ICMC-USP

Lecture Notes
Graduate SME5802, Undergrad SME0253

Introduction to Computational Fluid Mechanics

with an emphasis in the Finite Volume Method for Elliptic, Parabolic and Hyperbolic problems

Roberto F. Ausas & Fabricio S. Sousa

June 29, 2025

Instituto de Ciências Matemáticas e de Computação
University of São Paulo

Preface

These lecture notes provide a general overview of classical discretization methods to solve problems arising in fluid mechanics. Originally, they were intended for graduate students, however, by omitting certain technical details they can be used by undergrad students without major difficulties, provided appropriate guidance. We study several problems with different mathematical structure (elliptic, parabolic and hyperbolic), from incompressible to compressible flows, from laminar to turbulent flows and cover theoretical as well as implementation aspects, mainly by the finite volume method, although other methods are also considered for discretization.

What This Course Covers

As a summary of the content of this document, let us enumerate the main topics to be covered:

Chapter |01| Governing principles in Fluid Mechanics;
Chapter |02| Discretization of Elliptic and parabolic problems;
Chapter |03| Numerical solution of Compressible Potential flows;
Chapter |04| Discretization of Hyperbolic problems;
Chapter |05| Numerical solution of the Navier-Stokes equations;
Chapter |06| Computational modeling of Turbulent flows;

Bibliographical remarks

Throughout this document we do not follow a single books or author, but we take ideas from several sources. Particularly, in the first chapter we follow some books on fluid mechanics, such as [1–3] and also from the lecture notes of [4, 5]. The latter is also used in other chapters, however, significant changes have been introduced in the presentation, the excercices, both theoretical and computational, as well as in notational aspects with respect to previous years.

RFA & FSS

Contents

Preface ii

Contents iii

1 GOVERNING PRINCIPLES IN FLUID MECHANICS 1
- 1.1 Prelude . . . 1
- 1.2 Solids and Fluids, The continuum hypothesis . . . 1
- 1.3 Scalar, Vector and Tensor fields in Cartesian coordinates . . . 2
- 1.4 Kinematics of a continuous medium . . . 4
  - 1.4.1 Material, Referential and Spatial descriptions . . . 4
  - 1.4.2 Representation of fields . . . 5
  - 1.4.3 Material time derivative . . . 5
- 1.5 Time derivatives of volume integrals: Reynolds Transport theorem . . . 6
- 1.6 Conservation laws . . . 8
  - 1.6.1 Conservation of mass . . . 8
  - 1.6.2 Conservation of momentum . . . 9
  - 1.6.3 Conservation of energy . . . 11
- 1.7 Constitutive laws . . . 11
  - 1.7.1 Specific heat capacity . . . 11
  - 1.7.2 Fourier's law . . . 12
  - 1.7.3 Newtonian and quasi-Newtonian behavior . . . 12
- 1.8 Assignment 1: Warm up . . . 13

2 DISCRETIZATION OF SCALAR ELLIPTIC AND PARABOLIC PROBLEMS 15
- 2.1 The second order prototypical problem . . . 15
  - 2.1.1 Poisson's equation . . . 15
  - 2.1.2 Transient Poisson's problem . . . 16
- 2.2 1st application in fluid mechanics: Fully developed flow in ducts . . . 16
  - 2.2.1 Application of the conservation laws . . . 17
- 2.3 Overview of discretization methods . . . 19
- 2.4 Finite difference discretization . . . 20
- 2.5 Assignment 1: A *simple* finite difference (FD) code . . . 22
- 2.6 Finite volume discretization . . . 24
  - 2.6.1 Structured case - Orthogonal meshes . . . 24
- 2.7 Assignment 2: A *not so simple* finite volume (FV) code . . . 28
  - 2.7.1 Unstructured case - Non-orthogonal meshes . . . 29
  - 2.7.2 Gradient recovery . . . 32
- 2.8 Assignment 3: Non-orthogonal meshes: A practice with `OpenFOAM` . . . 34
  - 2.8.1 The `openFOAM` platform . . . 34
- 2.9 Finite element discretization: The Galerkin method . . . 37
- 2.10 Assignment 4: A FE formulation implemented in `Firedrake` . . . 41
  - 2.10.1 The `Firedrake` platform . . . 41

3 NUMERICAL SOLUTION OF POTENTIAL FLOWS 43
- 3.1 Prelude . . . 43
- 3.2 Potential functions . . . 43

3.3 Incompressible potential flows . . . 43
3.3.1 Boundary conditions for the potential function . . . 44
3.4 Stream functions . . . 45
3.4.1 Boundary conditions for the stream function . . . 46
3.5 Potential lines and streamlines . . . 47
3.6 Bernoulli's equation . . . 47
3.7 Slightly compressible potential flows . . . 48
3.8 Finite-volume discretizations . . . 50
3.8.1 Discretization of the incompressible model . . . 50
3.8.2 Discretization of boundary conditions . . . 51
3.9 Assignment: Implementation of an incompressible potential flow . . . 53
3.10 Discretization of the compressible model . . . 53
3.10.1 Computation of densities . . . 55
3.10.2 Solution of the nonlinear problem . . . 55
3.11 Assignment 2: Nonlinear potential flow . . . 57

4 NUMERICAL METHODS FOR HYPERBOLIC CONSERVATION LAWS 58
4.1 Balance and conservation laws . . . 58
4.2 Linear Hyperbolic Conservation Laws . . . 60
4.2.1 Solution of the Advection Equation . . . 60
4.2.2 Characteristic Curves . . . 61
4.2.3 Boundary Conditions . . . 62
4.2.4 Riemann Problem . . . 62
4.2.5 Variable Coefficients . . . 63
4.3 Finite volume methods for hyperbolic conservation laws . . . 63
4.3.1 Central scheme . . . 65
4.3.2 Lax-Friedrichs . . . 65
4.3.3 Lax-Wendroff . . . 66
4.3.4 Upwind . . . 66
4.4 The CFL condition . . . 68
4.5 Consistency, Stability, and Convergence . . . 70
4.5.1 Local Truncation Error . . . 71
4.5.2 Flux consistency . . . 73
4.5.3 Linear stability . . . 73
4.5.4 The von Neumann stability criterion . . . 74
4.6 Assignment 1: Linear advection equation . . . 77
4.7 Nonlinear hyperbolic conservation laws . . . 77
4.7.1 Characteristic curves . . . 77
4.7.2 Weak solutions . . . 78
4.7.3 The Rankine-Hugoniot condition . . . 79
4.7.4 Solution of the Riemann Problem . . . 80
4.7.5 Entropy Conditions . . . 81
4.7.6 Rarefaction waves . . . 82
4.8 Finite volume methods for nonlinear hyperbolic conservation laws . . . 83
4.8.1 The Godunov method . . . 84
4.8.2 The Roe Method . . . 85
4.8.3 The Lax-Friedrichs Method . . . 86
4.8.4 The Rusanov Method . . . 87
4.8.5 The Engquist-Osher Method . . . 87
4.9 High-Order Methods . . . 87
4.9.1 The REA Algorithm . . . 88

4.9.2 TVD Methods . . . 89
4.9.3 Slope Limiters . . . 90
4.9.4 Semi-Discrete Formulation . . . 91
4.9.5 Time Discretization . . . 91
4.10 Assignment 2: Nonlinear traffic flow . . . 92
4.11 Assignment 3: Numerical solution of 1D Euler's equations . . . 93
4.11.1 1D Euler's equations . . . 93
4.11.2 Sod shock tube . . . 93

5 NUMERICAL METHODS FOR MIXED EQUATIONS 96
5.1 Examples of mixed equations . . . 96
5.2 Fully coupled Taylor series methods . . . 97
5.3 Fully coupled method of lines . . . 97
5.4 Implicit-explicit (IMEX) methods . . . 98
5.5 Fractional step methods . . . 98

6 DISCRETIZATION OF THE INCOMPRESSIBLE NAVIER-STOKES EQUATIONS 100
6.1 Prelude . . . 100
6.2 The Navier-Stokes equations . . . 100
6.2.1 Initial and Boundary conditions . . . 101
6.3 Discretization by the FVM . . . 102
6.4 Monolithic vs. Segregated approach . . . 103
6.5 Spatial discretization: Colocated vs. Staggered . . . 105
6.5.1 Colocated grids . . . 105
6.5.2 Comments on the nonlinear advective terms . . . 108
6.5.3 Treatment of boundary conditions . . . 109
6.5.4 Spurious checkboard modes . . . 109
6.5.5 One remedy: One-sided discretization of div(·) and grad(·) . . . 110
6.5.6 Another remedy: Pressure-Weighted-Interpolation (PWI) . . . 110
6.6 Assignment 1: A practice with `OpenFOAM` - Flow around obstacle . . . 111
6.7 The ultimate remedy to cure the spurious checkboard modes: Staggered grids . . . 112
6.7.1 Laplacian form of the viscous term . . . 114
6.7.2 Treatment of boundary conditions . . . 115
6.8 Assignment 2: A simple Finite Volume Staggered code - Cavity flow . . . 117
6.9 Further comments . . . 119
6.9.1 Other temporal schemes: ABCN . . . 119
6.9.2 Other decoupling strategies . . . 120

7 COMPUTATIONAL ASPECTS OF TURBULENCE MODELING 121
7.1 Prelude . . . 121
7.2 What is turbulence? Qualitative aspects . . . 121
7.3 The Averaged Navier-Stokes equations (RANS) . . . 122
7.4 Computational Modeling of Turbulence . . . 127
7.4.1 Turbulence models . . . 127
7.4.2 Boundary conditions - Wall laws . . . 128
7.4.3 Final comments - LES models . . . 129
7.5 Assignment 1: Turbulent flows . . . 129
7.6 Assignment 2: RANS equations in `openFOAM` . . . 130

Bibliography 131

Alphabetical Index 133

GOVERNING PRINCIPLES IN FLUID MECHANICS

1

1.1 Prelude

This chapter is devoted to present in a very synthetic form, fundamental concepts of relevance in fluid mechanics that are worth having in mind for the rest of the course, prior to starting the study of methods and techniques to solve problems arising in fluid mechanics by numerical means. Our aim is not to provide full details, a more comprehensive discussion being found in any textbook on fluid mechanics such as [1] or [2] (as an engineering textbook), from which we take some explanations and concepts.

1.2 Solids and Fluids, The continuum hypothesis

Let us begin by recalling a few ideas:

- We all have an intuitive notion of what a solid and a fluid is. Putting this in mechanical terms, whereas a solid can resist **shear**, a fluid (be it a gas or a liquid) cannot (as illustrated in Figure 1.1).
- Fluids are aggregations of molecules, widely spaced for a gas and closely spaced for a liquid.
- For a fluid, the molecules are not "fixed" in a lattice, as occurs with solid materials.
- Although a molecular description of fluids involving statistical mechanics is certainly possible and sometimes necessary[1], in this course, we will describe the fluids by a macroscopic mathematical model known as **continuous medium**.
- A central concept is that a continuous medium is made of elements, called **material points** or **material particles**. This concept is introduced axiomatically in the same way as a geometrical point in elementary geometry.
- For a continuous medium, we have that:

> "Physical properties can be assumed to vary continuously in space and each property is essentially a *pointwise function*. This does not preclude the presence of discontinuities, since they may occur across interfaces separating two phases and across shock waves. Differential calculus is applicable! (L. Euler, 1755)

1.1 Prelude 1
1.2 Solids and Fluids, The continuum hypothesis . . 1
1.3 Scalar, Vector and Tensor fields in Cartesian coordinates 2
1.4 Kinematics of a continuous medium 4
1.5 Time derivatives of volume integrals: Reynolds Transport theorem 6
1.6 Conservation laws 8
1.7 Constitutive laws 11
1.8 Assignment 1: Warm up . 13

[1]: Kundu et al. (2008), *Fluid Mechanics, Fourth Edition*

[2]: White (2011), *Fluid Mechanics, Seventh Edition*

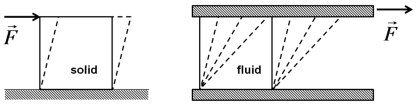

Figure 1.1: Solid vs fluid.

1: Typically when we study gas flows at very small scales, in rarefied regime. This can be characterized by the so called Knudsen number, which is a dimensionless quantity defined as

$$Kn = \frac{\lambda}{L}$$

being λ the mean free path of particles (mean distance travelled between collisions with other particles) and L a characteristic length scale of the problem.

Leonhard Euler (1707(Switzerland)-1783(Russia)).

- It is common to introduce these ideas by examining the definition of density of a fluid (i.e., mass per unit volume) which is

$$\rho = \lim_{\mathcal{V} \to \mathcal{V}_{\min}} \frac{m}{\mathcal{V}}$$

where m is the molecular mass and $\mathcal{V}_{\min}$ is a limiting volume below which molecular variations becomes relevant. This limiting volume is in practice $\sim 10^{-9}\,\mathrm{mm}^3$. Above this volume, properties can be thought to vary continuously as depicted in Figure 1.3.

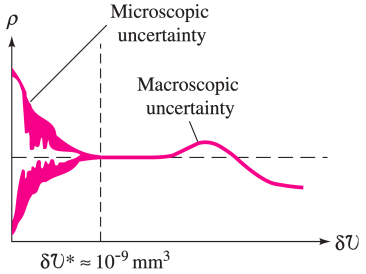

Figure 1.3: Density vs. elemental size volume (taken from [2]).

- The practical problems we aim to solve in this course involve physical dimensions that are certainly larger than $\mathcal{V}_{\min}$, so it is perfectly reasonable to consider the density (or any other quantity) a pointwise function that changes continuously, for which differential calculus is applicable.

1.3 Scalar, Vector and Tensor fields in Cartesian coordinates

In this course, we will be dealing with:

- *scalar quantities*, such as temperature and density;
- *vector quantities*, such as velocity and force;
- *tensor quantities*, such as stress and gradients of vector fields.

A scalar field, is any quantity whose value at a certain location is independent of the coordinate system. However, for vectors and tensors we need to specify the coordinate directions. In this course we will consider vectors and tensors in cartesian basis. We will denote the Cartesian coordinates by[2]

$$\{x_1,\ x_2,\ x_3\}$$

and the Cartesian basis vectors by

$$\{\check{\mathbf{e}}^{(1)},\ \check{\mathbf{e}}^{(2)},\ \check{\mathbf{e}}^{(3)}\}$$

which are unit vectors in three mutually perpendicular directions (an orthonormal base). Vectors, such as position $\mathbf{x}$ and velocity $\mathbf{u}$ are denoted by boldfaces[3]

$$\mathbf{x} = \sum_{i=1}^{3} x_i\, \check{\mathbf{e}}^{(i)} = [x_1, x_2, x_3]^\intercal$$

$$\mathbf{u} = \sum_{i=1}^{3} u_i\, \check{\mathbf{e}}^{(i)} = [u_1, u_2, u_3]^\intercal$$

This column matrix is the representation of the vector with respect to the set of base vectors $\{\check{\mathbf{e}}^{(i)}\}$.

A tensor $\boldsymbol{\sigma}$ is a linear transformation, such that for any two vectors $\mathbf{u}$ and $\mathbf{v}$ and α, β scalars

$$\boldsymbol{\sigma}(\alpha\mathbf{u} + \beta\mathbf{v}) = \alpha\boldsymbol{\sigma}(\mathbf{u}) + \beta\boldsymbol{\sigma}(\mathbf{v})$$

2: Notice that the supraindex (i) in $\check{\mathbf{e}}^{(i)}$ denotes the i–th vector and not the component.

3: Recall that, in order to follow the rules of linear algebra, vectors have to be written as columns, i.e.,

$$\mathbf{x} = \begin{bmatrix} x_1 \\ x_2 \\ x_3 \end{bmatrix} = [x_1, x_2, x_3]^\intercal$$

Usually, instead of $\sigma(\mathbf{u})$, we write $\sigma\mathbf{u}$ or $\sigma \cdot \mathbf{u}$.

The tensor product of $\mathbf{v}$ and $\mathbf{w}$ is a tensor defined such that for any vector $\mathbf{u}$

$$(\mathbf{v} \otimes \mathbf{w})\mathbf{u} = (\mathbf{w} \cdot \mathbf{u})\mathbf{v}$$

The symbol $\otimes$ denotes the dyadic product of the two vectors, such that, in cartesian components $\mathbf{v} \otimes \mathbf{w} = \mathbf{v}\mathbf{w}^\intercal$ (or simply $\mathbf{v}\,\mathbf{w}$) is defined by[4]

$$(\mathbf{v} \otimes \mathbf{w})_{ij} = \sum_{i=1}^{3} \sum_{j=1}^{3} v_i w_j \, \check{\mathbf{e}}^{(i)} \otimes \check{\mathbf{e}}^{(j)}$$

4: Note that, the set of matrizes $\check{\mathbf{e}}^{(i)} \otimes \check{\mathbf{e}}^{(j)}, i, j = 1, \ldots, d$, form a base for the space $\mathbb{R}^{d \times d}$.

Gradients of fields

The gradient of a scalar field f is denoted

$$\nabla f = \sum_{i=1}^{3} \frac{\partial f}{\partial x_i} \check{\mathbf{e}}^{(i)} = [f_{,1}, f_{,2}, f_{,3}]^\intercal$$

where ∇ is called the nabla operator. Notice the abbreviated notation $f_{,i}$ to denote the partial derivative of f with respect to x_i, $\partial f / \partial x_i$. Similarly, the gradient of a vector field is

$$\nabla \mathbf{u} = \sum_{i=1}^{3} \sum_{j=1}^{3} \frac{\partial u_i}{\partial x_j} \check{\mathbf{e}}^{(i)} \otimes \check{\mathbf{e}}^{(j)} = \begin{bmatrix} u_{1,1} & u_{1,2} & u_{1,3} \\ u_{2,1} & u_{2,2} & u_{2,3} \\ u_{3,1} & u_{3,2} & u_{3,3} \end{bmatrix}$$

This array is called the matrix of the tensor with respect to the set of base vectors $\{\check{\mathbf{e}}^{(i)}\}$.

The Kronecker delta

The Kronecker symbol is a tensor defined as

$$\delta_{ij} = \begin{cases} 1 & \text{if} \quad i = j \\ 0 & \text{if} \quad i \neq j \end{cases}$$

that is the identity tensor, since $\sum_{i=1}^{d} \delta_{ij} x_j = x_i$.

Einstein's convention

As an example, consider operations such as the scalar product (the **dot** product of two vectors or the double contraction of two tensors):

$$\mathbf{u} \cdot \mathbf{v} = u_1 v_1 + u_2 v_2 + u_3 v_3 = \sum_{i=1}^{3} u_i v_i,$$

or

$$\boldsymbol{\sigma} : \boldsymbol{\tau} = \sigma_{11}\tau_{11} + \sigma_{12}\tau_{12} + \cdots + \sigma_{32}\tau_{32} + \sigma_{33}\tau_{33} = \sum_{i=1}^{3} \sum_{j=1}^{3} \sigma_{ij}\tau_{ij}$$

Einstein's summation convention

Whenever an index is repeated once, it is a dummy index indicating a summation with the index running through the integer numbers $1, \ldots, d$.

Albert Einstein (Germany(1879)–USA(1955)).

For the examples above, applying the convention, these operations can be abbreviated to

$$\mathbf{u} \cdot \mathbf{v} = u_i v_i, \qquad \boldsymbol{\sigma} : \boldsymbol{\tau} = \sigma_{ij}\tau_{ij}$$

and similarly for other operations, for instance, the **divergence** of a vector field is

$$\nabla \cdot \mathbf{u} = \sum_{k=1}^{3} \frac{\partial u_k}{\partial x_k} = \frac{\partial u_k}{\partial x_k} = u_{k,k}$$

or the application of a linear tranformation

$$(\boldsymbol{\sigma} \cdot \check{\mathbf{n}})_i = \sum_{j=1}^{3} \sigma_{ij}\check{n}_j = \sigma_{ij}\check{n}_j$$

1.4 Kinematics of a continuous medium

1.4.1 Material, Referential and Spatial descriptions

We begin with a body $\mathfrak{B}$ made of **material particles** . All these particles together form a continuous medium as we have seen. The motion of $\mathfrak{B}$ is specified by a mapping $\hat{\boldsymbol{\chi}}$, such that, for any particle P of $\mathfrak{B}$, its position $\mathbf{x}$ on the body's configuration at arbitrary time t is given by

$$\mathbf{x} = \hat{\boldsymbol{\chi}}(\mathsf{P}, t) = \hat{\boldsymbol{\chi}}_t(\mathsf{P})$$

so, the configuration of $\mathfrak{B}$ at time t may be denoted by $\mathscr{V} = \hat{\boldsymbol{\chi}}(\mathfrak{B}, t)$.

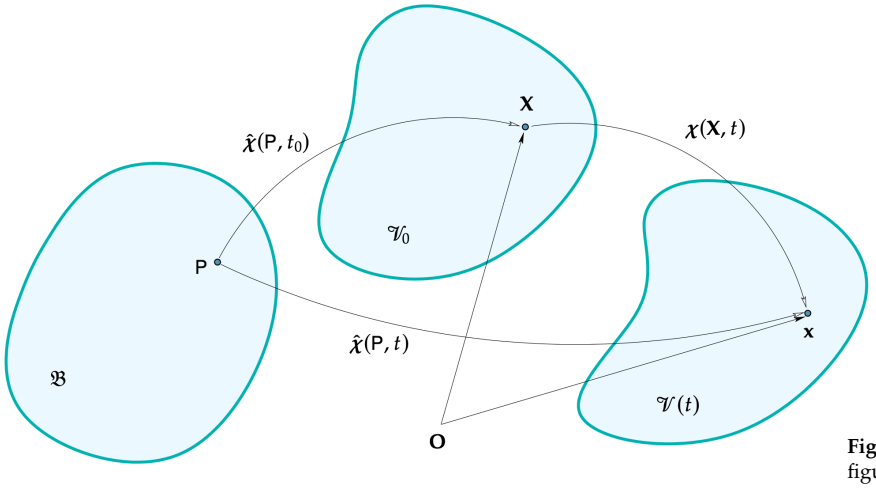

Figure 1.5: Material body, reference configuration and current configuration.

This material description is of limited practical interest. However, it can be useful to introduce a reference configuration. To that end, we consider

the position $\mathbf{x}$ at time t of a particle P, that at the reference time t_0, is at position $\mathbf{X} = \hat{\boldsymbol{\chi}}(\mathsf{P}, t_0) = \hat{\boldsymbol{\chi}}_{t_0}(\mathsf{P})$, by defining[5]

$$\mathbf{x} = \hat{\boldsymbol{\chi}}(\hat{\boldsymbol{\chi}}_{t_0}^{-1}(\mathbf{X}), t) = \boldsymbol{\chi}(\mathbf{X}, t)$$

The function $\boldsymbol{\chi}$ must be twice-differentiable with respect to t, such that we can compute velocities and accelerations of the particles, i.e.,

$$\mathbf{u} = \frac{\partial \boldsymbol{\chi}(\mathbf{X}, t)}{\partial t}, \quad \mathbf{a} = \frac{\partial^2 \boldsymbol{\chi}(\mathbf{X}, t)}{\partial t^2}$$

or, componentwise

$$v_i = \frac{\partial \chi_i(\mathbf{X}, t)}{\partial t}, \quad a_i = \frac{\partial^2 \chi_i(\mathbf{X}, t)}{\partial t^2}$$

5: The configuration at time t is called the current configuration.

1.4.2 Representation of fields

The following discussion applies to any scalar, vector or tensor field. We have different representations of a field or any quantity, say ℓ. Since $\mathsf{P} = \hat{\boldsymbol{\chi}}_t^{-1}(\mathbf{x})$ and $\mathbf{X} = \boldsymbol{\chi}_t^{-1}(\mathbf{x})$, we may write[6]:

$$\ell = \bar{f}(\mathsf{P}, t) = f(\mathbf{x}, t) = \tilde{f}(\mathbf{X}, t)$$

The three functions $\bar{f}$, $\tilde{f}$ and f represent the same quantity ℓ:

- **Material description:** Function $\bar{f}$ applies for a given time t and material point P;
- **Referential description:** Function $\tilde{f}$ applies for a given time t and position $\mathbf{X}$ that particle P occupied at the reference time t_0;
- **Spatial description**[7]**:** Function f applies for a given time t and position $\mathbf{x}$ that particle P occupies at this time t.

6: In these notes, we will use in general the notation with a bar (e.g., $\bar{f}$) for the material description, with a tilde (e.g., $\tilde{f}$) for the referential description and "nothing" for the Spatial description, which is the most widely used one in this course.

7: This is also called the *Eulerian description*.

1.4.3 Material time derivative

We must provide a way to compute the total time derivative of a quantity which may be given in the different configurations, namely, the Material, Referential or Spatial description. Clearly, the rate of change of quantity ℓ is

$$\dot{\ell} = \frac{d\ell}{dt} = \frac{\partial \bar{f}(\mathsf{P}, t)}{\partial t} = \frac{\partial \tilde{f}(\mathbf{X}, t)}{\partial t}$$

because both, P and $\mathbf{X}$ are fixed. However, if we are dealing with the spatial (or Eulerian) description f, we have[8]

$$\begin{aligned}
\dot{\ell} &= \frac{\partial f(\mathbf{x}, t)}{\partial t} + \frac{\partial f(\mathbf{x}, t)}{\partial \mathbf{x}} \cdot \frac{\partial \boldsymbol{\chi}(\mathbf{X}, t)}{\partial t} \\
&= \frac{\partial f(\mathbf{x}, t)}{\partial t} + \frac{\partial f(\mathbf{x}, t)}{\partial \mathbf{x}} \cdot \mathbf{u}(\mathbf{x}, t) \\
&= \frac{\partial f(\mathbf{x}, t)}{\partial t} + \nabla_{\mathbf{x}} f \cdot \mathbf{u}(\mathbf{x}, t)
\end{aligned}$$

8: Recall, we in general ommit the subindex $\mathbf{x}$ in gradient operator ∇, since it is understood the derivatives are being taken with respect to the spatial variables.

Definition 1.4.1 *(**Material or total time derivative**) The material derivative of a scalar, vector or tensor quantity ℓ expressed by $f(\mathbf{x}, t)$ in Eulerian description in a continuous medium, with velocity $\mathbf{u}$, is denoted by $\dfrac{Df}{Dt}$ and is given by*

$$\dot{\ell} = \frac{Df(\mathbf{x},t)}{Dt} = \frac{\partial f(\mathbf{x},t)}{\partial t} + \underbrace{\nabla_{\mathbf{x}} f(\mathbf{x},t)\cdot\mathbf{u}(\mathbf{x},t)}_{\text{Convective derivative}} \tag{1.1}$$

The first term corresponds to the rate of change of quantity ℓ for a fixed position $\mathbf{x}$ in space and the second term corresponds to the *convective* (also termed *advective*) rate of change of ℓ as the material particle which occupies $\mathbf{x}$ at time t is transported with velocity $\mathbf{u}$[9].

9: In general, and when there is no confussion, the arguments $(\mathbf{x}, t)$ will be omited in the functions for simplicity of notation.

Be cautious in Equation 1.1 with the convective term for vector or tensor fields. In particular, for a vector field $\mathbf{f}$ we have

$$\frac{D\mathbf{f}}{Dt} = \frac{\partial \mathbf{f}}{\partial t} + (\nabla \mathbf{f})\cdot\mathbf{u}$$

for the second term, working with components

$$[(\nabla\mathbf{f})\cdot\mathbf{u}]_i = \frac{\partial f_i}{\partial x_j}u_j = \left(u_j\frac{\partial}{\partial x_j}\right)(f_i) = [(\mathbf{u}\cdot\nabla)\mathbf{f}]_i$$

An example corresponds to the case $\mathbf{f} = \mathbf{u}$, so in this case the material derivative is

$$\frac{D\mathbf{u}}{Dt} = \frac{\partial \mathbf{u}}{\partial t} + (\nabla\mathbf{u})\cdot\mathbf{u} = \frac{\partial \mathbf{u}}{\partial t} + (\mathbf{u}\cdot\nabla)\mathbf{u} \tag{1.2}$$

which is nothing but the acceleration $\mathbf{a}$ in Eulerian description, that is nonlinear in $\mathbf{u}$.

Steady motion

If for the quantity at hand, it happens that there is no explicit dependence of f with the time independent variable t, then the first term is simply zero

$$\frac{Df(\mathbf{x},t)}{Dt} = \nabla_{\mathbf{x}} f(\mathbf{x},t)\cdot\mathbf{u}(\mathbf{x},t)$$

This is called **Steady motion** .

1.5 Time derivatives of volume integrals: Reynolds Transport theorem

In the chapter we discuss certain conservation laws for a continuous medium, fluids in particular. To that end, we first need to be able to compute quantities such as

$$\mathcal{I}(t) = \int_{\mathcal{V}(t)} f(\mathbf{x},t)\,dv \quad \text{and} \quad \frac{d}{dt}\mathcal{I}(t)$$

where $\mathcal{V}(t)$ is a subset of the current configuration[10] (at time t) of a body $\mathfrak{B}$ made of material particles. Let $\mathcal{V}_0$ be the subset in the (fixed) reference configuration (defined at time t_0) occupied by the same material particles currently in $\mathcal{V}(t)$, and f the Eulerian description of a quantity ℓ (scalar, vector or tensor).

10: We have left the time dependence in $\mathcal{V}(t)$ to emphasized that we aim to compute the integral of a quantity over a region of space changing with time.

We can't simply interchange the integral and the derivative signs because the domain of integration depends on time. However, we can proceed as follows. Let J be the determinant of the Jacobian of the transformation between $\mathcal{V}_0$ and $\mathcal{V}$, if dv and dV denote the infinitesimal volume elements in the reference and current configurations, then

$$dv = J\, dV$$

It can be shown that the time derivative of J is given by[11]

$$\dot{J} = J\, \nabla \cdot \mathbf{u}$$

Osborne Reynolds (Ireland, 1842–1912).

Then,

$$\begin{aligned}
\frac{d}{dt}\int_{\mathcal{V}(t)} f\, dv &= \frac{d}{dt}\int_{\mathcal{V}_0} \tilde{f}\, J\, dV \quad \text{(pull-back)} \\
&= \int_{\mathcal{V}_0} \frac{d}{dt}\left(\tilde{f} J\right) dV \\
&= \int_{\mathcal{V}_0} \left(\dot{\ell}\, J + \tilde{f}\, \dot{J}\right) dV \\
&= \int_{\mathcal{V}_0} \left[\dot{\ell}\, J + \tilde{f}\, (J\, \nabla \cdot \mathbf{u})\right] dV \\
&= \int_{\mathcal{V}(t)} \left(\dot{\ell} + f\, \nabla \cdot \mathbf{u}\right) dv \quad \text{(push-forward)} \qquad (1.3)
\end{aligned}$$

11: In order to show such result, we need to take the time derivative of

$$\begin{aligned} dv &= d\mathbf{x}^{(1)} \cdot \left(d\mathbf{x}^{(2)} \times d\mathbf{x}^{(3)}\right) \\ &= \mathbf{F}\, d\mathbf{X}^{(1)} \cdot \left(\mathbf{F}\, d\mathbf{X}^{(2)} \times \mathbf{F}\, d\mathbf{X}^{(3)}\right) \end{aligned}$$

in which $\mathbf{F} = \dfrac{\partial \boldsymbol{\chi}(\mathbf{X}, t)}{\partial \mathbf{X}}$ (see [4] for the details).

substituting the expression for $\dot{\ell}$ given in Equation 1.1 we obtain:

Theorem 1.5.1 ***(Reynolds transport)*** *The rate of change of the integral of a quantity ℓ over $\mathcal{V}(t)$ following the particles that occupy that region is given by*

$$\begin{aligned}
\frac{d\mathcal{I}(t)}{dt} = \frac{d}{dt}\int_{\mathcal{V}(t)} f\, dv &= \int_{\mathcal{V}(t)} \left[\frac{\partial f}{\partial t} + \nabla \cdot (f\, \mathbf{u})\right] dv \\
&= \underbrace{\int_{\mathcal{V}(t)} \frac{\partial f}{\partial t}\, dv}_{\substack{\text{Rate of change of } \ell \\ \text{inside the region}}} + \underbrace{\int_{\partial\mathcal{V}(t)} f\, \mathbf{u} \cdot \check{\mathbf{n}}\, ds}_{\substack{\text{Flux of } \ell \\ \text{across the boundary}}} \qquad (1.4)
\end{aligned}$$

Carl Friedrich Gauss (Germany, 1777–1855).

Notice that, the Gauss (or divergence) theorem has been used to transform the volume integral in the left hand side to a surface integral in the right[12]. A particular case, very often encountered, is when the region $\mathcal{V}(t) = \bar{\mathcal{V}}$,

12: Recall, the Gauss' theorem: If $\mathcal{V} \subset \mathbb{R}^d$ is compact and has piecewise smooth boundary $\partial\mathcal{V}$, for a continuously differentiable vector-valued function $\mathbf{F}$, then

$$\int_{\mathcal{V}} (\nabla \cdot \mathbf{F})\, dv = \int_{\partial\mathcal{V}} \mathbf{F} \cdot \check{\mathbf{n}}\, ds$$

a fixed region in space. In such case we can write

$$\frac{d}{dt}\int_{\bar{\mathcal{V}}} f\,dv = \frac{\partial}{\partial t}\int_{\bar{\mathcal{V}}} f\,dv + \int_{\partial\bar{\mathcal{V}}} f\mathbf{u}\cdot\check{\mathbf{n}}\,ds$$

1.6 Conservation laws

In sequel we formulate some conservation principles that are essential for the rest of the course, namely, the conservation of mass, linear momentum and Energy. The idea is to apply the Reynolds transport theorem to derive these laws in integral form. However, we may also be interested in the differential formulation, for which the following theorem will be of importance to us[13]:

13: The theorem applies componentwise in case g is a vector-valued function.

Theorem 1.6.1 ***(The localization theorem)*** *Let $g : \mathcal{V}\times\mathbb{R}\to\mathbb{R}$ be a continuous function in the spatial variable, then*

$$\int_\Omega g(\mathbf{x},t)\,dv = 0 \;\; \forall\Omega\subset\mathcal{V}$$

if and only if $g(\mathbf{x},t)=0\;\forall\mathbf{x}\in\mathcal{V}(t)$.

1.6.1 Conservation of mass

Consider a material volume $\mathcal{V}$, the amount of mass inside it being

$$\mathcal{M} = \int_{\mathcal{V}} \rho(\mathbf{x},t)\,dv$$

since this material volume has fixed identity and we assume there is no exchange of mass with the surroundings (e.g., this would be the case if the body loses mass by evaporation to the ambient) we have that

$$\frac{d\mathcal{M}}{dt} = \frac{d}{dt}\int_{\mathcal{V}} \rho\,dv = 0$$

so, the function f in Theorem 1.5.1 is $f=\rho$.

Conservation of mass

By applying the Reynolds transport theorem, the principle reads

$$\int_{\mathcal{V}}\left[\frac{\partial\rho}{\partial t}+\nabla\cdot(\rho\mathbf{u})\right]dv = \int_{\mathcal{V}}\frac{\partial\rho}{\partial t}\,dv + \int_{\partial\mathcal{V}}\rho\mathbf{u}\cdot\check{\mathbf{n}}\,ds = 0 \qquad (1.5)$$

and using the Localization theorem we obtain the differential form

$$\frac{\partial\rho}{\partial t}+\nabla\cdot(\rho\mathbf{u}) = \frac{D\rho}{Dt}+\rho\nabla\cdot\mathbf{u} = 0 \qquad (1.6)$$

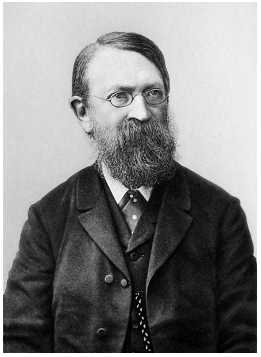

Ernst Waldfried Josef Wenzel Mach (Austria(1838)–Germany(1916)).

- The first term $\dfrac{D\rho}{Dt}$ is the rate of change of the density following the particles.

- An **incompressible fluid** is one in which density does not change with pressure. Liquids are almost incompressible and gases, in the low Mach number[14] regime can also be considered incompressible fluids.

- From Equation 1.6, we immediately see that for a flow in which the material particles have constant density, the velocity is solenoidal (**incompressible flow**), i.e.,

$$\nabla \cdot \mathbf{u} = 0$$

14: The Mach number is a nondimensional quantity defined as

$$\mathrm{Ma} = \frac{\|\mathbf{u}\|}{c}$$

where $\|\mathbf{u}\|$ is the magnitude of $\mathbf{u}$ and c is the speed of sound (the speed at which waves propagates in that medium.

1.6.2 Conservation of momentum

The amount of linear momentum inside $\mathcal{V}$

$$\mathcal{P} = \int_{\mathcal{V}} \rho(\mathbf{x}, t)\, \mathbf{u}(\mathbf{x}, t)\, dv$$

By Newton's second law of motion the principle of conservation of momentum states that the rate of change of linear momentum must be equal to the applied volumetric forces[15] given

$$\frac{d\mathcal{P}}{dt} = \frac{d}{dt}\int_{\mathcal{V}} \rho\mathbf{u}\, dv = \int_{\mathcal{V}} \mathbf{b}\, dv + \int_{\partial\mathcal{V}} \mathcal{F}\, ds$$

so, the function f in Theorem 1.5.1 is $f = \rho\mathbf{u}$.

15: These are also called *body forces*. A typical example of a body force is due to gravity

$$\mathbf{b} = -\rho\, g\check{\mathbf{e}}_3$$

Cauchy stress tensor

At this point, we must introduce a central concept in continuum mechanics (be it solid or fluid mechanics), which is the concept of stress tensor due to Cauchy. The idea is that if we take a surface $\partial\mathcal{V}$ in the continua and at any arbitrary point $\mathbf{x} \in \partial\mathcal{V}$ the region is subject to a surface force $\mathcal{F}$, the continuum inside *reacts with an equal and opposite force*, this is summarized in the:

Augustin-Louis Cauchy (France, 1789–1857).

Theorem 1.6.2 ***(Cauchy's stress)*** *There exists a symmetric tensor $\boldsymbol{\sigma}$, called the Cauchy stress tensor, such that, at any time t the local stress vector is*

$$\mathcal{F}(\mathbf{x}, t) = \boldsymbol{\sigma}(\mathbf{x}, t) \cdot \check{\mathbf{n}}(\mathbf{x}, t) \quad \forall \mathbf{x} \in \partial\mathcal{V}$$

where $\check{\mathbf{n}}$ is the unit normal vector of the plane on which the force acts.

Conservation of momentum

Noticing that[16]

$$\rho\mathbf{u}\,(\mathbf{u}\cdot\check{\mathbf{n}}) = \rho(\mathbf{u}\otimes\mathbf{u})\cdot\check{\mathbf{n}}$$

and using Theorem 1.6.2 the Reynolds' transport theorem applied to

16: Using index notation:

$$[\mathbf{u}\,(\mathbf{u}\cdot\check{\mathbf{n}})]_i = u_i(u_k\,\check{n}_k) = (u_i u_k)\check{n}_k = [(\mathbf{u}\otimes\mathbf{u})\cdot\check{\mathbf{n}}]_i$$

this case reads

$$\int_{\mathcal{V}} \frac{\partial(\rho\mathbf{u})}{\partial t}\, dv + \int_{\partial\mathcal{V}} \rho(\mathbf{u}\otimes\mathbf{u})\cdot\check{\mathbf{n}}\, ds = \\ = \int_{\mathcal{V}} \left[\frac{\partial(\rho\mathbf{u})}{\partial t} + \nabla\cdot(\rho\mathbf{u}\otimes\mathbf{u})\right] dv = \int_{\mathcal{V}} \mathbf{b}\, dv + \int_{\partial\mathcal{V}} \boldsymbol{\sigma}\cdot\check{\mathbf{n}}\, ds \quad (1.7)$$

or in differential form

$$\frac{\partial(\rho\mathbf{u})}{\partial t} + \nabla\cdot(\rho\mathbf{u}\otimes\mathbf{u}) - \nabla\cdot\boldsymbol{\sigma} = \mathbf{b} \quad (1.8)$$

which can also be written as using the conservation of mass Equation 1.6

$$\rho\left(\frac{\partial\mathbf{u}}{\partial t} + (\mathbf{u}\cdot\nabla)\mathbf{u}\right) - \nabla\cdot\boldsymbol{\sigma} = \mathbf{b} \quad (1.9)$$

- Equation 1.8 is called the conservative form of the momentum equation.

- If we define the *momentum flux* as

  $$\boldsymbol{\mathcal{p}} = -\boldsymbol{\sigma} + \rho\,(\mathbf{u}\otimes\mathbf{u})$$

  we write the equation in conservative form more compactly as

  $$\frac{\partial(\rho\mathbf{u})}{\partial t} + \nabla\cdot\boldsymbol{\mathcal{p}} = \mathbf{b}$$

- Equation 1.9 is called the non-conservative form and it is perhaps the form of the **Navier-Stokes equations** we find more frequently in the literature. Using Equation 1.2 we get

  $$\rho\frac{D\mathbf{u}}{Dt} - \nabla\cdot\boldsymbol{\sigma} = \mathbf{b} \quad (1.10)$$

- Until now, we haven't provided details about the boundary conditions so as to end up with a well-posed mathematical problem. In most fluid mechanics problems to be solved in this course we consider two types of boundary conditions at **physical walls**, namely,

  - **Dirichlet conditions:** The velocity field is specified

    $$\mathbf{u}(\mathbf{x},t) = \mathbf{u}_w(\mathbf{x},t) \quad \forall\mathbf{x}\in\partial\mathcal{V}_D$$

    In some cases we enforce conditions, either for the normal component to the surface, which for a *stationary* and *impermeable* wall is[17]

    $$u_n = \mathbf{u}\cdot\check{\mathbf{n}} = 0$$

    or for the tangent component, which again, for a stationary wall corresponds to[18]

    $$\mathbf{u}_t = \mathbf{u} - u_n\check{\mathbf{n}} = 0$$

  - **Neumann conditions:** The stresses are specified

    $$\boldsymbol{\sigma}\cdot\check{\mathbf{n}} = \boldsymbol{\mathcal{F}}_w \quad \forall\mathbf{x}\in\partial\mathcal{V}_N$$

17: This is called the **no-penetration condition** and is a kinematic condition, which is deduced from a conservation principle.

18: This is called the **no-slip** condition, which is a dynamic boundary condition, that can not be deduced from other principles, instead, it is a *postulate* which agrees well with physical observations.

We suggest to have a look for instance at [3] (section 1.6) for a more detailed discussion on boundary conditions for problems in fluid mechanics.

[3]: Kirby (2010), *Micro- and Nanoscale Fluid Mechanics: Transport in Microfluidic Devices*

1.6.3 Conservation of energy

The amount of energy inside $\mathcal{V}$

$$\mathscr{E} = \int_{\mathcal{V}} \rho \left(\frac{1}{2} \|\mathbf{u}\|^2 + e \right) dv$$

where the first contribution corresponds to the **Kinetic energy** and the second one to the **internal energy** (per unit of mass) which accounts for the capability of a medium storing thermal energy and is a function of its local state (tipically, temperature and pressure). The first law of thermodynamic establishes that

$$\frac{d\mathscr{E}}{dt} = \frac{d}{dt} \int_{\mathcal{V}} \rho \left(\frac{1}{2} \|\mathbf{u}\|^2 + e \right) dv = \mathbb{Q} + \mathcal{W}$$

where $\mathbb{Q}$ and $\mathcal{W}$ stands for the amount of heat and work received from the surroundings. We have volume and surface contributions to these terms which materializes in the conservation law as

$$\frac{d\mathscr{E}}{dt} = \int_{\mathcal{V}} \left(\mathbf{b} \cdot \mathbf{u} + \mathfrak{s}_Q \right) dv + \int_{\partial\mathcal{V}} (\mathbf{u} \cdot \boldsymbol{\sigma} - \boldsymbol{q}) \cdot \check{\mathbf{n}} \, ds \tag{1.11}$$

where

- $\mathbf{b} \cdot \mathbf{u}$ is the power of the body forces;
- $\mathfrak{s}_Q$ are the volumetric sources/sinks of heat;
- $\mathbf{u} \cdot (\boldsymbol{\sigma} \cdot \check{\mathbf{n}})$ is the power of tractions through $\partial\mathcal{V}$;
- $\boldsymbol{q} \cdot \check{\mathbf{n}}$ is the flux of heat entering/leaving the region through $\partial\mathcal{V}$.

The complete derivation of the conservation of energy principle and its differential form which is obtained by applying the Reynolds transport and localization theorems is

$$\rho \frac{De}{Dt} + \nabla \cdot \boldsymbol{q} = \mathfrak{s}_Q + \Phi \tag{1.12}$$

where $\Phi = \boldsymbol{\sigma} : \nabla \mathbf{u}$ is the the local viscous dissipation. This is left as an exercice (see below).

1.7 Constitutive laws

In most part of this course we consider three constitutive relations that allow us to have a closure of the problems above. We need laws for e, $\boldsymbol{q}$ and $\boldsymbol{\sigma}$ which are briefly explained below.

1.7.1 Specific heat capacity

The internal energy of a continuous medium is related to its capacity to store thermal energy. This can be expressed by using the specific heat

capacity c, which is essentially the amount of heat we must supplied to 1 unit of mass of the material so as to increase its temperature in 1 unit. In thermodynamics, it is defined as

$$c = \frac{1}{\mathcal{M}} \frac{\partial \mathbb{Q}}{\partial T}$$

so, we can write for the internal energy per unit mass

$$e = c\,T$$

where in general c is a function of temperature and pressure.

1.7.2 Fourier's law

In thermal problems the constitutive law universally adopted relates the heat flux to the temperature gradient ∇T, i.e.,

$$\boldsymbol{q} = -\boldsymbol{\kappa} \cdot \nabla T$$

where the **thermal conductivity** $\boldsymbol{\kappa}$ is in general a $d \times d$ symmetric positive definite matrix. The simple scalar case corresponding to

$$\boldsymbol{\kappa} = \kappa\, \mathbf{I}_{d\times d} \quad \Rightarrow \quad \boldsymbol{q} = -\kappa \nabla T$$

Jean-Baptiste Joseph Fourier (France, 1768–1830).

1.7.3 Newtonian and quasi-Newtonian behavior

The simplest constitutive behavior corresponds to that of viscous Newtonian fluids, which relates the local stresses to the rate of deformation tensor. The reader is possibly familiar from basic courses that for parallel flows the shear stress at a surface element parallel to a flat plate is

$$\tau(z) = \mu \frac{\partial u}{\partial z}$$

so the wall shear strees is $\tau_w = \tau(z = 0)$, where μ is the dynamic viscosity and z is the height above the plate. The law above can be generalized to arbitrary geometries to

$$\boldsymbol{\sigma} = (-p + \lambda \nabla \cdot \mathbf{u})\mathbf{I} + \mu(\nabla \mathbf{u} + \nabla \mathbf{u}^\intercal)$$

where λ and μ are the first and second viscosity coefficients. The first two terms account for the spherical state of stresses. Clearly, for incompressible flows, the second term vanishes.

If λ and μ are constants (or eventually dependent on the temperature) the fluid is simply referred to as *Newtonian*, however, for the so called Generalized-Newtonian fluids, these coefficients may depend locally on the invariants of the rate of deformation tensor[19]

$$\boldsymbol{\varepsilon}(\mathbf{u}) = \frac{1}{2}(\nabla \mathbf{u} + \nabla \mathbf{u}^\intercal)$$

so as the model is said to be **objective**.

19: The invariants of $\boldsymbol{\varepsilon}$ are:

$$\begin{aligned} I_1 &= \text{trace}(\boldsymbol{\varepsilon}) = \nabla \cdot \mathbf{u} \\ I_2 &= \frac{1}{2}\left(I_1^2 - \boldsymbol{\varepsilon} : \boldsymbol{\varepsilon}\right) \\ I_3 &= \det(\boldsymbol{\varepsilon}) \end{aligned}$$

1.8 Assignment 1: Warm up

To conclude this chapter you must solve the following:

Exercices

1. Consider the motion

$$\begin{aligned} x_1 &= \chi_1(\mathbf{X}, t) = X_1\, e^t \\ x_2 &= \chi_2(\mathbf{X}, t) = X_2 + t X_3 \\ x_3 &= \chi_3(\mathbf{X}, t) = X_3 - t X_2 \end{aligned}$$

   Note that, at $t = 0$ the body occupies the reference configuration , (i.e., $\mathbf{x} = \boldsymbol{\chi}(\mathbf{X}, 0) = \mathbf{X}$). Compute:

   - The inverse mapping $\boldsymbol{\chi}^{-1}$;
   - The velocity and acceleration in the referential description;
   - The velocity and acceleration in the spatial description ;

2. Let $\mathcal{V}$ be a connected volume in 3D, with boundary $\partial\mathcal{V}$. Assume that the fluid inside $\mathcal{V}$ is at constant pressure, exerting a force

$$\mathbf{F} = -p\, \check{\mathbf{n}}$$

   per unit area on $\partial\mathcal{V}$. Prove that the total force exerted by the inner fluid on the boundary is zero.

3. Let $\mathcal{V}$ be a connected region in $\mathbb{R}^d$ with boundary $\partial\mathcal{V}$. Prove that the total area/volume can be obtained from line/surface integrals:

$$\text{meas}(\mathcal{V}) = \int_{\mathcal{V}} 1\, dv = \frac{1}{d} \int_{\partial\mathcal{V}} \mathbf{x} \cdot \check{\mathbf{n}}\, ds$$

4. Complete the details that take you from the last step in Equation 1.3 to the Reynolds Transport Theorem 1.5.1.

5. In the Navier-Stokes problem in 3D (Equation 1.10), considering a Newtonian fluid with constant density and viscosity, write *in extensum* the 3 equations corresponding to each component.

6. Complete the details that take you from Equation 1.8 to Equation 1.9.

7. Consider the following **manufactured** solution in 2D for the Navier-Stokes equations:

$$\begin{aligned} \mathbf{u}(x_1, x_2, t) &= [\sin(x_1)\sin(x_2 + t),\ \cos(x_1)\cos(x_2 + t)]^\intercal\,, \\ p(x_1, x_2, t) &= \cos(x_1)\sin(x_2 + t), \end{aligned}$$

   for a Newtonian fluid with viscosity μ and density $\rho = 1$. By using the differential form of the momentum equation, compute to which body force $\mathbf{b}$ and boundary conditions it corresponds.

8. In the previous exercice, consider the region $\mathcal{V} = [0,1]^2$. Show that the manufactured solution satisfies

$$\int_{\mathcal{V}} \frac{\partial \rho}{\partial t}\, dv + \int_{\partial\mathcal{V}} \rho \mathbf{u} \cdot \check{\mathbf{n}}\, ds = 0$$

$$\int_{\mathcal{V}} \frac{\partial (\rho \mathbf{u})}{\partial t}\, dv + \int_{\partial\mathcal{V}} \rho (\mathbf{u} \otimes \mathbf{u}) \cdot \check{\mathbf{n}}\, ds = \int_{\mathcal{V}} \mathbf{b}\, dv + \int_{\partial\mathcal{V}} \boldsymbol{\sigma} \cdot \check{\mathbf{n}}\, ds$$

If necessary use a symbolic library to compute the integrals.

9. Let ψ be the *mass fraction* of some species A dispersed in a medium. The mass of this species in some volume $\mathcal{V}$ is

$$\mathcal{M}_A = \int_{\mathcal{V}} \rho\, \psi\, dv\ .$$

Derive conservation laws in differential and integral form for ψ. Also prove that

$$\frac{D\psi}{Dt} = 0\ .$$

10. Knowing that the velocity field of a rigid body motion is given by

$$\mathbf{u}(\mathbf{x}, t) = \mathbf{z}(t) + \mathbf{r}(t) \times \mathbf{x}\ ,$$

a) Prove that $\boldsymbol{\varepsilon}(\mathbf{u})$ is zero.
b) Compute the **vorticity** $\boldsymbol{\omega} = \nabla \times \mathbf{u}$ and find its relation to $\mathbf{r}$ and to the **antisymmetric part** of the velocity gradient, $\nabla^A \mathbf{u} = \frac{1}{2}\left(\nabla \mathbf{u} - \nabla \mathbf{u}^T\right)$.

11. Write the nondimensional form of the incompressible Navier-Stokes equations in terms of nondimendional variables $\hat{\mathbf{u}}$, $\hat{\mathbf{x}}$, $\hat{p}$, $\hat{t}$, $\hat{\mathbf{b}}$ and the parameter Re= $\dfrac{\rho U L}{\mu}$ (a.k.a. the Reynolds number).

12. Show Equation 1.12 from Equation 1.11 by applying the Reynolds transport theorem.

DISCRETIZATION OF SCALAR ELLIPTIC AND PARABOLIC PROBLEMS

2

2.1 The second order prototypical problem

2.1.1 Poisson's equation

The simplest second order problem we consider in this course is Poisson's equations that models several physical phenomena, such as, heat conduction, mass transport by diffusion or even fully developed flows in ducts as we will see later on in this chapter. The problem reads: Given a region $\Omega \subset \mathbb{R}^d$, $d = 1, 2$ or 3 with boundary $\partial\Omega$, find u such as

$$\begin{cases} -\nabla \cdot (\mu(\mathbf{x})\nabla u(\mathbf{x})) &= f(\mathbf{x}) \quad \mathbf{x} \in \Omega \\ u(\mathbf{x}) &= g(\mathbf{x}) \quad \mathbf{x} \in \partial\Omega \end{cases} \tag{2.1}$$

where the source term $f : \Omega \to \mathbb{R}$ is a given function and the boundary data $g : \partial\Omega \to \mathbb{R}$ is also a given function. This problem falls into the cathegory of **elliptic** problems. The scalar field u represents different physical quantities depending on the problem. Notice that if μ is a constant, the left hand side becomes the Laplace equation, i.e.,

$$\nabla \cdot (\mu(\mathbf{x})\nabla u(\mathbf{x})) = \mu \nabla^2 u(\mathbf{x}) \tag{2.2}$$

Study of this problem and its discretization is essential since this operator appears in several problems in fluid mechanics we consider throughout this course. Of importance to us is a variant of this problem which includes flux boundary conditions over all or in some part of $\partial\Omega$ (ommiting the $\mathbf{x}$ dependence for simplificity of notation)

$$\begin{cases} -\nabla \cdot (\mu \nabla u) &= f \quad \text{in } \Omega \\ u &= g \quad \text{on } \Gamma_D \\ -\mu \nabla u \cdot \check{\mathbf{n}} &= h \quad \text{on } \Gamma_N \end{cases} \tag{2.3}$$

where $\partial\Omega = \Gamma_D \cup \Gamma_N$ and $\Gamma_D \cap \Gamma_N = \emptyset$. The so called mixed formulation introduces an additional field to represent the flux of the quantity of interest

$$\begin{cases} \nabla \cdot \boldsymbol{\mathcal{J}} &= f \quad \text{in } \Omega \\ \boldsymbol{\mathcal{J}} &= -\mu \nabla u \quad \text{in } \Omega \\ u &= g \quad \text{on } \Gamma_D \\ \boldsymbol{\mathcal{J}} \cdot \check{\mathbf{n}} &= h \quad \text{on } \Gamma_N \end{cases} \tag{2.4}$$

Although both problems are equivalent in the exact setting we are focused now, in the discrete setting things may differ, distinct approaches being needed to deal with each formulation. The equation defining the relation

2.1 The second order prototypical problem 15
2.2 1st application in fluid mechanics: Fully developed flow in ducts 16
2.3 Overview of discretization methods 19
2.4 Finite difference discretization 20
2.5 Assignment 1: A *simple* finite difference (FD) code 22
2.6 Finite volume discretization 24
2.7 Assignment 2: A *not so simple* finite volume (FV) code 28
2.8 Assignment 3: Non-orthogonal meshes: A practice with OpenFOAM . 34
2.9 Finite element discretization: The Galerkin method 37
2.10 Assignment 4: A FE formulation implemented in Firedrake 41

Siméon Denis Poisson (France, 1781–1840).

Pierre-Simon Laplace (France, 1749–1827).

between $\boldsymbol{\mathcal{J}}$ and u is a **constitutive law** as we have seen. Finally, it is instructive to interpret the different quantities according to the physical problem being solved, as summarized in Table 2.1.

Table 2.1: Physical interpretation of quantities in Poisson's problem. Units in SI.

Physical problem	u	f	$\boldsymbol{\mathcal{J}}$	μ
Heat conduction	Temperature $[^\circ K]$	Heat source $[\frac{\mathrm{W}}{\mathrm{m}^3}]$	Heat flux $[\frac{\mathrm{W}}{\mathrm{m}^2}]$	Conductivity $[\frac{\mathrm{W}}{\mathrm{m}^\circ\mathrm{K}}]$
Mass diffusion	Mass $[\frac{\mathrm{mol}}{\mathrm{m}^3}]$	Mass source $[\frac{\mathrm{mol}}{\mathrm{m}^3\mathrm{s}}]$	Mass flux $[\frac{\mathrm{mol}}{\mathrm{m}^2\mathrm{s}}]$	Diffusivity $[\frac{\mathrm{m}^2}{\mathrm{s}}]$
Flow in ducts	Velocity $[\frac{\mathrm{m}}{\mathrm{s}}]$	Pressure gradient $[\frac{\mathrm{N}}{\mathrm{m}^3}]$	Shear stress [Pa]	Viscosity [Pa · s]

2.1.2 Transient Poisson's problem

The transient or unsteady version of the previous problems includes an additional term involving the rate of change of the physical quantity of interest. For the heat conduction problem with constant density and heat capacity, the equation reads

$$\begin{cases} a\,\dfrac{\partial u(\mathbf{x},t)}{\partial t} - \nabla\cdot(\mu(\mathbf{x},t)\nabla u(\mathbf{x},t)) &= f(\mathbf{x},t) \quad \mathbf{x}\in\Omega,\ \ t\in[0,T] \\ u(\mathbf{x},t) &= g(\mathbf{x},t) \quad \mathbf{x}\in\partial\Omega,\ \ t\in[0,T] \\ u(\mathbf{x},0) &= u_0(\mathbf{x}) \quad \mathbf{x}\in\Omega \end{cases} \tag{2.5}$$

where now an initial condition for the scalar unknown (e.g. the temperature) has been provided. This problem falls into the cathegory of **parabolic** problems. The parameter a in front of the time derivative has different meanings depending on the problem at hand (see Table 2.2). The different forms of this problem, such as the one with a flux boundary condition or the mixed formulation can be formulated in a similar way as in the stationary case [1].

1: Recalling from the previous chapter, in terms of conserved quantities, for each physical problem we have the following cases:

- **Heat conduction:** $\epsilon = \rho c\, u$ (Internal energy);
- **Mass difussion:** $m = \rho u$ (Amount of species);
- **Parallel flow in ducts:** $l = \rho u$ (Linear momentum).

Table 2.2: Physical interpretation of the a factor in front of $\partial_t u$ in the transient Poisson's problem. Units in SI.

Problem	Factor a	Description
Heat conduction	$\rho\, c$	$[\frac{\mathrm{Kg}}{\mathrm{m}^3}\ \frac{\mathrm{J}}{\mathrm{Kg}^\circ\mathrm{K}}]$
Mass diffusion	1	[-]
Flow in ducts	ρ	$[\frac{\mathrm{Kg}}{\mathrm{m}^3}]$

2.2 1st application in fluid mechanics: Fully developed flow in ducts

Fully developed flow in ducts is a particular case of flow governed by the Navier-Stokes equations, which corresponds to the following situation (see Figure 2.3):

- Incompressible flow in a **long** cylinder of cross section $\Omega \subset \mathbb{R}^2$. The flow domain is $b = \Omega \times (0, L)$.

- The flow is driven by a uniform pressure gradient

$$\mathcal{G}(t) = \frac{p(L,t) - p(0)}{L} \tag{2.6}$$

The pressure field is thus linear as a function of x_3. Also, notice that when $\mathcal{G}(t) > 0$ we expect $u_3 < 0$ and viceversa.

- If L is sufficiently large, the entry and exit effects can be neglected and all cross sections are essentially identical, except for the pressure.

- The flow is in principle assumed isothermal

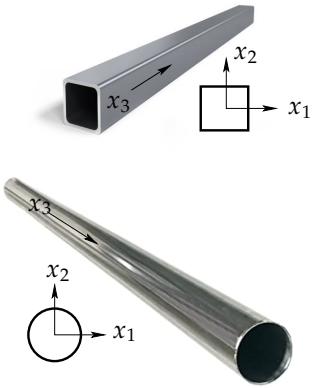

Figure 2.3: Domain for the fully developed flow.

2.2.1 Application of the conservation laws

First, consider an arbitrary region $\omega \subset \Omega$ and the corresponding cylinder

$$\mathcal{V} = \omega \times (0, L)$$

this cylinder being enclosed by

$$\partial\mathcal{V} = \omega_0 \cup \mathcal{S} \cup \omega_L$$

where ω_0 and ω_L correspond to the cylinder caps at $x_3 = 0$ and $x_3 = L$ respectively and $\mathcal{S} = \partial\omega \times (0, L)$.

Mass conservation

Recall, the mass conservation in integral form, for an arbitrary region V:

$$\int_{\mathcal{V}} \frac{\partial \rho}{\partial t}\, dv + \int_{\partial\mathcal{V}} \rho \mathbf{u} \cdot \check{\mathbf{n}}\, ds = 0$$

since ρ is assumed constant

$$0 = \int_{\partial\mathcal{V}} \mathbf{u} \cdot \check{\mathbf{n}}\, ds = \int_{\omega_0} \mathbf{u} \cdot \check{\mathbf{n}}_{\omega_0}\, ds + \int_{\omega_L} \mathbf{u} \cdot \check{\mathbf{n}}_{\omega_L}\, ds + \int_{\mathcal{S}} \mathbf{u} \cdot \check{\mathbf{n}}_{\mathcal{S}}\, ds$$

being $\check{\mathbf{n}}_{\omega_0} = -\check{\mathbf{e}}^{(3)}$ and $\check{\mathbf{n}}_{\omega_L} = \check{\mathbf{e}}^{(3)}$

$$0 = \int_{\partial\mathcal{V}} \mathbf{u} \cdot \check{\mathbf{n}}\, ds = -\int_{\omega_0} u_3\, ds + \int_{\omega_L} u_3\, ds + \int_{\mathcal{S}} \mathbf{u} \cdot \check{\mathbf{n}}_{\mathcal{S}}\, ds$$

Since $\check{\mathbf{n}}_{\mathcal{S}} \perp \check{\mathbf{e}}^{(3)}$, we see that velocity fields of the form:

$$\mathbf{u} = [0, 0, u(x_1, x_2, t)]^\intercal \tag{2.7}$$

satisfy the conservation of mass (the last term vanishing). Clearly, for any differentiable u, the proposed velocity is divergence free [2].

- Decomposing the stress tensor in pressure and non-pressure components, we have

$$\boldsymbol{\sigma}(x_1, x_2, x_3, t) = -p(x_3, t)\mathbf{I} + \boldsymbol{\sigma}^*(x_1, x_2, t)\,. \tag{2.8}$$

2: Indeed, the divergence for such velocity field is

$$\frac{\partial u_1}{\partial x_1} + \frac{\partial u_2}{\partial x_2} + \frac{\partial u_3}{\partial x_3} = \frac{\partial u}{\partial x_3} = 0$$

where, if the fluid is Newtonian ,

$$\boldsymbol{\sigma}^* = \mu \begin{pmatrix} 0 & 0 & u_{,1} \\ 0 & 0 & u_{,2} \\ u_{,1} & u_{,2} & 0 \end{pmatrix} \quad \Rightarrow \quad \boldsymbol{\tau} = \mu \nabla u \ , \tag{2.9}$$

being $\boldsymbol{\tau}$ a vector having the shear stresses as its components.

Momentum conservation

First, recall the general form

$$\frac{d}{dt}\left(\int_{\mathcal{V}} \rho\, \mathbf{u}\, dv\right) = \int_{\mathcal{V}} \mathbf{f}\, dv + \int_{\partial\mathcal{V}} [\boldsymbol{\mathcal{F}} - \rho\, (\mathbf{u} \otimes \mathbf{u}) \cdot \check{\mathbf{n}}]\, ds$$

where

- For the body force we consider $\mathbf{f} = 0$;
- For the inertial terms we have: $(\mathbf{u} \otimes \mathbf{u}) \cdot \check{\mathbf{n}} = [0, 0, u^2\, \check{n}_3]^\intercal$;
- For the surface force: $\boldsymbol{\mathcal{F}} = \boldsymbol{\sigma} \cdot \check{\mathbf{n}} = -p\check{\mathbf{n}} + \boldsymbol{\sigma}^* \cdot \check{\mathbf{n}}$.

Considering the different parts of $\partial\mathcal{V}$, we get for the 3rd component

$$\frac{d}{dt}\left(\int_{\mathcal{V}} \rho\, u\, dv\right) = \int_{\omega_0} (p(0) + \rho u^2)\, ds + \int_{\omega_L} (-p(L,t) - \rho u^2)\, ds + \\ + \int_{\mathcal{S}} \boldsymbol{\tau} \cdot \check{\mathbf{n}}_{\mathcal{S}}\, ds$$

since $|\omega_0| = |\omega_L| = |\omega|$[3]. Using Equation 2.6 yields

$$L\frac{d}{dt}\left(\int_{\omega} \rho\, u\, ds\right) = -\mathcal{G}(t) L|\omega| + L \int_{\partial\omega} \boldsymbol{\tau} \cdot \check{\mathbf{n}}_{\mathcal{S}}\, d\ell \tag{2.10}$$

3: We denote by $|\omega|$ the measure of ω (the area in this case), i.e.,

$$|\omega| = \int_{\omega} 1\, ds$$

.

- Notice that in **incompressible** and **isothermal** flow, the mass and momentum conservation laws form a closed system, i.e., no additional equations are needded.
- We can obtain the differential (or strong) form. To that end apply Gauss' theorem in the last term to arrive at

$$\int_{\omega} [\rho\, \partial_t u + \mathcal{G}(t) - \nabla \cdot (\mu \nabla u)]\, ds = 0$$

and since ω is arbitrary (using the localization theorem)

$$\rho \frac{\partial u}{\partial t} - \nabla \cdot (\mu\, \nabla u) = -\mathcal{G}(t) \quad \forall \mathbf{x} \in \Omega \ , \tag{2.11}$$

or, in conservative form, defining $\boldsymbol{\mathcal{F}}_\tau = -\boldsymbol{\tau} = -\mu \nabla u$

$$\frac{\partial}{\partial t}(\rho\, u) + \nabla \cdot \boldsymbol{\mathcal{F}}_\tau = -\mathcal{G}(t), \tag{2.12}$$

- Finally, for the boundary conditions we assume the standard

hypothesis of **no-slip**, which implies

$$u = 0 \quad \forall \mathbf{x} \in \partial\Omega \tag{2.13}$$

This means that the fluid is attached to the lateral walls of the domain, which is a physical observation valid in most of the cases[4].

4: More general conditions, such as **slip** conditions observed in rarefied flows (typically, gas flows at very small scale) can be considered as well.

- We conclude by noticing that this problem is mathematically identical to the transient heat conduction problem presented above, and in the stationary case ($\partial_t u = 0$) to the Poisson's problem. Physically, the quantity being diffused is linear momentum.

2.3 Overview of discretization methods

Among the classical numerical methods to solve PDEs arising in fluid mechanics which are of relevance to us, we have:

- **Finite differences** (FDM);
- **Finite elements** (FEM);
- **Finite volumes** (FVM);

Table 2.3 summarizes the pros and cons of each method as well as some general characteristic features of the methods. However, be aware that these are general comments that should be taken with caution. For instance, when we state a certain method has "arbitrary accuracy", this will depend on the regularity of the domain, the PDE at hand and the data (source terms, initial and boundary conditions).

Table 2.3: Pros & cons and some features of the FD, FE and FV methods.

Method	Implementation	Accuracy	Geometry	BCs	Based on
FDM	very simple	arbitrary (regular grids)	limited	simple	approximate differential operators
FEM	moderately simple	arbitrary	arbitrary	simple	Variational principle
FVM	simple on regular grids, difficult on general grids	generally limited to 1st or 2nd order	arbitrary	difficult	Conservation principle

Now, to have a glance on how these methods work, we embark in the task of solving the problem of fully develop flow in ducts in its differential form (Equation 2.11) by the finite difference method, in variational form by the finite element method and in the integral form (Equation 2.10) by the finite volume method.

2.4 Finite difference discretization

We consider a pipe with rectangular cross section defined by

$$\Omega = [0, L_1] \times [0, L_2]$$

and a Cartesian grid with (n_1, n_2) divisions of uniform spacings $(h_1, h_2) = (L_1/n_1, L_2/n_2)$ in each direction, the nodes being at positions

$$\mathbf{x}_{i_1,i_2} = [i_1 h_1, i_2 h_2]$$

(see Figure 2.4)[5]. We define the number of points in each direction $N_i = n_i + 1$ and the total number of points in the grid $N_p = N_1 \times N_2$.

5: Notice that, since we will be using `python` for implementation, we consider the indices starting in 0.

The starting point for the discretization by a finite difference is the differential problem Equation 2.11. In the sequel we assume further that both, the density ρ and viscosity μ are constants. The ideia is to find an approximate solution at each grid point $\mathbf{x}_{i_1 i_2}$ and time t, i.e.,

$$u(\mathbf{x}_{i_1,i_2}, t) \approx U_{i_1,i_2}(t)$$

If the point $\mathbf{x}_{i_1,i_2}$ is in the set of boundary nodes

$$\mathcal{N}_b = \{(i_1, i_2) \text{ s.t. } i_1 = 0 \text{ or } i_1 = N_1 - 1 \text{ or } i_2 = 0 \text{ or } i_2 = N_2 - 1\}$$

we simply set

$$U_{i_1 i_2}(t) = 0$$

so as to obey the Dirichlet boundary condition, otherwise, if it is in the set of interior nodes, we approximate the viscous operator at the point $\mathbf{x}_{i_1,i_2}$ and time t by a second order finite difference formula

$$\mathcal{L}_\mu(u(\mathbf{x},t))|_{\mathbf{x}_{i_1,i_2}} = -\mu \nabla^2 u(\mathbf{x},t)|_{\mathbf{x}_{i_1,i_2}} = -\mu \left[\frac{\partial^2 u(\mathbf{x},t)}{\partial x_1^2} + \frac{\partial^2 u(\mathbf{x},t)}{\partial x_2^2} \right]_{\mathbf{x}_{i_1,i_2}} \approx$$

$$\approx -\mu \frac{U_{i_1+1,i_2}(t) - 2\,U_{i_1,i_2}(t) + U_{i_1-1,i_2}(t)}{h_1^2} - \mu \frac{U_{i_1,i_2+1}(t) - 2\,U_{i_1,i_2}(t) + U_{i_1,i_2-1}(t)}{h_2^2}$$

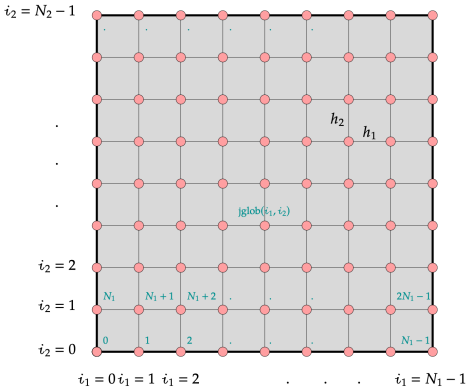

Figure 2.4: Finite difference grid.

Implementation aspects and Time discretization

The previous discretization leads to a linear system of equations which relates the $N_p = N_1 \times N_2$ velocity values and that must be assembled. To that end, it is convenient to define a mapping so as to associate to each pair (i_1, i_2) a unique global index

$$j_g = \text{jglob}(i_1, i_2)$$

thus giving

$$U_{i_1,i_2}(t) = \mathsf{U}_{\text{jglob}(i_1,i_2)}(t) = \mathsf{U}_{j_g}(t), \;\; j_g = 0, \ldots, (N_p - 1), \; i_1 = 0, \ldots, (N_1 - 1), \; i_2 = 0, \ldots, (N_2 - 1)$$

The local-to-global map can be for instance as follows:

$$j_g = i_1 + i_2\, N_1$$

```
def jglob(i1, i2, N1):
    jg = i1 + i2*N1
    return jg
```

although other numberings are possible[6].

6: We could alternatively number the points as

$$j_g = i_2 + i_1\, N_2$$

We must also discretize in time. We consider a partition of the time interval $[0, T]$ into N steps of uniform size $\Delta t = T/N$, i.e.,

$$0 = t_0 < t_1 < \cdots < t_N = T, \quad t_n = n\,\Delta t$$

and consider

$$\mathsf{U}_{j_g}(t_n) \approx \mathsf{U}^n_{j_g}$$

so, at some arbitrary time $t_{n+\theta} = (1-\theta)\,t_n + \theta\, t_{n+1}$, $\theta \in [0,1]$, the discrete viscous operator takes the form:

$$\mathcal{L}_\mu(u(\mathbf{x},t))\big|_{(\mathbf{x}_{j_g}, t_{n+\theta})} \approx -\frac{\mu}{h_1^2}\left(\mathsf{U}^{n+\theta}_r - 2\,\mathsf{U}^{n+\theta}_{j_g} + \mathsf{U}^{n+\theta}_\ell\right) - \frac{\mu}{h_2^2}\left(\mathsf{U}^{n+\theta}_t - 2\,\mathsf{U}^{n+\theta}_{j_g} + \mathsf{U}^{n+\theta}_b\right)$$

where

$$\left.\begin{array}{rcl} r &=& \mathrm{jglob}\,(i_1+1 \;,\; i_2\;\;) \\ \ell &=& \mathrm{jglob}\,(i_1-1 \;,\; i_2\;\;) \\ t &=& \mathrm{jglob}\,(i_1\;\;\;\; ,\; i_2+1) \\ b &=& \mathrm{jglob}\,(i_1\;\;\;\; ,\; i_2-1) \end{array}\right\} \tag{2.14}$$

We must also provide an approximation for the time derivative of u in Equation 2.11, for which we consider a finite difference (in time) formula that is applied throughout the time step, from t_n until t_{n+1}

$$\rho\,\frac{\partial u}{\partial t}\bigg|_{(\mathbf{x}_{j_g}, [t_n, t_{n+1}])} \approx \rho\,\frac{\mathsf{U}^{n+1}_{j_g} - \mathsf{U}^n_{j_g}}{\Delta t}$$

If all the discrete values of u on the underlying grid and at time index n, are arranged into a column vector $\mathbf{U}^n \in \mathbb{R}^{N_p}$,

$$\mathbf{U}^n = \begin{bmatrix} \mathsf{U}^n_0 \\ \mathsf{U}^n_1 \\ \cdot \\ \cdot \\ \cdot \\ \mathsf{U}^n_{N_p-1} \end{bmatrix}$$

the scheme can be written as

$$\frac{\rho}{\Delta t}\left(\mathbf{U}^{n+1} - \mathbf{U}^n\right) + \mathbb{A}\,\mathbf{U}^{n+\theta} = -\mathcal{G}(t_{n+\theta})\,\mathbf{b} \tag{2.15}$$

where $\mathbf{U}^{n+\theta} = (1-\theta)\,\mathbf{U}^n + \theta\,\mathbf{U}^{n+1}$ and $\mathbb{A} \in \mathbb{R}^{N_p \times N_p}$ is the matrix, which in row $j_g = \mathrm{jglob}(i_1, i_2)$, corresponding to an internal node, has entries

$$\begin{cases} a_{j_g\, j_g} &= \dfrac{2\mu}{h_1^2} + \dfrac{2\mu}{h_2^2} \\ a_{j_g\, r} = a_{j_g\, \ell} &= -\dfrac{\mu}{h_1^2} \\ a_{j_g\, t} = a_{j_g\, b} &= -\dfrac{\mu}{h_2^2} \end{cases}$$

with the column indices defined as in Equation 2.14, whereas for points belonging to the set of boundary nodes, we have

$$a_{j_g\, j_c} = \begin{cases} 1 & \text{if } j_g = j_c \\ 0 & \text{otherwise} \end{cases}$$

This is essentially a penta-diagonal matrix, except for a few lines that are stolen from the identity matrix $\mathbb{I}_{N_p \times N_p}$. Lastly, $\mathbf{b} \in \mathbb{R}^{N_p}$ is a vector with all its components equal to 1, if they correspond to an interior node and zero otherwise.

2.5 Assignment 1: A *simple* finite difference (FD) code

Consider a pipe of rectangular cross section $(0, W) \times (0, H)$ and length L. Consider water as the fluid with density $\rho = 1000$ kg/m^3 and viscosity $\mu = 10^{-3}$ Pa-s. Take $W = 20$ microns, $H = 10$ microns and $L = 3$ mm.

1. Show that Equation 2.15 can be written as:

$$\left(\frac{\rho}{\Delta t}\mathbb{I} + \theta\, \mathbb{A}\right) \mathbf{U}^{n+1} = \left(\frac{\rho}{\Delta t}\mathbb{I} - (1-\theta)\, \mathbb{A}\right) \mathbf{U}^{n} - \mathcal{G}(t_{n+\theta})\, \mathbf{b}$$

2. Program a `python` script that implements the above FD scheme. Program a function to save the solution in `vtk` format that can be visualized in `Paraview`.
   In order to assembly the finite difference matrix, consider the following two alternatives:
   - Looping over the points and setting each row individually

```
from scipy import sparse

def AssemblyMatLoop(N1,N2, ...):
    nunk = N1*N2;
    A = np.zeros(shape=(nunk,nunk))
    h1, h2 = ...
    ...
    for i1 in range(1,N1-1):
        for i2 in range(1,N2-1):
            jg = jglob(i1,   i2,  N1)
            jr = jglob(i1+1, i2,  N1)
            jl = jglob(i1-1, i2,  N1)
            .
            .
    return sparse.csr_matrix(A)
```

In the code above for simplicity we create a *dense* matrix and then convert to *sparse* format, however, it would be better to preallocate a sparse matrix directly by setting the symbolic structure and corresponding coefficients using e.g., `sparse.coo_matrix` or as suggested in the next item:

- Constructing a pentadiagonal matrix directly. The following code may be useful:

```
from scipy.sparse import diags

def AssemblyMatDiags(N1,N2, ...):
    nunk = N1*N2
    h1, h2 = ...
    ...
    d1 =  np.ones(nunk)  * ( ... )
    d2 = -np.ones(nunk-1)* ( ... )
    d3 = -np.ones(nunk-N)* ( ... )
    return diags([d3,d2,d1,d2,d3], [-N1,-1,0,1,N1])
```

Compare the two approaches in terms of computational efficiency.

3. Consider non-slip boundary conditions at all walls. Apply a pressure gradient $\mathcal{G}(t) = \cos(2\pi\, t/T_G)$, in which T_G is a given period. Consider values of $\theta = 0,\ 0.5$ and 1. Plot the solution in `Paraview`. Extract profiles of the velocity field along lines.

4. Provide a discrete formula to compute the flow rate

$$Q = \int_\Omega \mathbf{u}\cdot\check{\mathbf{e}}_3\, dv = \int_\Omega u\, dv$$

and compute Q as a function of time. Plot the results for the different values of θ considered in the previous item. Determine the phase difference with respect to $\mathcal{G}(t)$. Consider $\mu = 10^{-2}$ and $\mu = 10^{-4}$ and repeat the calculations.

5. Prepare a short report/presentation.

2.6 Finite volume discretization

The starting point for a finite volume discretization is Equation 2.10. We subdivide the computational domain Ω into non-overlapping cells or **finite volumes**. The first thing to decide is how to construct this partition. For simple geometries we naturally use *structured* meshes, whereas for more complicated geometries we rely on *unstructured* meshes. We must also specify to which geometrical location to associate the unknowns. This leads to Vertex-centered and Cell-Centered approximations, which are illustrated in Figure 2.5. Let begin with the structured case for simplicity to introduce the ideas of the finite volume method. The unstructured case will be presented later on.

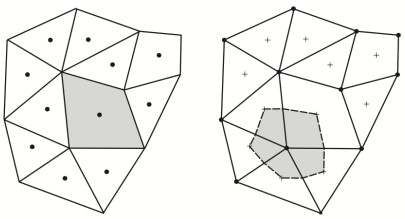

Figure 2.5: Examples of cell-centered and vertex-centered finite volume meshes.

2.6.1 Structured case - Orthogonal meshes

We consider a cell-centered cartesian finite volume discretization of the domain $\Omega = [0, L_1] \times [0, L_2]$ as shown in Figure 2.6. into $N_c = n_1 \times n_2$ non-overlapping rectangles that conform a covering of Ω. We distinguish between cell values (located at the centroid of the cell) and face values (located at the centroid of the face) and introduce the following notation. We denote the finite volumes by the letter K

$$K_{i_1,i_2} = (x_{i_1}, x_{i_1+1}) \times (y_{i_2}, y_{i_2+1})$$

the centroids being located at

$$\hat{\mathbf{x}}_{i_1,i_2} = (\hat{x}_{i_1,i_2},\ \hat{y}_{i_1,i_2}) = \left(\frac{x_{i_1} + x_{i_1+1}}{2},\ \frac{y_{i_2} + y_{i_2+1}}{2}\right)$$

so, we allow for variable spacing.

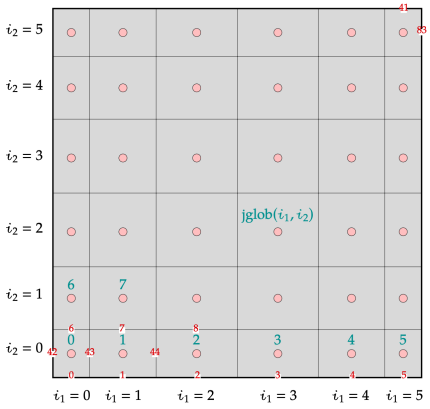

Figure 2.6: Cell-centered structured cartesian grid showing the numbering of cells and faces.

The local-to-global map of the cells, that associates a unique (global) index to each pair (i_1, i_2) is the same as in the finite difference case, so for each finite volume cell we have[7]

$$K_{i_1,i_2} = K_g, \quad g = i_1 + i_2\, n_1$$

The accuracy of the method depends on the assumed variation for the unknown field. If we consider a Taylor expansion inside cell K_g

$$u(\mathbf{x}, t) = u(\hat{\mathbf{x}}_g, t) + \left[\nabla u(\hat{\mathbf{x}}_g, t)\right] \cdot \left(\mathbf{x} - \hat{\mathbf{x}}_g\right) \ + \ \text{h.o.t.}, \quad \mathbf{x} \in K_g \tag{2.16}$$

so, if we discard the h.o.t., we expect to end up with a second order accurate method. Notice that

$$\int_{K_g} u(\mathbf{x})\, dv = |K_g|\, u(\hat{\mathbf{x}}_g) \tag{2.17}$$

where $|K_g|$ is the measure (area in 2D) of the cell, given in this simple case by

$$|K_g| = \underbrace{(x_{i_1+1} - x_{i_1})}_{\Delta x_g}\ \underbrace{(y_{i_2+1} - y_{i_2})}_{\Delta y_g}$$

7: Notice that the cell index is denoted by a lowercase caligraphic letter (e.g., g, r, ℓ, t, b).

We aim to write a discrete set of equations to approximate u, such that

$$u(\hat{\mathbf{x}}_g, t) \approx U_g(t)$$

Now, let recall the conservation of linear momentum principle for the problem under consideration, applied to each finite volume cell K_g

$$L\frac{d}{dt}\left(\int_{K_g} \rho\, u\, dv\right) \;=\; -\mathcal{G}(t)\, L\, |K_g| \;+\; L\int_{\partial K_g} \boldsymbol{\tau}\cdot\check{\mathbf{n}}_{\partial K_g}\, d\ell \tag{2.18}$$

the factor L obviously cancels out. In Equation 2.18, $d\ell$ stands for the differential of arc in the 2D case we are dealing with. The last term is in turn written as a sum over the faces of K_g

$$\int_{\partial K_g} \boldsymbol{\tau}\cdot\check{\mathbf{n}}_{\partial K_g}\, d\ell = \sum_{f\in\partial K_g}\int_f \boldsymbol{\tau}_f\cdot\check{\mathbf{n}}_f\, d\ell$$

so, we need an estimate of the momentum flux $\boldsymbol{\tau} = \mu\,\nabla u$ at cell faces. To that end consider auxiliary values u_f located at the centroid (or midpoint) of cell faces. Based on Equation 2.16, an approximation is thus given by

$$\boldsymbol{\tau}_f\cdot\check{\mathbf{n}}_f = -\mu_f\,\frac{U_g(t) - u_f(t)}{d_{gf}}$$

where d_{gf} is the distance between the centroid of g and the midpoint of f, i.e.[8],

$$d_{gf} = \begin{cases} \Delta x_g/2 & \text{if } f \text{ is a vertical face} \\ \Delta y_g/2 & \text{if } f \text{ is a horizontal face} \end{cases}$$

8: Notice that the face index is denoted by a lowercase press letter (e.g., f, r, l, t, b).

We group the set of faces between internal faces $\mathcal{E}_{\text{int}}$ and boundary faces $\mathcal{E}_\partial$. If the face $f \in \mathcal{E}_\partial$ we set $u_f = 0$ so as to obey the Dirichlet condition. For an internal face shared by two cells, K_g and K_n, we realize that the flux should be the same when approaching $\mathbf{x}_f$ from either cell, i.e.[9],

9: The time dependence has been omitted here for simplicity of notation.

$$-\mu_f\,\frac{U_g - u_f}{d_{gf}} = \mu_f\,\frac{U_n - u_f}{d_{nf}}$$

Eliminating, we obtain for u_f

$$u_f = \frac{U_g\, d_{nf} + U_n\, d_{gf}}{d_{gf} + d_{nf}} \tag{2.19}$$

that can be eliminated[10], to obtain

10: In the jargon, we also say that u_f is being statically condensed.

$$\boldsymbol{\tau}_f\cdot\check{\mathbf{n}}_f = -\mu_f\frac{U_g - U_n}{d_{gn}} \tag{2.20}$$

where d_{gn} is the distance between the cell centroid of g and the centroid of its neighbor cell K_n, i.e., $\frac{\Delta x_g + \Delta x_n}{2}$ if they share a vertical face or $\frac{\Delta y_g + \Delta y_n}{2}$ if they share a horizontal face. Notice that if μ is a function of $\mathbf{x}$, its face value is simply that function evaluated at $\mathbf{x}_f$, i.e., $\mu_f = \mu(\mathbf{x}_f)$. Finally, for

the transient term we write, recalling density is constant

$$L\frac{d}{dt}\left(\int_{K_g}\rho\,u\,dv\right) = L\,\rho\,|K_g|\frac{dU_g(t)}{dt}\bigg|_{[t_n,t_{n+1}]} \approx L\,\rho\,|K_g|\frac{U_g^{n+1}-U_g^n}{\Delta t}$$

Now, we are in position to write the equation for finite volume cell K_n. We begin with the so called **mixed formulation** in which we treat fluxes and cell values as unknowns, i.e. for cell g we have

$$\left[\begin{aligned} \mathsf{J}_{\tau,r} &= \mu_r\frac{U_g^{n+\theta}-u_r^{n+\theta}}{d_{gr}} \\ \mathsf{J}_{\tau,l} &= \mu_l\frac{U_g^{n+\theta}-u_l^{n+\theta}}{d_{gl}} \\ \mathsf{J}_{\tau,t} &= \mu_t\frac{U_g^{n+\theta}-u_t^{n+\theta}}{d_{gt}} \\ \mathsf{J}_{\tau,b} &= \mu_b\frac{U_g^{n+\theta}-u_b^{n+\theta}}{d_{gb}} \\ \rho\,|K_g|\frac{U_g^{n+1}-U_g^n}{\Delta t} &+ (\mathsf{J}_{\tau,r}+\mathsf{J}_{\tau,l})\,\Delta y_g + (\mathsf{J}_{\tau,t}+\mathsf{J}_{\tau,b})\,\Delta x_g = -\mathcal{G}(t_{n+\theta})\,|K_g| \end{aligned}\right.$$

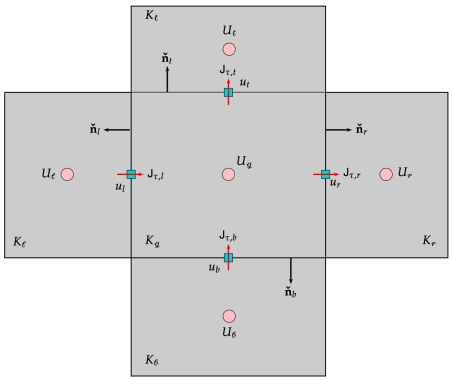

Figure 2.7: Cells and unknowns involved in the momentum balance for finite volume cell K_g.

This formula is written in terms of the local fluxes and serves both, cells having sides in $\mathcal{E}_\partial$, for which the corresponding value $u_f^{n+\theta}$, $f = r,l,t,b$ is prescribed and cells having faces in $\mathcal{E}_{\text{int}}$ for which the value is given by Equation 2.19. In fact, substituting J_τ in the last expression and using Equation 2.20, for a cell having all its faces in $\mathcal{E}_{\text{int}}$ we obtain the so called **primal formulation**

$$\rho\,|K_g|\frac{U_g^{n+1}-U_g^n}{\Delta t}+\left(\mu_r\frac{U_g^{n+\theta}-U_r^{n+\theta}}{d_{gr}}+\mu_l\frac{U_g^{n+\theta}-U_\ell^{n+\theta}}{d_{g\ell}}\right)\Delta y_g+\left(\mu_t\frac{U_g^{n+\theta}-U_t^{n+\theta}}{d_{gt}}+\mu_b\frac{U_g^{n+\theta}-U_b^{n+\theta}}{d_{gb}}\right)\Delta x_g = -\mathcal{G}(t_{n+\theta})\,|K_g|$$

from which the matrix form is more or less obvious based on our previous experience with finite differences. The matrix form of the mixed formulation requires an additional effort, since we need a global numbering of the flux unknowns.

First, let introduce a numbering of the of the face fluxes J_τ of which we have:

- $N_h = n_1 \times (n_2+1)$ horizontal faces;
- $N_v = n_2 \times (n_1+1)$ vertical faces;

giving in total $N_f = N_h + N_v$. We can enumerate first the horizontal faces

$$f_h(k_1,k_2) = k_1 + k_2 n_1, \quad k_1 \in [0, n_1-1],\ k_2 \in [0, n_2]$$

followed by the vertical ones

$$f_v(k_1,k_2) = n_1(n_2+1) + k_1 + k_2(n_1+1), \quad k_1 \in [0, n_1],\ k_2 \in [0, n_2-1]$$

At this point it is convenient to introduce a **cell-to-face** connectivity, which for finite volume cell $g = \text{jglob}(i_1,i_2)$ can be for instance

$$\text{CF}[\,g,:\,] = [\,f_h(i_1,i_2),\ f_v(i_1+1,i_2),\ f_h(i_1,i_2+1),\ f_v(i_1,i_2)\,]$$

and a **face-to-cell** connectivity, such as

$$\mathrm{FC}[\, f, :\,] = [\, g(f),\ n(f)\,]$$

where

- If $f = f_h(k_1, k_2),\ k_1 \in [0, n_1 - 1],\ k_2 \in [0, n_2]$

$$[g(f), n(f)] = \begin{cases} (\mathrm{jglob}(k_1, k_2),\ -1) & \text{if} \quad k_2 = 0 \\ (\mathrm{jglob}(k_1, k_2 - 1),\ \mathrm{jglob}(k_1, k_2)) & \text{if} \quad k_2 \in [1, n_2 - 1] \\ (\mathrm{jglob}(k_1, k_2 - 1),\ -3) & \text{if} \quad k_2 = n_2 \end{cases}$$

- If $f = f_v(k_1, k_2),\ k_1 \in [0, n_1],\ k_2 \in [0, n_2 - 1]$

$$[g(f), n(f)] = \begin{cases} (\mathrm{jglob}(k_1, k_2),\ -2) & \text{if} \quad k_1 = 0 \\ (\mathrm{jglob}(k_1 - 1, k_2),\ \mathrm{jglob}(k_1, k_2)) & \text{if} \quad k_1 \in [1, n_1 - 1] \\ (\mathrm{jglob}(k_1 - 1, k_2),\ -4) & \text{if} \quad k_1 = n_1 \end{cases}$$

Notice that the first index is always a valid index (i.e. greater or equal than zero) and the second index may be a negative number that indicates to which wall the face belongs (bottom: -1, right: -2, top: -3, left: -4)[11].

11: This numbering of the walls is unused in the current context, since the same homogeneous Dirichlet boundary conditions is being applied at all walls, however, it may be useful if the boundary value differs at each wall, as it may be the case if solving a heat transfer problem.

The vector of unknowns has now two parts

$$\mathbf{X}^n = \begin{bmatrix} \mathbf{J}_\tau^n \\ \\ \mathbf{U}^n \end{bmatrix}, \quad \mathbf{J}_\tau^n = \begin{bmatrix} \mathsf{J}_0^n \\ . \\ . \\ . \\ \mathsf{J}_{N_f-1}^n \end{bmatrix} \in \mathbb{R}^{N_f}, \quad \mathbf{U}^n = \begin{bmatrix} \mathsf{U}_0^n \\ . \\ . \\ . \\ \mathsf{U}_{N_c-1}^n \end{bmatrix} \in \mathbb{R}^{N_c}$$

and the corresponding matrix is given by blocks as

$$\begin{bmatrix} \mathbb{O} & \mathbb{O} \\ \\ \mathbb{O} & \mathbb{M} \end{bmatrix} \begin{bmatrix} \mathbf{J}_\tau^{n+1} \\ \\ \mathbf{U}^{n+1} \end{bmatrix} + \begin{bmatrix} \mathbb{K}^{-1} & -\mathbb{A} \\ \\ \mathbb{C} & \mathbb{O} \end{bmatrix} \begin{bmatrix} \mathbf{J}_\tau^{n+1} \\ \\ \mathbf{U}^{n+\theta} \end{bmatrix} = \begin{bmatrix} \mathbb{O} & \mathbb{O} \\ \\ \mathbb{O} & \mathbb{M} \end{bmatrix} \begin{bmatrix} \mathbf{J}_\tau^{n} \\ \\ \mathbf{U}^{n} \end{bmatrix} + \begin{bmatrix} \mathbf{g}^{n+1} \\ \\ \mathbf{b}^{n+\theta} \end{bmatrix}$$

where

- $\mathbb{M} \in \mathbb{R}^{N_c \times N_c}$ is diagonal with elements

$$m_{gg} = \frac{\rho |K_g|}{\Delta t}$$

- $\mathbb{K} \in \mathbb{R}^{N_f \times N_f}$ is diagonal with elements

$$k_{ff} = \frac{\mu_f}{d_f}$$

  where d_f is given by

$$d_f = \begin{cases} d_{\mathrm{FC}[f,0]\,\mathrm{FC}[f,1]} & \text{if} \quad \mathrm{FC}[\, f, 1] \geq 0 \\ \\ d_{\mathrm{FC}[f,0]\, f} & \text{if} \quad \mathrm{FC}[\, f, 1] < 0 \end{cases}$$

i.e., if f is an internal face, we take the distance between the centroids of the two cells sharing the face, otherwise, if f is located over the boundary, we take the distance between the cell centroid to which it belong and the corresponding boundary face.

- $\mathbb{A} \in \mathbb{R}^{N_f \times N_c}$ having elements

$$a_{fg} = \begin{cases} +1 & \text{if } g = \text{FC}[f, 0] \\ -1 & \text{if } g = \text{FC}[f, 1] \geq 0 \\ 0 & \text{otherwise} \end{cases}$$

- $\mathbb{C} \in \mathbb{R}^{N_c \times N_f}$ having elements

$$c_{gf} = \begin{cases} +s_f & \text{if } f = \text{CF}[g, :] \text{ and } g = \text{FC}[f, 0] \\ -s_f & \text{if } f = \text{CF}[g, :] \text{ and } g \neq \text{FC}[f, 0] \\ 0 & \text{otherwise} \end{cases}$$

where s_f is the size of the corresponding face (if it is a face of cell g, $s_f = \Delta x_g$ if horizontal and Δy_g otherwise).

Remark

In the mixed formulation presented above we can simply eliminate the fluxes as unknowns. This is actually left as an exercise below. In the current context, no gain is obtained by using such formulation, however, we have done it mainly for didactical reasons and because it is the starting point for other more general formulations.

2.7 Assignment 2: A *not so simple* finite volume (FV) code

Consider the same pipe of the previous assignment, the finite volume formulation above and the script `FV_mixed.py`.

1. In the context of our finite volume method, explain Equation 2.17. Also, explain why the following is true:

$$\int_f u(\mathbf{x})\, d\ell = s_f\, u(\hat{\mathbf{x}}_f)$$

where s_f is the measure of the face f and $\hat{\mathbf{x}}_f$ is the location of its midpoint.

2. Read the script carefully and identify the different ingredients involved in the formulation.

3. Test the implementation on different finite volume grids repeating the calculations of the previous assignment. Consider:

- Grids with uniform spacing h_1 and h_2. In this simple case, write the finite volume formulation to see how it looks and compare to the finite difference formulation of the previous assignment.
- Grids locally refined near the walls and coarsened near the center of the domain. Consider different transitions from the fine to the coarse cells.
- Explain, how the code would be adapted to solve the problem on a pipe with irregular geometry (e.g., circular cross section).
- Plot the velocity field in `Paraview` and extract profiles along lines to compare the results on different grids. A typical result on a square domain is shown in Figure 2.8. For the sake of comparison we also show the finite difference result obtained with the formulation of the previous assignment.
- Considering a small case, visualize the symbolic structure of the matrix using the command `plt.spy`. Notice the symmetry relations between the block $\mathbb{A}$ and $\mathbb{C}$.
- **Graduate students:** How would you use this code to impose a homogeneous boundary condition in the flux unknown on some part of the boundary? Explain.
- (**Bonus**): Implement the previous item.

4. **Graduate students:** Eliminate the fluxes as unknowns (at the algebraic level) and implement the primal formulation. Test the implementation.
5. In the mixed formulation, implement the case of a variable viscosity coefficient

$$\mu(x_1, x_2) = \mu_0 + \mu_0 e^{-50\left[\frac{(x_1-0.5L_1)^2}{L_1^2}+\frac{(x_2-0.5L_2)^2}{L_2^2}\right]}$$

   where μ_0 takes the values considered in the previous assignment.
6. (**Bonus**): Write a vertex-centered finite volume formulation of the same problem. Explain how it differs with the one above and with the finite difference formulation to as the treatment of boundary conditions.
7. Prepare a short report/presentation.

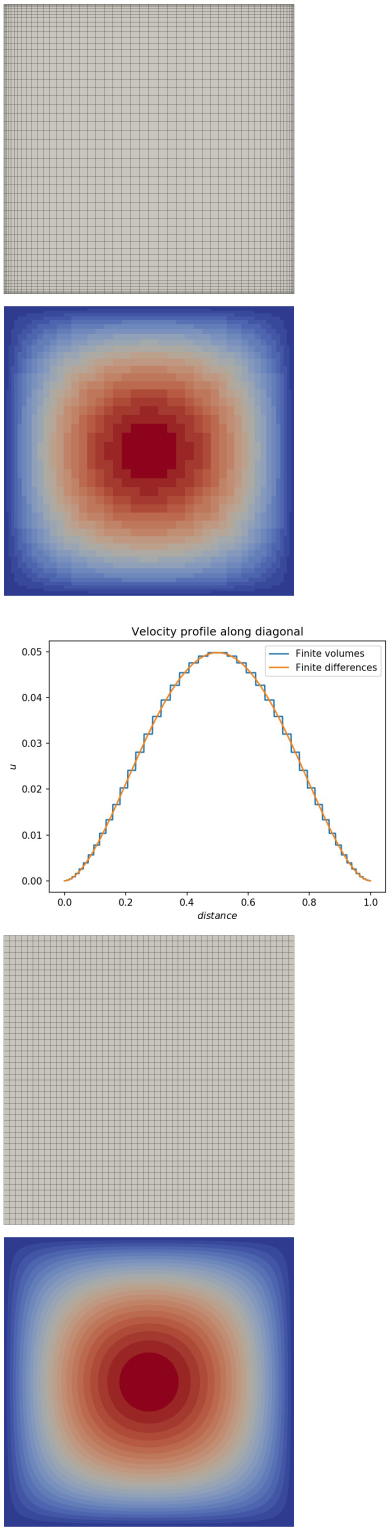

Figure 2.8: Comparison of the finite volume (on a locally refined grid) and the finite difference formulation on a square domain.

2.7.1 Unstructured case - Non-orthogonal meshes

So far we have been dealing with structured orthogonal meshes. This clearly simplifies things a lot. The need for unstructured general meshes

is quite obvious when we are faced to solve a problem on irregular geometries. Examples of such meshes were shown in Figure 2.5. Notice, that an interesting aspect of the finite volume method, with respect to the finite element method, is that dealing with *mixed-meshes* (i.e., meshes that mixture cells of different geometrical shape) is relatively simpler to code.

Rigorous numerical analysis of the finite volume method on arbitrary geometries and meshes can rapidly become too tecnhical. A comprehensive text is [6]. There, a scheme similar to the previous finite volume method, is derived for more general orthogonal meshes that satisfy the definition of **finite volume admissible mesh** :

[6]: Eymard et al. (2003), *Finite Volume Methods*

Definition 2.7.1 (***Finite volume admissible mesh***) *Let Ω be an open bounded polygonal domain in $\mathbb{R}^d$ ($d = 2$ or 3). An admissible finite volume mesh $\mathcal{T}_h$ is a family of open polygonal/polyhedral (in 2D/3D) control volumes, a set of edges/faces (in 2D/3D) denoted by $\mathcal{E}_h$, with strictly $d-1$ measure and a set of points, denoted by $\mathcal{P}_h$ that satisfies:*

- *The closure of the union of all the K_q's of $\mathcal{T}_h$ is $\bar{\Omega}$;*
- *For any K_q of $\mathcal{T}_h$, there is a $\mathcal{E}_{K_q} \subset \mathcal{E}_h$, $\partial K_q = \bar{K}_q \setminus K_q = \bigcup_{f \in \mathcal{E}_{K_q}} \bar{f}$;*
- *For any pair of finite volumes K_q and K_n of $\mathcal{T}_h$, either $\bar{K}_q \cap \bar{K}_n$ is empty or a complete edge/face, i.e., $\bar{K}_q \cap \bar{K}_n = \bar{\sigma}$;*
- *The set of points $\mathcal{P}_h = \{\mathbf{x}_q\}$ is such that $\mathbf{x}_q \in \bar{K}_q$ and if f is a face shared by control volumes K_q and K_n, then $\mathbf{x}_q \neq \mathbf{x}_n$ and the straight line $\mathbf{d}_{qn}$ going from $\mathbf{x}_q$ to $\mathbf{x}_n$ is orthogonal to f;*
- *If the face f of a control volume K_q is on the boundary (i.e., $f \in \partial\Omega$), the orthogonal line to f passing through $\mathbf{x}_q$ intersects f.*

This definition looks pretty restrictive on the type of grids. However, convergence of FV schemes can be shown for such class of meshes.

Unfortunately, orthogonal meshes are an exception in computational mechanics. In most cases we have to deal with **mesh non-orthogonality** and **skewness errors** (see Figure 2.9): this is the topic to be discussed now. The idea is to present an overview of some numerical and implementation aspects involved in such cases. We restrict ourselves to the treatment of diffusive terms, which is the main topic in this chapter. Other terms usually appearing in CFD, such as convective terms, need a separate discussion. So, let us begin with the expression for the diffusive part in Equation 2.18

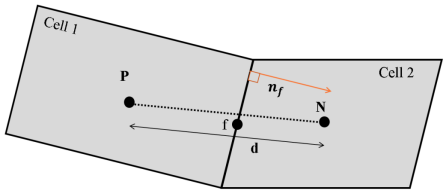

Figure 2.9: Non-orthogonal and skew mesh.

$$\int_{\partial K_q} \boldsymbol{\tau} \cdot \check{\mathbf{n}}_{\partial K_q} \, d\ell = \sum_{f \in \partial K_q} \int_f \boldsymbol{\tau}_f \cdot \check{\mathbf{n}}_f \, d\ell = \sum_{f \in \partial K_q} s_f \, [\mu \nabla u]_f \cdot \check{\mathbf{n}}_f$$

where s_f is the measure of the face[12]. We seek for an approximation of the face value $[\nabla u]_f \cdot \check{\mathbf{n}}_f$. The key point is how to discretize the diffusion term when the cells are non-orthogonal, i.e., the line joining the centroids of two adjacent finite volume cells is not parallel to the face normal $\check{\mathbf{n}}_f$ as illustrated in Figure 2.10. The normal vector admits and additive

12: The measure of the face corresponds to the length in 2D or the area in 3D.

decomposition

$$\check{\mathbf{n}}_f = \mathbf{n}_d + \mathbf{n}_\delta$$

such that

$$[\nabla u]_f \cdot \check{\mathbf{n}}_f = [\nabla u]_f \cdot \mathbf{n}_d + [\nabla u]_f \cdot \mathbf{n}_\delta \tag{2.21}$$

where $\mathbf{n}_d$ is a vector parallel to the line joining g and n, which we denote by $\mathbf{d}_{gn} = \mathbf{x}_n - \mathbf{x}_g$, whose Euclidean norm we denote by $\|\mathbf{d}_{gn}\| = d_{gn}$ and $\check{\mathbf{n}}_\delta$ is the residual vector, i.e.[13],

$$\mathbf{n}_\delta = \check{\mathbf{n}}_f - \mathbf{n}_d$$

There are infinitely many decompositions. Three commonly used in CFD softwares are:

- **Method 1:** Compute the projection of $\mathbf{n}_f$ onto $\mathbf{d}_{gn}$:

$$\mathbf{n}_d = \frac{\mathbf{d}_{gn} \cdot \check{\mathbf{n}}_f}{d_{gn}^2} \mathbf{d}_{gn}$$

- **Method 2:** Define $\mathbf{n}_d$ as a unit vector along $\mathbf{d}_{gn}$:

$$\mathbf{n}_d = \frac{\mathbf{d}_{gn}}{d_{gn}}$$

- **Method 3:** Compute the projection of $\mathbf{n}_d$ onto $\mathbf{n}_f$

$$\mathbf{n}_d = \frac{\mathbf{d}_{gn}}{\check{\mathbf{n}}_f \cdot \mathbf{d}_{gn}} = \frac{1}{\cos\theta_f} \frac{\mathbf{d}_{gn}}{d_{gn}}$$

Once we have done this, we can approximate the first term in Equation 2.21 by

$$[\nabla u]_f \cdot \mathbf{n}_d = \|\mathbf{n}_d\| \frac{U_n - U_g}{d_{gn}}$$

So, the final approximation reads

$$[\nabla u]_f \cdot \check{\mathbf{n}}_f = \|\mathbf{n}_d\| \frac{U_n - U_g}{d_{gn}} + \underbrace{[\nabla u]_f \cdot \mathbf{n}_\delta}_{\text{cross-diffusion}} = \|\mathbf{n}_d\| \frac{U_n - U_g}{d_{gn}} + [\nabla u]_f \cdot (\check{\mathbf{n}}_f - \mathbf{n}_d) \tag{2.22}$$

Generally, the first term is treated implicitly, so the values of U_g and U_n are taken at time $n+1$, whereas the second term is treated explicitly, taking the value of $[\nabla u]_f$ at the known time n, or iteratively, by executing *non-orthogonal correction* steps, i.e.[14],

$$[\nabla u]_f^{n+1,k+1} \cdot \check{\mathbf{n}}_f = \|\mathbf{n}_d\| \frac{U_n^{n+1,k+1} - U_g^{n+1,k+1}}{d_{gn}} + [\nabla u]_f^{n+1,k} \cdot \mathbf{n}_\delta, \quad k = 1, 2, \ldots$$

in any case the cross-diffusion term will appear in the right-hand-side of the system as a source term.

But, we still need an estimate for $[\nabla u]_f$ in order to compute the so called **cross-diffusion** term. In turn, several options are at our disposal, which we comment in the sequel.

13: Notice that the vectors $\mathbf{n}_d$ and $\mathbf{n}_\delta$ are not necessarily unitary.

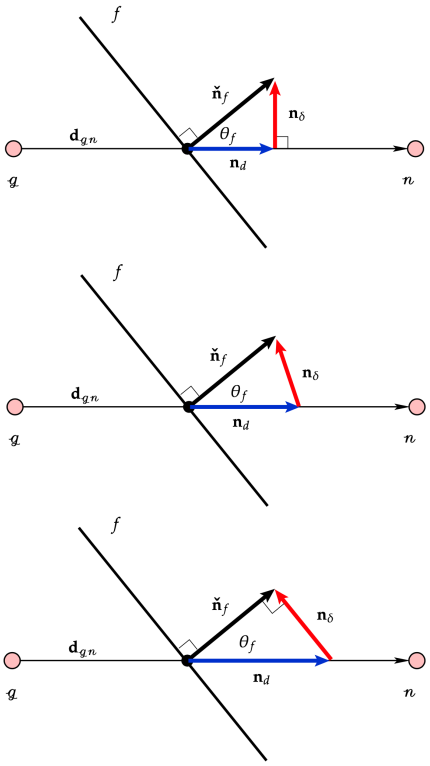

Figure 2.10: Additive decomposition of $\check{\mathbf{n}}_f$: Method 1 (top), Method 2 (middle), Method 3 (bottom).

14: Notice that, if the non-orthogonal correction term becomes too large, as it would be the case in bad quality meshes ($\theta_f \gtrsim 70°$), the method may exhibit instabilities. For this reason, this correction is sometimes limited.

2.7.2 Gradient recovery

Recall that in our cell-centered finite volume formulation the primary variables are stored at cell centroids. This is also the case for majority of software used in the industry, such as `Fluent` or `OpenFOAM`. We thus need a way to estimate the gradient of quantities at other locations, such as nodes (or vertices) and, in particular faces.

Green-Gauss methods

First, recall the vector identity[15]

$$\int_{K_g} \nabla u \, dv = \int_{\partial K_g} u \, \check{\mathbf{n}}_{\partial K_g} \, d\ell = \sum_{f \in \partial K} \int_f u \, \check{\mathbf{n}}_f \, d\ell \tag{2.23}$$

and from the assumed linear variation for u inside the control volume, we obtain an expression for the gradient at cell-centroids in terms of face values

$$[\nabla u]_g = \frac{1}{|K_g|} \sum_{f \in \partial K_g} s_f \, u_f \, \check{\mathbf{n}}_f \tag{2.24}$$

Now, in order to compute the face values u_f we need and interpolation. One reasonable alternative is to compute u_f by interpolating the two cell values

$$u_f \approx \alpha_g \, U_g + \alpha_n \, U_n \tag{2.25}$$

where α_g and α_n are taken to be the normalized inverse distances from g and n to the intersection of the line segment between g and n and the face f (see Figure 2.11), i.e.,

$$\alpha_g = \frac{d_{gf}^{-1}}{d_{gf}^{-1} + d_{nf}^{-1}} = \frac{d_{nf}}{d_{gn}}, \qquad \alpha_n = \frac{d_{nf}^{-1}}{d_{gf}^{-1} + d_{nf}^{-1}} = \frac{d_{gf}}{d_{gn}}$$

This is the cell-based Green-Gauss method. The method leads to an error for non-orthogonal meshes since the intersection point (the black dot) does not necessarily coincide with the midpoint of the face (the cyan square). This is known as a **skewness error**, which is, in fact, an integration error. The effect is more severe as the mesh gets more distorted.

An alternative that circumvents this skewness error, is the node-based Green-Gauss method, which consists in estimating the face values of u by averaging the vertex values. Referring to Figure 2.12, if we denote by nodes(f) the set of mesh vertices connected by face f (the blue dots), the face value is simply[16]

$$u_f = \frac{1}{n_v} \sum_{v \in \text{nodes}(f)} \mathcal{U}_v$$

and the vertex values $\mathcal{U}_v$'s are in turn computed by averaging the cell values (the pink dots, which are the actual unknowns of the problem), i.e.,

$$\mathcal{U}_v = \frac{1}{\mathcal{N}_c} \sum_{c \in \text{cells}(v)} U_c \tag{2.26}$$

15: The identity is proved by applying Gauss theorem to the vector field $u \, \check{\mathbf{e}}^{(i)}$ to obtain

$$\int_K \nabla \cdot (u \, \check{\mathbf{e}}^{(i)}) \, dv = \int_{\partial K} u \, (\check{\mathbf{e}}^{(i)} \cdot \check{\mathbf{n}}) \, d\ell$$

Therefore giving

$$\int_K \frac{\partial u}{\partial x_i} \, dv = \int_{\partial K} u \, \check{n}_i \, d\ell$$

from which Equation 2.23 yields.

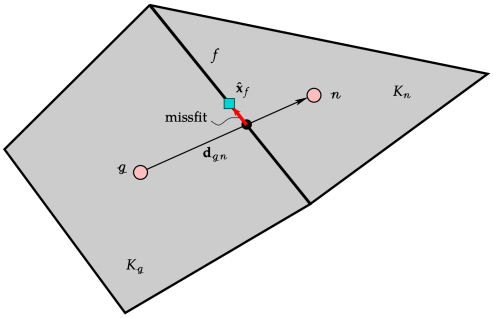

Figure 2.11: Linear interpolation to find an approximation for u_f and associated skewness error.

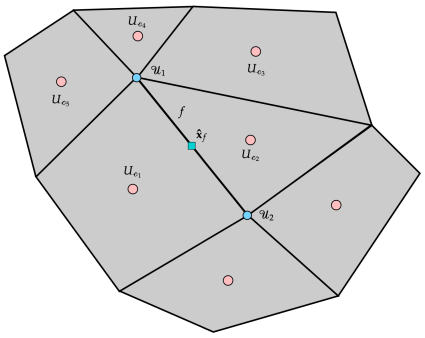

Figure 2.12: Computation of nodal values and face values based on cell values.

16: Notice that in 2D a face (an edge) is always defined by two vertices (i.e., $n_v = 2$), but in 3D, a face may be a polygonal with arbitrary number of points.

where $\mathcal{N}_c$ is the number of cells that share vertex c, which can be arbitrary on general meshes. This method avoids the skewness error, however notice that, the computational cost is slightly higher. Also, more sophisticated schemes, rather than the arithmetic mean Equation 2.26, could be used to compute the vertex values.

Least square method

This method does not make use of the identity Equation 2.23. Consider Figure 2.13. For each cell g in the grid, consider all its neighbours n_i, $i = 1, \dots, \mathcal{N}$, such that, by extrapolating the linear behavior from g to the different neighboring cells, we obtain

$$\begin{aligned} U_{n_1} &= U_g + [\nabla u]_g \cdot \mathbf{d}_{gn_1} \\ U_{n_2} &= U_g + [\nabla u]_g \cdot \mathbf{d}_{gn_2} \\ &\dots \\ U_{n_\mathcal{N}} &= U_g + [\nabla u]_g \cdot \mathbf{d}_{gn_\mathcal{N}} \end{aligned}$$

In order to obtain $[\nabla u]_g = [u_{,1}, u_{,2}]_g^\intercal$, we must solve the following overdetermined system

$$\underbrace{\begin{bmatrix} \leftarrow & \mathbf{d}_{gn_1}^\intercal & \rightarrow \\ \leftarrow & \mathbf{d}_{gn_2}^\intercal & \rightarrow \\ . & . & . \\ . & . & . \\ \leftarrow & \mathbf{d}_{gn_\mathcal{N}}^\intercal & \rightarrow \end{bmatrix}}_{\mathbb{D} \in \mathbb{R}^{\mathcal{N} \times 2}} \begin{bmatrix} u_{,1} \\ u_{,2} \end{bmatrix}_g = \begin{bmatrix} U_{n_1} - U_g \\ U_{n_2} - U_g \\ . \\ . \\ U_{n_\mathcal{N}} - U_g \end{bmatrix} \tag{2.27}$$

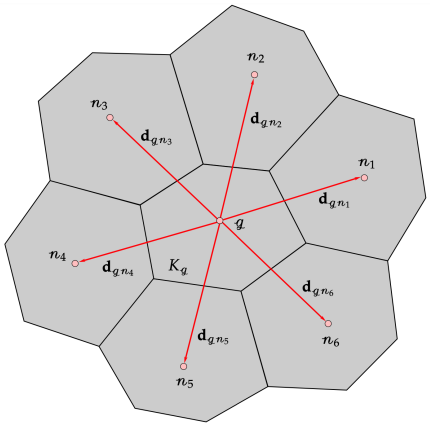

Figure 2.13: Finite volume cell and its neighbours for the least square computation of $[\nabla u]_g$.

The generalization to 3D is straightforward. This overdetermined algebraic problem is solved in the least square sense, either by the normal equations or by the QR factorization of the matrix[17]. In the former case, the square system to be solved reads

$$\mathbb{D}^\intercal \, \mathbb{D} \, [\nabla u]_g = \mathbb{D}^\intercal \, \delta \mathbf{U}$$

where $\delta \mathbf{U}$ is the vector in the rhs of Equation 2.27. Recall that the least square solution in the case above considers the standard Euclidean norm, so it minimizes the norm of the residual $\mathbf{r} = \mathbb{D} \, [\nabla u]_g - \delta \mathbf{U}$

$$\| \mathbb{D} \, [\nabla u]_g - \delta \mathbf{U} \|_2 = \| \mathbf{r} \|_2 = \sqrt{\mathbf{r}^\intercal \mathbf{r}}$$

however, notice that we could choose a generalized inner product

$$\| \mathbf{r} \|_\mathbb{W} = \sqrt{\mathbf{r}^\intercal \, \mathbb{W} \, \mathbf{r}}$$

where $\mathbb{W} \in \mathbb{R}^{\mathcal{N} \times \mathcal{N}}$ is a symmetric positive definite matrix[18]. This allows us to assign weights to each equation, which is a common practice on highly stretched grids (as the one shown in Figure 2.8), so as to assign larger weights to points in the direction perpendicular to the wall, with respect to points in the other direction. In such case the set o normal equations reads

$$\mathbb{D}^\intercal \mathbb{W} \mathbb{D} \, [\nabla u]_g = \mathbb{D}^\intercal \mathbb{W} \delta \mathbf{U} \tag{2.28}$$

17: Recall from our numerical analysis course that the method based on QR factorization is in general more stable than the normal equations. This is expected to affect on some pathological cases, involving highly stretched meshes.

18: Typically, $\mathbb{W}$ is chosen to be a diagonal matrix with positive coefficients

Having the gradients of u at the cell-centroids at our disposal, whether obtained by one method or another, namely, the Green-Gauss or the Least square, we end up computing a weighted average of the cell values shared by the face, i.e.,

$$[\nabla u]_f \approx \alpha_g [\nabla u]_g + \alpha_n [\nabla u]_n \tag{2.29}$$

This last interpolation does not involve a skewness error (Explain why?). Finally, additional references that may be consulted are [7, 8]

[7]: Versteeg et al. (2007), *An Introduction to Computational Fluid Dynamics. The finite volume method.*
[8]: Jasak (1996), 'Error Analysis and Estimation for the Finite Volume Method with Applications to Fluid Flows'

2.8 Assignment 3: Non-orthogonal meshes: A practice with `OpenFOAM`

2.8.1 The `openFOAM` platform

In this last assignment we will use the famous open source CFD Toolbox `OpenFOAM`[19]. There are currently two main branches of `OpenFOAM`, of which we will use `https://www.openfoam.com/` (please, pay attention to the `.com` at the end!).

19: `FOAM` is an acronism for Field Operation And Manipulation

- For installation refer to the Download tab in the site above. Detailed instructions for different platforms being available. For some linux distibuitions go to `openFOAM:Debian-Ubuntu`.

- The assignment is based on the `scalarTransportFoam` tutorial, available in the `OpenFOAM` repository. You can download from Tidia a `ZIP` archive containing the case files, including some pre-built meshes using the open source software `https://gmsh.info/`.

The problem to be solved is:

Find $T : \Omega \times [t_i, t_f] \longrightarrow \mathbf{R}$ such that

$$\frac{\partial T}{\partial t} + \nabla \cdot (\mathbf{U}\, T) - \nabla \cdot (\mu \nabla T) = f \quad \text{in } \Omega\,,$$

where

- Ω is the parallelogram shown in Figure 2.14;
- $T = 0$ on $\partial\Omega$;
- $\mu = f = 0.01$;
- $\mathbf{U} = \mathbf{0}$.

Notice that, what we have called u in the previous assignments, is now being called T and $\mathbf{U}$ is now the convective velocity, which is taken to be identically zero, so the problem is formally identical to the ones solved before, except for the right hand side which is assumed constant in time for simplicity.

- The following files inside the main directory `NonOrth-example/` are important:
  - `Allrun.pre`: Pre-processing script

- `Allrun`: Solution script
- `paraFoam`: Post-processing script
- `0/T`: Sets the initial and boundary conditions
- `system/controlDict`: Specifies parameters such as the time step, initial and final time, output frequency, etc.
- `system/fvSchemes`: Sets the temporal and spatial discretization options, such as the gradient and laplacian schemes, the interpolation, etc.
- `system/fvSolution`: Specifies the linear solver options and the number of **non-orthogonal corrector** steps

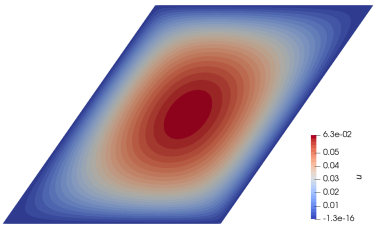

Figure 2.14: Reference solution obtained by the FEM on a very fine mesh to be used for comparison with `OpenFOAM` results.

To run a case, type the following commands in a terminal at the location of your case files:

```
NonOrth-example> cp grids/xxx.msh domain.msh
NonOrth-example> ./Allrun.pre
NonOrth-example> rm log.scalarTransportFoam
NonOrth-example> ./Allrun
NonOrth-example> paraFoam
```

Notice that the first and second steps are necessary only the first time you run the case on a new mesh. The different meshes are located in the directory `grids`[20].

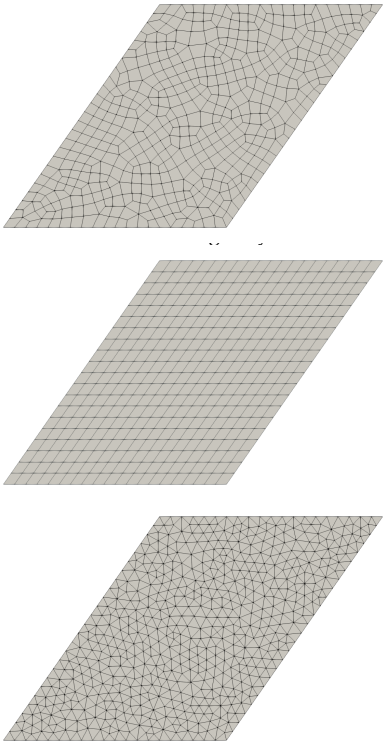

Figure 2.15: Finite volume grids M1c, M2c, M3c (coarser level) to be used in `OpenFOAM`.

1. Discuss the examples of admissible meshes in [6] (pag. 39) and the connections with the definition given above.

2. In the main directory `NonOrth-example/`, there are 3 types of finite volume grids (M1, M2, M3) and two levels of refinement for each (c: coarse and f: fine), so as to assess the accuracy of the numerical scheme (see Figure 2.15). The first step is to solve the **steady state** problem directly, by setting the appropriate parameters in `system/fvSchemes`. Visualize and compare the solution using `paraFoam`. As a reference solution consider the file `fempoisson.xdmf`, that was obtained by a finite element method on a very fine mesh (see Figure 2.14).

3. Consider the following options for the treatment of the non-orthogonal terms in `system/fvSchemes`:

```
gradSchemes
{
    default         xxx;
}

laplacianSchemes
{
    default         none;
    laplacian(DT,T) Gauss linear yyy;
}
```

where xxx in `gradSchemes` specifies the method to compute the gradient at cell centes:

- `Gauss linear`: Green-Gauss cell based with linear interpolation to find the values u_f (Equation 2.24);
- `Gauss pointLinear`: Green-Gauss node based (Equation 2.26)
- `leastSquares`: least square method (Equation 2.28);

For the `laplacianSchemes` the keyword `Gauss` (the only available choice for such) means that for the diffusive term, Gauss theorem is being applied, `linear` refers to the interpolation used to estimate μ_f (μ at cell faces) and `yyy` refers to the treatment of the (explicit) non-orthogonal terms, which can be for instance:

- `orthogonal`: No correction at all;
- `uncorrected`: One single correction;
- `corrected`: Several corrections
- `limited` ψ (with ψ taking values 0.333 or 0.5): limited non-orthogonal correction

Finally, we can increase the number of non-orthogonal corrector sweps

```
SIMPLE
{
    nNonOrthogonalCorrectors xxx;
}
```

where xxx is the number times the correction is applied[21].

Assess the behavior of the various options given above on the different meshes by comparing the solution to the reference one.

4. Solve the **transient** problem from $t = 0$ until $t = 4$. Compare the solution at several times, considering different grids and discretization options so as to assess how the non-orthogonality errors accumulates in a transient case. To that end modify `system/fvSchemes` to set the integration scheme to

```
ddtSchemes
{
    default         none;
    ddt(T)          CrankNicolson xxx;
}
```

21: The `corrected` option applied a sufficient number of times should provide the best results.

where `xxx` can be set to 0 (Euler) or 1 (Crank-Nicolson). Also set the `endTime` parameter in `system/controlDict` to a larger value so as to be able to reach the steady state solution. Compare to previous results.

5. Create the case of circular geometry with radius $R = 0.5$. There are examples of `.geo` files for `gmsh` to create the geometry and mesh. Be aware that you will need to adapt other files such as `0/T` to correctly identify the boundaries of the domain.

2.9 Finite element discretization: The Galerkin method

The starting point for the finite element discretization of the problem under consideration is the differential form Equation 2.11, from which we will arrive at the so called **variational formulation**. Complete technical details are left for a finite element course. We will now proceed quite informally to gain some insight on how the method works so as to compare to the other methods being studied. To cast this problem into variational form, we multiply by a sufficiently regular **test** function w that satifies the boundary condition, i.e.,

$$w(\mathbf{x}) = 0 \quad \forall \mathbf{x} \in \partial\Omega \tag{2.30}$$

and integrate over Ω

$$\int_\Omega \rho \frac{\partial u}{\partial t}\, w\, dv - \int_\Omega \left[\nabla \cdot (\mu\, \nabla u)\right]\, w\, dv = \int_\Omega f\, w\, dv \tag{2.31}$$

where we have defined $f(t) = -\mathcal{G}(t)$. Now, we use the identity

$$\nabla \cdot [(\mu \nabla u)\, w] = [\nabla \cdot (\mu \nabla u)]\, w + (\mu \nabla u) \cdot \nabla w$$

We thus have

$$\int_\Omega \rho \frac{\partial u}{\partial t}\, w\, dv + \int_\Omega (\mu\, \nabla u) \cdot \nabla w\, dv - \int_\Omega \nabla \cdot [(\mu \nabla u)\, w]\, dv = \int_\Omega f\, w\, dv \tag{2.32}$$

For the third term in the left hand side we apply Gauss theorem

$$\int_\Omega \nabla \cdot [(\mu \nabla u)\, w]\, dv = \int_{\partial\Omega} w\, (\mu \nabla u) \cdot \check{\mathbf{n}}\, ds \tag{2.33}$$

which is identically zero by Equation 2.30, yielding[22]

$$\int_\Omega \rho \frac{\partial u}{\partial t}\, w\, dv + \int_\Omega \mu\, \nabla u \cdot \nabla w\, dv = \int_\Omega f\, w\, dv \tag{2.34}$$

This is valid **for any** $w : \Omega \to \mathbb{R}$ belonging to some space of functions (say $V(\Omega)$) that satisfy the homogeneous boundary condition at $\partial\Omega$, for which the integrals in the left and right hand sides at least don't blow up. We may formally write the weak[23] form of the problem

22: What we have done is also called integration by parts.

23: The problem is said to be in **weak** form because in this formulation we require less differentiability from u in contrast to the PDEs in **strong** form for which we require u to have at least continuous second order derivatives if we pretend the equation to be satisfied pointwise.

Weak (or variational) formulation

Find $u \in V(\Omega)$ such that

$$\begin{cases} \underbrace{\int_\Omega \rho\, \partial_t u\, w\, dv}_{(\rho\, \partial_t u, w)_{L^2(\Omega)}} + \underbrace{\int_\Omega \mu\, \nabla u \cdot \nabla w\, dv}_{a(u,w)} = \underbrace{\int_\Omega f\, w\, dv}_{\ell(w)} \\ \\ \forall w \in V(\Omega). \end{cases} \tag{2.35}$$

David Hilbert (Germany, 1862–1943).

What appear in the lhs is the bilinear form $a(\cdot,\cdot)$ and the $L^2(\Omega)$ scalar product $(\cdot,\cdot)_{L^2(\Omega)}$ (which is also a bilinear form), whereas in the rhs we have a linear form $\ell(\cdot)$.

The correct functional setting to solve this problem is provided by the the space

$$V(\Omega) = H_0^1(\Omega) = \left\{ w \in H^1(\Omega) : w|_{\partial\Omega} = 0 \right\}.$$

where $H^1(\Omega)$ is the Hilbert space[24]

$$H^1(\Omega) = \left\{ w : \Omega \to \mathbb{R} : \int_\Omega w^2\, dx < +\infty \text{ and } \int_\Omega (\nabla w \cdot \nabla w)\, dx < +\infty \right\}$$

24: A Hilbert space is a vector space equipped with an inner product, that is also a complete metric space with respect to the norm induced by the inner product.

This means, we seek a solution in a space of square integrable functions whose derivatives are also square integrable, a reasonable requirement by looking at the terms we are trying to integrate in the linear and bilinear forms above.

The Galerkin method

Boris Galerkin (Russia, 1871-1945).

The idea of the Galerkin method is simple: replace the infinite dimensional space V by a discrete subspace $V_h \subset V$, where the parameter $h > 0$ in the finite element method is related to the refinement of a partition of Ω (the mesh), such that $h \to 0$ as the dimension of the space $N \to \infty$. Considering for a moment the **stationary** case for simplicity, we replace the original continuous formulation by a discrete variational formulation: Find $u_h \in V_h$ such that

$$a(u_h, w_h) \quad = \quad \ell(w_h) \quad \forall\, w_h \in V_h \tag{2.36}$$

Now, we define $u_h \in V_h$ by

$$u_h(\mathbf{x}) = \sum_{j=1}^{N} U_j\, \psi_j(\mathbf{x}) \tag{2.37}$$

The interesting thing about the Galerkin method is that it provides the **methodology** to compute u_h. If we choose a basis $\{\psi_1, \psi_2, \ldots, \psi_N\}$ of V_h, replace the Equation 2.37 and take $w_h = \psi_i$ in Equation 2.36, we obtain

$$a\left(\sum_{j=1}^{N} U_j \psi_j, \psi_i \right) = \sum_{j=1}^{N} \underbrace{a(\psi_j, \psi_i)}_{A_{ij}} U_j = \underbrace{\ell(\psi_i)}_{b_i}, \quad i = 1, \ldots, N \tag{2.38}$$

which is clearly a linear system of equations

$$\mathbb{A}\,\mathbf{U} = \mathbf{b} \tag{2.39}$$

where $\mathbf{U} = [U_1, U_2, \ldots, U_N]^\intercal$, $\mathbb{A} \in \mathbb{R}^{N\times N}$ and $\mathbf{b} \in \mathbb{R}^N$ are defined by

$$A_{ij} = a(\psi_j, \psi_i) = \int_\Omega \left(\mu\,\nabla\psi_j\right)\cdot\nabla\psi_i\,dv, \quad b_i = \ell(\psi_i) = \int_\Omega f\psi_i\,dv. \tag{2.40}$$

About matrix $\mathbb{A}$ we can say:

- Since $a(v,w) = a(w,v)\ \forall v, w \in V$ (i.e., $a(\cdot,\cdot)$ is symmetric), clearly $\mathbb{A}$ is also symmetric;
- if $a(w,w) > 0\ \forall w \in V$ (then, $(\cdot,\cdot)$ is said to be strongly coercive[25]), taking any arbitrary nonzero $w_h = \sum_{j=1}^N W_j\,\psi_j$ and defining $\mathbf{W} = [W_1, W_2, \ldots, W_N]^\intercal$, we get

$$a\left(\sum_{j=1}^N W_j\psi_j, \sum_{i=1}^N W_i\psi_i\right) = \sum_{i=1}^N\sum_{j=1}^N W_i\,A_{ij}\,W_j = \mathbf{W}^\intercal\mathbb{A}\mathbf{W} > 0,\ \ \mathbf{W}\neq\mathbf{0} \tag{2.41}$$

  thus, $\mathbb{A}$ is positive definite and therefore **invertible**, so, we can safely solve the system and find the unique $\mathbf{U}$ that defines u_h.

25: Strong coercivity is also referred to as V-ellipticity. For the bilinear form at hand, it can be shown this property holds.

The question that arises is how to construct a discrete space. The typical choice is to construct piecewise polynomial spaces associated to a **conforming partition** (a finite element mesh) of the computational domain, i.e.,

$$V_h = \{w \in C^0(\bar\Omega),\ \ w|_K \in P_k(K)\ \ \forall K \in \mathcal{T}_h\}$$

where $P_k(K)$ is the space of polynomials of degree k on K. For instance, for $k = 1$ in 2D we have the classical *hat* nodal functions on 3-node triangular elements illustrated in Figure 2.18.

$$P_1(K) = \{p : K \to \mathbb{R},\ p = \alpha + \beta x + \gamma\, y\}$$

With these local functions, a global nodal base $\{\psi_1, \ldots, \psi_n\}$, can be constructed, such that there is one function for each vertex (node) of the mesh. Any piecewise linear function can be written as a linear combination of such functions. They are constructed such that the delta Kronecker property holds, i.e.,

$$\psi_i(\mathbf{x}_j) = \delta_{ij}$$

These are called *Lagrangian* elements. Similarly, in 3D, for 4-node tetrahedral elements we have

$$P_1(K) = \{p : K \to \mathbb{R},\ p = \alpha + \beta x + \gamma\, y + \delta\, z\}$$

By looking at the basis functions illustrated in Figure 2.18, we notice that they have **compact support**, i.e, they are different than zero only in the cluster of elements shared by a given node, thus leading to a sparse matrix $\mathbb{A}$. For completness, the definition of a finite element conforming mesh is:

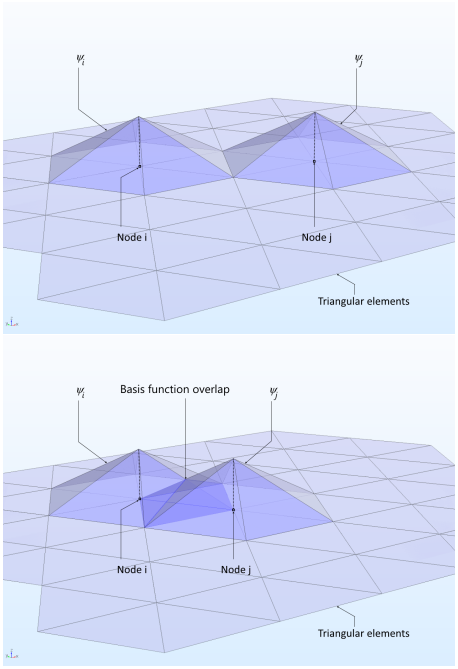

Figure 2.18: Examples of P_1 basis functions associated to the nodes of a 2D triangular mesh. Source: https://https://www.comsol.com/.

Definition 2.9.1 *A partition $\mathcal{T}_h$ of a domain Ω is* ***conforming*** *if $\bar{K}_i \cap \bar{K}_j$ is either*

- *empty, or,*
- *a vertex, or*
- *a complete edge.*
- *a complete face (in 3D)*

otherwise the partition is said to be ***nonconforming****.*

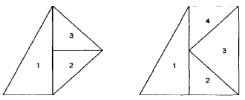

Figure 4.1. *Two examples of nonconforming triangulations. In both examples, the intersection of triangles 1 and 2 is a line segment that is not an edge of triangle 1.*

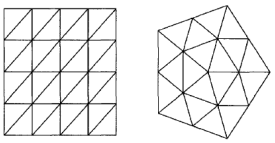

Figure 4.2. *Triangulations of two polygonal domains.*

Figure 2.19: Conforming vs. nonconforming partitions of Ω.

In the general **transient** case we write:

$$u_h(\mathbf{x}, t) = \sum_{j=1}^{N} U_j(t)\, \psi_j(\mathbf{x}) \tag{2.42}$$

and proceed similarly. We replace into the complete variational problem, so for the inertial term we have

$$\left(\sum_{j=1}^{N} \partial_t U_j(t)\, \psi_j, \psi_i \right)_{L^2(\Omega)} = \sum_{j=1}^{N} \dot{U}_j(t) \left(\psi_j, \psi_i \right)_{L^2(\Omega)} = \sum_{j=1}^{N} M_{ij} \partial_t U_j(t), \quad i = 1, \ldots, N$$

where

$$\dot{U}_j(t) = \partial_t U_j(t) = \frac{\partial U_j(t)}{\partial t}$$

and the *mass* matrix $\mathbb{M}$ has coefficients[26]

$$M_{ij} = \left(\psi_j, \psi_i \right)_{L^2(\Omega)} = \int_\Omega \psi_j\, \psi_i \, dv$$

26: Notice that the matrix $\mathbb{M}$ will also be sparse, however, as with the FDM and the FVM, this matrix is not diagonal.

As with the other methods we write

$$\mathsf{U}_j^n \approx U_j(t_n) \quad \text{and} \quad \left. \frac{\partial U_j(t)}{\partial t} \right|_{[t_n, t_{n+1}]} \approx \frac{\mathsf{U}_j^{n+1} - \mathsf{U}_j^n}{\Delta t}$$

and put all the unknowns into a column vector

$$\mathbf{U}^n = \begin{bmatrix} \mathsf{U}_1^n \\ \mathsf{U}_2^n \\ \cdot \\ \cdot \\ \cdot \\ \mathsf{U}_N^n \end{bmatrix}$$

so as the method in matrix form reads

$$\frac{\rho}{\Delta t} \mathbb{M} \left(\mathbf{U}^{n+1} - \mathbf{U}^n \right) + \mathbb{A}\, \mathbf{U}^{n+\theta} = f(t_{n+\theta})\, \mathbf{b} \tag{2.43}$$

Depending on how the FEM is implemented, the resulting matrizes and right hand side vector may need to be adapted so as to obey the Dirichlet boundary condition, i.e.,

$$u(\mathbf{x}_i, t_n) = \mathsf{U}_i^n = 0, \quad \mathbf{x}_i \in \partial\Omega, \quad n = 0, 1, \ldots$$

2.10 Assignment 4: A FE formulation implemented in `Firedrake`

2.10.1 The `Firedrake` platform

We will use the finite element library `Firedrake` to solve the fully developed flow in a circular pipe of radius R and with center at the origin. We consider as usual $u = 0$ on $\partial\Omega$ and $f = 1$, $\rho = 1000$ and $\mu = 0.001$.

You need first to install the library. I suggest to follow the instructions in `Firedrake` which generally work well in Linux systems. Other alternative would be to use `FEM on Colab`, which offers installations of the `Firedrake` library through `google colab`.

1. Read the script carefully to identify the different sections, in particular, the mesh creation and variational formulation.

2. Run the script by setting the mesh refinement parameter `Lc` to different values. Consider the stationary case by setting `flag_only_linear_steady = True`

3. Compare the solution to the finite volume case obtained in the previous assignment in the stationary case.

4. An interesting thing about the finite element method is that nonlinearities can be dealt easily, specially when using a library like `FEniCS` or `Firedrake`, which are capable of performing automatic differentiation. As an example, we consider the flow in the circular pipe with a nonlinear viscosity, i.e., we solve the following discrete variational problem in **residual form**: Given an initial condition u_h^0, find $u_h^{n+1} \in V_h$, $n = 0, 1, \ldots$ such that

$$\mathcal{R}(u_h^{n+1}) = \int_\Omega \rho \frac{u_h^{n+1} - u_h^n}{\Delta t} w_h \, dv + \\ + \int_\Omega \left[\mu + \mu_t(u_h^{n+\gamma})\right] \nabla u_h^{n+\theta} \cdot \nabla w_h \, dv - \int_\Omega f \, w_h \, dv = 0$$

forall $w_h \in V_h$. Notice that, we have already discretized in time and the unknown is u_h^{n+1}. The viscosity μ_t is defined by the relation

$$\mu_t(u) = \rho \, l^2(\mathbf{x}) \sqrt{\nabla u \cdot \nabla u}$$

where

$$\frac{l(\mathbf{x})}{R} = 0.14 - 0.08 \left(\frac{r}{R}\right)^2 - 0.06 \left(\frac{r}{R}\right)^4$$

with $r = \sqrt{x_1^2 + x_2^2}$ the distance to the origin. The parameter γ can be set to 0 so as to linearized the problem[27] or can be set to $\theta > 0$ to have the full nonlinear problem. In the latter case, the problem is solved by a Newton-Raphson scheme and the `Firedrake` library computes the Jacobian of the system $\partial\mathcal{R}/\partial u$ automatically, as needed. Solve the problem and plot the solu-

27: In this case, it is expected that the time step should be fine enough to avoid instabilities.

tion in `paraview`. Extract profiles of the velocity field along lines.

5. (**Bonus**) Solve the problem of fully developed flow in a pipe of annular cross section, with internal radius $r_i = 0.3$ and external radius $r_e = 0.5$. Consider the linear and stationary case. Compare the solution to the analytical one:

$$u(r) = \frac{f}{4\mu}\left[r_e^2 - r^2 + \frac{r_e^2 - r_i^2}{\ln(r_i/r_e)}\ln\left(\frac{r_e}{r}\right)\right]$$

(Use the script `annular_pipe_flow.py`). By adding the following line to the code, compute the flow rate:

```
.
Q = assemble (u * dx)
.
```

and compare to the exact value.

NUMERICAL SOLUTION OF POTENTIAL FLOWS

3

3.1 Prelude

"When a flow is both frictionless and irrotational, pleasant things happen."

– F.M. White [2]

The simplistic structure of potential flows, being inviscid and irrotational, allows the construction of analytical solutions. This subject is well explored in traditional fluid mechanics books, such as [1] and [2]. In this chapter, however, this simple model is used to introduce the full discretization by the finite volume method, including the correct treatment of different boundary conditions and numerical techniques to solve the resulting nonlinear algebraic problem.

3.1 Prelude 43
3.2 Potential functions 43
3.3 Incompressible potential flows 43
3.4 Stream functions 45
3.5 Potential lines and streamlines 47
3.6 Bernoulli's equation . . . 47
3.7 Slightly compressible potential flows 48
3.8 Finite-volume discretizations 50
3.9 Assignment: Implementation of an incompressible potential flow 53
3.10 Discretization of the compressible model . . . 53
3.11 Assignment 2: Nonlinear potential flow 57

[1]: Kundu et al. (2008), *Fluid Mechanics, Fourth Edition*

[2]: White (2011), *Fluid Mechanics, Seventh Edition*

3.2 Potential functions

Potential flows are mainly characterized by being inviscid (no friction) and irrotational (fluid particles are not rotated). Usually, viscous effects are limited to a thin layer next to the flow boundaries (think of a flow around a body, for example), called the boundary layer. Hence, neglecting the viscous effects of the boundary layer might be a good approximation for high-speed flows away from this region. As a result, there is no separation of the boundary layer, as happens in viscous flows.

By definition, a velocity vector field $\mathbf{u}(\mathbf{x})$ of an irrotational flow has zero vorticity, i.e.

$$\boldsymbol{\omega} = \nabla \times \mathbf{u} = \mathbf{0}.$$

Moreover, consider $\phi(\mathbf{x})$, $\phi : \mathbb{R}^d \to \mathbb{R}$, a smooth scalar field. The following result is easy to prove:

$$\nabla \times \nabla\phi = \mathbf{0},$$

which leads to the conclusion that if $\mathbf{u}(\mathbf{x})$ is irrotational, then there exists a scalar field $\phi(\mathbf{x})$ such that $\mathbf{u} = \nabla\phi$. This scalar field is defined as **potential function**.

3.3 Incompressible potential flows

If the potential flow is incompressible, we have from Equation 1.6 that $\nabla \cdot \mathbf{u} = 0$, resulting in

$$0 = \nabla \cdot \mathbf{u} = \nabla \cdot \nabla\phi$$

or simply,

$$\nabla^2\phi = 0 \tag{3.1}$$

which is a Laplace equation modeling the incompressible potential flow. This equation is defined over a domain $\Omega \subset \mathbb{R}^d$ and can also be written as

$$\frac{\partial^2 \phi}{\partial x_i \partial x_i} = 0$$

using Einstein's notation, or, for $d = 2$, one can write

$$\frac{\partial^2 \phi}{\partial x_1^2} + \frac{\partial^2 \phi}{\partial x_2^2} = 0.$$

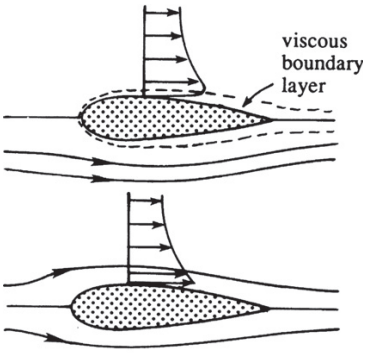

Figure 3.1: Approximation of a viscous flow by a potential flow. Source: [1].

3.3.1 Boundary conditions for the potential function

Being an elliptic equation, we need to specify boundary conditions for Equation 3.1 on $\partial\Omega$, which can be of the following types:

- **Dirichlet:** $\phi(\mathbf{x}) = f(\mathbf{x})$ for $\mathbf{x} \in \Gamma_D$;
- **Neumann:** $\nabla\phi(\mathbf{x}) \cdot \check{\mathbf{n}} = g(\mathbf{x})$ for $\mathbf{x} \in \Gamma_N$;
- **Robin:** $\phi(\mathbf{x}) + \beta\nabla\phi(\mathbf{x}) \cdot \check{\mathbf{n}} = h(\mathbf{x})$ for $\mathbf{x} \in \Gamma_R$;

where $\Gamma_D \cup \Gamma_N \cup \Gamma_R = \partial\Omega$, and $\Gamma_D \cap \Gamma_N \cap \Gamma_R = \emptyset$. Recalling that ϕ is a potential function, these types can be used to specify boundaries with different physical meanings, which are usually prescribed in terms of fluid velocity.

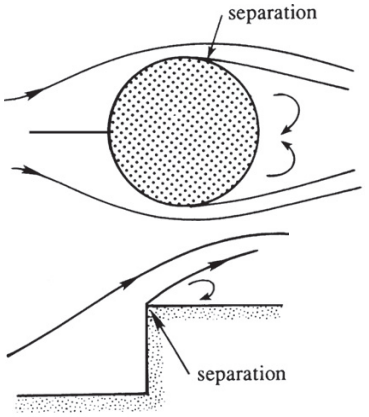

Figure 3.2: No boundary layer separation can occur in a potential flow. Source: [1].

- **Imposed flux (inflow/outflow):** Boundaries where the velocity $\mathbf{u} = \mathbf{U}$ is prescribed in some part $\Gamma_1 \in \partial\Omega$. Using the definition of the potential function, we get $\nabla\phi = \mathbf{U}$. However, we cannot impose both components of this gradient in an elliptic equation. The closest we can get is to impose only the normal component, leading to a Neumann-type boundary condition:

$$\nabla\phi \cdot \check{\mathbf{n}} = U_n \quad \text{or} \quad \frac{\partial\phi}{\partial n} = U_n;$$

- **Non-penetrating boundaries:** Boundaries where fluid particles cannot cross, leading to a normal null flux, which can be easily specified as a homogeneous Neumann-type boundary:

$$\nabla\phi \cdot \check{\mathbf{n}} = 0 \quad \text{or} \quad \frac{\partial\phi}{\partial n} = 0,$$

  on some $\Gamma_2 \in \partial\Omega$. Using the same arguments above, one can see that we cannot impose a no-slip boundary condition.

- **Free flux (outflow):** The free flux boundary is usually modeled by imposing that the variation of the normal flux in the normal direction is zero, meaning that

$$\frac{\partial u_n}{\partial n} = 0 \quad \Rightarrow \quad \frac{\partial^2\phi}{\partial n^2} = 0 \quad \text{on some } \Gamma_3 \subset \partial\Omega.$$

  This condition can be achieved if $\nabla\phi \cdot \check{\mathbf{n}}$ is constant in the normal direction, leading to a condition equivalent to an **imposed flux**

boundary, instead. A better effect is achieved by setting $\phi = 0$ on Γ_3, which is not exactly equivalent to an outflow condition; however, it not only satisfies the above equation but also simplifies the solution of the Laplace problem.

Example 3.3.1 Consider the domain given by Figure 3.3. In this case, the boundary conditions for the potential function Laplace problem Equation 3.1 are given by

- Solid walls (green and blue): we can use the non-penetrating boundaries by imposing $\nabla\phi \cdot \check{\mathbf{n}} = 0$, leading to

$$\frac{\partial \phi}{\partial x} = 0 \quad \text{or} \quad \frac{\partial \phi}{\partial y} = 0$$

  depending on the normal vector to the wall.
- Inflow: Imposed inflow condition leads to

$$\nabla\phi \cdot \check{\mathbf{n}} = 5 \quad \Rightarrow \quad \frac{\partial \phi}{\partial x} = -5$$

- Outflow: Imposed outflow condition leads to

$$\nabla\phi \cdot \check{\mathbf{n}} = 5 \quad \Rightarrow \quad \frac{\partial \phi}{\partial x} = 5$$

Notice, however, that Equation 3.1, together with these boundary conditions, results in a Neumann boundary problem and the well-known indeterminacy of the solution (any constant function satisfy this boundary problem).

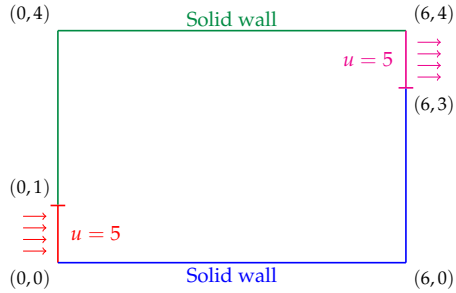

Figure 3.3: Example of a confined potential flow with inflow and outflow boundary conditions.

3.4 Stream functions

Another useful function is derived in terms of velocity. According to White [2], this concept only works if the continuity equation Equation 1.6 can be reduced to two terms, with the most common application being to steady-state two-dimensional incompressible flows. In this case, by defining a function $\psi : \Omega \subset \mathbb{R}^2 \to \mathbb{R}$ such that

$$u_1 = \frac{\partial \psi}{\partial x_2} \quad \text{and} \quad u_2 = -\frac{\partial \psi}{\partial x_1},$$

the continuity equation is automatically satisfied. We can rewrite the velocity field $\mathbf{u}$ as

$$\mathbf{u} = \frac{\partial \psi}{\partial x_2}\,\check{\mathbf{e}}^{(1)} - \frac{\partial \psi}{\partial x_1}\,\check{\mathbf{e}}^{(2)}$$

such that the vorticity of $\mathbf{u}$ is given by

$$\nabla \times \mathbf{u} = -\nabla^2\psi\,\check{\mathbf{e}}^{(3)},$$

and by applying the hypothesis of an irrotational flow, one can derive the Laplace equation

$$\nabla^2\psi = 0 \tag{3.2}$$

that can be solved, with suitable boundary conditions, to obtain the stream function ψ.

In two dimensions, both potential and stream functions, $\phi(x_1, x_2)$ and $\psi(x_1, x_2)$ respectively, satisfy the Cauchy-Riemann equations, given as

Definition 3.4.1 *Given two real-valued functions $\phi, \psi : \mathbb{R}^2 \to \mathbb{R}$, they are said to satisfy the Cauchy-Riemann equations if*

$$\frac{\partial \phi}{\partial x_1} = \frac{\partial \psi}{\partial x_2} \quad \textit{and} \quad \frac{\partial \phi}{\partial x_2} = -\frac{\partial \psi}{\partial x_1}. \tag{3.3}$$

3.4.1 Boundary conditions for the stream function

Usually, the stream functions are applied to describe incompressible, irrotational external flows, and therefore boundary conditions are mainly given at the boundary of an immersed body of interest and at infinity (a reference position), such that

- **At the body:** The stream function is assumed to be constant around the body of interest ($\psi = \psi_0$);
- **At infinity:** At a position away from the boundary, the stream function is assumed to be constant ($\psi = \psi_\infty$), but its value depends on the condition imposed at the body and the flux between boundaries. We will see how to impose that in an example.
- **Imposed flux (inflow/outflow):** We can impose a normal flux U_n through some boundary by using the definition of stream function

  $$\mathbf{u} \cdot \check{\mathbf{n}} = \left(\frac{\partial \psi}{\partial x_2} \check{\mathbf{e}}^{(1)} - \frac{\partial \psi}{\partial x_1} \check{\mathbf{e}}^{(2)} \right) \cdot \check{\mathbf{n}} = U_n,$$

  however, to effectively apply this condition, one has to integrate this equation over the boundary since $\mathbf{u}$ is not the gradient of ψ, as it was for the potential function. We will see more details in a working example.

Example 3.4.1 Consider the domain given by Figure 3.3. The boundary conditions for the stream function Laplace problem Equation 3.2 are given by

- Bottom wall: The bottom wall is a streamline itself, hence ψ is constant. Lets assume $\psi_0 = 0$ on this boundary.
- Top wall: The top wall is also a streamline, with constant ψ value, say, ψ_∞. However, we need to compute its value depending on ψ_0. The difference between ψ_∞ and ψ_0 is given by the flux passing between these two boundaries, i.e.,

  $$\psi_{\text{top}} - \psi_{\text{bot}} = \int_0^1 \frac{\partial \psi}{\partial y} dy = \int_0^1 u dy = 5$$

  which implies that $\psi_\infty = 5$. Notice that since inflow and outflow fluxes are the same, the same value would be achieved should we have integrated on the right boundary (outflow).

- Inflow: It is clear that ψ is a function of y, varying from ψ_0 to ψ_∞, as y goes from 0 to 1. This function can be obtained by integrating the boundary condition from 0 to y:

$$u = 5 \Rightarrow \frac{\partial \psi}{\partial y} = 5 \Rightarrow \int_0^y \frac{\partial \psi}{\partial y}\, ds = \int_0^y 5\, ds \Rightarrow \psi(y) = 5y$$

- Outflow: The same idea can be used to find $\psi(y)$ on the outflow:

$$u = 5 \Rightarrow \frac{\partial \psi}{\partial y} = 5 \Rightarrow \int_3^y \frac{\partial \psi}{\partial y}\, ds = \int_3^y 5\, ds \Rightarrow \psi(y) = 5y - 15$$

Since all imposed boundary conditions are of the Dirichlet type, there is no problem with the indeterminacy of the solution, as in the previous example.

3.5 Potential lines and streamlines

In a two-dimensional setup ($d = 2$), both potential and stream functions define a set of lines that brings some geometric interpretation to the incompressible potential flow. To simplify the notation, consider $\mathbf{x} = (x, y)$ and $\mathbf{u} = (u, v)$. Variations of $\phi(x, y)$ and $\psi(x, y)$ are given by

$$d\phi = \frac{\partial \phi}{\partial x} dx + \frac{\partial \phi}{\partial y} dy = u\, dx + v\, dy$$
$$d\psi = \frac{\partial \psi}{\partial x} dx + \frac{\partial \psi}{\partial y} dy = -v\, dx + u\, dy$$

Lines of constant potential, called **potential lines**, are given by

$$d\phi = 0 \quad \Rightarrow \quad \frac{dy}{dx} = -\frac{u}{v},$$

while lines of constant stream function values, called **streamlines**, are given by

$$d\psi = 0 \quad \Rightarrow \quad \frac{dy}{dx} = \frac{v}{u},$$

hence they are orthogonal. The concept of streamlines is useful to visualize and interpret the flow since they follow the trajectory of the fluid particles.

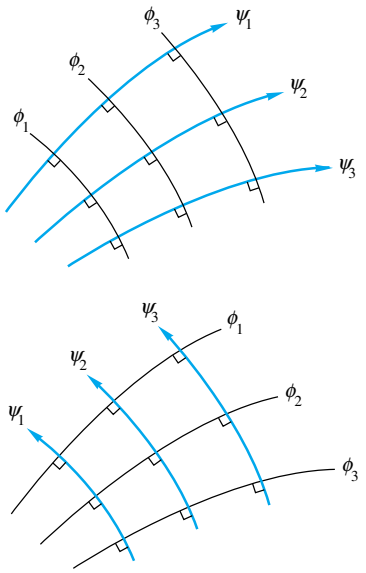

Figure 3.4: Potential lines and streamlines. Source: [2].

3.6 Bernoulli's equation

From the principle of conservation of linear momentum in Equation 1.9, we can apply the simplifications seen in this chapter. First, considering an incompressible and inviscid flow, the Cauchy stress tensor σ can be thoroughly simplified

$$\sigma = (-p + \lambda \nabla \cdot \mathbf{u})\mathbf{I} + \mu(\nabla \mathbf{u} + \nabla \mathbf{u}^\intercal) = -p\mathbf{I}$$

Daniel Bernoulli (Dutch Republic, 1700 – Swiss, 1782).

leading to the equation known as Euler's equation:

$$\rho\left(\frac{\partial \mathbf{u}}{\partial t} + (\mathbf{u}\cdot\nabla)\mathbf{u}\right) + \nabla p = \mathbf{b} \tag{3.4}$$

To derive Bernoulli's equation, we will use the following result from vector calculus:

Theorem 3.6.1 *Let* $\mathbf{u}$ *be a vector field defined in* $\mathbb{R}^d$*, with* $d = 2, 3$*. The following identity holds:*

$$(\mathbf{u}\cdot\nabla)\mathbf{u} = \nabla\left(\frac{\mathbf{u}\cdot\mathbf{u}}{2}\right) - \mathbf{u}\times(\nabla\times\mathbf{u}). \tag{3.5}$$

From Equation 3.4 and Equation 3.5, we can write

$$\frac{\partial \mathbf{u}}{\partial t} + \nabla\left(\frac{\mathbf{u}\cdot\mathbf{u}}{2}\right) - \mathbf{u}\times(\nabla\times\mathbf{u}) + \frac{1}{\rho}\nabla p = \frac{1}{\rho}\mathbf{b}.$$

If we consider a steady-state flow, such that $\partial\mathbf{u}/\partial t = 0$, and that the body force $\mathbf{b}$ accounts only for gravity effects in the vertical direction (say x_d, with $d = 2, 3$), such that $\mathbf{b} = -\rho g\,\check{\mathbf{e}}^{(d)}$, following that $\mathbf{b} = \nabla(-\rho g x_d)$. Therefore,

$$\frac{1}{\rho}\nabla p + \nabla\left(\frac{\mathbf{u}\cdot\mathbf{u}}{2}\right) + \nabla(g x_d) = \mathbf{u}\times(\nabla\times\mathbf{u}),$$

that is known as Bernoulli's equation. For an irrotational flow, we can further simplify it by vanishing the right-hand side, resulting in

$$\nabla\left(\frac{p}{\rho} + \frac{\mathbf{u}\cdot\mathbf{u}}{2} + g x_d\right) = 0,$$

which implies that

$$\frac{p}{\rho} + \frac{\mathbf{u}\cdot\mathbf{u}}{2} + g x_d = C \tag{3.6}$$

with C an arbitrary constant. This equation is the most popular version of Bernoulli's equation for potential flows. It can be used to compute the pressure once the velocity field is known. Note that the actual pressure values are not important in this context, only its gradient since C is unknown.

Exercises

1. Let $\phi : \mathbb{R}^d \to \mathbb{R}$ be a smooth scalar function. Show that $\nabla\times\nabla\phi = \mathbf{0}$.
2. Prove theorem 3.6.1.
3. Show that equipotential lines and streamlines are orthogonal by showing that $\nabla\phi\cdot\nabla\psi = 0$.

3.7 Slightly compressible potential flows

An approximation of the external flow of air (around a body such as an airplane, for example) might take into account the compressibility of

fluid, resulting in a compressible flow. In fact, this choice depends on the Mach number, presented in Chapter 1, defined as

$$\mathrm{Ma} = \frac{\|\mathbf{u}\|}{c}$$

where c is the speed of sound. The exact limit as to where to consider a compressible or incompressible flow is a matter of discussion. However, some authors consider that subsonic flows with $\mathrm{Ma} < 0.3$ a reasonable limit for incompressible flows. For supersonic flows, $\mathrm{Ma} > 1$, the model has to take into account the nonlinearities of the flow, and simplifications like potential flows are not suitable anymore. Therefore for subsonic flows where $0.3 < \mathrm{Ma} < 1$, we still might approximate the model by potential flows and introduce some compressibility in the model.

By recalling the mass conservation Equation 1.6 again, dropping the time derivative by considering a steady-state flow, we get

$$\nabla \cdot (\rho \mathbf{u}) = 0 \quad \Rightarrow \quad \nabla \cdot (\rho \nabla \phi) = 0 \tag{3.7}$$

for a potential function ϕ. Now, since we are considering compressibility, ρ is not constant. Therefore we cannot conclude that $\mathbf{u}$ is solenoidal.

We consider an isentropic flow, i.e., when the change of flow variables is small and gradual. In thermodynamics, this is equivalent to an adiabatic and reversible process[1] [9, 10]. By using several thermodynamic relations, we can arrive in the following equations

$$\frac{\rho_0}{\rho} = \left(1 + \frac{\gamma - 1}{2}\mathrm{Ma}^2\right)^{\frac{1}{\gamma-1}}$$
$$\frac{p_0}{p} = \left(1 + \frac{\gamma - 1}{2}\mathrm{Ma}^2\right)^{\frac{\gamma}{\gamma-1}}$$

where γ is the fluid's specific heat ratio. For ideal gases, γ is considered to be constant, and for air at moderate temperature, $\gamma = 1.4$. Moreover, ρ_0 and p_0 are the density and pressure at stagnation, i.e., where the fluid velocity is taken isentropically to zero.

The density in Equation 3.7 depends on the Mach number, which depends on velocity, which is defined in terms of the potential function. By using $\gamma = 1.4$, we can write the equation for density as

$$\rho(\phi) = \rho_0 \left(1 + \frac{1}{5}\mathrm{Ma}^2\right)^{-\frac{5}{2}}$$

and the Mach number as

$$\mathrm{Ma}^2 = \frac{\|\mathbf{u}\|^2}{c^2} = \frac{\mathbf{u} \cdot \mathbf{u}}{c^2} = \frac{1}{c^2}\left[\left(\frac{\partial \phi}{\partial x}\right)^2 + \left(\frac{\partial \phi}{\partial y}\right)^2\right].$$

The pressure can no longer be computed by Bernoulli's equation due to the incompressibility assumption. Instead, we can use the above relation,

1: That also means that no heat is added to the flow, and no energy transformations occur due to friction or dissipative effects.

[9]: Pontes et al. (2019), *An Introduction to Compressible Flows with Applications: Quasi-One-Dimensional Approximation and General Formulation for Subsonic, Transonic and Supersonic Flows*
[10]: Pontes et al. (2021), *Fenômeos de Transferência*

which leads to the equation

$$p(\phi) = p_0 \left(1 + \frac{1}{5}\mathrm{Ma}^2\right)^{-\frac{7}{2}}.$$

Therefore, Equation 3.7 is a nonlinear elliptic equation that requires linearization either before or after the finite volume discretization.

3.8 Finite-volume discretizations

Following what has been done in Section 2.6, we intend to discretize $\Omega = [0, L_1] \times [0, L_2]$ by an admissible finite volume mesh, structured and orthogonal, with $n_1 \times n_2$ elements. For the sake of simplicity, let us introduce the notation of Figure 3.6.

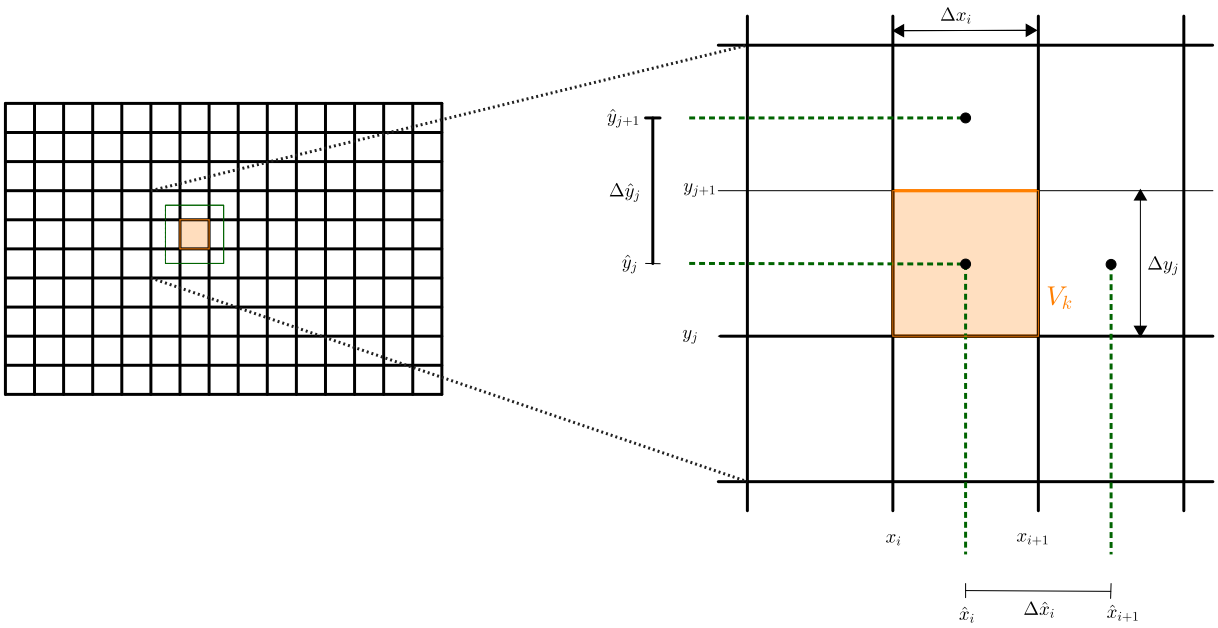

Figure 3.6: Standard cell-centered orthogonal finite volume mesh and notation.

Additionally, each straight edge of ∂V_k is identified as E, N, W, and S, representing the east, north, west, and south edges, respectively, such as in Figure 3.7.

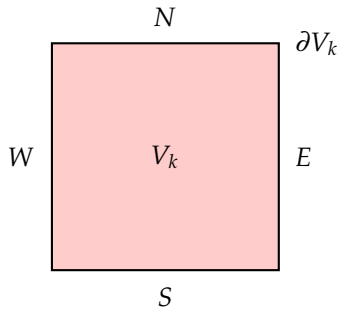

Figure 3.7: Finite volume element with edges.

3.8.1 Discretization of the incompressible model

We will follow the discretization of the incompressible model, given by Equation 3.1. By integrating over a single generic volume V_k, we get

$$\begin{aligned}\int_{V_k} \nabla^2\phi \, dv &= \int_{\partial V_k} \nabla\phi \cdot \check{\mathbf{n}} \, ds \\ &= \int_E \nabla\phi \cdot \check{\mathbf{n}} \, ds + \int_N \nabla\phi \cdot \check{\mathbf{n}} \, ds + \int_W \nabla\phi \cdot \check{\mathbf{n}} \, ds + \int_S \nabla\phi \cdot \check{\mathbf{n}} \, ds\end{aligned}$$

Integrating the E-side, using $\check{\mathbf{n}} = (1, 0)$, we have:

$$\int_E \nabla\phi \cdot \check{\mathbf{n}}\, ds = \int_{y_j}^{y_{j+1}} \frac{\partial\phi}{\partial x}(x_{i+1}, y) dy$$

By considering

$$\phi_{i,j} = \phi_k = \frac{1}{|V_k|} \int_{V_k} \phi(x, y)\, dv$$

we can approximate

$$\int_{y_j}^{y_{j+1}} \frac{\partial\phi}{dx}(x_{i+1}, y)\, dy \simeq \int_{y_j}^{y_{j+1}} \frac{\phi_{i+1,j} - \phi_{i,j}}{\Delta\hat{x}_i}\, dy = \frac{\Delta y_j}{\Delta\hat{x}_i}(\phi_{i+1,j} - \phi_{i,j})$$

Integrating the S-side, using $\check{\mathbf{n}} = (0, -1)$, we have:

$$\begin{aligned}\int_S \nabla\phi \cdot \check{\mathbf{n}}\, ds \simeq \int_{x_i}^{x_{i+1}} -\frac{\partial\phi}{dy}(x, y_j)\, dx \simeq \int_{x_i}^{x_{i+1}} -\frac{\phi_{i,j} - \phi_{i,j-1}}{\Delta\hat{y}_{j-1}}\, dx \\ = \frac{\Delta x_i}{\Delta\hat{y}_{j-1}}(\phi_{i,j-1} - \phi_{i,j})\end{aligned}$$

The other sides are integrated analogously. The final discrete set of equations to be solved are

$$\underbrace{\frac{\Delta y_j}{\Delta\hat{x}_i}(\phi_{i+1,j} - \phi_{i,j})}_{(E)} + \underbrace{\frac{\Delta x_i}{\Delta\hat{y}_j}(\phi_{i,j+1} - \phi_{i,j})}_{(N)} + \underbrace{\frac{\Delta y_j}{\Delta\hat{x}_{i-1}}(\phi_{i-1,j} - \phi_{i,j})}_{(W)} + \underbrace{\frac{\Delta x_i}{\Delta\hat{y}_{j-1}}(\phi_{i,j-1} - \phi_{i,j})}_{(S)} = 0, \tag{3.8}$$

$\forall\, i = 1, \ldots, n_1, \;\; \forall\, j = 1, \ldots, n_2.$

3.8.2 Discretization of boundary conditions

Let us work on the finite volume treatment of boundary conditions with some examples. First, consider the elements touching a solid-wall boundary Γ. The treatment of such condition is straightforward since $\nabla\phi \cdot \check{\mathbf{n}} = 0$ on Γ, meaning that the contribution of the integral corresponding to the side of V_k in Γ vanishes completely.

Example 3.8.1 If the E-side of an element V_k is touching Γ, then

$$\frac{\partial\phi}{\partial\check{\mathbf{n}}} = 0 \quad \text{on} \quad \Gamma \cap \partial V_k$$

which means that the E-side corresponding integral is given by

$$\int_E \nabla\phi \cdot \check{\mathbf{n}}\, ds = \int_E \frac{\partial\phi}{\partial\check{\mathbf{n}}}\, ds = 0$$

such that its contribution vanishes from Equation 3.8.

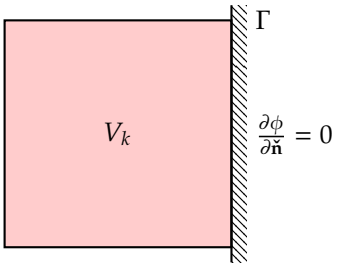

Figure 3.8: Boundary on the E-side of the element V_k.

Analogously, if a non-homogeneous Neumann boundary is given, such as an imposed inflow or outflow condition, the contribution in Equation

3.8 is adjusted accordingly.

Example 3.8.2 Suppose the S-side of an element V_k is touching Γ, where we want to impose a non-homogeneous Neumann boundary condition

$$\frac{\partial \phi}{\partial \check{\mathbf{n}}} = g(x, y) \quad \text{on} \quad \Gamma \cap \partial V_k$$

and the corresponding integral is given by

$$\int_S \nabla\phi \cdot \check{\mathbf{n}}\, ds = \int_{x_i}^{x_{i+1}} \frac{\partial \phi}{\partial \check{\mathbf{n}}}\, dx = \int_{x_i}^{x_{i+1}} g(x, y_1)\, dx.$$

Notice, however, that now the function g should be numerically integrated. The trapezoidal rule can be used to result in

$$\int_{x_i}^{x_{i+1}} g(x, y_1)\, dx \simeq \frac{\Delta x_i}{2}\left[g(x_i, y_1) + g(x_{i+1}, y_1)\right].$$

Once again, the corresponding contribution to the S-side integral should be modified in Equation 3.8 to reflect the imposed boundary condition.

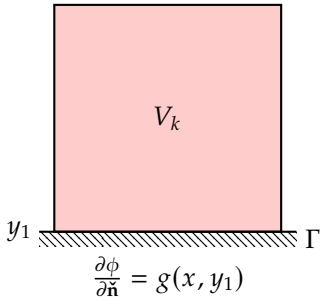

Figure 3.9: Boundary on the S-side of the element V_k.

In the case of Dirichlet-type boundary conditions, such as in a free flux outflow conditions, the imposition is not as straightforward. The following example shows how to do that in the considered mesh.

Example 3.8.3 Suppose now that an element W-side is touching a boundary Γ where we want to impose a Dirichlet boundary condition such as

$$\phi(x, y) = g(x, y) \quad \text{on} \quad \Gamma \cap \partial V_k$$

This boundary condition will affect the integral on the W-side so that we need to recompute its contribution to the discrete equation:

$$\begin{aligned}\int_W \nabla\phi \cdot \check{\mathbf{n}} &\simeq \int_{y_j}^{y_{j+1}} -\frac{\partial \phi}{\partial x}(x_1, y)\, dy \simeq \int_{y_j}^{y_{j+1}} -\frac{\phi_{1,j} - g(x_1, y)}{\hat{x}_1 - x_1}\, dy \\ &= -\frac{2\Delta y_j}{\Delta x_1}\phi_{1,j} + \frac{2}{\Delta x_1}\int_{y_j}^{y_{j+1}} g(x_1, y)\, dy \\ &\simeq -\frac{2\Delta y_j}{\Delta x_1}\phi_{1,j} + \frac{\Delta y_j}{\Delta x_1}\left[g(x_1, y_j) + g(x_1, y_{j+1})\right]\end{aligned}$$

where the trapezoidal rule was applied in the last line to approximate the integral of the function g. With this value at hand, we can update the W-side integral contribution in Equation 3.8.

If a homogeneous Dirichlet boundary is to be imposed, notice that the W-side integral does not vanish completely, and its contribution should be updated as

$$\int_W \nabla\phi \cdot \check{\mathbf{n}} \simeq -\frac{2\Delta y_j}{\Delta x_1}\phi_{1,j}.$$

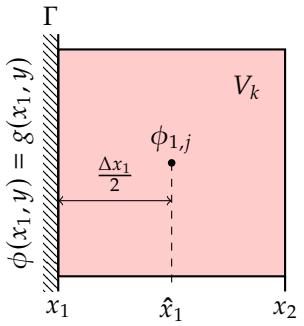

Figure 3.10: Boundary on the W-side of the element V_k.

3.9 Assignment: Implementation of an incompressible potential flow

Consider the domain given by Figure 3.3 (reproduced on the right).

1. Implement a finite volume method to solve an incompressible potential flow modeled by Equation 3.1 in this domain, with the given boundary conditions.
2. When solving for the potential function, this is a Neumann problem. How can you solve the constant space indeterminacy? What happens if we change the imposed outflow to a free flux outflow?
3. Perform a convergence study with different mesh characteristic sizes, using a reference solution computed in a much finer grid. What is the expected and observed orders of convergence?
4. Implement the same problem, now solving Equation 3.2 for the stream function. Adapt the boundary conditions accordingly.
5. Compute the pressure by using Bernoulli's Equation 3.6.
6. Plot side by side the streamlines and constant potential lines.

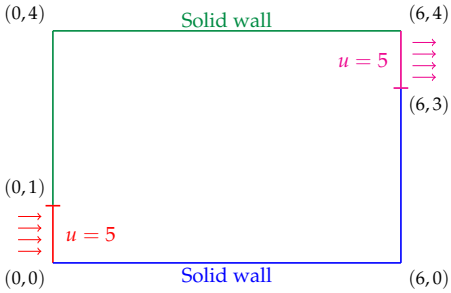

3.10 Discretization of the compressible model

Equation 3.7 can be discretized by finite volumes in a similar way. First, let us integrate this equation over one generic finite volume V_k:

$$\int_{V_k} \nabla \cdot (\rho \nabla \phi) dv = 0 \implies \int_{\partial V_k} \rho \nabla \phi \cdot \check{\mathbf{n}}\, ds = 0.$$

Notice that $\rho = \rho(\phi)$ is part of the integrand and shound be adequately discretized. To do that, in order to simplify the notation, let us consider a one-dimensional version of Equation 3.7, given by

$$\frac{d}{dx}\left(\rho \frac{d\phi}{dx}\right) = 0.$$

Consider a discretization such as in Figure 3.11. Integrating the equation above results in

$$\int_{x_i}^{x_{i+1}} \frac{d}{dx}\left(\rho \frac{d\phi}{dx}\right) dx = \rho \frac{d\phi}{dx}\bigg|_{x_{i+1}} - \rho \frac{d\phi}{dx}\bigg|_{x_i}.$$

For the discretization to be conservative, the value of ρ at the interfaces (x_{i+1}, for instance) should be carefully evaluated. In fact the mass flux should be equal in both sides of the interface in x_{i+1}, leading to

$$\lim_{x \to x_{i+1}^-} \rho \frac{d\phi}{dx} = \lim_{x \to x_{i+1}^+} \rho \frac{d\phi}{dx}.$$

Suppose that $\phi_{i+\frac{1}{2}}$ is the value of ϕ at x_{i+1}. By discretizing both sides of the equality, we get

$$\rho_i \frac{\phi_{i+\frac{1}{2}} - \phi_i}{\Delta x_i/2} = \rho_{i+1} \frac{\phi_{i+1} - \phi_{i+\frac{1}{2}}}{\Delta x_{i+1}/2},$$

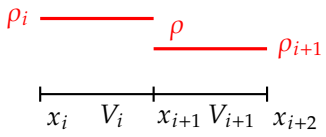

Figure 3.11: Finite volume discretization in 1D.

and by isolating $\phi_{i+\frac{1}{2}}$, we get

$$\phi_{i+\frac{1}{2}} = \frac{\Delta x_{i+1}\rho_i\phi_i + \Delta x_i\rho_{i+1}\phi_{i+1}}{\Delta x_{i+1}\rho_i + \Delta x_i\rho_{i+1}}.$$

This value can be inserted back into the discretization of the fluxes, resulting in

$$\lim_{x\to x_{i+1}^-} \rho\frac{d\phi}{dx} \simeq \rho_i\frac{\phi_{i+\frac{1}{2}} - \phi_i}{\Delta x_i/2} = 2\rho_i\rho_{i+1}\left(\frac{\phi_{i+1} - \phi_i}{\Delta x_{i+1}\rho_i + \Delta x_i\rho_{i+1}}\right),$$

which is equal to the flux on the right side of x_{i+1}. Notice that if we take $\Delta x_{i+1} = \Delta x_i = \Delta x$, this equation simplifies to

$$\rho\frac{\partial\phi}{\partial x}\bigg|_{x_{i+1}} = \underbrace{\frac{2\rho_i\rho_{i+1}}{\rho_i + \rho_{i+1}}}_{\text{harmonic mean}}\left(\frac{\phi_{i+1} - \phi_i}{\Delta x}\right).$$

Therefore, the value of ρ at the interfaces that leads to a conservative discretization is the harmonic mean of the surrounding densities.

Going back to the Laplace equation,

$$\int_{\partial V_k} \rho\nabla\phi\cdot\check{\mathbf{n}}\,ds = 0$$

can be written as

$$\int_E \rho\nabla\phi\cdot\check{\mathbf{n}}\,ds + \int_N \rho\nabla\phi\cdot\check{\mathbf{n}}\,ds + \int_W \rho\nabla\phi\cdot\check{\mathbf{n}}\,ds + \int_S \rho\nabla\phi\cdot\check{\mathbf{n}}\,ds = 0.$$

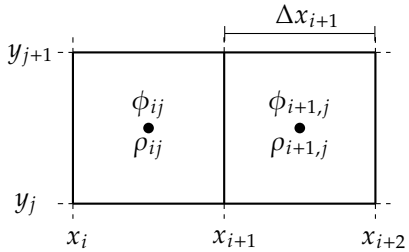

Figure 3.12: Discretization of the fluxes through the E-side of a finite volume.

Each term can be integrated as before. As an example, consider the integral of the E-side, that can be computed as

$$\begin{aligned}\int_E \rho\nabla\phi\cdot\check{\mathbf{n}}\,ds &= \int_{y_j}^{y_{j+1}} \rho\frac{\partial\phi}{\partial x}\bigg|_{(x_{i+1},y)} dy \\ &= \frac{2\rho_{ij}\rho_{i+1,j}\Delta y_j}{\Delta x_{i+1}\rho_{ij} + \Delta x_i\rho_{i+1,j}}(\phi_{i+1,j} - \phi_{ij}).\end{aligned}$$

The discrete system can be written as

$$\begin{aligned}&\underbrace{\frac{2\rho_{ij}\rho_{i+1,j}\Delta y_j}{\Delta x_{i+1}\rho_{ij} + \Delta x_i\rho_{i+1,j}}(\phi_{i+1,j} - \phi_{ij})}_{(E)} + \underbrace{\frac{2\rho_{ij}\rho_{i,j+1}\Delta x_i}{\Delta y_{j+1}\rho_{ij} + \Delta y_j\rho_{i,j+1}}(\phi_{i,j+1} - \phi_{ij})}_{(N)} + \\ &\underbrace{\frac{2\rho_{ij}\rho_{i-1,j}\Delta y_j}{\Delta x_{i-1}\rho_{ij} + \Delta x_i\rho_{i-1,j}}(\phi_{i-1,j} - \phi_{ij})}_{(W)} + \underbrace{\frac{2\rho_{ij}\rho_{i,j-1}\Delta x_i}{\Delta y_{j-1}\rho_{ij} + \Delta y_j\rho_{i,j-1}}(\phi_{i,j-1} - \phi_{ij})}_{(S)} = 0\end{aligned} \tag{3.9}$$

$\forall\, i = 1,\ldots,n_1,\ \ \forall\, j = 1,\ldots,n_2.$

3.10.1 Computation of densities

As seen before, the discrete densities $\rho_k = \rho_{ij}$ are piecewise constant in each finite volume V_k. To compute that, we need to recall the formula

$$\rho(\phi) = \left(1 + \frac{1}{5}\mathrm{Ma}^2\right)^{-\frac{5}{2}},$$

that depends on the Mach number, which can be written as

$$\mathrm{Ma}^2 = \frac{\|\mathbf{u}\|_2^2}{c^2} = \frac{1}{c^2}(\mathbf{u}\cdot\mathbf{u}) = \frac{1}{c^2}\left(\left(\frac{\partial\phi}{\partial x}\right)^2 + \left(\frac{\partial\phi}{\partial y}\right)^2\right),$$

where we used the definition of the velocities in terms of the potential ϕ. To be consistent with the finite volume approximation used, the velocities are first approximated at the edges of V_k using the same discretization employed for the fluxes between elements

$$\left.\frac{\partial\phi}{\partial x}\right|_E \simeq \frac{\phi_{i+1,j} - \phi_{ij}}{\Delta\hat{x}_i} \qquad \left.\frac{\partial\phi}{\partial x}\right|_W \simeq \frac{\phi_{ij} - \phi_{i-1,j}}{\Delta\hat{x}_{i-1}}$$
$$\left.\frac{\partial\phi}{\partial y}\right|_N \simeq \frac{\phi_{i,j+1} - \phi_{ij}}{\Delta\hat{y}_j} \qquad \left.\frac{\partial\phi}{\partial y}\right|_S \simeq \frac{\phi_{ij} - \phi_{i,j-1}}{\Delta\hat{y}_{j-1}}$$

and finally computing the piecewise constant velocity $\mathbf{u}_k = [u_k, v_k]$ by averaging

$$u_k = \frac{1}{2}\left(\left.\frac{\partial\phi}{\partial x}\right|_E + \left.\frac{\partial\phi}{\partial x}\right|_W\right), \quad v_k = \frac{1}{2}\left(\left.\frac{\partial\phi}{\partial y}\right|_N + \left.\frac{\partial\phi}{\partial y}\right|_S\right).$$

Finally, we can compute ρ_k by

$$\rho_k = \left(1 + \frac{1}{5c^2}\left(u_k^2 + v_k^2\right)\right)^{-\frac{5}{2}}.$$

3.10.2 Solution of the nonlinear problem

The discrete system Equation 3.9 is a non-linear algebraic system of dimension $N = n_1 n_2$ (for $d = 2$), of the form

$$\mathbf{g}(\boldsymbol{\phi}) = \mathbf{0},$$

where $\mathbf{g} : \mathbb{R}^N \to \mathbb{R}^N$ and $\boldsymbol{\phi} = [\phi_1, \ldots, \phi_N]^T$, that have to be solved for $\boldsymbol{\phi}$ by some linearization technique.

Newton's method

Newton's method is an iterative method that computes the next approximation $\boldsymbol{\phi}^{(s+1)}$ in terms of $\boldsymbol{\phi}^{(s)}$ by

$$\boldsymbol{\phi}^{(s+1)} = \boldsymbol{\phi}^{(s)} - J_{\mathbf{g}}(\boldsymbol{\phi}^{(s)})^{-1}\mathbf{g}(\boldsymbol{\phi}^{(s)})$$

where $J_{\mathbf{g}}$ is the Jacobian of $\mathbf{g}$. Some coments about the method:

1. If $\boldsymbol{\phi}^{(0)}$ is close enough to the true solution $\boldsymbol{\phi}^*$, and the Jacobian

is non-singular in this neighborhood, then the convergence of Newton's method is guarateed to be quadratic, meaning that $\|\boldsymbol{\phi}^* - \boldsymbol{\phi}^{(s+1)}\| \leq C\|\boldsymbol{\phi}^* - \boldsymbol{\phi}^{(s)}\|^2$. As a consequence, only few iterations should be enough to drop the error to machine precision.
2. The computation of the inverse of the Jacobian matrix can be avoided by rearranging the above equation to transform it in a linear system, to be solved every time step.
3. Major drawbacks are the computation of the Jacobian and finding a suitable initial guess.
4. The Jacobian can also be approximated somehow (for instance by finite differences), resulting in quasi-Newton methods.

Successive iterations

An alternative to Newton's method is to compute successive iterations, by evaluating some variables in the previous iteration. There are many ways to do that, but the suggested method in our context is to evaluate all density values in Equation 3.9 in the previous iteration s, so that Equation 3.9 can be written as the linear system

$$\mathbf{A}\left(\boldsymbol{\rho}^{(s)}\right)\boldsymbol{\phi}^{(s+1)} = \mathbf{b}\left(\boldsymbol{\rho}^{(s)}\right)$$

where the right-hand-side is due to known boundary conditions.

1. The convergence is linear, much slower than Newton's method.
2. The initial guess is not as restrictive as in Newton's method.
3. Implementation is much simpler.
4. Can be used in combination with Newton's method to find a better initial guess.

Algorithm 1: Successive iterations, given $s = 0$ e $\boldsymbol{\phi}^{(0)}$

while $E > \varepsilon$ **do**
  for $i = 1$ to M **do**
    for $j = 1$ to N **do**
      Compute the equation index $k \leftarrow (i, j)$;
      Compute velocities $u_k^{(s)}$ e $v_k^{(s)}$ in terms of $\boldsymbol{\phi}^{(s)}$;
      Compute $\mathrm{Ma}_k^{(s)}$ and $\rho_k^{(s)}$;
      Assemble the k-th line of matrix $\mathbf{A}(\boldsymbol{\rho}^{(s)})$ and rhs $\mathbf{b}(\boldsymbol{\rho}^{(s)})$;
    end for
  end for
  Solve the linear system $\mathbf{A}(\boldsymbol{\rho}^{(s)})\boldsymbol{\phi}^{(s+1)} = \mathbf{b}(\boldsymbol{\rho}^{(s)})$;
  Compute $E = \|\boldsymbol{\phi}^{(s+1)} - \boldsymbol{\phi}^{(s)}\|/\|\boldsymbol{\phi}^{(s+1)}\|$;
  Update $s \leftarrow s + 1$ and $\boldsymbol{\phi}^{(s)} \leftarrow \boldsymbol{\phi}^{(s+1)}$;
end while

3.11 Assignment 2: Nonlinear potential flow

Consider again the domain given by Figure 3.3 (reproduced on the right).

1. Implement a finite volume method to solve a slightly compressible potential flow modeled by Equation 3.7 in this domain, with the given boundary conditions.
2. Implement the Successive Iterations method for the nonlinear problem.
3. **Graduate students:** Solve the nonlinear problem by the Newton's method (use a NumPy package or implement your own version). Compare both methods in terms of number of iterations, initial guess sensitivity and overall execution time.
4. The imposed velocity values (in m/s) in Figure 3.3 are too low to develop a compressible flow (check it with your simulation). Set inflow and outflow velocities to one third of the speed of sound. What happens if we increse this value even further? How it affects the solution of the nonlinear problem?
5. Plot the potential function, potential lines, velocity field, pressure, density and Mach number. Use any visualization tool to plot the streamlines (no need to solve the stream function).
6. **Graduate students:** It is easy to put an obstacle inside the domain, by defining a mask (essentially a matrix defining the type of all cells). Compute the compressible flow around a rectangular obstacle.

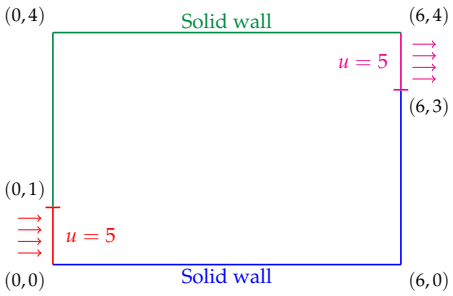

NUMERICAL METHODS FOR HYPERBOLIC CONSERVATION LAWS

4

4.1 Balance and conservation laws 58
4.2 Linear Hyperbolic Conservation Laws 60
4.3 Finite volume methods for hyperbolic conservation laws 63
4.4 The CFL condition 68
4.5 Consistency, Stability, and Convergence 70
4.6 Assignment 1: Linear advection equation 77
4.7 Nonlinear hyperbolic conservation laws 77
4.8 Finite volume methods for nonlinear hyperbolic conservation laws 83
4.9 High-Order Methods . . 87
4.10 Assignment 2: Nonlinear traffic flow 92
4.11 Assignment 3: Numerical solution of 1D Euler's equations 93

4.1 Balance and conservation laws

Partial differential equations are used to describe a large number of phenomena, including various types of fluid flow applications. To physically understand how these equation arise, we will derive a balance law to determine the conservation of a given property in a domain $\Omega \subset \mathbb{R}^d$ over time. Let us consider a fluid property $\mathbf{q}(\mathbf{x}, t)$, and the balance law states that the temporal variation of the amount of $\mathbf{q}$ contained in the domain Ω is equal to the flux rate of $\mathbf{q}$ through the boundaries of Ω plus the total amount of $\mathbf{q}$ injected or removed from Ω through source terms. Mathematically, we have

$$\frac{\partial}{\partial t}\int_\Omega \mathbf{q}(\mathbf{x},t)\,d\mathbf{x} = -\int_{\partial\Omega}\mathbf{f}(\mathbf{q}(\mathbf{x},t))\cdot\check{\mathbf{n}}\,ds + \int_\Omega \mathbf{s}(\mathbf{x},t)\,d\mathbf{x}, \tag{4.1}$$

where $\check{\mathbf{n}}$ is the normal vector to Ω, $\mathbf{f}(\mathbf{q})$ is the flux function, which depends on $\mathbf{q}$ (not necessarily in a linear way), and $\mathbf{s}$ is the source term.

More general balance laws can be determined when the flux function $\mathbf{f}$ depends on $\mathbf{q}, \nabla\mathbf{q}, \nabla^2\mathbf{q}, \ldots$, however, in this chapter, we are interested only on those cases when $\mathbf{f}$ depends only on $\mathbf{q}$, which usually results in a first order system of hyperbolic equations.

Applying the divergence theorem, we obtain

$$\frac{\partial}{\partial t}\int_\Omega \mathbf{q}(\mathbf{x},t)\,d\mathbf{x} + \int_\Omega \nabla\cdot\mathbf{f}(\mathbf{q}(\mathbf{x},t))\,d\mathbf{x} = \int_\Omega \mathbf{s}(\mathbf{x},t)\,d\mathbf{x}, \tag{4.2}$$

that is,

$$\int_\Omega \left(\frac{\partial}{\partial t}\mathbf{q}(\mathbf{x},t) + \nabla\cdot\mathbf{f}(\mathbf{q}(\mathbf{x},t)) - \mathbf{s}(\mathbf{x},t)\right) d\mathbf{x} = 0. \tag{4.3}$$

Since the equation above holds for any arbitrary domain Ω, it is possible to obtain the following differential form:

$$\mathbf{q}_t + \nabla\cdot\mathbf{f}(\mathbf{q}) = \mathbf{s}. \tag{4.4}$$

The above balance law is known as a hyperbolic conservation law when $\mathbf{s} = \mathbf{0}$. When $\mathbf{f}$ is a linear function of $\mathbf{q}$, we have a linear hyperbolic conservation law, whose solution is simply transported through the domain. On the other hand, when $\mathbf{f}$ is a nonlinear function of $\mathbf{q}$, the solution deforms as it evolves. Let us look at some classic examples of hyperbolic conservation laws:

Example 4.1.1 Linear transport equation. Let q denote the concentration of some material (a pollutant dispersed in water, for instance). If the water is flowing with velocity $\mathbf{u}$, the pollutant will be transported by this velocity, such that the flux is given by $\mathbf{f}(q) = \mathbf{u}q$. The conservation

law can be derived from (4.4) as

$$\frac{\partial q}{\partial t} + \nabla \cdot (\mathbf{u} q) = 0,$$

In one dimension, we have

$$\frac{\partial q}{\partial t} + \frac{\partial}{\partial x}(uq) = 0, \tag{4.5}$$

or equivalently,

$$q_t + u q_x = 0,$$

which is known as the advection equation [11].

[11]: LeVeque (2002), *Finite volume methods for hyperbolic problems*

Example 4.1.2 The Burgers' equation is a simple model that captures important properties of gas dynamics [12]. It can be obtained by choosing

$$f(q) = \frac{q^2}{2},$$

such that the conservation law reads

$$q_t + \left(q^2\right)_x = 0. \tag{4.6}$$

Can be often be presented in a non-conservative form

$$q_t + q\, q_x = 0.$$

This is a nonlinear hyperbolic equation that can develop discontinuities, and it is commonly used as a benchmark test for numerical methods.

[12]: Burgers (1948), 'A mathematical model illustrating the theory of turbulence'

Johannes Martinus Burgers (Netherlands, 1895 — USA, 1981).

Example 4.1.3 The Buckley-Leverett equation is nonlinear conservation equation used to model two-phase flow in porous media [13]. It describes an immiscible displacement process, such as the displacement of oil by water, in a one-dimensional or quasi-one-dimensional reservoir. This equation can be derived from the mass conservation equations of two-phase flows in porous media. Let $s(\mathbf{x}, t)$ be the variable of interest representing the water saturation in a fully saturated media, the model states that

$$\frac{\partial s}{\partial t} + \nabla \cdot \left(\varphi(s)\mathbf{u}\right) = 0, \tag{4.7}$$

with

$$\varphi(s) = \frac{Ms^2}{Ms^2 + (1-s)^2} \quad \text{and} \quad M = \frac{\mu_o}{\mu_w}. \tag{4.8}$$

The vector field $\mathbf{u}$ is the flow velocity, and μ_o and μ_w are the viscosities of oil and water, respectively.

[13]: Buckley et al. (1942), 'Mechanism of fluid displacement in sands'

Example 4.1.4 The Euler's equations of gas dynamics can be derived from the principles of conservation of mass, momentum and energy, leading to the multidimensional system of nonlinear hyperbolic equations given by

$$\mathbf{q}_t + \operatorname{div}(\mathbf{f}(\mathbf{q})) = \mathbf{0}$$

where

$$\mathbf{q} = \begin{bmatrix} \rho \\ \rho\mathbf{u} \\ E \end{bmatrix} \quad \text{and} \quad \mathbf{f}(\mathbf{q}) = \begin{bmatrix} \rho\mathbf{u} \\ \rho\mathbf{u} \otimes \mathbf{u} + p\mathbf{I} \\ (E+p)\mathbf{u} \end{bmatrix}.$$

This equation describes the evolution of density ρ, momentum $\rho\mathbf{u}$ and total energy $E = E_k + E_i$ which is the sum of kinetic (E_k) and internal (E_i) energies. The pressure is related to the internal energy through a equation of state of the form

$$E_i = \frac{p}{\gamma - 1}$$

where the constant γ is the gas' specific heat ratio as seen in Chapter 3. In three-dimensional space, this system has five unknowns, three of them are the components of the momentum, due to velocity. Another benchmark for numerical methods for nonlinear conservation laws is the one-dimensional version of this system, with only three unknowns.

4.2 Linear Hyperbolic Conservation Laws

To develop the mathematical theory and numerical methods for solving hyperbolic conservation laws, we begin by considering simple one-dimensional problems.

4.2.1 Solution of the Advection Equation

Let us first consider the advection (4.5), which can also be written as

$$q_t + uq_x = 0, \tag{4.9}$$

where u is the constant given velocity of the moving fluid.

To determine the solution of problem in (4.9) with initial condition $q(x,0) = q_0(x)$, we consider a parameterization of the variables x and t in the form $x = x(\zeta)$, $t = t(\zeta)$, so that

$$q(x,t) = q(x(\zeta), t(\zeta)).$$

Then,

$$\frac{dq}{d\zeta} = \frac{\partial q}{\partial t}\frac{dt}{d\zeta} + \frac{\partial q}{\partial x}\frac{dx}{d\zeta} = q_t\frac{dt}{d\zeta} + q_x\frac{dx}{d\zeta}.$$

This expression matches (4.9) when

$$\frac{dx}{d\zeta} = u \qquad \text{and} \qquad \frac{dt}{d\zeta} = 1, \tag{4.10}$$

yielding

$$\frac{dq}{d\zeta} = q_t + uq_x = 0,$$

meaning that the solution $q(x,t)$ is constant along the parameter ζ. Solving the system in (4.10), we find

$$x(\zeta) = x_0 + u\zeta \qquad \text{and} \qquad t(\zeta) = t_0 + \zeta = \zeta,$$

assuming $t_0 = 0$. Hence,

$$q(x,t) = q(x(\zeta), t(\zeta)) = q(x_0 + u\zeta, \zeta).$$

Since $q(x,t)$ is constant with respect to ζ and, at $\zeta = 0$, we have $q(x,t) = q(x_0, 0)$, using the initial condition, we obtain

$$q(x,t) = q_0(x_0) = q_0(x - u\zeta) = q_0(x - ut), \tag{4.11}$$

i.e., the values of the solution $q(x,t)$ are simply transported with velocity

$$\frac{dx}{dt} = u. \tag{4.12}$$

One of the fundamental properties of hyperbolic equations is wave propagation, meaning the solution consists of a translation of the initial condition, preserving its shape [14, 15]. Figure 4.2 illustrates this behavior for the case of constant $u > 0$.

It is important to note that initial conditions for hyperbolic problems may include discontinuities, which are propagated over time [11, 14]. Figure 4.3 illustrates this behavior with $u = 1$ and a discontinuous initial condition:

$$q_0(x) = \begin{cases} 1, & \text{if } x \leq 0, \\ 0, & \text{if } x > 0. \end{cases} \tag{4.13}$$

[14]: Thomas (2013), *Numerical partial differential equations: finite difference methods*
[15]: Cuminato et al. (2013), *Discretização de equações diferenciais parciais: técnicas de diferenças finitas*

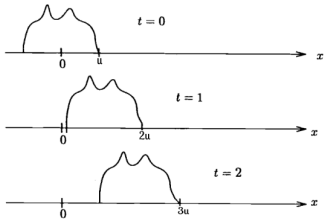

Figure 4.2: Behavior of the solution $q(x,t)$ for constant $u > 0$.

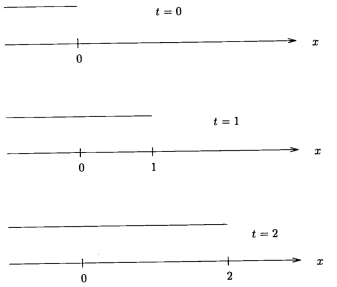

Figure 4.3: Solution $q(x,t)$ with $u = 1$ and discontinuous initial condition.

4.2.2 Characteristic Curves

The trajectories

$$X(t) = x_0 + ut, \tag{4.14}$$

solutions of equation (4.12), are called **characteristic curves** of (4.9), along which the equation simplifies to:

$$\frac{d}{dt} q(X(t), t) = q_t + uq_x = 0. \tag{4.15}$$

Therefore, the solution $q(x,t)$ remains constant along each characteristic. If u is constant, the characteristics are parallel straight lines, as illustrated in Figure 4.4 for $u > 0$ and $u < 0$, respectively.

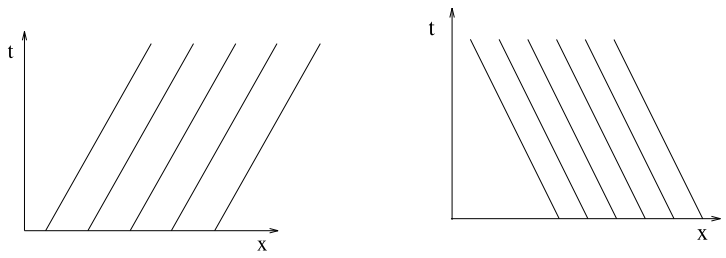

Figure 4.4: Characteristic curves for $u > 0$ and $u < 0$ constants, respectively.

In more general cases, the characteristics are not necessarily straight. For the case $u = u(t) = t$, the characteristics are:

$$X(t) = x_0 + \frac{t^2}{2}, \tag{4.16}$$

whereas for $u = u(x) = x$, they are given by

$$X(t) = x_0 e^t, \tag{4.17}$$

both cases illustrated in Figure 4.5.

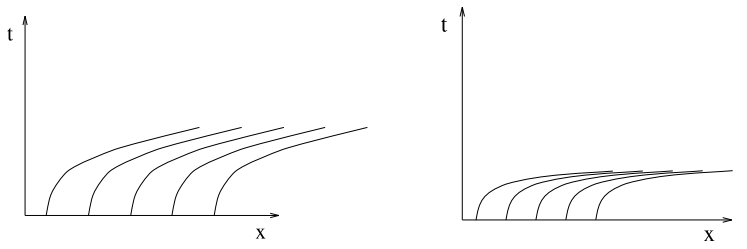

Figure 4.5: Characteristic curves for $u(t) = t$ and $u(x) = x$, respectively.

4.2.3 Boundary Conditions

In addition to the initial values, the appropriate specification of boundary conditions is an essential part of formulating hyperbolic problems.

Each point on the initial curve influences the solution along the characteristic that passes through it. This information is critical when defining boundary data. For instance, for $a < x < b$ with constant velocity $u > 0$, the concentration must be specified at the inflow boundary $x = a$. If $u < 0$, the boundary condition must be imposed at $x = b$. Figure 4.6 illustrates these two cases.

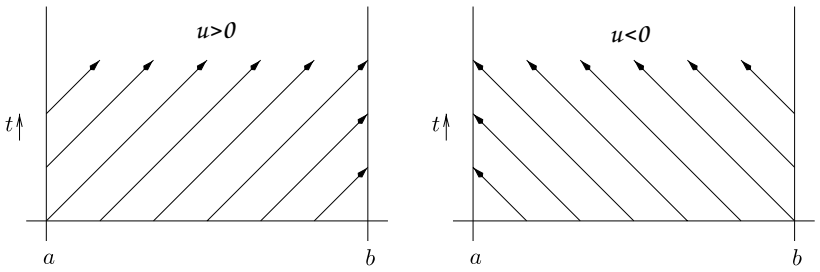

Figure 4.6: Specification of boundary conditions at inflow boundaries for constant u and $a < x < b$.

4.2.4 Riemann Problem

A Riemann problem consists of a conservation law with an initial condition given by a Heaviside-type function:

$$q(x,0) = \begin{cases} q_L, & x \le 0, \\ q_R, & x > 0, \end{cases} \tag{4.18}$$

with $q_L \neq q_R$. For the advection (4.9) with constant $u > 0$, the solution is piecewise constant:

$$q(x,t) = \begin{cases} q_L, & x \le ut, \\ q_R, & x > ut, \end{cases} \tag{4.19}$$

as shown Figure 4.3 for $u = 1$, $q_L = 1$, and $q_R = 0$.

Bernhard Riemann
(Germany, 1826 — Italy, 1866).

4.2.5 Variable Coefficients

If the fluid velocity varies with position, i.e., $u = u(x)$, we obtain the advection equation with variable coefficients:

$$q_t + \big(u(x)q\big)_x = 0. \tag{4.20}$$

In this case, the characteristic curves $X(t)$ satisfy the ordinary differential equation:

$$X'(t) = u(X(t)), \tag{4.21}$$

and are therefore not straight lines in general.

Along the characteristics, the equation becomes:

$$\begin{aligned}\frac{d}{dt}q(X(t),t) &= q_t + X'(t)q_x \\ &= q_t + u(X(t))q_x \\ &= q_t + \big(u(X(t))q\big)_x - u'(X(t))q \\ &= -u'(X(t))q(X(t),t).\end{aligned}$$

Thus, the solution q is no longer constant along characteristics, but the equation reduces to an ODE system, which admits a solution as long as u is Lipschitz continuous.

Equation (4.20) is written in conservative form. It is also common to encounter the non-conservative form:

$$q_t + u(x)q_x = 0.$$

In this case, the characteristics still satisfy (4.21), but the total derivative of the solution along each curve is zero, meaning q remains constant along each characteristic.

4.3 Finite volume methods for hyperbolic conservation laws

Since the numerical solution of hyperbolic equations admits discontinuities, for the computed solution to be representative of the physical problem, these discontinuities must be properly handled by the numerical methods. These methods must take into account the direction and speed of information propagation throughout the computational domain. Finite volume schemes, which are derived from the integral form of the conservation law, are suitable for this type of problem.

Finite volume methods consider hyperbolic conservation laws of the form (4.4), with source $s = 0$, or, in the one-dimensional case:

$$\frac{\partial q}{\partial t} + \frac{\partial}{\partial x}f(q) = 0. \tag{4.22}$$

We consider a discretization of the computational domain in space and time, as shown in Figure 4.8. For simplicity, we consider a uniform

discretization centered at the points x_j, $j = 1, \cdots, N$, such that the interfaces between two control volumes V_{j-1} and V_j are given by

$$x_{j-\frac{1}{2}} = x_j - \frac{\Delta x}{2}. \tag{4.23}$$

Thus, each control volume is defined by

$$V_j = [x_{j-\frac{1}{2}}, x_{j+\frac{1}{2}}). \tag{4.24}$$

Time discretization is also uniform, with each time step of size Δt, and time levels denoted by $t^n = n\Delta t$.

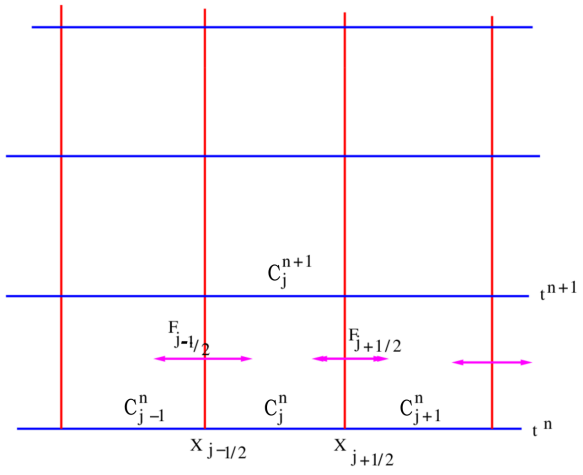

Figure 4.8: Representation of a finite volume discretization for hyperbolic conservation laws.

At each time step t^n, the approximation of the solution in control volume V_j is given by an average value of the concentration in that computational cell:

$$Q_j^n = Q(x_j, t^n) \approx \frac{1}{\Delta x} \int_{x_{j-\frac{1}{2}}}^{x_{j+\frac{1}{2}}} q(x, t^n) dx. \tag{4.25}$$

If the approximation Q_j^n is known at some time step t^n, the finite volume method computes the approximation Q_j^{n+1} at the next time step t^{n+1} by integrating the conservation law (4.22) over the domain $[x_{j-\frac{1}{2}}, x_{j+\frac{1}{2}}) \times [t^n, t^{n+1})$, that is,

$$\int_{t^n}^{t^{n+1}} \int_{x_{j-\frac{1}{2}}}^{x_{j+\frac{1}{2}}} \left(\frac{\partial q}{\partial t} + \frac{\partial}{\partial x} f(q) \right) dx\, dt = 0. \tag{4.26}$$

Integrating results in

$$\begin{aligned} \int_{x_{j-\frac{1}{2}}}^{x_{j+\frac{1}{2}}} q(x, t^{n+1}) dx - \int_{x_{j-\frac{1}{2}}}^{x_{j+\frac{1}{2}}} q(x, t^n) dx \\ = - \int_{t^n}^{t^{n+1}} f\left(q(x_{j+\frac{1}{2}}, t)\right) dt + \int_{t^n}^{t^{n+1}} f\left(q(x_{j-\frac{1}{2}}, t)\right) dt. \end{aligned} \tag{4.27}$$

Defining the time average of the flux function:

$$\bar{F}_{j+\frac{1}{2}}^n = \frac{1}{\Delta t} \int_{t^n}^{t^{n+1}} f\left(q(x_{j+\frac{1}{2}}, t)\right) dt, \tag{4.28}$$

and dividing both sides of (4.27) by Δx, we obtain:

$$Q_j^{n+1} = Q_j^n - \frac{\Delta t}{\Delta x}\left(\bar{F}^n_{j+\frac{1}{2}} - \bar{F}^n_{j-\frac{1}{2}}\right). \tag{4.29}$$

The equation above establishes a conservation principle: the average change in concentration in the cell is given by the difference in fluxes at its boundaries. Different finite volume schemes can be obtained using different approximations

$$F^n_{j+\frac{1}{2}} \simeq \bar{F}^n_{j+\frac{1}{2}},$$

which are called **discrete fluxes**, used to approximate the time average of the flux function given in (4.28), resulting in the following numerical method

$$Q_j^{n+1} = Q_j^n - \frac{\Delta t}{\Delta x}\left(F^n_{j+\frac{1}{2}} - F^n_{j-\frac{1}{2}}\right). \tag{4.30}$$

We now present some choices for the approximations of the discrete fluxes $F^n_{j+\frac{1}{2}}$ for linear hyperbolic conservation laws with constant coefficients, that is, $f(q) = uq$, with u constant.

4.3.1 Central scheme

The most intuitive attempt to define the flux at $x_{j+\frac{1}{2}}$ is to take the average between the data to the left, Q_j, and to the right, Q_{j+1}:

$$F^n_{j+\frac{1}{2}} = \frac{1}{2}\left(f(Q_j^n) + f(Q_{j+1}^n)\right) = \frac{u}{2}\left(Q_j^n + Q_{j+1}^n\right) \tag{4.31}$$

and thus, equation (4.29) becomes

$$Q_j^{n+1} = Q_j^n - \frac{u\Delta t}{2\Delta x}\left(Q_{j+1}^n - Q_{j-1}^n\right). \tag{4.32}$$

In practice, this method is not useful, as it is not a stable method for hyperbolic problems, as we will see below.

Peter David Lax (Hungary, 1926 –).

4.3.2 Lax-Friedrichs

The Lax-Friedrichs method, whose fluxes are given by

$$F^n_{j+\frac{1}{2}} = \frac{u}{2}\left(Q_{j+1}^n + Q_j^n\right) - \frac{\Delta x}{2\Delta t}\left(Q_{j+1}^n - Q_j^n\right), \tag{4.33}$$

is a small modification of the central scheme to provide a stable approximation. Writing the Lax-Friedrichs method in the form of equation (4.29), we obtain

$$Q_j^{n+1} = \frac{1}{2}\left(Q_{j-1}^n + Q_{j+1}^n\right) - \frac{u\Delta t}{2\Delta x}\left(Q_{j+1}^n - Q_{j-1}^n\right). \tag{4.34}$$

Note that the modification with respect to the central method is that the value of Q_j^n in equation (4.32) has been replaced by the average $(Q_{j-1}^n + Q_{j+1}^n)/2$.

4.3.3 Lax-Wendroff

The Lax-Wendroff method, with numerical fluxes defined by

$$F^n_{j+\frac{1}{2}} = \frac{u}{2}\left(Q^n_{j+1} + Q^n_j\right) - \frac{u^2\Delta t}{2\Delta x}\left(Q^n_{j+1} - Q^n_j\right), \tag{4.35}$$

is a method that uses Taylor series expansions in time of the solution $q(x,t)$ to achieve formal second-order accuracy. Writing the Lax-Wendroff method in the form of equation (4.29) gives

$$Q^{n+1}_j = Q^n_j - \frac{u\Delta t}{2\Delta x}\left(Q^n_{j+1} - Q^n_{j-1}\right) + \frac{u^2(\Delta t)^2}{2(\Delta x)^2}\left(Q^n_{j+1} - 2Q^n_j + Q^n_{j-1}\right). \tag{4.36}$$

Note that

$$q_t = -\big(f(q)\big)_x = -uq_x \tag{4.37}$$

and

$$q_{tt} = \big(-uq_x\big)_t = -u\big(q_x\big)_t = -u\big(q_t\big)_x = -u\big(-uq_x\big)_x = u^2 q_{xx}, \tag{4.38}$$

therefore, if we consider Taylor series expansions in time for a smooth function $q(x,t)$, we obtain:

$$q(x_j, t^{n+1}) = q(x_j, t^n) + \Delta t\, q_t(x_j, t^n) + \frac{\Delta t^2}{2} q_{tt}(x_j, t^n) + \mathcal{O}(\Delta t^3),$$

that is,

$$q(x_j, t^{n+1}) = q(x_j, t^n) - u\Delta t\, q_x(x_j, t^n) + \frac{u^2\Delta t^2}{2} q_{xx}(x_j, t^n) + \mathcal{O}(\Delta t^3).$$

Approximating the spatial derivatives by second-order central finite differences [16]

$$q_x(x_j, t^n) \approx \frac{Q^n_{j+1} - Q^n_{j-1}}{2\Delta x} \tag{4.39}$$

and

$$q_{xx}(x_j, t^n) \approx \frac{1}{(\Delta x)^2}(Q^n_{j+1} - 2Q^n_j + Q^n_{j-1}), \tag{4.40}$$

we obtain the same approximation as in equation (4.36).

[16]: LeVeque (2007), *Finite difference methods for ordinary and partial differential equations: steady-state and time-dependent problems*

4.3.4 Upwind

The methods considered previously were all centered methods, symmetric with respect to the point where we are updating the solution. However, for hyperbolic problems, we expect information to propagate as waves moving along characteristics. Therefore, it makes sense to try to use the knowledge of the solution structure to define the numerical flux functions. This idea leads to upwind methods, where the information at each point is obtained by looking in the direction from which this information is propagating.

For the scalar advection equation, there is only one velocity, which is either positive or negative, and therefore, an upwind method is a unilateral method, with values determined based on information either to the left or to the right.

In Figure 4.10, we illustrate how information in a cell is propagated from the time step t^n to t^{n+1}. For positive u, the flux at the face $x_{j+\frac{1}{2}}$ depends only on Q^n_{j-1}, while this same flux depends only on Q^n_{j+1} when u is negative.

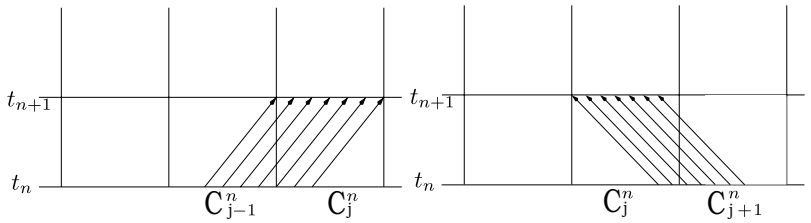

Figure 4.10: Information propagation in a cell from time step t^n to t^{n+1}.

These observations suggest that the numerical flux be defined as follows:

$$F^n_{j+\frac{1}{2}} = \begin{cases} uQ^n_j, & \text{if } u > 0 \\ uQ^n_{j+1}, & \text{if } u < 0. \end{cases} \tag{4.41}$$

Thus, the equation (4.29) for the upwind method is given by:

$$Q^{n+1}_j = Q^n_j - \frac{u\Delta t}{\Delta x}\left(Q^n_j - Q^n_{j-1}\right), \quad \text{if } u > 0 \tag{4.42}$$

and

$$Q^{n+1}_j = Q^n_j - \frac{u\Delta t}{\Delta x}\left(Q^n_{j+1} - Q^n_j\right), \quad \text{if } u < 0. \tag{4.43}$$

We can also analyze the upwind method from a wave propagation perspective. Consider the jump functions:

$$\mathcal{W}_{j+\frac{1}{2}} = Q^n_{j+1} - Q^n_j \tag{4.44}$$

and

$$\mathcal{W}_{j-\frac{1}{2}} = Q^n_j - Q^n_{j-1}, \tag{4.45}$$

which represent, respectively, the waves moving towards cells V_{j+1} and V_j with velocity u. Returning to the expressions (4.42) and (4.43), we have:

$$Q^{n+1}_j = Q^n_j - \frac{u\Delta t}{\Delta x}\mathcal{W}_{j-\frac{1}{2}}, \quad \text{if } u > 0 \tag{4.46}$$

and

$$Q^{n+1}_j = Q^n_j - \frac{u\Delta t}{\Delta x}\mathcal{W}_{j+\frac{1}{2}}, \quad \text{if } u < 0. \tag{4.47}$$

Defining the discrete fluxes as:

$$F^n_{j+\frac{1}{2}} = u^+Q^n_j + u^-Q^n_{j+1}, \tag{4.48}$$

where $u^+ = \max\{u, 0\}$ and $u^- = \min\{u, 0\}$, we can combine (4.46) and (4.47) into a single formula:

$$\begin{aligned} Q^{n+1}_j &= Q^n_j - \frac{\Delta t}{\Delta x}\left(u^+Q^n_j + u^-Q^n_{j+1} - u^+Q^n_{j-1} - u^-Q^n_j\right) \\ &= Q^n_j - \frac{\Delta t}{\Delta x}\left(u^+\mathcal{W}_{j-\frac{1}{2}} + u^-\mathcal{W}_{j+\frac{1}{2}}\right). \end{aligned} \tag{4.49}$$

4.4 The CFL condition

Richard Courant
(Poland, 1888 — USA, 1972).

The CFL condition (after Richard Courant, Kurt Friedrichs, and Hans Lewy) is a necessary, but not sufficient, condition to ensure convergence of the finite volume method for the differential equation as the mesh is refined. This means that if the CFL condition is satisfied, the method may or may not converge, depending on its consistency and stability properties. However, if it is not satisfied, the numerical method has no chance of converging.

The solution of (4.9) is given by (4.11), where the value of q is constant along each characteristic. For example, if the characteristic curve is a straight line, then for each time step, the exact solution satisfies

$$q(x, t^{n+1}) = q(x - u\Delta t, t^n), \tag{4.50}$$

i.e., the solution at (x_j, t^{n+1}) depends on the information located at the point $(x_j - u\Delta t, t^n)$. Since the finite volume method computes spatial averages, the approximate solution Q_j^n should be compared with

$$q_j^n = \frac{1}{\Delta x} \int_{x_{j-\frac{1}{2}}}^{x_{j+\frac{1}{2}}} q(x, t^n)\, dx, \tag{4.51}$$

which is the exact value of this average.

Kurt Otto Friedrichs
(Germany, 1901 — USA, 1982).

The finite volume schemes presented so far are explicit methods and can be written with an update function of the form

$$Q_j^{n+1} = \mathscr{H}(Q_{j-1}^n, Q_j^n, Q_{j+1}^n), \tag{4.52}$$

depending on the chosen scheme. Therefore, the construction of the numerical solution Q_j^{n+1} in the control volume V_j depends on the information confined in V_j and neighboring volumes V_{j-1} and V_{j+1}, i.e., in the interval $[x_{j-\frac{3}{2}}, x_{j+\frac{3}{2}}]$ at time t^n.

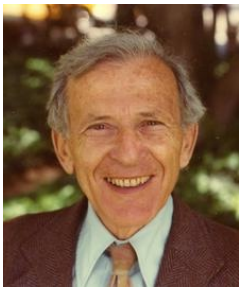

Hans Lewy
(Poland, 1904 — USA, 1988).

Unfolding the recurrences up to $t^0 = 0$, it is easy to see that the analytical solution is given by

$$q(x, t^{n+1}) = q_0(x - u\ t^{n+1}) = q_0(x - (n+1)u\Delta t), \tag{4.53}$$

so the information composing the average q_j^{n+1} of the exact solution, which is propagated along characteristics, is contained in the interval

$$\left[x_{j-\frac{1}{2}} - u\ t^{n+1},\ x_{j+\frac{1}{2}} - u\ t^{n+1}\right] = \left[x_{j-\frac{1}{2}} - (n+1)u\Delta t,\ x_{j+\frac{1}{2}} - (n+1)u\Delta t\right]. \tag{4.54}$$

On the other hand, the numerical solution will be computed based on the values $Q_{j-1-n}^0, \ldots, Q_j^0, \ldots, Q_{j+1+n}^0$, and therefore the information propagated for the construction of Q_j^{n+1} is confined in the interval

$$\left[x_{j-\frac{1}{2}-(n+1)},\ x_{j+\frac{1}{2}+(n+1)}\right] = \left[x_{j-\frac{1}{2}} - (n+1)\Delta x,\ x_{j+\frac{1}{2}} + (n+1)\Delta x\right]. \tag{4.55}$$

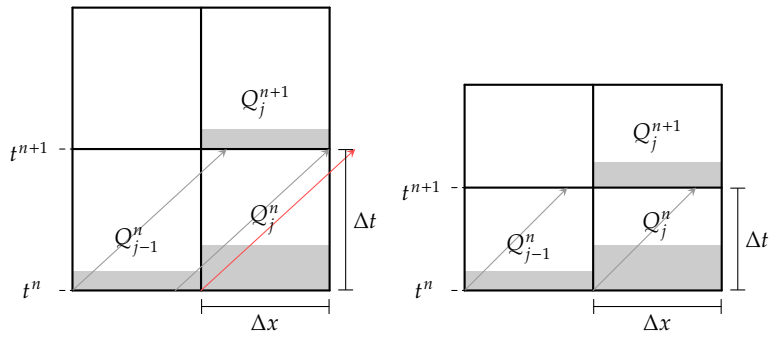

Figure 4.14: Information propagation from t^n to t^{n+1}, for $u = 1$, showing a case where the choice of Δt and Δx does not satisfy CFL (left), and one where Δt and Δx do satisfy CFL (right).

The main idea of the CFL condition is that the numerical method will only have a chance of converging to the exact solution with the refinement of Δt and Δx if the original information carried by the characteristic curves comes from a region covered by the numerical method's recurrence. In other words, if the interval defined in (4.54) is contained in the interval defined in equation (4.55). An algebraic calculation shows that this only happens if

$$\nu := u\frac{\Delta t}{\Delta x} \leq 1, \tag{4.56}$$

where u is constant and ν is known as the Courant number [11]. If this condition is not satisfied, the numerical method has no chance of converging, since the numerical solution will be built using information that does not lead to the exact solution of the problem.

We can generalize these concepts using the following definition and by stating Theorem 4.4.1.

Definition 4.4.1 (Domain of dependence) *The domain of dependence $\mathcal{D}$ of a solution of a hyperbolic conservation law at a certain time t is the set of points at $t = 0$ that can influence the solution value at time t.*

Example 4.4.1 According to the calculations above, for $u > 0$ we have

$$\begin{aligned}\mathcal{D}(q(x_j, t^{n+1})) &= \{x_j - u\ t^{n+1}\}\\ \mathcal{D}(q_j^{n+1}) &= \left[x_{j-\frac{1}{2}} - u\ t^{n+1},\ x_{j+\frac{1}{2}} - u\ t^{n+1}\right]\\ \mathcal{D}(Q_j^{n+1}) &= \left[x_{j-\frac{1}{2}} - (n+1)\Delta x,\ x_{j+\frac{1}{2}} + (n+1)\Delta x\right].\end{aligned}$$

Theorem 4.4.1 (CFL condition) *A necessary (but not sufficient) condition for the convergence of a finite-volume approximation to the exact solution of a hyperbolic conservation law is that the domain of dependence of the exact solution must be contained in the domain of dependence of the approximate solution, for all $\Delta t, \Delta x \to 0$.*

Therefore, according to Theorem 4.4.1, for the finite volume method we must have

$$\mathcal{D}(q_j^{n+1}) \subset \mathcal{D}(Q_j^{n+1}). \tag{4.57}$$

Figure 4.14 presents two examples of mesh spacing choices Δt and Δx that may or may not satisfy the CFL condition, with the same velocity

$u = 1$. In Figure 4.14 (left), the choice does not satisfy CFL since $\Delta t > \Delta x$, a situation in which Theorem 4.4.1 guarantees that the method will not converge. It is possible to see that from time t^n to t^{n+1}, information can propagate beyond one cell. On the other hand, in Figure 4.14 (right), where $\Delta t < \Delta x$, there is a chance (but no guarantee) that the method is convergent according to Theorem 4.4.1. In this case, we see that information never propagates beyond neighboring volumes.

Remark 4.4.1 The observation made in the previous paragraph is, in fact, another interpretation of the CFL condition: It is satisfied if a wave $\mathcal{W}_{j+\frac{1}{2}}$ originating at $x_{j+\frac{1}{2}}$ does not travel a distance greater than Δx in a time interval Δt.

4.5 Consistency, Stability, and Convergence

To assess the accuracy and convergence of finite volume methods for hyperbolic conservation laws, we define the global error at a fixed time $T = N\Delta t$ by

$$\mathbf{e}^N = \mathbf{Q}^N - \mathbf{q}^N, \tag{4.58}$$

where $\mathbf{Q}^N$ is the vector of finite volume approximations and $\mathbf{q}^N$ is the vector of the exact solution. In the context of one-dimensional finite volumes, for each cell j we compare Q_j^N with

$$q_j^N = \frac{1}{\Delta x}\int_{x_{j-\frac{1}{2}}}^{x_{j+\frac{1}{2}}} q(x, t^N)\, dx. \tag{4.59}$$

To simplify the notation, it is usually assumed that Δt and Δx are related. Since the CFL condition for this problem requires that (4.56) be satisfied to ensure the possibility of convergence, the ratio $\Delta t/\Delta x$ is fixed (in this case equal to $1/u$). In this context, we have the following definition:

Definition 4.5.1 *(Convergence) A finite volume method of the form (4.29) converges to the analytical solution of (4.22), in a norm $\|\cdot\|$, if*

$$\lim_{\substack{\Delta t \to 0 \\ T = N\Delta t}} \|\mathbf{e}^N\| = 0,$$

for all $0 < T < T_{\max}$, with $T = N\Delta t$.

The convergence of finite volume methods for hyperbolic equations is governed by the following theorem.

Theorem 4.5.1 (Lax equivalence theorem) *A consistent finite volume scheme of the form* (4.30) *is convergent if, and only if, it is stable [16].*

Thus, we must analyze consistency and stability of a numerical method to determine whether it is convergent or not, which will be summarized in the next sections.

4.5.1 Local Truncation Error

Any explicit numerical method can be written as

$$\mathbf{Q}^{n+1} = \mathcal{N}(\mathbf{Q}^n), \tag{4.60}$$

where $\mathcal{N}(\cdot)$ represents the numerical operator that approximates the solution at the time step t^{n+1}, given the previously computed solution at time t^n. At each time step, a local error is introduced, defined as the difference between the exact solution at t^{n+1} ($\mathbf{q}^{n+1}$) and the value that the method would compute at time t^{n+1}, assuming all previous steps were computed exactly ($\mathcal{N}(\mathbf{q}^n)$). The accumulation of this difference at each step is called the local truncation error, given by

$$\boldsymbol{\tau}^n = \frac{1}{\Delta t}\left(\mathcal{N}(\mathbf{q}^n) - \mathbf{q}^{n+1}\right). \tag{4.61}$$

The local truncation error provides an indication of the behavior of the global error in terms of its order of accuracy.

Definition 4.5.2 (Consistency) *A method $\mathcal{N}(\cdot)$ is said to be consistent with the differential equation if its the local truncation error goes to zero as $\Delta t \to 0$:*

$$\lim_{\Delta t \to 0} \|\boldsymbol{\tau}^n\| = 0.$$

It is possible to estimate the truncation error of the methods mentioned here by using Taylor series expansions of the solution. However, we need the additional requirement of sufficient smoothness of the solution $q(x,t)$, a property that is not straightforwardly guaranteed, especially with non-smooth initial conditions. Below we illustrate how the local truncation error can be estimated for some of the methods previously introduced, always supposing enough smoothness of q.

Upwind

Consider the upwind scheme for the advection equation with constant velocity $u > 0$, given by

$$Q_j^{n+1} = Q_j^n - \frac{u\Delta t}{\Delta x}\left(Q_j^n - Q_{j-1}^n\right).$$

Applying this method to the exact solution, we obtain the following local truncation error

$$\boldsymbol{\tau}^n = \frac{1}{\Delta t}\left[q(x_j,t^n) - \frac{u\Delta t}{\Delta x}\left(q(x_j,t^n) - q(x_{j-1},t^n)\right) - q(x_j,t^{n+1})\right].$$

Assuming sufficient smoothness for q, the terms $q(x_{j-1},t^n)$ and $q(x_j,t^{n+1})$ can be expanded in Taylor series around (x_j,t^n), resulting in

$$q(x_{j-1},t^n) = q(x_j,t^n) - \Delta x q_x(x_j,t^n) + \frac{\Delta x^2}{2} q_{xx}(x_j,t^n) - \mathcal{O}\left(\Delta x^3\right)$$

and

$$q(x_j, t^{n+1}) = q(x_j, t^n) + \Delta t\, q_t(x_j, t^n) + \frac{\Delta t^2}{2} q_{tt}(x_j, t^n) + \mathcal{O}(\Delta t^3).$$

Therefore,

$$\begin{aligned}\tau^n &= \frac{1}{\Delta t}\Bigg[q(x_j, t^n) - \frac{u\Delta t}{\Delta x}\Big(q(x_j, t^n) - q(x_j, t^n) + \Delta x\, q_x(x_j, t^n) \\ &\quad - \frac{\Delta x^2}{2} q_{xx}(x_j, t^n) + \mathcal{O}(\Delta x^3)\Big) - q(x_j, t^n) - \Delta t\, q_t(x_j, t^n) \\ &\quad - \frac{\Delta t^2}{2} q_{tt}(x_j, t^n) - \mathcal{O}(\Delta t^3)\Bigg] \\ &= -\Big(q_t(x_j, t^n) + u\, q_x(x_j, t^n)\Big) + \frac{u\Delta x}{2} q_{xx}(x_j, t^n) \\ &\quad - \mathcal{O}(\Delta x^2) - \frac{\Delta t}{2} q_{tt}(x_j, t^n) - \mathcal{O}(\Delta t^2).\end{aligned}$$

Since q is a solution of the advection equation, $q_t(x_j, t^n) + u\, q_x(x_j, t^n) = 0$, some terms vanish due to the equation

$$\tau^n = \frac{u\Delta x}{2} q_{xx}(x_j, t^n) - \mathcal{O}(\Delta x^2) - \frac{\Delta t}{2} q_{tt}(x_j, t^n) - \mathcal{O}(\Delta t^2).$$

Note that $q_{tt} = (q_t)_t = (-uq_x)_t = -u(q_t)_x = u^2(q_x)_x = u^2 q_{xx}$, due to the assumed smoothness of q. Thus, the local truncation error of the upwind method is given by

$$\tau^n = \frac{u\Delta x}{2}(1 - \nu) q_{xx}(x_j, t^n) + \mathcal{O}(\Delta t^2),$$

where $\nu = u\Delta t/\Delta x$ is the Courant number, which establishes the relation between Δt and Δx that must be satisfied in a convergent setting. Therefore, the truncation error is governed by Δx (or Δt), and the method is first-order consistent.

Lax-Friedrichs

The local truncation error of the Lax-Friedrichs scheme is given by

$$\begin{aligned}\tau^n &= \frac{1}{2}\left(\frac{\Delta x^2}{\Delta t} - u^2\Delta t\right) q_{xx}(x_j, t^n) + \mathcal{O}(\Delta t^2) \\ &= \frac{u\Delta x}{2}\left(\frac{1}{\nu} - \nu\right) q_{xx}(x_j, t^n) + \mathcal{O}(\Delta t^2).\end{aligned}$$

That is, the truncation error is dominated by a term of order Δx (or Δt), and the method is first-order.

Lax-Wendroff

The local truncation error of the Lax-Wendroff scheme is given by

$$\tau^n = -\frac{u\Delta x^2}{6}(1 - \nu^2) q_{xxx}(x_j, t^n) + \mathcal{O}(\Delta t^3).$$

Therefore, the truncation error is dominated by a term of order Δx^2, and the method is second-order.

4.5.2 Flux consistency

In finite volume schemes, it is common to check the consistency by analyzing the numerical flux. Note that the numerical fluxes defined above are all two-point flux formulas, meaning that

$$F^n_{j+\frac{1}{2}} = \mathcal{F}(Q^n_j, Q^n_{j+1}).$$

If the solution is constant in x, it will also not change in time, therefore $q(x,t) = \bar{q}$ and the time average of the flux function reduces to $f(\bar{q})$. As a result, if $Q^n_j = Q^n_{j+1} = \bar{q}$, then we expect that

$$\mathcal{F}(\bar{q}, \bar{q}) = f(\bar{q})$$

for any value of $\bar{q}$, which is often used as a definition of flux consistency. In fact, as $Q^n_j, Q^n_{j+1} \to \bar{q}$, we expect that $\mathcal{F}(Q^n_j, Q^n_{j+1}) \to f(\bar{q})$ continuously, therefore an additional assumption of *Lipschitz continuity* is also required:

$$|\mathcal{F}(u,v) - f(\bar{q})| \leq L \max\left(|u-\bar{q}|, |v-\bar{q}|\right),$$

for any $u, v, \bar{q}$.

Exercises

1. Compute the truncation errors of Lax-Friedrichs and Lax-Wendroff schemes.
2. What does it mean the Courant number $\nu = 1$? What effect it produces on the aforementioned methods? Why?

4.5.3 Linear stability

Before analyzing the stability of the methods discussed, it is necessary to review some basic properties of stability. Suppose that at time step t^n, we have an approximation $\mathbf{Q}^n$ with error $\mathbf{e}^n$. Recalling equation (4.58), we can write

$$\mathbf{Q}^n = \mathbf{q}^n + \mathbf{e}^n.$$

By applying the numerical method to obtain $\mathbf{Q}^{n+1}$, we have

$$\mathbf{Q}^{n+1} = \mathcal{N}(\mathbf{Q}^n) = \mathcal{N}(\mathbf{q}^n + \mathbf{e}^n),$$

so that

$$\begin{aligned}
\mathbf{e}^{n+1} &= \mathbf{Q}^{n+1} - \mathbf{q}^{n+1} \\
&= \mathcal{N}(\mathbf{q}^n + \mathbf{e}^n) - \mathbf{q}^{n+1} \\
&= \mathcal{N}(\mathbf{q}^n + \mathbf{e}^n) - \mathcal{N}(\mathbf{q}^n) + \mathcal{N}(\mathbf{q}^n) - \mathbf{q}^{n+1} \\
&= \mathcal{N}(\mathbf{q}^n + \mathbf{e}^n) - \mathcal{N}(\mathbf{q}^n) + \Delta t\, \boldsymbol{\tau}^n. \qquad (4.62)
\end{aligned}$$

Thus, the global error will be the accumulation of $\mathcal{N}(\mathbf{q}^n + \mathbf{e}^n) - \mathcal{N}(\mathbf{q}^n)$, which measures the effect of the numerical method on the global error

from the previous step, and the accumulation of $\Delta t\ \boldsymbol{\tau}^n$, which accounts for the error introduced in the current time step. We have previously seen that the study of the local truncation error allows us to bound the accumulation of the term $\Delta t\ \boldsymbol{\tau}^n$. The stability theory, in turn, will be developed to bound the term $\mathcal{N}(\mathbf{q}^n + \mathbf{e}^n) - \mathcal{N}(\mathbf{q}^n)$. Combining the two techniques will allow us to bound the global error, which is part of the proof of the Lax theorem 4.5.1 for hyperbolic equations.

If the operator $\mathcal{N}(\cdot)$ is linear, then

$$\mathcal{N}(\mathbf{q}^n + \mathbf{e}^n) - \mathcal{N}(\mathbf{q}^n) = \mathcal{N}(\mathbf{q}^n) + \mathcal{N}(\mathbf{e}^n) - \mathcal{N}(\mathbf{q}^n) = \mathcal{N}(\mathbf{e}^n)$$

and thus, by unrolling the recurrence in equation (4.62) and applying a norm to both sides, we get

$$\|\mathbf{e}^{n+1}\| \leq \|\mathcal{N}^n(\mathbf{e}^0)\| + \Delta t \sum_{\ell} \|\boldsymbol{\tau}^\ell\|. \tag{4.63}$$

Note that n appears as an index on the left-hand side and as an exponent on the right-hand side of (4.63), representing the number of successive applications of the operator $\mathcal{N}$. Since the method is consistent, the local truncation error will be bounded, so it remains to ensure that $\mathcal{N}^n(\mathbf{e}^0)$ is also bounded in order to achieve convergence. Therefore, we derive a condition on the norm of the linear operator $\mathcal{N}$ for each time T:

$$\|\mathcal{N}^n\| \leq L,$$

for all $n \leq N = T/\Delta t$, where L is a constant independent of n. In other words, for the global error to be bounded, we require that the nth power of the linear operator $\mathcal{N}$ be uniformly bounded up to the time of interest T. For linear methods, this form of stability is known as Lax-Richtmyer stability [11, 16].

4.5.4 The von Neumann stability criterion

For linear Cauchy problems with constant coefficients, stability is particularly simple to analyze in the 2-norm, since Fourier analysis can be used to simplify the problem [15]. This is the basis of the von Neumann stability criterion, where it is assumed that Q_j^n has finite norm and, therefore, can be expressed as a Fourier series:

$$Q_j^n = \frac{1}{\sqrt{2\pi}} \int_{-\infty}^{\infty} \hat{Q}^n(\xi) e^{i\xi j \Delta x} d\xi,$$

John von Neumann (Hungary, 1903 — USA, 1957).

where $i = \sqrt{-1}$. Applying linear finite volume schemes to Q_j^n, and manipulating the exponentials, it is possible to find an expression of the form

$$Q_j^{n+1} = \frac{1}{\sqrt{2\pi}} \int_{-\infty}^{\infty} \hat{Q}^n(\xi) g(\xi, \Delta x, \Delta t) e^{i\xi j \Delta x} d\xi,$$

where $g(\xi, \Delta x, \Delta t) \in \mathbb{C}$ is called the amplification factor for the wavenumber ξ, since one can define the recurrence

$$\hat{Q}^{n+1}(\xi) = g(\xi, \Delta x, \Delta t) \hat{Q}^n(\xi). \tag{4.64}$$

From Parseval's relation we have

$$\|\mathbf{Q}^n\|_2 = \|\hat{Q}^n\|_2,$$

where

$$\|\mathbf{Q}^n\|_2 = \left(\Delta x \sum_{j=-\infty}^{\infty} |Q_j^n|^2\right)^{\frac{1}{2}} \quad \text{and} \quad \|\hat{Q}^n\|_2 = \left(\int_{-\infty}^{\infty} |\hat{Q}^n(\xi)|^2 \, d\xi\right)^{\frac{1}{2}}.$$

To show that the 2-norm of $\mathbf{Q}^n$ is bounded, it is enough to show that the 2-norm of $\hat{Q}^n$ remains bounded. Note that the function $\hat{Q}^n$ satisfies equation (4.64) as ξ varies. Therefore, it is sufficient to consider an arbitrary wavenumber ξ and

$$Q_j^n = e^{i\xi j\Delta x}, \tag{4.65}$$

so that we can compute $g(\xi, \Delta x, \Delta t)$ using the recurrence

$$Q_j^{n+1}(\xi) = g(\xi, \Delta x, \Delta t) Q_j^n(\xi). \tag{4.66}$$

instead of equation (4.64). If we ensure that

$$|g(\xi, \Delta x, \Delta t)| \leq 1,$$

for all ξ, then numerical stability is guaranteed, as there will be no catastrophic amplification of Fourier modes.

The application of the von Neumann criterion is quite straightforward, and is best illustrated through a few examples:

Central scheme

Considering the central scheme

$$Q_j^{n+1} = Q_j^n - \frac{u\Delta t}{2\Delta x}\left(Q_{j+1}^n - Q_{j-1}^n\right),$$

and Q_j^n given by (4.65), so that

$$Q_j^{n+1} = g(\xi, \Delta x, \Delta t) e^{i\xi j\Delta x},$$

we have:

$$g(\xi, \Delta x, \Delta t) e^{i\xi j\Delta x} = e^{i\xi j\Delta x} - \frac{u\Delta t}{2\Delta x}\left(e^{i\xi(j+1)\Delta x} - e^{i\xi(j-1)\Delta x}\right),$$

that is,

$$\begin{aligned} g(\xi, \Delta x, \Delta t) &= 1 - \frac{u\Delta t}{2\Delta x}\left(e^{i\xi\Delta x} - e^{-i\xi\Delta x}\right) \\ &= 1 - \frac{u\Delta t}{2\Delta x}\left(2i\sin(\xi\Delta x)\right) \\ &= 1 - \nu\left(i\sin(\xi\Delta x)\right), \end{aligned}$$

where $\nu = u\Delta t/\Delta x$ is the Courant number. Thus we have

$$|g(\xi, \Delta x, \Delta t)| = \left(1 + \left(\nu \sin(\xi \Delta x)\right)^2\right)^{\frac{1}{2}}.$$

From the above expression we can conclude that $|g(\xi, \Delta x, \Delta t)| \geq 1$ always, and therefore, the central scheme is unstable, as we had mentioned in Section 4.3.1.

Upwind

Consider the upwind scheme for the advection equation with constant speed $u > 0$:

$$Q_j^{n+1} = (1 - \nu)Q_j^n + \nu\, Q_{j-1}^n,$$

where $\nu = u\Delta t/\Delta x$ is the Courant number. Writing Q_j^n as in (4.65) we have

$$\begin{aligned} g(\xi, \Delta x, \Delta t)e^{i\xi j\Delta x} &= (1 - \nu)e^{i\xi j\Delta x} + \nu e^{i\xi(j-1)\Delta x} \\ &= \left((1 - \nu) + \nu e^{-i\xi\Delta x}\right)e^{i\xi j\Delta x}, \end{aligned}$$

therefore,

$$g(\xi, \Delta x, \Delta t) = (1 - \nu) + \nu e^{-i\xi\Delta x}.$$

Note that $g(\xi, \Delta x, \Delta t)$ lies on a circle of radius ν in the complex plane, centered on the real axis at $1 - \nu$. This circle is entirely contained within the unit circle, that is, $|g| \leq 1\ \forall\, \xi$ if and only if $0 \leq \nu \leq 1$. As this inequality is always satisfied due to the CFL condition, we can conclude that the upwind method is stable whenever the CFL condition is satisfied.

Lax-Friedrichs

Writing Q_j^n according to (4.65) and (4.66) and considering the Lax-Friedrichs scheme (4.34), it can be shown that $|g| \leq 1$ whenever $|\nu| \leq 1$, that is, the method is conditionally stable.

Lax-Wendroff

Writing Q_j^n according to (4.65) and (4.66) and considering the Lax-Wendroff scheme (4.36), it can also be shown that the method is conditionally stable when $|\nu| \leq 1$.

Exercises

1. Analyze the stability of Lax-Friedrichs and Lax-Wendroff schemes.
2. **Graduate students:** Prove that a consistent and stable finite volume method is necessarily convergent.

4.6 Assignment 1: Linear advection equation

1. Consider the linear advection equation (4.9), with constant velocity $u = 1$, and two different initial conditions:
   a) A *smooth* initial data
   $$q_0(x) = \sin(2\pi x)$$
   b) A *Riemann* initial data given in equation (4.13):
   $$q_0(x) = \begin{cases} 1, & \text{if } x \leq 0, \\ 0, & \text{if } x > 0. \end{cases}$$
2. Implement the finite volume schemes: Central, Upwind, Lax-Friedrichs and Lax-Wendroff.
3. Test the numerical solutions for cases whether or not the CFL condition is satisfied ($\nu < 1$ and $\nu > 1$).
4. Verify if the numerical results converge with expected theoretical order to the analytical solution, for both initial data. Plot the convergence curves in terms of Δt and Δx.
5. Do you observe any difference in the results of these methods for both initial conditions?

4.7 Nonlinear hyperbolic conservation laws

The Burger's equation (4.6) and the water saturation transport modeled by the Buckley-Leverett equation (4.7) are examples of nonlinear hyperbolic conservation laws. This type of equation presents additional difficulties for numerical methods when compared to linear conservation laws [17–19].

[17]: Whitham (2011), *Linear and nonlinear waves*
[18]: Holden et al. (2015), *Front tracking for hyperbolic conservation laws*
[19]: Smith (1985), *Numerical solution of partial differential equations: finite difference methods*

Consider the following nonlinear hyperbolic conservation law

$$\frac{\partial q}{\partial t} + \nabla \cdot \mathbf{f}(q) = 0, \tag{4.67}$$

where $\mathbf{f}(q)$ is a given nonlinear function of q. The one-dimensional form of equation (4.67) can be written as

$$q_t + f(q)_x = 0, \tag{4.68}$$

in the conservative form.

4.7.1 Characteristic curves

Let's consider the nonlinear hyperbolic conservation law (4.68), from which we can obtain the quasi-linear form

$$q_t + f'(q)q_x = 0.$$

Analogously to the advection equation case in section 4.2.2, the characteristic curves satisfy

$$X'(t) = f'\big(q(X(t),t)\big),$$

that is,

$$\frac{d}{dt}q(X(t),t) = q_t(X(t),t) + X'(t)q_x(X(t),t) = q_t + f'\big(q(X(t),t)\big)q_x = 0.$$

Therefore, $q(x,t)$ is constant along the characteristic curves. Note that the characteristic curves

$$X(t) = x_0 + f'\big(q(X(t),t)\big)t$$

depend on the solution, unlike the linear case [20]. To understand the nature of this problem, let's consider Burgers' equation (4.6), which can also be written as

$$q_t + qq_x = 0.$$

In this case, the characteristic curves are given by

$$X(t) = x_0 + q(X(t),t)t.$$

Since $q(x,t)$ must be constant along the characteristics, we have that

$$X(t) = x_0 + q_0(x_0)t,$$

where q_0 is the initial condition. If we consider q_0 given by the Riemann problem:

$$q_0(x) = \begin{cases} 1, & \text{if } x < 0 \\ 0, & \text{if } x > 0, \end{cases} \tag{4.69}$$

we have the respective characteristic curves illustrated in figure 4.16, which collide, generating a discontinuity in the solution, called a **shock** [11, 20].

Even smooth initial data can lead to the intersection of characteristics after a short time interval, see an example in figure 4.18.

[20]: Mishra (2010), 'Numerical methods for conservation laws and related equations'

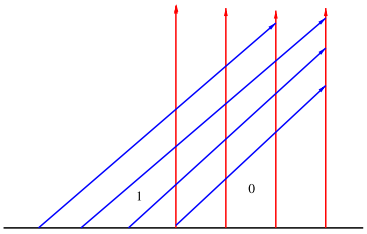

Figure 4.16: Intersection of characteristic curves with the initial condition given by the Riemann problem (4.69).

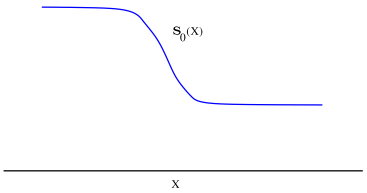

Figure 4.17: Smooth initial condition.

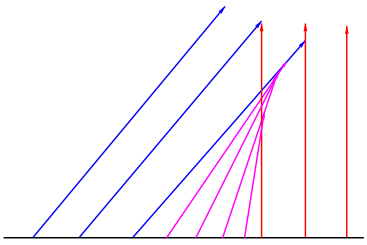

Figure 4.18: Occurrence of intersection of characteristic curves even with smooth initial condition.

4.7.2 Weak solutions

Smooth or classical solutions of the conservation law (4.68) may not exist. However, these models arise from physics and admit weak solutions, which are constructed from the integral formulation.

Let $\mathscr{C}_c^1(\mathbb{R}\times\mathbb{R}_+)$ the space of all continuously differentiable functions from $\mathbb{R}\times\mathbb{R}_+ \longrightarrow \mathbb{R}$ with compact support, i.e., the functions that vanish outside a compact subset of $\mathbb{R}\times\mathbb{R}_+$. Assuming a solution exists for (4.68), and multiplying by a smooth test function $\varphi \in \mathscr{C}_c^1(\mathbb{R}\times\mathbb{R}_+)$, results in

$$q_t\varphi + f(q)_x\varphi = 0,$$

integrating over $x \in \mathbb{R}$ and $t \in \mathbb{R}_+$ we have

$$\int_{\mathbb{R}\times\mathbb{R}_+} (q_t\varphi + f(q)_x\varphi)\,dxdt = 0.$$

Now, integrating by parts we obtain

$$\begin{aligned}0 = &\lim_{t\to\infty}\int_{\mathbb{R}} q(x,t)\varphi(x,t)dx - \int_{\mathbb{R}} q(x,0)\varphi(x,0)dx\\ &- \int_{\mathbb{R}\times\mathbb{R}_+} q(x,t)\varphi_t(x,t)dxdt\\ &+ \lim_{x\to\infty}\int_{\mathbb{R}_+} q(x,t)\varphi(x,t)dt - \lim_{x\to-\infty}\int_{\mathbb{R}_+} q(x,t)\varphi(x,t)dt\\ &- \int_{\mathbb{R}\times\mathbb{R}_+} f\big(q(x,t)\big)\varphi_x(x,t)dxdt.\end{aligned}$$

Since the test function has compact support, we find

$$\int_{\mathbb{R}\times\mathbb{R}_+} q(x,t)\varphi_t(x,t) + f\big(q(x,t)\big)\varphi_x(x,t)dxdt + \int_{\mathbb{R}} q_0(x)\varphi(x,0)dx = 0, \quad (4.70)$$

and thus, we formulate the following definition:

Definition 4.7.1 *A function $q(x,t)$ is a weak solution of the conservation law (4.68) with initial condition $q_0(x)$ if (4.70) is satisfied for all smooth test functions φ with compact support in a bounded subset of $\mathbb{R}\times\mathbb{R}_+$.*

Weak solutions are not necessarily differentiable, nor even continuous. This implies that solutions can contain discontinuities that arise as shock waves and propagate as the solution evolves.

4.7.3 The Rankine-Hugoniot condition

Let us assume the existence of an isolated discontinuity moving along a smooth curve $\gamma(t)$ through a compact subset $\omega \subset \mathbb{R}\times\mathbb{R}_+$ as illustrated in Figure 4.19. The solution $q(x,t)$ is smooth in each domain ω^+ and ω^- (sufficiently close to $\gamma(t)$) and satisfies equation (4.68) pointwise in $\omega^- \cup \omega^+$, where

$$\begin{aligned}\omega^- &= \{(x,t)\in\mathbb{R}\times\mathbb{R}_+,\ x<\gamma(t)\},\\ \omega^+ &= \{(x,t)\in\mathbb{R}\times\mathbb{R}_+,\ x>\gamma(t)\}.\end{aligned}$$

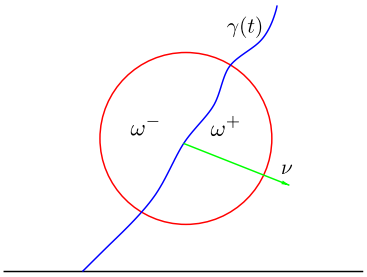

Figure 4.19: A discontinuity propagating along a $\gamma(t)$ curve.

Consider a test function φ with support entirely contained in ω. We can define

$$\mathcal{q} = (f(q), q) \quad \text{and} \quad \nabla = (\partial_x, \partial_t)$$

such that, on one hand we have

$$\int_\omega \mathcal{q}\cdot\nabla\varphi\, d\omega = -\underbrace{\int_\omega \varphi\nabla\cdot\mathcal{q}\, d\omega}_{=0\text{ (diff. equation)}} + \underbrace{\int_{\partial\omega}\varphi\mathcal{q}\cdot\check{\mathbf{n}}\, d(\partial\omega)}_{=0\ (\varphi\text{ vanishes})} = 0. \quad (4.71)$$

This equation is another version of integration by parts, that can be easily verified. On the other hand, we can integrate over each side of $\gamma(t)$,

yielding

$$\begin{aligned}\int_\omega \boldsymbol{q}\cdot\nabla\varphi\, d\omega &= \int_{\omega^+} \boldsymbol{q}\cdot\nabla\varphi\, d\omega + \int_{\omega^-} \boldsymbol{q}\cdot\nabla\varphi\, d\omega \\ &= -\int_{\omega^+} \varphi\nabla\cdot\boldsymbol{q}\, d\omega + \int_{\partial\omega^+} \varphi\boldsymbol{q}^+\cdot\check{\mathbf{n}}^+\, d(\partial\omega) \\ &\quad -\int_{\omega^-} \varphi\nabla\cdot\boldsymbol{q}\, d\omega + \int_{\partial\omega^-} \varphi\boldsymbol{q}^-\cdot\check{\mathbf{n}}^-\, d(\partial\omega) \\ &= \int_{\partial\omega^+} \varphi\boldsymbol{q}^+\cdot\check{\mathbf{n}}^+\, d(\partial\omega) + \int_{\partial\omega^-} \varphi\boldsymbol{q}^-\cdot\check{\mathbf{n}}^-\, d(\partial\omega), \quad (4.72)\end{aligned}$$

where $\boldsymbol{q}^\pm = (f(q^\pm), q^\pm)$, and $q^\pm = q|_{\omega^\pm}$. In the last steps, we applied integration by parts to each side of $\gamma(t)$, followed by the vanishing of the integral in $\omega^+ \cup \omega^-$ since $\nabla\cdot\boldsymbol{q} = f(q)_x + q_t = 0$. The curve $x = \gamma(t)$ describes a trajectory in $\mathbb{R}\times\mathbb{R}_+$, given by $\vec{\boldsymbol{\gamma}}(t) = (\gamma(t), t)$. Therefore the tangent vector to the curve is $d\vec{\boldsymbol{\gamma}}/dt = (\gamma'(t), 1)$, and a reference normal vector to the curve can be computed as $\check{\boldsymbol{\nu}} = (1, -\gamma'(t))$. Now notice that the integrals over $\partial\omega^+$ and $\partial\omega^-$ vanish over the boundary of ω, due to the compact support of φ. Now joining the equations (4.71) and (4.72), results in

$$\begin{aligned}0 &= \int_{\partial\omega^+} \varphi\boldsymbol{q}^+\cdot\check{\mathbf{n}}^+\, d(\partial\omega) + \int_{\partial\omega^-} \varphi\boldsymbol{q}^-\cdot\check{\mathbf{n}}^-\, d(\partial\omega) \\ &= \int_\gamma \varphi\boldsymbol{q}^+\cdot\check{\mathbf{n}}^+\, d\gamma + \int_\gamma \varphi\boldsymbol{q}^-\cdot\check{\mathbf{n}}^-\, d\gamma \\ &= \int_\gamma \varphi\left(\boldsymbol{q}^-\cdot\check{\boldsymbol{\nu}} - \boldsymbol{q}^+\cdot\check{\boldsymbol{\nu}}\right)\, d\gamma, \quad (4.73)\end{aligned}$$

where the reference normal vector $\check{\boldsymbol{\nu}}$ aligns with $\check{\mathbf{n}}^-$, and it is opposite to $\check{\mathbf{n}}^+$. Equation (4.73) holds for any test function φ and therefore the integrand must be zero, leading to

$$f(q^-(t)) - \gamma'(t)q^-(t) - f(q^+(t)) + \gamma'(t)q^+(t) = 0$$

that allows us to conclude that the discontinuity propagation speed $\mathfrak{s}(t) = \gamma'(t)$ must satisfy

$$\mathfrak{s}(t) = \frac{f(q^+(t)) - f(q^-(t))}{q^+(t) - q^-(t)}, \quad (4.74)$$

which is known as the **Rankine-Hugoniot** condition and expresses the conservation of $q(x,t)$ across discontinuities.

Example 4.7.1 For the Burgers equation we have $f(q) = q^2/2$, therefore

$$\mathfrak{s}(t) = \frac{\frac{(q^+)^2}{2} - \frac{(q^-)^2}{2}}{q^+ - q^-} = \frac{q^+ + q^-}{2}.$$

4.7.4 Solution of the Riemann Problem

If we consider the Burgers problem with initial condition given by the Riemann problem (4.69), the solution develop a shock discontinuity, and

its speed can be computed by the Rankine-Hugoniot condition as

$$\dot{s}(t) = \frac{1}{2}$$

such that its weak solution is of the form

$$q(x,t) = \begin{cases} 1, & \text{if } x < \frac{1}{2}t \\ 0, & \text{if } x > \frac{1}{2}t. \end{cases} \tag{4.75}$$

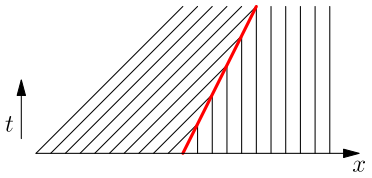

Figure 4.20: Characteristics for the Riemann problem (4.75).

This solution is illustrated in Figure 4.20, where we can see that the characteristics flow into the shock. Thus, every point in the x-t plane is mapped by the characteristics, allowing the solution to be determined by the initial condition.

On the other hand, if the Riemann problem is given by

$$q_0(x) = \begin{cases} 0, & \text{if } x < 0 \\ 1, & \text{if } x > 0, \end{cases} \tag{4.76}$$

then, following the characteristics emanating from the x-axis, as in the previous problem, we now obtain a region where no characteristics can reach (see Figure 4.21). The missing information in this region can be filled in various ways. Using the Rankine-Hugoniot condition, one possible weak solution is given by

$$q(x,t) = \begin{cases} 0, & \text{if } x < \frac{1}{2}t \\ 1, & \text{if } x > \frac{1}{2}t, \end{cases} \tag{4.77}$$

see Figure 4.22. Note that this solution has a shock curve, drawn in red in the figure. However, this solution is not the only possible weak solution. Adding an intermediate state with value $q = \frac{2}{3}$ and using the Rankine-Hugoniot condition, we obtain the weak solution

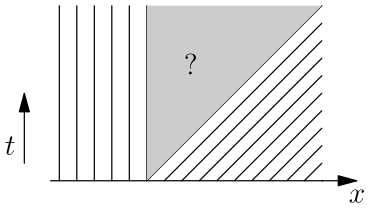

Figure 4.21: Characteristics for the Riemann problem (4.76).

$$q(x,t) = \begin{cases} 0, & \text{if } x < \frac{1}{3}t \\ \frac{2}{3}, & \text{if } \frac{1}{3}t < x < \frac{5}{6}t \\ 1, & \text{if } x > \frac{5}{6}t, \end{cases} \tag{4.78}$$

whose characteristics are shown in Figure 4.23.

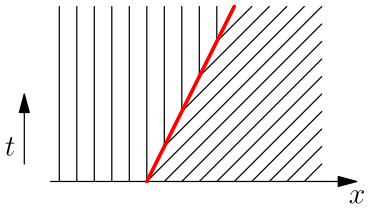

Figure 4.22: Solution (4.77).

These solutions represent an expansion of characteristics and are known as **rarefaction waves**. Similarly, arbitrarily many other weak solutions can be constructed using the Rankine-Hugoniot condition with different intermediate states. That is, the solutions are not necessarily unique and therefore some additional conditions must be imposed.

4.7.5 Entropy Conditions

There are several conditions that can be applied directly to weak solutions of hyperbolic equations to check whether they are physically admissible. These are usually called entropy conditions.

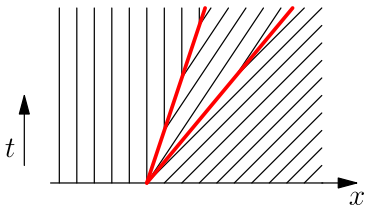

Figure 4.23: Solution (4.78).

In the case of scalar equations, one requirement is that the information be derived from the initial data, including discontinuities. For example, in the case of a shock, the discontinuity will form if the slope of the characteristics

to the left is greater than to the right of the initial discontinuity. Let q^- and q^+ be the states on both sides of a shock moving at speed $\mathfrak{s}$, and assume $f(q)$ is convex[1]. Then the solution $q(x,t)$ is entropic if, along the discontinuity,

$$f'(q^-) > \mathfrak{s} > f'(q^+). \tag{4.79}$$

This is Lax's entropy condition [21], which allows as valid the weak solutions for which the characteristics flow into a discontinuity, and not out of it. A more general condition was established by Oleĭnik [22] and guarantees that the solution is entropic if

$$\frac{f(q) - f(q^-)}{q - q^-} \geq \mathfrak{s} \geq \frac{f(q) - f(q^+)}{q - q^+}, \tag{4.80}$$

for all q between the states q^- and q^+.

Another condition also established by Oleĭnik [22] guarantees that a solution is entropic in the case of rarefaction, assuming $f'' > 0$, if there exists a constant $E > 0$ such that for $\delta > 0$, $t > 0$, and any $x \in \mathbb{R}$, we have

$$\frac{q(x+\delta, t) - q(x,t)}{\delta} < \frac{E}{t}. \tag{4.81}$$

4.7.6 Rarefaction waves

Let us consider the conservation law (4.68) with a convex flux function and initial condition given by the following Riemann problem:

$$q_0(x) = \begin{cases} q_l, & \text{if } x < 0 \\ q_r, & \text{if } x > 0. \end{cases} \tag{4.82}$$

When $q_l > q_r$, the entropic solution contains a shock between the two states and is given by

$$q(x,t) = \begin{cases} q_l, & \text{if } x < \mathfrak{s}t \\ q_r, & \text{if } x > \mathfrak{s}t, \end{cases} \tag{4.83}$$

where the shock speed $\mathfrak{s}$ is given by the Rankine-Hugoniot condition. Note that (4.83) satisfies the Lax entropy condition.

Now, let us understand how to determine the entropic solution in the case where $q_l < q_r$, where the two states will be separated by a rarefaction wave.

A rarefaction wave is a self-similar solution of the form

$$q(x,t) = \psi\left(\frac{x}{t}\right),$$

therefore,

$$\begin{aligned} q_t(x,t) + f(q(x,t))_x &= -\frac{x}{t^2}\psi'(x/t) + \frac{1}{t} f'\big(\psi(x/t)\big)\psi'(x/t) \\ &= \psi'(x/t)\left(-\frac{x}{t^2} + \frac{1}{t} f'\big(\psi(x/t)\big)\right). \end{aligned}$$

1: A function $f : \Omega \subset \mathbb{R} \to \mathbb{R}$ is convex if, for any $x_1, x_2 \in \Omega$, and $0 \leq \alpha \leq 1$, we have

$$f(\alpha x_1 + (1-\alpha)x_2) \leq \alpha f(x_1) + (1-\alpha) f(x_2).$$

If f is twice differentiable, it is convex if and only if $f''(x) \geq 0, \ \forall x \in \Omega$.

[21]: Lax (1957), 'Hyperbolic systems of conservation laws II'

[22]: Oleinik (1957), 'Discontinuous solutions of non-linear differential equations'

Since q satisfies (4.68), and $t > 0$, we must have

$$\psi'(x/t)\Big(-\frac{x}{t} + f'\big(\psi(x/t)\big)\Big) = 0. \tag{4.84}$$

The case in which the solutions are not constant satisfies

$$f'\big(\psi(x/t)\big) = x/t. \tag{4.85}$$

Equivalently, using the fact that f' is strictly increasing (f convex), we obtain

$$\psi(x/t) = (f')^{-1}(x/t). \tag{4.86}$$

This self-similar solution determines the rarefaction wave for the Riemann problem (4.82) with $q_l < q_r$, and therefore the entropic solution of the conservation law (4.68) is given by

$$q(x,t) = \begin{cases} q_l, & \text{if } x \le f'(q_l)t \\ (f')^{-1}(x/t), & \text{if } f'(q_l)t < x \le f'(q_r)t \\ q_r, & \text{if } x > f'(q_r)t. \end{cases} \tag{4.87}$$

Figure 4.24 illustrates the solution (4.87) for the particular case of the Burgers equation with $q_l = 0$ and $q_r = 1$.

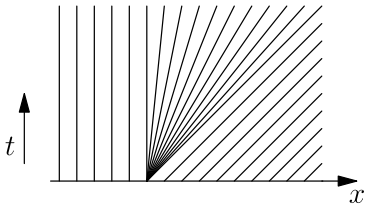

Figure 4.24: Rarefaction solution of problem (4.87).

In the scalar case with f convex or concave, a Riemann problem always yields either a shock or a rarefaction wave as the entropic solution. However, when f has inflection points, both types of entropic solutions may develop simultaneously.

4.8 Finite volume methods for nonlinear hyperbolic conservation laws

The integral form for hyperbolic conservation laws introduced in Section 4.3 covers the nonlinear case, as well as the discretization presented in equation (4.29) do método de volumes finitos para leis de conservação hiperbólicas na forma

$$q_t + f(q)_x = 0.$$

Therefore, we consider the approximation of the solution in each control volume V_j for each time t^n, dada por

$$Q_j^n \approx \frac{1}{\Delta x}\int_{x_{j-\frac{1}{2}}}^{x_{j+\frac{1}{2}}} q(x,t^n)dx$$

to compute

$$Q_j^{n+1} = Q_j^n - \frac{\Delta t}{\Delta x}\Big(\bar{F}^n_{j+\frac{1}{2}} - \bar{F}^n_{j-\frac{1}{2}}\Big) \tag{4.88}$$

and define discrete fluxes that approximate the time average of the flux function

$$F^n_{j+\frac{1}{2}} \approx \bar{F}^n_{j+\frac{1}{2}} = \frac{1}{\Delta t}\int_{t^n}^{t^{n+1}} f\big(q(x_{j+\frac{1}{2}},t)\big)dt, \tag{4.89}$$

that should be approximated by schemes that are able to handle the difficulties introduced by the nonlinear problems. Next, we introduce some classical finite volume schemes for nonlinear hyperbolic conservation laws.

Sergei Konstantinovich Godunov (Russia, 1929 — Russia, 2023).

4.8.1 The Godunov method

The Godunov method [23] takes into account that for each time step, the average approximations Q_j^n define the following Riemann problems at each interface $x_{j+\frac{1}{2}}$:

$$\begin{cases} q_t + f(q)_x &= 0 \\ q(x,t^n) &= \begin{cases} Q_j^n & \text{if } x < x_{j+\frac{1}{2}} \\ Q_{j+1}^n & \text{if } x > x_{j+\frac{1}{2}}, \end{cases} \end{cases} \tag{4.90}$$

as illustrated in Figure 4.26.

[23]: Godunov (1959), 'A difference scheme for numerical solution of discontinuous solution of hydrodynamic equations'

In the previous section, we saw that the exact solution to this type of problem is given by shock waves, rarefaction waves, or both. Therefore, at each time step, we can solve the Riemann problem in terms of the waves coming from each interface $x_{j+\frac{1}{2}}$. Waves from neighboring Riemann problems may cross after some time, as shown in Figure 4.27. However, each wave has a finite propagation speed, and the maximum wave speed for any Riemann problem is bounded by

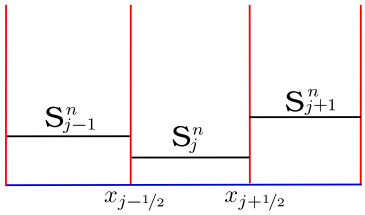

Figure 4.26: Riemann problems defined at each interface $x_{j+\frac{1}{2}}$.

$$\max_j |f'(Q_j^n)|.$$

Therefore, by imposing the CFL condition

$$\max_j |f'(Q_j^n)| \frac{\Delta t}{\Delta x} \leq \frac{1}{2} \tag{4.91}$$

we ensure that waves from neighboring problems do not interact before they reach the next time level, as shown in Figure 4.28. The condition in equation (4.91) can be less restrictive, but it is commonly used for simplicity [20].

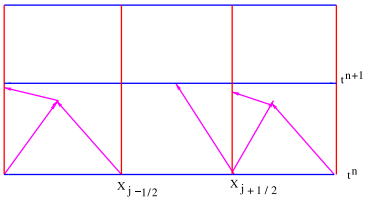

Figure 4.27: Waves interacting.

Assuming that $f(q)$ is convex, we have that $f''(q)$ does not change sign, and the solution to the Riemann problem (4.90) consists of a single shock or rarefaction wave, within the five possibilities illustrated in Figure 4.29. That is, we can have: (a) a shock moving to the left; (b) a rarefaction moving to the left; (c) a rarefaction wave spreading partially to the left and partially to the right; (d) a rarefaction moving to the right; (e) a shock moving to the right. The situation described in Figure 4.29 (c) is called transonic rarefaction, and the solution in this case is q_s, which corresponds to the unique value of q that propagates with zero velocity (also known as the sonic point), i.e., $f'(q_s) = 0$. This happens, for example, when $f''(q) > 0$, which generates a rarefaction wave whenever $Q_j^n < Q_{j+1}^n$, and a transonic rarefaction when $Q_j^n < q_s < Q_{j+1}^n$. In this

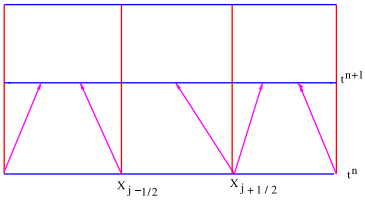

Figure 4.28: Non-interacting waves.

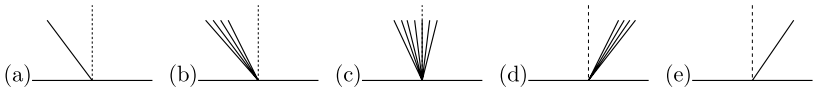

Figure 4.29: Possible configurations for the solution to the Riemann problem between the states Q_j^n and Q_{j+1}^n.

case, the Godunov flux function is given by

$$F_{j+\frac{1}{2}}^n = \begin{cases} f(Q_j^n), & \text{if } Q_j^n > q_s \text{ and } \vartheta > 0, \\ f(Q_{j+1}^n), & \text{if } Q_{j+1}^n < q_s \text{ and } \vartheta < 0, \\ f(q_s), & \text{if } Q_j^n < q_s < Q_{j+1}^n, \end{cases} \tag{4.92}$$

where

$$\vartheta = \frac{f(Q_{j+1}^n) - f(Q_j^n)}{Q_{j+1}^n - Q_j^n}$$

is the shock speed given by the Rankine-Hugoniot condition.

Note that if $f'(q) > 0$ for both states Q_j^n and Q_{j+1}^n, then

$$F_{j+\frac{1}{2}}^n = f(Q_j^n),$$

whereas if $f'(q) < 0$ for both states Q_j^n and Q_{j+1}^n, then

$$F_{j+\frac{1}{2}}^n = f(Q_{j+1}^n),$$

and the Godunov method reduces to the first-order upwind method.

Equation (4.92) can be written more compactly as

$$F_{j+\frac{1}{2}}^n = \begin{cases} \min\limits_{Q_j^n \le q \le Q_{j+1}^n} f(q), & \text{if } Q_j^n \le Q_{j+1}^n, \\ \max\limits_{Q_{j+1}^n \le q \le Q_j^n} f(q), & \text{if } Q_{j+1}^n \le Q_j^n, \end{cases} \tag{4.93}$$

considering that q_s is the global minimum or maximum of f in the convex case. The formula above is also valid when $f''(q) < 0$ and for non-convex fluxes, where there may be multiple sonic points.

One final case not considered in Figure 4.29 is when a stationary shock occurs, with $\vartheta = 0$. In this case, the solution to the Riemann problem is discontinuous at $x_{j+\frac{1}{2}}$, but by the Rankine-Hugoniot condition $f(Q_j^n) = f(Q_{j+1}^n)$, and $F_{j+\frac{1}{2}}^n$ is well defined, with the formula (4.93) still valid.

4.8.2 The Roe Method

The Roe method [24] proposes replacing the exact solution of the Riemann problem (4.90) with an approximation, which considers a local linearization of the flux function $f(q)$ given by

[24]: Roe (1981), 'Approximate Riemann solvers, parameter vectors, and difference schemes'

$$f(q)_x = f'(q)q_x \approx A_{j+\frac{1}{2}} q_x,$$

where $A \approx f'$ is a constant state where f is linearized. The linearization proposed by Roe consists of choosing an average flux given by

$$A_{j+\frac{1}{2}} = \begin{cases} \dfrac{f(Q^n_{j+1}) - f(Q^n_j)}{Q^n_{j+1} - Q^n_j}, & \text{if } Q^n_{j+1} \neq Q^n_j, \\ f'(Q^n_j), & \text{if } Q^n_{j+1} = Q^n_j. \end{cases}$$

Note that the Roe average is a linear approximation of f', which when used in (4.90) provides:

$$\begin{cases} q_t + A_{j+\frac{1}{2}} q_x &= 0 \\ q(x, t^n) &= \begin{cases} Q^n_j & \text{if } x < x_{j+\frac{1}{2}} \\ Q^n_{j+1} & \text{if } x > x_{j+\frac{1}{2}}. \end{cases} \end{cases}$$

Above, we have a linear transport problem with constant velocity, whose solution allows us to compute the Roe numerical flux:

$$F^n_{j+\frac{1}{2}} = \begin{cases} f(Q^n_j), & \text{if } A_{j+\frac{1}{2}} \geq 0, \\ f(Q^n_{j+1}), & \text{if } A_{j+\frac{1}{2}} < 0. \end{cases}$$

4.8.3 The Lax-Friedrichs Method

The Lax-Friedrichs method [25], discussed in the previous chapter, can also be used to approximate problems with nonlinear flux functions.

[25]: Friedrichs et al. (1971), 'Systems of conservation equations with a convex extension'

In the context of Riemann problems, central methods consider two waves to approximate the solution: one moving to the left with velocity $\mathfrak{s}^l_{j+\frac{1}{2}}$ and another moving to the right with velocity $\mathfrak{s}^r_{j+\frac{1}{2}}$, as illustrated in figure 4.30. The problem (4.90) is approximated by:

$$q(x,t) = \begin{cases} Q^n_j & \text{if } x < \mathfrak{s}^l_{j+\frac{1}{2}} t \\ Q^*_{j+\frac{1}{2}} & \text{if } \mathfrak{s}^l_{j+\frac{1}{2}} t < x < \mathfrak{s}^r_{j+\frac{1}{2}} t \\ Q^n_{j+1} & \text{if } x > \mathfrak{s}^r_{j+\frac{1}{2}} t, \end{cases}$$

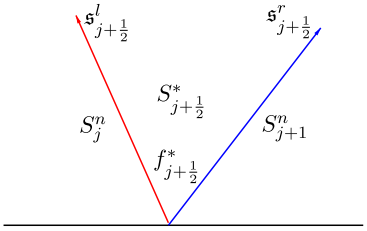

Figure 4.30: Approximation for the Riemann problem considering one wave moving in each direction.

where the intermediate state $Q^*_{j+\frac{1}{2}}$ can be determined by local conservation using the Rankine-Hugoniot conditions:

$$\begin{aligned} f(Q^n_{j+1}) - f^*_{j+\frac{1}{2}} &= \mathfrak{s}^r_{j+\frac{1}{2}}(Q^n_{j+1} - Q^*_{j+\frac{1}{2}}) \\ f(Q^n_j) - f^*_{j+\frac{1}{2}} &= \mathfrak{s}^l_{j+\frac{1}{2}}(Q^n_j - Q^*_{j+\frac{1}{2}}), \end{aligned} \tag{4.94}$$

where $f^*_{j+\frac{1}{2}}$ is the intermediate flux, as illustrated in figure 4.30. Solving the system (4.94) gives

$$f^*_{j+\frac{1}{2}} = \frac{\mathfrak{s}^r_{j+\frac{1}{2}} f(Q^n_j) - \mathfrak{s}^l_{j+\frac{1}{2}} f(Q^n_{j+1}) + \mathfrak{s}^r_{j+\frac{1}{2}} \mathfrak{s}^l_{j+\frac{1}{2}} (Q^n_{j+1} - Q^n_j)}{\mathfrak{s}^r_{j+\frac{1}{2}} - \mathfrak{s}^l_{j+\frac{1}{2}}}.$$

In particular, if we choose equal velocities but with opposite signs

$\mathfrak{d}^r = -\mathfrak{d}^l$, we obtain

$$f^*_{j+\frac{1}{2}} = \frac{f(Q^n_{j+1}) + f(Q^n_j)}{2} - \frac{\mathfrak{d}_{j+\frac{1}{2}}}{2}(Q^n_{j+1} - Q^n_j).$$

Moreover, if we specify

$$\mathfrak{d}^l_{j+\frac{1}{2}} = -\frac{\Delta x}{\Delta t} \qquad \text{and} \qquad \mathfrak{d}^r_{j+\frac{1}{2}} = \frac{\Delta x}{\Delta t}$$

and take the numerical flux $F^n_{j+\frac{1}{2}} = f^*_{j+\frac{1}{2}}$, we obtain the Lax-Friedrichs flux

$$F^n_{j+\frac{1}{2}} = \frac{f(Q^n_{j+1}) + f(Q^n_j)}{2} - \frac{\Delta x}{2\Delta t}(Q^n_{j+1} - Q^n_j).$$

4.8.4 The Rusanov Method

The Rusanov method [26] suggests local approximations for the velocities given by

$$\mathfrak{d}^l_{j+\frac{1}{2}} = -\mathfrak{d}_{j+\frac{1}{2}} \qquad \text{and} \qquad \mathfrak{d}^r_{j+\frac{1}{2}} = \mathfrak{d}_{j+\frac{1}{2}},$$

where

$$\mathfrak{d}_{j+\frac{1}{2}} = \max\left(|f'(Q^n_j)|, |f'(Q^n_{j+1})|\right),$$

resulting in numerical fluxes given by

$$F^n_{j+\frac{1}{2}} = \frac{f(Q^n_{j+1}) + f(Q^n_j)}{2} - \frac{\max\left(|f'(Q^n_j)|, |f'(Q^n_{j+1})|\right)}{2}(Q^n_{j+1} - Q^n_j).$$

[26]: Rusanov (1961), 'Calculation of interaction of non-steady shock waves with obstacles'

4.8.5 The Engquist-Osher Method

The Engquist-Osher method [27] assumes that the solution to each Riemann problem is a rarefaction wave, with numerical fluxes given by

$$F^n_{j+\frac{1}{2}} = \frac{f(Q^n_{j+1}) + f(Q^n_j)}{2} - \frac{1}{2}\int_{Q^n_j}^{Q^n_{j+1}} |f'(\theta)| d\theta.$$

In the case where the flux function has a single minimum point at q_s and no maximum point, the Engquist-Osher flux is given by

$$F^n_{j+\frac{1}{2}} = f\left(\max(Q^n_j, q_s)\right) + f\left(\min(Q^n_{j+1}, q_s)\right) - f(q_s).$$

Furthermore, if the flux function is convex and we neglect the constant term $f(q_s)$, we have that $f\left(\max(Q^n_j, q_s)\right)$ is the positive part and $f\left(\min(Q^n_{j+1}, q_s)\right)$ is the negative part of f, and then the Engquist-Osher method can be seen as a flux segregation scheme.

[27]: Engquist et al. (1980), 'Stable and entropy satisfying approximations for transonic flow calculations'

4.9 High-Order Methods

Methods with a high formal order of convergence are quite popular in the numerical solution of hyperbolic conservation laws. The Lax-Wendroff method, presented in section 4.3 for linear hyperbolic conservation laws,

is an example of a method with formal order 2, whose fluxes are defined by

$$F^n_{j+\frac{1}{2}} = \frac{f(Q^n_{j+1}) + f(Q^n_j)}{2} - \frac{a^n_{j+\frac{1}{2}}\Delta t}{2\Delta x}\left(f(Q^n_{j+1}) - f(Q^n_j)\right),$$

where

$$a^n_{j+\frac{1}{2}} = f'\left(\frac{Q^n_{j+1} + Q^n_j}{2}\right).$$

However, this scheme, like other methods of dispersive nature, produces spurious oscillations in the presence of discontinuities. In other words, increasing the order of accuracy may lead to stability issues, which motivates the development of new procedures to obtain high-order schemes.

4.9.1 The REA Algorithm

Revisiting the derivation of the Godunov scheme, we have three steps:

1. Reconstruction: At each time step t^n, the averages in the cells Q^n_j are assumed to be known, and the solution is defined as a piecewise constant function

$$q(x, t^n) = Q^n_j, \text{ for } x_{j-\frac{1}{2}} \leq x < x_{j+\frac{1}{2}}. \tag{4.95}$$

2. Evolution: The reconstructed function $q(x, t^n)$ evolves over time, solving the conservation law.
3. Solution averaging: The solution at the next time step is taken as an average over each control volume.

The three steps above constitute the REA (Reconstruction-Evolution-Averaging) algorithm [11, 20, 23].

[11]: LeVeque (2002), *Finite volume methods for hyperbolic problems*
[20]: Mishra (2010), 'Numerical methods for conservation laws and related equations'
[23]: Godunov (1959), 'A difference scheme for numerical solution of discontinuous solution of hydrodynamic equations'

The reconstruction step that uses piecewise constant functions is illustrated in figure 4.31. However, to obtain better accuracy than first-order, we can use a higher-order reconstruction, such as piecewise linear functions, as illustrated in figure 4.32. The solution defined as a piecewise linear function is given by

$$q(x, t^n) = Q^n_j + \sigma^n_j(x - x_j), \text{ for } x_{j-\frac{1}{2}} \leq x < x_{j+\frac{1}{2}}, \tag{4.96}$$

where σ^n_j is an approximation of the derivative of q at x_j. Notice that if $\sigma^n_j = 0,\ \forall j$, we fall back to the case of piecewise constant reconstruction. Some possibilities for choosing σ^n_j are:

- Central:

$$\sigma^n_j = \frac{Q^n_{j+1} - Q^n_{j-1}}{2\Delta x}; \tag{4.97}$$

- Backward:

$$\sigma^n_j = \frac{Q^n_j - Q^n_{j-1}}{\Delta x}; \tag{4.98}$$

- Forward:

$$\sigma^n_j = \frac{Q^n_{j+1} - Q^n_j}{\Delta x}. \tag{4.99}$$

Some of these choices provide methods for hyperbolic conservation laws based on Taylor series expansions.

Example 4.9.1 Considering the advection problem $q_t + uq_x = 0$ with $u > 0$, whose exact solution at time t^{n+1} is $q(x, t^{n+1}) = q(x - u\Delta t, t^n)$, we have that the average approximation of the solution Q_j^{n+1} is given by

$$\begin{aligned} Q_j^{n+1} &= \frac{u\Delta t}{\Delta x}\left(Q_{j-1}^n + \frac{1}{2}(\Delta x - u\Delta t)\sigma_{j-1}^n\right) + \left(1 - \frac{u\Delta t}{\Delta x}\right)\left(Q_j^n - \frac{1}{2}u\Delta t\,\sigma_j^n\right) \\ &= Q_j^n - \frac{u\Delta t}{\Delta x}\left(Q_j^n - Q_{j-1}^n\right) - \frac{1}{2}\frac{u\Delta t}{\Delta x}(\Delta x - u\Delta t)(\sigma_j^n - \sigma_{j-1}^n). \end{aligned}$$

Choosing σ_j^n as given in (4.99), we obtain the Lax-Wendroff method:

$$Q_j^{n+1} = Q_j^n - \frac{u\Delta t}{2\Delta x}\left(Q_{j+1}^n - Q_{j-1}^n\right) + \frac{u^2(\Delta t)^2}{2(\Delta x)^2}\left(Q_{j+1}^n - 2Q_j^n + Q_{j-1}^n\right).$$

However, as we mentioned above, the Lax-Wendroff scheme produces oscillations, and therefore other choices for σ_j^n must be considered. To understand how the aforementioned oscillations arise, consider the advection problem with σ_j^n given by (4.99) applied to piecewise constant data with values

$$Q_j^n = \begin{cases} 1 & \text{if} \quad x \le J, \\ 0 & \text{if} \quad x > J. \end{cases}$$

Thus, $\sigma_j^n = 0$, $\forall\, j \neq J$, as illustrated in figure 4.33. When advecting this profile by a distance $u\Delta t$, we find that the average over cell J is greater than 1 for $0 < u\Delta t < \Delta x$. Figure 4.34 illustrates the case $u\Delta t = \Delta x/2$. This type of oscillation increases with each time step. The slopes proposed in (4.97), (4.98), and (4.99) are based on the assumption that the solution is smooth, and do not improve accuracy near a discontinuity. Limiting the slope near the discontinuity can be a solution to avoid oscillations. Methods based on this idea are known as slope-limited methods [28] and will be introduced next.

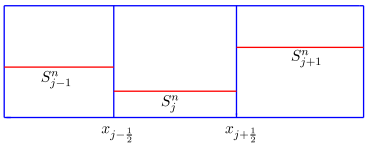

Figure 4.31: Piecewise constant functions used in the reconstruction step of the REA algorithm.

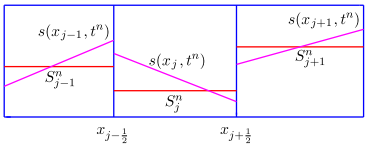

Figure 4.32: Piecewise linear functions used in the reconstruction step of the REA algorithm.

[28]: Yee (1989), 'A class of high resolution explicit and implicit shock-capturing methods'

4.9.2 TVD Methods

Methods that limit the slope must, in some way, measure the oscillations present in the solution. This is provided by the notion of the total variation of a function:

$$\mathrm{TV}(Q) = \sum_{j=-\infty}^{\infty} |Q_j^n - Q_{j-1}^n|. \tag{4.100}$$

If the method introduces oscillations, then the total variation of Q^n increases over time. We can, therefore, try to avoid oscillations by requiring that the method does not increase the total variation:

Definition 4.9.1 *A two-level method is called Total Variation Diminishing (TVD) if, for any set of data Q^n, the values Q^{n+1} calculated by the method satisfy*

$$TV(Q^{n+1}) \le TV(Q^n). \tag{4.101}$$

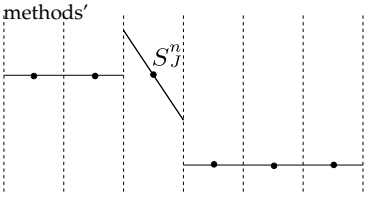

Figure 4.33: Oscillations produced by the choice of slope (4.99). Values of Q^n with reconstruction.

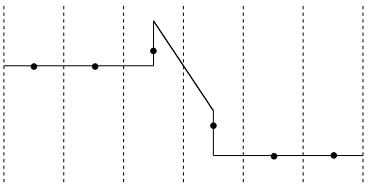

Figure 4.34: After advection with $u\Delta t = \Delta x/2$.

Note that the constant reconstruction is TVD, while slope choices such as (4.97), (4.98), and (4.99) are not TVD [11, 20]. The next subsection will present some slope limiter methods that are TVD, which prevent the introduction of oscillations in the solution approximation.

[11]: LeVeque (2002), *Finite volume methods for hyperbolic problems*
[20]: Mishra (2010), 'Numerical methods for conservation laws and related equations'

4.9.3 Slope Limiters

A slope choice that provides second-order accuracy for smooth solutions and satisfies the TVD property is given by

$$\sigma_j^n = \text{minmod}\left(\frac{Q_j^n - Q_{j-1}^n}{\Delta x}, \frac{Q_{j+1}^n - Q_j^n}{\Delta x}\right),$$

where *minmod* is the limiter function defined by

$$\text{minmod}(a,b) = \begin{cases} a & \text{if } |a| < |b| \text{ and } ab > 0, \\ b & \text{if } |b| < |a| \text{ and } ab > 0, \\ 0 & \text{if } ab \le 0. \end{cases}$$

Note that if a and b have the same sign, the smallest magnitude value is chosen; otherwise, zero is returned. In other words, the *minmod* limiter compares the two slopes (4.98) and (4.99) and chooses the one with the smallest magnitude. In the case where both slopes have opposite signs, Q_j^n is a local minimum or maximum, and then the value zero is chosen for the slope. Figure 4.35 shows the results using the *minmod* method for the previously considered advection problem.

A slope limiter, also with second-order accuracy, that provides the reconstruction illustrated in figure 4.36 for the advection problem is the so-called *superbee* limiter [29]:

$$\sigma_j^n = \text{maxmod}\left(\sigma_j^{(1)}, \sigma_j^{(2)}\right),$$

where

$$\sigma_j^{(1)} = \text{minmod}\left(\frac{Q_{j+1}^n - Q_j^n}{\Delta x}, 2\frac{Q_j^n - Q_{j-1}^n}{\Delta x}\right),$$

and

$$\sigma_j^{(2)} = \text{minmod}\left(2\frac{Q_{j+1}^n - Q_j^n}{\Delta x}, \frac{Q_j^n - Q_{j-1}^n}{\Delta x}\right).$$

Each one-sided slope is compared with twice the opposite one-sided slope. Then, the maxmod function selects the argument with the largest magnitude. In regions where the solution is smooth, this will tend to return the largest of the two one-sided slopes.

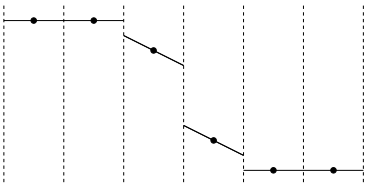

Figure 4.35: Reconstructed values of Q^n using the slope limiter *Minmod*.

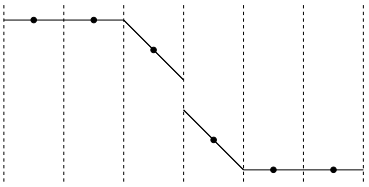

Figure 4.36: Reconstructed values of Q^n using the slope limiter *Superbee*.

Two other popular slope limiters are the MC (*monotonized central-difference limiter*) and the van Leer limiter, both proposed by van Leer [30], given by

$$\sigma_j^n = \text{minmod}\left(\frac{Q_{j+1}^n - Q_{j-1}^n}{2\Delta x}, 2\frac{Q_j^n - Q_{j-1}^n}{\Delta x}, 2\frac{Q_{j+1}^n - Q_j^n}{\Delta x}\right)$$

and

$$\sigma_j^n = \frac{r + |r|}{1 + |r|},$$

[30]: Van Leer (1977), 'Towards the ultimate conservative difference scheme. IV. A new approach to numerical convection'

where

$$r = \frac{Q_{j+1}^n - Q_j^n}{Q_j^n - Q_{j-1}^n}.$$

4.9.4 Semi-Discrete Formulation

Slope limiters and the REA algorithm can be applied to any conservation law. However, obtaining the finite volume flux form for nonlinear equations may be challenging.

To obtain high-resolution methods for nonlinear conservation laws such as (4.68) through reconstruction procedures, we consider a semi-discrete formulation, where we take the average in each cell as

$$Q_j(t) = \frac{1}{\Delta x} \int_{x_{j-\frac{1}{2}}}^{x_{j+\frac{1}{2}}} q(x,t)\, dx.$$

On the other hand, integrating the hyperbolic conservation law (4.68) in space gives

$$\frac{1}{\Delta x} \int_{x_{j-\frac{1}{2}}}^{x_{j+\frac{1}{2}}} q_t + \big(f(q)\big)_x \, dx = 0.$$

Therefore,

$$\frac{d}{dt} Q_j(t) + \frac{1}{\Delta x}\Big(f\big(q(x_{j+\frac{1}{2}}^-, t)\big) - f\big(q(x_{j-\frac{1}{2}}^+, t)\big)\Big) = 0,$$

where $q(x_{j+\frac{1}{2}}^-, t)$ represents the left limit of q at $x_{j+\frac{1}{2}}$:

$$q(x_{j+\frac{1}{2}}^-, t) = \lim_{x \to x_{j+\frac{1}{2}}^-} q(x,t).$$

Denoting F as the approximation for the flux terms:

$$F_{j+\frac{1}{2}}^{\pm}(t) \approx f\big(q(x_{j+\frac{1}{2}}^{\pm}, t)\big),$$

we obtain the semi-discrete form of the finite volume method (4.88):

$$\frac{d}{dt} Q_j(t) + \frac{1}{\Delta x}\Big(F_{j+\frac{1}{2}}^-(t) - F_{j-\frac{1}{2}}^+(t)\Big) = 0, \tag{4.102}$$

where the numerical fluxes $F_{j+\frac{1}{2}}^- = F_{j+\frac{1}{2}}^+$ are determined by methods for hyperbolic conservation laws such as Godunov, Rusanov, Engquist-Osher, etc., which use reconstructed solutions at the cell interfaces Q_j^+ and Q_{j+1}^-, as illustrated in figure 4.37.

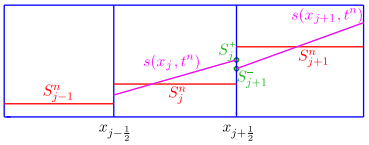

Figure 4.37: Non-oscillatory second-order reconstruction.

4.9.5 Time Discretization

Equation (4.102) leads to a system of ODEs that needs to be integrated in time using an appropriate method. If the forward Euler method is used for this system, we obtain the classical finite volume scheme (4.88), which is a first-order scheme. The advantage of the semi-discrete formulation is that we can separately increase the spatial and temporal accuracy.

Writing $\mathbf{Q}(t)$ as a vector

$$\mathbf{Q}(t) = [\cdots, Q_{j-1}(t), Q_j(t), Q_{j+1}(t), \cdots],$$

the finite volume scheme (4.102) can be rewritten as

$$\frac{d}{dt}\mathbf{Q}(t) = \mathscr{L}\big(\mathbf{Q}(t)\big),$$

where $\mathscr{L}$ is the operator given by

$$\mathscr{L}(\mathbf{Q}(t))_j = -\frac{1}{\Delta x}\Big(F_{j+\frac{1}{2}}(t) - F_{j-\frac{1}{2}}(t)\Big). \tag{4.103}$$

If the forward Euler method is used to integrate (4.103) in time, we have

$$\mathbf{Q}^{n+1} = \mathbf{Q}^n + \Delta t\, \mathscr{L}(\mathbf{Q}^n),$$

where $\mathbf{Q}^n = \mathbf{Q}(t^n)$ is the vector of the cell averages Q at time t^n, and Δt satisfies the CFL condition (4.91).

Another alternative is to use high-order time methods, such as Runge-Kutta methods [31]. More precisely, TVD Runge-Kutta methods are of interest [32, 33], such as the following:

[31]: Wanner et al. (1996), *Solving ordinary differential equations II*

[32]: Gottlieb et al. (1998), 'Total variation diminishing Runge-Kutta schemes'

[33]: Gottlieb et al. (2001), 'Strong stability-preserving high-order time discretization methods'

$$\begin{aligned}
\mathbf{Q}^* &= \mathbf{Q}^n + \Delta t\, \mathscr{L}(\mathbf{Q}^n) \\
\mathbf{Q}^{**} &= \mathbf{Q}^* + \Delta t\, \mathscr{L}(\mathbf{Q}^*) \\
\mathbf{Q}^{n+1} &= \frac{1}{2}(\mathbf{Q}^n + \mathbf{Q}^{**}),
\end{aligned}$$

which is a second-order method in time.

4.10 Assignment 2: Nonlinear traffic flow

The flux of cars in a single lane road can be modeled by the scalar conservation law

$$q_t + (q\, u(q))_x = 0$$

where $q(x,t)$ represents the density of cars in the position x of the road, at time t, varying from 0 (empty road) to 1 (no empty spaces, bumber-to-bumber traffic). This conservation law is hyperbolic nonlinear, since $f(q) = q\, u(q)$ is a nonlinear function of q. A simple model for $u(q)$ is given by

$$u(q) = u_{\max}(1 - q)$$

where $u_{\max}$ is the maximum velocity attained by the cars in a zero-density (empty) road.

1. Implement a finite volume framework to solve the traffic flow equation given above. You can use a domain $x \in [-30, 30]$, $t \in [0, 25]$, as well as $u_{\max} = 1$.
2. Implement the following methods: Godunov, Lax-Friedrichs, Lax-Wendroff, Roe and Rusanov.
3. Think about "outflow" boundary conditions for this problem.

4. Test all methods with different initial conditions: (a) a smooth gaussian density distribution; (b) a traffic jam; (c) a traffic light turning green; (d) a traffic light turning red.
5. **Graduate students:** Show car trajectories by positioning a initial car distribution according to the density function q, and integrating car velocities depending on the density function.
6. **Graduate students:** By implementing periodic boundary conditions, we can simulate this experiment `https://youtu.be/7wm-pZp_mi0`. Can you reproduce this effect with this model?

4.11 Assignment 3: Numerical solution of 1D Euler's equations

4.11.1 1D Euler's equations

Let us consider the following hyperbolic conservation law, modeling the incompressible flow of air, known as Euler's equations in one spatial dimension:

$$\mathbf{q}_t + \mathbf{f}(\mathbf{q})_x = \mathbf{0}$$

where

$$\mathbf{q} = \begin{bmatrix} \rho \\ \rho u \\ E \end{bmatrix} \quad \text{and} \quad \mathbf{f}(\mathbf{q}) = \begin{bmatrix} \rho u \\ \rho u^2 + p \\ (E + p)u \end{bmatrix},$$

along with the constitutive relation

$$E = \frac{1}{2}\rho u^2 + \frac{p}{\gamma - 1},$$

with $\gamma \approx 1.4$ for air flow at standard room temperature. Define

$$c = \sqrt{\frac{\gamma p}{\rho}} \quad \text{and} \quad \text{Ma} = \frac{|u|}{c}$$

as the speed of sound and corresponding Mach number, associated with this flow.

4.11.2 Sod shock tube

The Sod shock tube test was proposed by Gary A. Sod as a benchmark for Riemann solvers for computational fluid dynamics codes. It is an one-dimensional Riemann problem for the Euler's equations, where the left and right states are known, configuring a high-pressure state on the left and a low-pressure state on the right.

As the solution evolves, it developes a rarefaction wave, a contact discontinuity and a shock wave. The solution can be described by five different regions, separated by the positions x_1, x_2, x_3 and x_4, as in Figure 4.38. To compute the analytical solution, a number of steps are required:

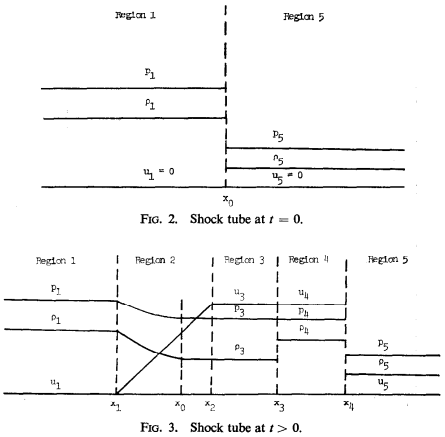

FIG. 2. Shock tube at $t = 0$.

FIG. 3. Shock tube at $t > 0$.

Figure 4.38: Structure of the Sod shock tube solution.

1. Compute sound velocities

$$c_1 = \sqrt{\frac{\gamma p_1}{\rho_1}}, \quad c_5 = \sqrt{\frac{\gamma p_5}{\rho_5}}$$

2. Compute the rarefaction waves as

$$u_2(x) = \frac{2}{\gamma+1}\left(c_1 + \frac{x-x_0}{t}\right)$$
$$\rho_2(x) = \rho_1\left(1 - \frac{(\gamma-1)u_2(x)}{2c_1}\right)^{\frac{2}{\gamma-1}}$$
$$p_2(x) = p_1\left(1 - \frac{(\gamma-1)u_2(x)}{2c_1}\right)^{\frac{2\gamma}{\gamma-1}}$$

3. Solve (numerically) the pressure p_3 from the nonlinear equation

$$\left(p_1^\beta - p_3^\beta\right)\sqrt{\frac{(1-\Gamma^2)p_1^{\frac{1}{\gamma}}}{\Gamma^2\rho_1}} - (p_3 - p_5)\sqrt{\frac{1-\Gamma}{\rho_5(p_3+\Gamma p_5)}} = 0$$

where $\Gamma = (\gamma-1)/(\gamma+1)$ and $\beta = (\gamma-1)/(2\gamma)$.

4. Compute ρ_3 and u_3 from

$$\rho_3 = \rho_1\left(\frac{p_3}{p_1}\right)^{\frac{1}{\gamma}}$$
$$u_3 = u_5 + \frac{p_3 - p_5}{\sqrt{\frac{1}{2}\rho_5\left((\gamma+1)p_3 + (\gamma-1)p_5\right)}}$$

5. Part IV is given by

$$p_4 = p_3$$
$$u_4 = u_3$$
$$\rho_4 = \rho_5\left(\frac{p_4 + \Gamma p_5}{p_5 + \Gamma p_4}\right)$$

6. Now solve for the discontinuities updated positions

$$x_1 = t(u_1 - c_1) + x_0$$
$$x_2 = t(u_3 - c_3) + x_0$$
$$x_3 = tu_3 + x_0$$
$$W = u_5 + c_5\sqrt{\beta + \left(\frac{\gamma+1}{2\gamma}\right)\frac{p_4}{p_5}}$$
$$x_4 = tW + x_0$$

1. Write the non-conservative form of Euler's equations

$$\mathbf{q}_t + \mathbf{f}'(\mathbf{q})\mathbf{q}_x = \mathbf{0}$$

with primitive variables $\mathbf{q} = (\rho, u, p)^T$.

2. The above system can be linearized by setting a constant state

$\bar{\mathbf{q}} = (\bar{\rho}, \bar{u}, \bar{p})$, to define the constant matrix $A = \mathbf{f}'(\bar{\mathbf{q}})$. Consider $\bar{\mathbf{q}} = (1, 0, 1)$ a constant state of interest, and solve the linearized Euler's equation in $[-1, 1]$, setting a Riemann problem with the initial condition given by

$$\mathbf{q}^0(x) = \begin{cases} \mathbf{q}_L = (1, 0, 1) & \text{if } x < 0 \\ \mathbf{q}_R = (0.2, 0, 0.2) & \text{if } x \geq 0 \end{cases}$$

For the numerical solution, implement the Godunov, Rusanov, Lax-Friedrichs and Lax-Wendroff schemes. Show a comparison of the numerical solutions for $t = 0.5$, computed with different resolutions.

3. **Graduate students:** Now consider the conservative nonlinear form of Euler's equations defined in $[0, 1]$, with the initial data given by

$$\mathbf{q}^0(x) = \begin{cases} \mathbf{q}_L = (1, 0, 1) & \text{if } x < \frac{1}{2} \\ \mathbf{q}_R = (0.125, 0, 0.1) & \text{if } x \geq \frac{1}{2} \end{cases}$$

configuring a Riemann problem known as Sod shock tube. Implement the computation of the analytical solution. Solve this problem with the finite volume schemes Roe, Lax-Friedrichs and Rusanov. Implement a sonic fix for the Roe scheme. Show the numerical solutions for $t = 0.15$ compared with the analytical solution and different resolutions.

NUMERICAL METHODS FOR MIXED EQUATIONS

5

5.1 Examples of mixed equations 96
5.2 Fully coupled Taylor series methods 97
5.3 Fully coupled method of lines 97
5.4 Implicit-explicit (IMEX) methods 98
5.5 Fractional step methods . . 98

5.1 Examples of mixed equations

$$q_t = \mathcal{A}_1(q) + \mathcal{A}_2(q) + \cdots + \mathcal{A}_N(q)$$

where each $\mathcal{A}_j(q)$ is a function or differential operator involving only spatial derivatives of q. The discussions in this chapter will consider only

$$q_t = \mathcal{A}(q) + \mathcal{B}(q), \tag{5.1}$$

where $\mathcal{A}$ and $\mathcal{B}$ are operators acting over $q(x,t)$.

Example 5.1.1 Two-dimensional hyperbolic conservation law

$$q_t + f(q)_x + g(q)_y = 0$$

where $\mathcal{A}(q) = -f(q)_x$ and $\mathcal{B}(q) = -g(q)_y$, and f, g are the corresponding flux functions of $q(x,y,t)$ in each spatial direction x, y respectively.

Example 5.1.2 Two-dimensional diffusion equation

$$q_t = \kappa(q_{xx} + q_{yy})$$

where $q = q(x,y,t)$, $\mathcal{A}(q) = \kappa q_{xx}$ and $\mathcal{B}(q) = \kappa q_{yy}$, with $\kappa > 0$ being the coefficient of thermal diffusivity.

Example 5.1.3 Advection-reaction equation

$$q_t + f(q)_x = \psi(q) \tag{5.2}$$

where $\psi(q)$ is a reaction term. This can be used to model the transport of a radioactive contaminant, when $f(q) = uq$, with transport velocity $u \in \mathbb{R}$ and ψ is usually a decay function of the form $\psi(q) = -\beta q$. For this case, $\mathcal{A}(q) = -uq_x$ and $\mathcal{B}(q) = -\beta q$.

Example 5.1.4 Advection-diffusion equation

$$q_t + f(q)_x = \mu\, q_{xx} \tag{5.3}$$

where $f(q)$ is a flux function and $\mu > 0$ is the diffusion coefficient. A common choice of flux function is a linear transport of the form $f(q) = uq$, where $u \in \mathbb{R}$ is the transport velocity. For this case, $\mathcal{A}(q) = -uq_x$ and $\mathcal{B}(q) = \mu q_{xx}$.

Example 5.1.5 Advection-diffusion-reaction equation

$$q_t + f(q)_x = \mu\, q_{xx} + \psi(q)$$

with terms already explained above. In this case, we can set $\mathcal{A}_1(q) = -f(q)_x$, $\mathcal{A}_2(q) = \mu q_{xx}$ and $\mathcal{A}_3(q) = \psi(q)$.

Example 5.1.6 The Korteweg-de Vries (KdV) equation

$$q_t + q\, q_x = \nu\, q_{xxx}$$

which is similar to the Burgers' equation, but with an added dispersion term. For this case, $\mathcal{A}(q) = -q\, q_x$ and $\mathcal{B}(q) = \nu q_{xxx}$.

5.2 Fully coupled Taylor series methods

This method is obtained by Taylor series expansions of the solution, leading to finite difference schemes of arbitrary order. Consider the *advectioin-reaction* equation (5.2) with $\psi(q) = -\beta q$. Under the suitable smoothness requirements over q, we can use the Taylor series expansions

$$\begin{aligned} q(x, t+\Delta t) &= \sum_{j=0}^{\infty} \frac{\Delta t^j}{j!} \partial_t^j q(x,t) = \sum_{j=0}^{\infty} \frac{\Delta t^j}{j!} (-u\partial_x - \beta)^j q(x,t) \\ &= e^{-\Delta t(u\partial_x + \beta)} q(x,t) \end{aligned}$$

to obtain an *upwind* method

$$Q_j^{n+1} = Q_j^n - \frac{u\Delta t}{h}(Q_j^n - Q_{j-1}^n) - \Delta t \beta Q_j^n$$

which is first-order accurate provided $0 < u\Delta t/h \leq 1$, or to obtain a 2nd-order accurate *Lax-Wendroff* method

$$\begin{aligned} Q_j^{n+1} = &\left(1 - \Delta t\beta + \frac{1}{2}\Delta t^2\beta^2\right) Q_j^n - \frac{u}{2}\frac{\Delta t}{h}(1 - \Delta t\beta)\left(Q_{j+1}^n - Q_{j-1}^n\right) \\ &+ \frac{u^2}{2}\frac{\Delta t^2}{h^2}\left(Q_{j-1}^n - 2Q_j^n + Q_{j+1}^n\right). \end{aligned}$$

5.3 Fully coupled method of lines

Semi-discretization in spatial coordinates x_j, $j = 0, 1, \ldots, m$, associated with an increment $h = \Delta x$. We seek functions $Q_j(t) \simeq q(x_j, t)$ that satisfy the fully couple ODE system

$$\mathbf{Q}'(t) = \mathbf{F}(\mathbf{Q}(t))$$

where each j-line of the system reads

$$Q_j'(t) = \mathcal{A}_j^h(\mathbf{Q}(t)) + \mathcal{B}_j^h(\mathbf{Q}(t))$$

where $\mathcal{A}_j^h$ and $\mathcal{B}_j^h$ are spatial discretizations of the operators $\mathcal{A}$ and $\mathcal{B}$, respectively. For example, if we consider the linear advection-diffusiion equation (5.3), with transport velocity $u > 0$, we can discretize $\mathcal{A}(q) = -uq_x$ by the upwind method, and $\mathcal{B}(q) = \mu q_{xx}$ by a central difference scheme, resulting in the discrete operators

$$\begin{aligned}\mathcal{A}_j^h(\mathbf{Q}(t)) &= -\frac{u}{h}\left(Q_j(t) - Q_{j-1}(t)\right)\\ \mathcal{B}_j^h(\mathbf{Q}(t)) &= \frac{\mu}{h^2}\left(Q_{j-1}(t) - 2Q_j(t) + Q_{j+1}(t)\right).\end{aligned}$$

Therefore the fully coupled system can be solved by any suitable method for IVPs. Note that in this case, implicit methods are preferable due to the stiff characteristic of the original system, causing stability restrictions to methods with bounded stability regions.

The application of the *trapezoidal* method to the fully coupled ODE system results

$$\begin{aligned}\mathbf{Q}^{n+1} &= \mathbf{Q}^n + \frac{\Delta t}{2}\left(\mathbf{F}(\mathbf{Q}^{n+1}) + \mathbf{F}(\mathbf{Q}^n)\right)\\ &= \mathbf{Q}^n + \frac{\Delta t}{2}\left(\underline{\mathcal{A}}^h(\mathbf{Q}^{n+1}) + \underline{\mathcal{B}}^h(\mathbf{Q}^{n+1}) + \underline{\mathcal{A}}^h(\mathbf{Q}^n) + \underline{\mathcal{B}}^h(\mathbf{Q}^n)\right)\end{aligned}$$

5.4 Implicit-explicit (IMEX) methods

Consider the equation (5.1), where $\mathcal{A}(q)$ represents stiff terms that would be better integrating with an implicit method, while $\mathcal{B}(q)$ represents nonstiff terms that can be handled by an explicit methods without severe restrictions to the time step, such as nonlinear reaction terms.

The idea of IMEX methods is to treat some terms explicitly and others implicitly. The simplest method is to employ the implicit Backward-Euler method to handle the $\mathcal{A}(q)$ operator, and the explicit Forward-Euler for the $\mathcal{B}(u)$ operator, resulting in

$$\mathbf{Q}^{n+1} = \mathbf{Q}^n + \Delta t\left(\underline{\mathcal{A}}^h(\mathbf{Q}^{n+1}) + \underline{\mathcal{B}}^h(\mathbf{Q}^n)\right).$$

Another example is the combination of 2nd-order Adams-Bashforth for the explicit term with trapezoidal method for the implicit term, yielding

$$\mathbf{Q}^{n+1} = \mathbf{Q}^n + \frac{\Delta t}{2}\left(\underline{\mathcal{A}}^h(\mathbf{Q}^n) + \underline{\mathcal{A}}^h(\mathbf{Q}^{n+1}) + 3\underline{\mathcal{B}}^h(\mathbf{Q}^n) - \underline{\mathcal{B}}^h(\mathbf{Q}^{n-1})\right).$$

5.5 Fractional step methods

The idea is to split the original equation (5.1) into two problems:

$$q_t = \mathcal{A}(q) \tag{5.4}$$

$$q_t = \mathcal{B}(q), \tag{5.5}$$

and combine the application of two different methods in an alternating manner. The main advantage is to apply directly standard methods for each part, taking advantage of accuracy and ease of implementation.

Take the advection-reaction equation (5.2), with linear fluxes $f(q) = uq$ and decay function $\psi(q) = -\beta q$, i.e.

$$q_t + u\, q_x = -\beta q.$$

By applying the split in (5.4) and (5.5), we have

$$\begin{aligned} q_t &= -u\, q_x \\ q_t &= -\beta q \end{aligned}$$

so that the first equation can be solved by the *upwind* method to obtain an intermediate approximate solution Q_j^*, and then the second equation can be integrated in time by the Forward-Euler method to obtain the final approximation Q_j^{n+1}. The resulting method reads

$$\begin{aligned} Q_j^* &= Q_j^n - \frac{u\Delta t}{h}\left(Q_j^n - Q_{j-1}^n\right) \\ Q_j^{n+1} &= Q_j^* - \beta \Delta t Q_j^* \end{aligned}$$

DISCRETIZATION OF THE INCOMPRESSIBLE NAVIER-STOKES EQUATIONS

6

6.1 Prelude

This aim of this chapter is to present an overview of finite volume methods for the direct numerical simulation of flows governed by the incompressible Navier-Stokes (NS) equations. The pressure in this case is not a thermodynamic variable, for which an equation of state can be invoked, but its sole role is to enforce the divergence-free constraint on the velocity field. This introduces some difficulties which are discussed next.

6.2 The Navier-Stokes equations

Let us first recall the different forms of the Navier-Stokes problem we aim to discretize. We write the mass and linear momentum conservation laws for the incompressible case over a fixed region Ω.

Navier-Stokes problem

Mass conservation

$$\int_{\partial\Omega} \mathbf{u}\cdot\check{\mathbf{n}}\, ds = 0 \quad \Rightarrow \quad \nabla\cdot\mathbf{u} = 0 \tag{6.1}$$

Momentum conservation

$$\int_\Omega \rho\frac{\partial \mathbf{u}}{\partial t}\, dv + \int_{\partial\Omega} \boldsymbol{\pi}\cdot\check{\mathbf{n}}\, ds = \int_\Omega \mathbf{f}\, dv \quad \Rightarrow \quad \rho\frac{\partial \mathbf{u}}{\partial t} + \nabla\cdot\boldsymbol{\pi} = \mathbf{f} \tag{6.2}$$

where the *momentum flux* is defined by

$$\boldsymbol{\pi} = -\boldsymbol{\sigma} + \rho\,(\mathbf{u}\otimes\mathbf{u})$$

and the stress tensor, for the Newtonian case is

$$\boldsymbol{\sigma} = -p\,\mathbf{I} + \mu(\nabla\mathbf{u} + \nabla\mathbf{u}^\intercal) = -p\,\mathbf{I} + 2\mu\mathbf{D}(\mathbf{u})$$

Substituting the expressions above we get the final form in *conservative form* to be used later on[1]

$$\int_\Omega \rho\frac{\partial \mathbf{u}}{\partial t}\, dv + \int_{\partial\Omega} [\rho\,(\mathbf{u}\otimes\mathbf{u}) + p\,\mathbf{I} - \mu(\nabla\mathbf{u} + \nabla\mathbf{u}^\intercal)]\cdot\check{\mathbf{n}}\, ds = \int_\Omega \mathbf{f} \tag{6.3}$$

or in differential form

$$\rho\frac{\partial \mathbf{u}}{\partial t} + \nabla\cdot[\rho\,(\mathbf{u}\otimes\mathbf{u}) + p\,\mathbf{I} - \mu(\nabla\mathbf{u} + \nabla\mathbf{u}^\intercal)] = \mathbf{f} \tag{6.4}$$

6.1 Prelude 100
6.2 The Navier-Stokes equations 100
6.3 Discretization by the FVM 102
6.4 Monolithic vs. Segregated approach 103
6.5 Spatial discretization: Colocated vs. Staggered 105
6.6 Assignment 1: A practice with OpenFOAM - Flow around obstacle 111
6.7 The ultimate remedy to cure the spurious checkboard modes: Staggered grids 112
6.8 Assignment 2: A simple Finite Volume Staggered code - Cavity flow 117
6.9 Further comments 119

1: Notice that the nonlinear term, can also be written as

$$\rho\,(\mathbf{u}\otimes\mathbf{u})\cdot\check{\mathbf{n}} = \rho\,\mathbf{u}\,(\mathbf{u}\cdot\check{\mathbf{n}})$$

This is easily seen bu using index notation:

$$[(\mathbf{u}\otimes\mathbf{u})\cdot\check{\mathbf{n}}]_i = (u_i\,u_j)\,\check{n}_j = u_i\,\underbrace{(u_j\,\check{n}_j)}_{\mathbf{u}\cdot\check{\mathbf{n}}} = [\mathbf{u}\,(\mathbf{u}\cdot\check{\mathbf{n}})]_i$$

The equations can also be written in the so called non-conservative form, as we usually find in most of the cases

$$\begin{cases} \rho\,\partial_t \mathbf{u} + \rho\,(\mathbf{u}\cdot\nabla)\,\mathbf{u} - \nabla\cdot\left[\mu\,(\nabla\mathbf{u} + \nabla\mathbf{u}^T)\right] + \nabla p &= \mathbf{f} \\ \nabla\cdot\mathbf{u} &= 0 \end{cases} \tag{6.5}$$

The non-uniform viscosity case is important to consider when dealing with generalized fluids and non-Newtonian behaviors or when using eddy viscosity models. In those cases the viscosity will exhibit spatial variations and μ can not be taken out of the divergence. Nevertheless, if we can assume μ as a constant parameter, the problem simplifies to[2]

2: Notice the Laplacian form of the viscous term in Equation 6.6.

$$\begin{cases} \rho\,\partial_t \mathbf{u} + \rho\,(\mathbf{u}\cdot\nabla)\,\mathbf{u} - \mu\,\nabla^2\mathbf{u} + \nabla p &= \mathbf{f} \\ \nabla\cdot\mathbf{u} &= 0 \end{cases} \tag{6.6}$$

6.2.1 Initial and Boundary conditions

We recall the discussion of Chapter 1 to as concerns boundary conditions for the NS equations.

- **Initial condition** The NS equations are first order in time and second order in space for the velocity. The well-posedness of the problem requires an initial velocity field, which has to be solenoidal, i.e.,

  $$\mathbf{u}(\mathbf{x}, t=0) = \mathbf{u}_0(\mathbf{x}) \qquad \text{with} \quad \nabla\cdot\mathbf{u}_0 = 0 \qquad in\Omega\,. \tag{6.7}$$

  and it is also required that the imposed normal velocity at the boundary be compatible with $\mathbf{u}_0$.

- **Imposed velocity:** The velocity field is specified

  $$\mathbf{u}(\mathbf{x}, t) = \mathbf{u}_w(\mathbf{x}, t) \quad \forall \mathbf{x} \in \partial\Omega_D$$

  In some cases we enforce conditions, either for the normal component to the surface, which for a *stationary* and *impermeable* wall is

  $$u_n = \mathbf{u}\cdot\check{\mathbf{n}} = 0$$

  recalling, this is a phenomenological condition. As for the tangent component, for a stationary wall it corresponds to

  $$\mathbf{u}_t = \mathbf{u} - u_n\check{\mathbf{n}} = 0$$

  Recall, this is a postulate that agrees well with physical observations.

- **Imposed force:** The stresses are specified

  $$\boldsymbol{\sigma}\cdot\check{\mathbf{n}} = \boldsymbol{\mathcal{F}}_w \quad \forall \mathbf{x} \in \partial\Omega_N$$

  for the case of the so called **Drag** force we have

  $$\boldsymbol{\sigma}\cdot\check{\mathbf{n}} = \mathbf{D}(\mathbf{u}) \quad \forall \mathbf{x} \in \partial\Omega_N$$

6.3 Discretization by the FVM

The main difficulties when discretizing the Navier-Stokes problem are related to the treatment of[3]:

- the pressure-velocity coupling (there is no equation for p);
- the convective nonlinear term $\rho\,(\mathbf{u}\cdot\nabla)\,\mathbf{u}$;
- boundary layers and turbulent flows.

3: In more complex situations, such as multiphase flows, additional difficulties have to be addressed, namely, immersed moving boundaries, jump conditions at interfaces, discontinuous material properties and so on. These are left for more advance courses.

Let us begin with the discretization in space and time of the NS equations 7.11-7.12. Denoting as usual the solution at time $t_n = n\,\Delta t$ with a supraindex in the variables, the unknown velocity vector by $\mathbf{U}^n \in \mathbb{R}^{\dim \mathbf{u}}$ and the unknown pressure by $\mathbf{P}^n \in \mathbb{R}^{\dim p}$, the discrete problem can be written in the following general form:

$$\left\{\begin{array}{rcl} \rho\,\dfrac{\mathbf{U}^{n+1}-\mathbf{U}^n}{\Delta t} + \rho\,\mathbb{A}(\mathbf{U}^{n+\gamma},\mathbf{U}^{n+\theta}) - \mathbb{V}(\mathbf{U}^{n+\theta}) + \mathbb{G}(\mathbf{P}^{n+1}) & = & \mathbf{F}^{n+\theta} \\ \\ \mathbb{D}(\mathbf{U}^{n+1}) & = & \mathbf{0} \end{array}\right. \tag{6.8}$$

A few comments are in order to as the previous discrete system:

- This problem is usually referred to as a Differential Algebraic Equation (DAE) system.
- For the moment the discrete operators appearing above are not specified. They emanate from a FD, FE or a FV discretization of the momentum and mass conservation equations.
- At this point it is clear that these operators, namely,
  - **Advection:** $\mathbb{A}(\cdot,\cdot) \leftrightarrow (\mathbf{u}\cdot\nabla)\,\mathbf{u}$
  - **Viscous:** $\mathbb{V}(\cdot) \leftrightarrow \nabla\cdot\left[\mu\,(\nabla\mathbf{u}+\nabla\mathbf{u}^T)\right]$ or $\mu\,\nabla^2\mathbf{u}$;
  - **Gradient:** $\mathbb{G}(\cdot) \leftrightarrow \nabla p$;
  - **Divergence:** $\mathbb{D}(\cdot) \leftrightarrow \nabla\cdot\mathbf{u}$;

  are represented by some sparse matrizes, as we have learned in previous chapters[4].
- Notice that the unknown vector $\mathbf{U}$ can be splitted into two/three parts (in 2D/3D), i.e.,

$$\text{in 2D:}\quad \mathbf{U} = \begin{bmatrix}\mathbf{U}_x\\ \mathbf{U}_y\end{bmatrix} \qquad \text{or in 3D:}\quad \mathbf{U} = \begin{bmatrix}\mathbf{U}_x\\ \mathbf{U}_y\\ \mathbf{U}_z\end{bmatrix}$$

- Depending on the choice for γ we may end up with a linearized problem or a nonlinear one, for which, Newton-Raphson, Picard or fixed-point iterations must be applied.

4: Note that for the nonlinear advection term this would actually be the case after linearization or if take $\gamma = 0$.

- Depending on the choice for θ we end up with an implicit or explicit formulation. The latter case requiring the time step to be bounded by, if we denote by $h = \min\{h_x, h_y, h_z\}$

$$\Delta t_\mu < C_\mu \frac{\rho\, h^2}{\mu}$$

where $C_\mu = 1/4$ in two dimensions and $1/6$ in the three dimensional case.

- The advection term is stabilized by viscosity if the time step is bounded by

$$\Delta t_a < \frac{2\mu}{\rho\,(\mathbf{u}\cdot\mathbf{u})}$$

- If we consider the Reynold number $\mathrm{Re}= \dfrac{\rho\, U\, L}{\mu}$ and nondimensionalize time as $\bar{t} = \dfrac{tU}{L}$, we see that

$$\bar{\Delta t}_a = \frac{2}{\mathrm{Re}} \xrightarrow[\mathrm{Re}\to\infty]{} 0 \quad \text{and} \quad \bar{\Delta t}_\mu = C_\mu \frac{h^2}{L^2}\mathrm{Re} \xrightarrow[\mathrm{Re}\to 0]{} 0,$$

which indicates the convenience of implicit schemes for the viscous terms at low Reynolds numbers, since the restriction scales as $\mathcal{O}(h^2)$. For high Re, the time step should also be controlled, however, stability also depends on the choice of the advection scheme[5].

5: For $\mathrm{Re}\gg 1$, the so called limited schemes and turbulent eddy viscosity models may be used to increase stability.

- We can put everything together into a single matrix as

$$\begin{bmatrix} \mathbb{B} & \mathbb{G} \\ \mathbb{D} & \mathbb{0} \end{bmatrix} \cdot \begin{bmatrix} \mathbf{U}^{n+1} \\ \mathbf{P}^{n+1} \end{bmatrix} = \begin{bmatrix} \tilde{\mathbf{F}} \\ \mathbf{G} \end{bmatrix}$$

where the right hand side may now include forces, boundary conditions and terms computed at the previous time level.

- We will discuss how to solve this mixed problem, whether **Monolithic** or **Segregated** and its finite volume discretization in **Collocated** and **Staggered grids**.

6.4 Monolithic vs. Segregated approach

The **Monolithic** approach, which is usually quite expensive, consists in solving for $\mathbf{U}^{n+1}$ and $\mathbf{P}^{n+1}$ at once. This is mainly done in problems at very low Reynolds numbers or for **Stokes flows** (in the absence of inertial terms). The algebraic system exhibits the typical structure of saddle-point problems, with a zero diagonal block, and efficient preconditioning is a challenge. On the other hand, the segregated approach, which is essentially based on Chorin's projection methods [34] can be more convenient for problems at finite Reynolds numbers. Let us recall the projection method and the famous Helmholtz-Hodge decomposition theorem.

[34]: Chorin (1968), 'Numerical Solution of the Navier-Stokes Equations'

Theorem 6.4.1 (***Helmholtz-Hodge***:) *Any sufficiently smooth vector field* $\mathbf{u} : \Omega \to \mathbb{R}^d$ *defined over a bounded domain* Ω *with smooth boundary, can be written as:*

$$\mathbf{u} = \mathbf{u}_{sol} + \mathbf{u}_{irrot}$$

where

- $\mathbf{u}_{sol}$ *is divergence-free (solenoidal), i.e.,* $\nabla \cdot \mathbf{u}_{sol} = 0$.
- $\mathbf{u}_{irrot}$ *is curl-free (irrotational), i.e.,* $\nabla \times \mathbf{u}_{irrot} = 0$, *therefore* $\mathbf{u}_{irrot} = \nabla\phi$, *with* ϕ *a scalar potential function.*

Consider the semi-discrete NS problem (continuous in space, discrete in time)

$$\frac{\mathbf{u}^{n+1} - \mathbf{u}^n}{\Delta t} = -(\mathbf{u}^n \cdot \nabla)\mathbf{u}^n - \frac{1}{\rho}\nabla p^{n+1} + \frac{\mu}{\rho}\nabla^2\mathbf{u}^n$$

and split the problem by introducing an intermediate field $\hat{\mathbf{u}}$

$$\mathbf{u}^{n+1} - \mathbf{u}^n = \mathbf{u}^{n+1} - \hat{\mathbf{u}} + \hat{\mathbf{u}} - \mathbf{u}^n$$

and solve:

1. **Predictor:** Find $\hat{\mathbf{u}}$ s.t.

$$\frac{\hat{\mathbf{u}} - \mathbf{u}^n}{\Delta t} = -(\mathbf{u}^n \cdot \nabla)\mathbf{u}^n + \frac{\mu}{\rho}\nabla^2\mathbf{u}^n$$

2. **Corrector:** Find $\mathbf{u}^{n+1}$ s.t.

$$\frac{\mathbf{u}^{n+1} - \hat{\mathbf{u}}}{\Delta t} = -\frac{1}{\rho}\nabla p^{n+1} \implies \mathbf{u}^{n+1} = \hat{\mathbf{u}} - \frac{\Delta t}{\rho}\nabla p^{n+1}$$

In order to compute the corrector we obviously need p^{n+1}, for which, by taking the divergence in the second equation and assuming $\nabla \cdot \mathbf{u}^{n+1} = 0$

$$\frac{\nabla \cdot \mathbf{u}^{n+1} - \nabla \cdot \hat{\mathbf{u}}}{\Delta t} = \frac{0 - \nabla \cdot \hat{\mathbf{u}}}{\Delta t} = -\frac{1}{\rho}\nabla \cdot \nabla p^{n+1} = -\frac{1}{\rho}\nabla^2 p^{n+1} \implies \nabla^2 p^{n+1} = \frac{\rho}{\Delta t}\nabla \cdot \hat{\mathbf{u}} \tag{6.9}$$

which is a **Poisson's equation**, we have seen many times before, in which p^{n+1} is the unknown and $\nabla \cdot \hat{\mathbf{u}}$ is the source term. The key point is to notice that

$$\hat{\mathbf{u}} = \underbrace{\mathbf{u}^{n+1}}_{\mathbf{u}_{\text{sol}}} + \underbrace{(\Delta t/\rho)\nabla p^{n+1}}_{\mathbf{u}_{\text{irrot}}}$$

from which we see the connection to Theorem 6.4.1.

Now, apply these ideas to the fully discrete problem. Assume for simplicity $\theta = \gamma = 0$ in Equation 6.8 and simplify a bit the notation. Again, we use the trick of substituting the numerator of the time derivative by

$$\mathbf{U}^{n+1} - \mathbf{U}^n = \mathbf{U}^{n+1} - \hat{\mathbf{U}} + \hat{\mathbf{U}} - \mathbf{U}^n$$

and split the problem into two separate problems[6]

6: Clearly, the sum of the two equations in 6.10 gives the original problem.

$$\begin{cases} \rho \dfrac{\hat{\mathbf{U}} - \mathbf{U}^n}{\Delta t} + \rho \mathbb{A}\,\mathbf{U}^n - \mathbb{V}\,\mathbf{U}^n = \mathbf{F}^n \\ \rho \dfrac{\mathbf{U}^{n+1} - \hat{\mathbf{U}}}{\Delta t} + \mathbb{G}\,\mathbf{P}^{n+1} = \mathbf{0} \end{cases} \tag{6.10}$$

so, the algorithm proceeds as follows:

Projection algorithm

- **Velocity predictor solver:** In the first step we ignore the pressure term and compute a guess velocity $\hat{\mathbf{U}}$, according to:

$$\rho \frac{\hat{\mathbf{U}} - \mathbf{U}^n}{\Delta t} + \rho \mathbb{A}\,\mathbf{U}^n - \mathbb{V}\,\mathbf{U}^n = \mathbf{F}^n \tag{6.11}$$

  There is no reason for $\hat{\mathbf{U}}$ to satisfy $\mathbb{D}\,\hat{\mathbf{U}} = \mathbf{0}$. We need to project into the space of discrete incompressible fields.

- **Pressure solver:** *"Take the divergence"* in the second equation of 6.10 to obtain[7]:

$$\mathbb{D}\,\mathbb{G}\,\mathbf{P}^{n+1} = \frac{\rho}{\Delta t}\mathbb{D}\,\hat{\mathbf{U}} \tag{6.12}$$

- **Velocity corrector:** Compute the gradient of the obtained pressure above and assert the velocity:

$$\mathbf{U}^{n+1} = \hat{\mathbf{U}} - \frac{\Delta t}{\rho}\mathbb{G}\,\mathbf{P}^{n+1} \tag{6.13}$$

6.5 Spatial discretization: Colocated vs. Staggered

We have to provide the precise form of the operators introduced above. Two clear options appear, namely, **Colocated grids**, in which all unknowns (velocity and pressure) reside at cell centers of the finite volumes and **Staggered grids**, in which scalar variables (the pressure in this case) are located at cell centers and vector-valued unknowns (the velocity) are located at cell faces (see Figure 6.1). These two options are detailed next. For simplicity we consider 2D orthogonal cartesian grids. The extension to the 3D case is quite straightforward, whereas, the extension to non-orthogonal grids can be done by using the numerical tools introduced in Chapter 2[8].

6.5.1 Colocated grids

Consider a uniform cell centered orthogonal cartesian grid made of finite volumes $K_{i,j}$, $i = 0, \ldots, N_x$, $j = 0, \ldots, N_y$ of size (h_x, h_y) of a rectangular domain with dimensions (L_x, L_y) as shown in Figure 6.2. Notice that the unknowns are stored at the cell centers (the circular and triangular dots of Figure 6.1), whereas the square blue dots shown in the figure are only for auxiliary computations.

7: Note that the matrix $\mathbb{D}\,\mathbb{G}$ in (Equation 6.12) will be some discrete version of ∇^2 that appeared in 6.9, whose precise form will depend on the discretization scheme adopted.

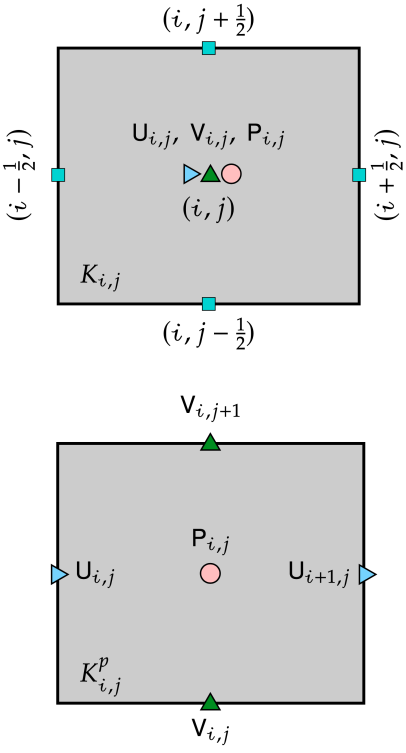

Figure 6.1: Colocated and staggered arranges of unknowns.

8: In the first computational assignment, the non-orthogonal case will considered in an example by using the `openFOAM` platform.

From now on we will denote the x and y velocity components of $\mathbf{u}$ by (u, v) or (U, V), depending on the case, instead of (u_x, u_y) or $(\mathsf{U}_x, \mathsf{U}_y)$, since now subindices in the variables stand for the grid unknowns. We begin with the continuity equation, integrate over control volume $K_{i,j}$ and use the midpoint rule for the face integrals, yielding[9]

$$\int_{K_{i,j}} \nabla \cdot \mathbf{u}^{n+1}\, dv = \int_{\partial K_{i,j}} \mathbf{u}^{n+1} \cdot \check{\mathbf{n}}\, d\ell \approx h_y \left(u^{n+1}_{i+\frac{1}{2},j} - u^{n+1}_{i-\frac{1}{2},j} \right) + h_x \left(v^{n+1}_{i,j+\frac{1}{2}} - v^{n+1}_{i,j-\frac{1}{2}} \right) = 0$$

9: Recall, in the finite volume method we assume linear variation for all fields, so a midpoint rule over the faces integrates exactly.

The face values in the equation above must be obtained by linear interpolation of cell values as we have done before, i.e.[10]

$$u^{n+1}_{i+\frac{1}{2},j} = \frac{1}{2}\left(\mathsf{U}^{n+1}_{i,j} + \mathsf{U}^{n+1}_{i+1,j} \right), \quad u^{n+1}_{i-\frac{1}{2},j} = \frac{1}{2}\left(\mathsf{U}^{n+1}_{i-1,j} + \mathsf{U}^{n+1}_{i,j} \right), \quad \text{and so on} \ldots$$

thus giving the equation for $K_{i,j}$

$$\frac{h_y}{2}\left(\mathsf{U}^{n+1}_{i+1,j} - \mathsf{U}^{n+1}_{i-1,j} \right) + \frac{h_x}{2}\left(\mathsf{V}^{n+1}_{i,j+1} - \mathsf{V}^{n+1}_{i,j-1} \right) = 0 \tag{6.14}$$

10: Although not obvious from the formulas (since we are working with integrals over faces) this is equivalent to using a central scheme to approximate $\left.\frac{\partial u}{\partial x}\right|_{i\pm\frac{1}{2},j}$ and $\left.\frac{\partial v}{\partial y}\right|_{i,j\pm\frac{1}{2}}$. We will see later on, this choice is quite unfortunate.

From now on, we will omit the time supra index to alleviate a bit the notation, since we are now focus on the spatial discretization of the momentum equation. Consider the momentum balance in integral form

$$\int_{K_{i,j}} \{\rho\, \partial_t \mathbf{u} + \nabla \cdot [\rho\, \mathbf{u} \otimes \mathbf{u} - \mu\, (\nabla \mathbf{u} + \nabla^\intercal \mathbf{u}) + \mathbb{I} p]\}\, dv = \int_{K_{i,j}} \mathbf{f}\, dv$$

where the time derivative has been left undiscretized. This term is approximated as

$$\int_{K_{i,j}} \rho\, \partial_t \mathbf{u}\, dv \approx \underbrace{h_x\, h_y}_{|K_{i,j}|} \left[\rho\, \partial_t \mathbf{u}\right]_{i,j} \tag{6.15}$$

and the time derivative with a finite difference approximation as usual. Similarly, for the forcing term in the right hand side, we have

$$\int_{K_{i,j}} \mathbf{f}\, dv \approx |K_{i,j}|\, \mathbf{f}_{i,j} \tag{6.16}$$

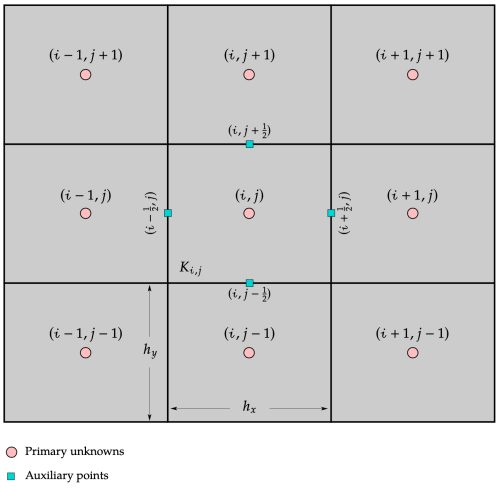

Figure 6.2: Colocated grid.

The volume integral of the divergence term is transformed into a surface integral

$$\int_{K_{i,j}} \{\nabla \cdot [\rho\, (\mathbf{u} \otimes \mathbf{u}) - \mu\, (\nabla \mathbf{u} + \nabla^\intercal \mathbf{u}) + \mathbb{I} p]\}\, dv = \int_{\partial K_{i,j}} [\rho\, (\mathbf{u} \otimes \mathbf{u}) - \mu\, (\nabla \mathbf{u} + \nabla^\intercal \mathbf{u}) + \mathbb{I} p] \cdot \check{\mathbf{n}}\, d\ell$$

Discretize the equation for the x-direction

$$\int_{\partial K_{i,j}} \left[\rho\, u\, (\mathbf{u} \cdot \check{\mathbf{n}}) - 2\mu \frac{\partial u}{\partial x} \check{n}_x - \mu \left(\frac{\partial u}{\partial y} + \frac{\partial v}{\partial x} \right) \check{n}_y + p \check{n}_x \right] d\ell \approx$$

$$+ h_y \rho \left[u^2_{i+\frac{1}{2},j} - u^2_{i-\frac{1}{2},j} \right] + h_x \rho \left[(u\, v)_{i,j+\frac{1}{2}} - (u\, v)_{i,j-\frac{1}{2}} \right] -$$

$$- h_y \left(2\mu \left.\frac{\partial u}{\partial x}\right|_{i+\frac{1}{2},j} - 2\mu \left.\frac{\partial u}{\partial x}\right|_{i-\frac{1}{2},j} \right) - h_x \left[\mu \left(\frac{\partial u}{\partial y} + \frac{\partial v}{\partial x} \right)_{i,j+\frac{1}{2}} - \mu \left(\frac{\partial u}{\partial y} + \frac{\partial v}{\partial x} \right)_{i,j-\frac{1}{2}} \right] +$$

$$+ h_y \left(p_{i+\frac{1}{2},j} - p_{i-\frac{1}{2},j} \right) \qquad (6.17)$$

and introduce some aproximations, namely

Right/Left sides: $\left[\begin{array}{lcl} u^2_{i+\frac{1}{2},j} & = & \frac{1}{2}\left(\mathsf{U}^2_{i,j} + \mathsf{U}^2_{i+1,j} \right), \\ u^2_{i-\frac{1}{2},j} & = & \frac{1}{2}\left(\mathsf{U}^2_{i,j} + \mathsf{U}^2_{i-1,j} \right), \end{array} \right.$ Top/Bottom sides: $\left[\begin{array}{lcl} (u\,v)_{i,j+\frac{1}{2}} & = & \frac{1}{2}\left(\mathsf{U}_{i,j}\mathsf{V}_{i,j} + \mathsf{U}_{i,j+1}\mathsf{V}_{i,j+1} \right), \\ (u\,v)_{i,j-\frac{1}{2}} & = & \frac{1}{2}\left(\mathsf{U}_{i,j}\mathsf{V}_{i,j} + \mathsf{U}_{i,j-1}\mathsf{V}_{i,j-1} \right) \end{array} \right.$

Right/Left sides: $\left[\begin{array}{lcl} \mu \left.\frac{\partial u}{\partial x}\right|_{i+\frac{1}{2},j} & = & \mu_{i+\frac{1}{2},j} \frac{\mathsf{U}_{i+1,j} - \mathsf{U}_{i,j}}{h_x}, \\ \mu \left.\frac{\partial u}{\partial x}\right|_{i-\frac{1}{2},j} & = & \mu_{i-\frac{1}{2},j} \frac{\mathsf{U}_{i,j} - \mathsf{U}_{i-1,j}}{h_x}, \end{array} \right.$ Top/Bottom sides: $\left[\begin{array}{lcl} \mu \left.\frac{\partial u}{\partial y}\right|_{i,j+\frac{1}{2}} & = & \mu_{i,j+\frac{1}{2}} \frac{\mathsf{U}_{i,j+1} - \mathsf{U}_{i,j}}{h_y}, \\ \mu \left.\frac{\partial u}{\partial y}\right|_{i,j-\frac{1}{2}} & = & \mu_{i,j-\frac{1}{2}} \frac{\mathsf{U}_{i,j} - \mathsf{U}_{i,j-1}}{h_y} \end{array} \right.$

Top/Bottom sides: $\left[\begin{array}{lcl} \mu \left.\frac{\partial v}{\partial x}\right|_{i,j+\frac{1}{2}} & = & \frac{\mu_{i,j+\frac{1}{2}}}{2} \left(\frac{\mathsf{V}_{i+1,j+1} - \mathsf{V}_{i-1,j+1}}{2h_x} + \frac{\mathsf{V}_{i+1,j} - \mathsf{V}_{i-1,j}}{2h_x} \right), \\ \mu \left.\frac{\partial v}{\partial x}\right|_{i,j-\frac{1}{2}} & = & \frac{\mu_{i,j-\frac{1}{2}}}{2} \left(\frac{\mathsf{V}_{i+1,j} - \mathsf{V}_{i-1,j}}{2h_x} + \frac{\mathsf{V}_{i+1,j-1} - \mathsf{V}_{i-1,j-1}}{2h_x} \right) \end{array} \right.$

Right/Left sides: $\left[\begin{array}{lcl} p_{i+\frac{1}{2},j} & = & \frac{1}{2}\left(\mathsf{P}_{i+1,j} + \mathsf{P}_{i,j} \right), \\ p_{i-\frac{1}{2},j} & = & \frac{1}{2}\left(\mathsf{P}_{i,j} + \mathsf{P}_{i-1,j} \right) \end{array} \right.$

As with the continuity equation, now for the pressure term, although not obvious from the previous formulas, since we are integrating over the boundary of $K_{i,j}$, the proposed approximation ends up being equivalent to using a central scheme to approximate $\left.\frac{\partial p}{\partial x}\right|_{i\pm\frac{1}{2}}$. We will come back to this shortly.

For the y-direction we have similarly,

$$\int_{\partial K_{i,j}} \left[\rho\, v\, (\mathbf{u}\cdot\check{\mathbf{n}}) - \mu \left(\frac{\partial u}{\partial y} + \frac{\partial v}{\partial x} \right) \check{n}_x - 2\mu \frac{\partial v}{\partial y} \check{n}_y + p\check{n}_y \right] d\ell \approx$$

$$+ h_y \rho \left[(v\,u)_{i+\frac{1}{2},j} - (v\,u)_{i-\frac{1}{2},j} \right] + h_x \rho \left[v^2_{i,j+\frac{1}{2}} - v^2_{i,j-\frac{1}{2}} \right] -$$

$$+ h_y \left[\mu \left(\frac{\partial u}{\partial y} + \frac{\partial v}{\partial x} \right)_{i+\frac{1}{2},j} - \mu \left(\frac{\partial u}{\partial y} + \frac{\partial v}{\partial x} \right)_{i-\frac{1}{2},j} \right] - h_x \left(2\mu \left.\frac{\partial v}{\partial y}\right|_{i,j+\frac{1}{2}} - 2\mu \left.\frac{\partial v}{\partial y}\right|_{i,j-\frac{1}{2}} \right) +$$

$$+ h_x \left(p_{i,j+\frac{1}{2}} - p_{i,j-\frac{1}{2}}\right)$$

and the aproximations are analogous to the previous ones

$$\text{Right/Left sides:} \quad \left[\begin{array}{rcl} (u\,v)_{i+\frac{1}{2},j} &=& \frac{1}{2}\left(\mathsf{U}_{i,j}\mathsf{V}_{i,j} + \mathsf{U}_{i+1,j}\mathsf{V}_{i+1,j}\right), \\ (u\,v)_{i-\frac{1}{2},j} &=& \frac{1}{2}\left(\mathsf{U}_{i,j}\mathsf{V}_{i,j} + \mathsf{U}_{i-1,j}\mathsf{V}_{i-1,j}\right), \end{array}\right. \quad \text{Top/Bottom sides:} \quad \left[\begin{array}{rcl} u^2_{i,j+\frac{1}{2}} &=& \frac{1}{2}\left(\mathsf{U}^2_{i,j} + \mathsf{U}^2_{i,j+1}\right), \\ u^2_{i,j-\frac{1}{2}} &=& \frac{1}{2}\left(\mathsf{U}^2_{i,j} + \mathsf{U}^2_{i,j-1}\right) \end{array}\right.$$

$$\text{Top/Bottom sides:} \quad \left[\begin{array}{rcl} \mu \left.\dfrac{\partial v}{\partial y}\right|_{i,j+\frac{1}{2}} &=& \mu_{i,j+\frac{1}{2}} \dfrac{\mathsf{V}_{i,j+1} - \mathsf{V}_{i,j}}{h_y}, \\ \mu \left.\dfrac{\partial v}{\partial y}\right|_{i,j-\frac{1}{2}} &=& \mu_{i,j-\frac{1}{2}} \dfrac{\mathsf{V}_{i,j} - \mathsf{V}_{i,j-1}}{h_y}, \end{array}\right. \quad \text{Right/Left sides:} \quad \left[\begin{array}{rcl} \mu \left.\dfrac{\partial v}{\partial x}\right|_{i+\frac{1}{2},j} &=& \mu_{i+\frac{1}{2},j} \dfrac{\mathsf{V}_{i+1,j} - \mathsf{V}_{i,j}}{h_x}, \\ \mu \left.\dfrac{\partial v}{\partial x}\right|_{i-\frac{1}{2},j} &=& \mu_{i-\frac{1}{2},j} \dfrac{\mathsf{V}_{i,j} - \mathsf{V}_{i-1,j}}{h_x} \end{array}\right.$$

$$\text{Right/Left sides:} \quad \left[\begin{array}{rcl} \mu \left.\dfrac{\partial u}{\partial y}\right|_{i+\frac{1}{2},j} &=& \dfrac{\mu_{i+\frac{1}{2},j}}{2}\left(\dfrac{\mathsf{U}_{i+1,j+1} - \mathsf{U}_{i+1,j-1}}{2h_y} + \dfrac{\mathsf{U}_{i,j+1} - \mathsf{U}_{i,j-1}}{2h_y}\right), \\ \mu \left.\dfrac{\partial u}{\partial y}\right|_{i-\frac{1}{2},j} &=& \dfrac{\mu_{i-\frac{1}{2},j}}{2}\left(\dfrac{\mathsf{U}_{i,j+1} - \mathsf{U}_{i,j-1}}{2h_y} + \dfrac{\mathsf{U}_{i-1,j+1} - \mathsf{U}_{i-1,j-1}}{2h_y}\right) \end{array}\right.$$

$$\text{Top/Bottom sides:} \quad \left[\begin{array}{rcl} p_{i,j+\frac{1}{2}} &=& \frac{1}{2}\left(\mathsf{P}_{i,j+1} + \mathsf{P}_{i,j}\right), \\ p_{i,j-\frac{1}{2}} &=& \frac{1}{2}\left(\mathsf{P}_{i,j} + \mathsf{P}_{i,j-1}\right) \end{array}\right.$$

6.5.2 Comments on the nonlinear advective terms

The nonlinear convective terms deserve some further attention. There are two aspects we have to deal with, namely

- **Spatial discretization**
- **Treatment of nonlinearities**

As for the former, the discretization adopted above corresponds to central differencing, while we have seen that **upwind** schemes may be more appropriate in problems where convective effects are strong. Consider as an example the equation for the x-direction. We use for the face values of the nonlinear term

$$(u\,v)_{i,j+\frac{1}{2}} \approx \begin{cases} \mathsf{U}_{i,j}\mathsf{V}_{i,j} & \text{if} \quad \mathsf{V}_{i,j} + \mathsf{V}_{i,j+1} \geq 0 \\ \mathsf{U}_{i,j+1}\mathsf{V}_{i,j+1} & \text{if} \quad \mathsf{V}_{i,j} + \mathsf{V}_{i,j+1} < 0 \end{cases}$$

and similarly for other terms and faces. More sophisticated schemes based on **limiters** can be consulted in the literature (see e.g. [35], Chapters 4 and 6).

[35]: Wesseling (2001), *Principles of Computational Fluid Dynamics*

As for the treatment of nonlinearities, we must linearize or apply an iterative procedure, such as the Newton's or fixed point method. The

simplest approach would be to approximate the nonlinear terms as

$$u\,(\mathbf{u}\cdot\check{\mathbf{n}}) \approx u\,(\bar{\mathbf{u}}\cdot\check{\mathbf{n}}) \quad \text{and} \quad v\,(\mathbf{u}\cdot\check{\mathbf{n}}) \approx v\,(\bar{\mathbf{u}}\cdot\check{\mathbf{n}}),$$

where $\bar{\mathbf{u}}$ would be the velocity computed at a previous iteration or time level. Notice that for the u-equation the unknown is u and for the v-equation the unknown is v, therefore, as commented in [35], it would be a bad ideia to do the other way around. Otherwise, if Newton's method is used the corresponding Jacobian must be computed. In that case the nonlinear term can be approximated by linearizing around the last computed state $(\bar{u}, \bar{v})$ as

$$u\,v \approx \bar{u}\,\bar{v} + \bar{v}\,\delta u + \bar{u}\,\delta v = u\,\bar{v} + \bar{u}\,v - \bar{u}\,\bar{v}$$

and similarly for other terms.

6.5.3 Treatment of boundary conditions

For the sake of brevity, it is left as an exercice to discuss how to deal with the boundary conditions, be it, Dirichlet (imposed velocity) or Neumann (imposed force) in cell-centered finite volume discretizations using a colocated grid. As a reference, you may go back to previous discussions in Chapter 2 and 3, where FV methods have been extensively applied to solve diffusion-type equations and [35] (Chapter 3).

6.5.4 Spurious checkboard modes

In this subsection we follow [35], although the phenomenon of spurious checkboard patterns is discussed and illustrated in any textbook on the subject. Considering constant and uniform density and viscosity for simplicity, the ideia is to realize that the following **unphysical checkboard function** is a solution of the discrete scheme detailed above

$$\mathsf{U}_{i,j} = \mathsf{V}_{i,j} = (-1)^{i+j}\,\psi(t), \quad \mathsf{P}_{i,j} = (-1)^{i+j}$$

(see Figure 6.3) where $\psi(t)$ satisfy the following Ordinary Differential Equation (ODE)[11]

$$\frac{d\psi}{dt} + a\,\psi = 0$$

in which $a = \dfrac{12\mu}{\rho}\left(\dfrac{1}{h_x^2} + \dfrac{1}{h_y^2}\right)$ and whose solution is known to be

$$\psi(t) = \psi_0\, e^{-a\,t}$$

so, this means that a constant checkboard pressure solution of the discrete system coexists with a damped checkboard solution for the velocity, which eventually tends to zero[12]. The existence of such modes shows that the previous discretization scheme on colocated grids needs to be corrected so as to avoid these *spurious* solutions. A similar phenomenon is observed in finite element discretizations when the same discrete spaces (equal order) are used for velocity and pressure. For such reason, FE discretizations adopt a velocity space that is richer than the pressure

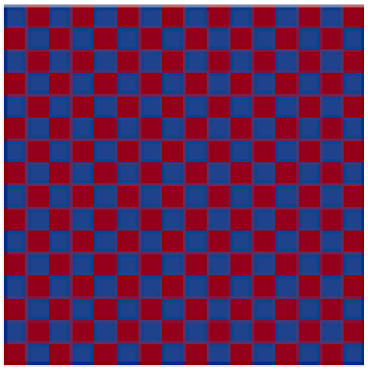

Figure 6.3: Typical checkboard patterns in unstabilized colocated grids.

11: See the details in [35] or better, verify it yourself.

12: Notice that the damping would be slow if Re$\gg$ 1.

space[13] or otherwise, stabilization terms are added to the variational formulation.

13: The tipical FE discretization of the Navier-Stokes equations uses P_2 quadratic elements for velocity and P_1 linear elements for pressure, which is referred to as the Taylor-Hood element.

6.5.5 One remedy: One-sided discretization of div$(\cdot)$ and grad$(\cdot)$

From the previous subsection we can see that the reason for the spurious modes is the central difference scheme for the div terms in the discretization of the continuity equation 6.14

$$\frac{h_y}{2}\left(\mathsf{U}^{n+1}_{i+1,j} - \mathsf{U}^{n+1}_{i-1,j}\right) + \frac{h_x}{2}\left(\mathsf{V}^{n+1}_{i,j+1} - \mathsf{V}^{n+1}_{i,j-1}\right) = 0$$

and for the grad terms in the momentum equations

$$h_y\,(p_{i+\frac{1}{2},j} - p_{i-\frac{1}{2},j}) \approx \frac{h_y}{2}\left(\mathsf{P}_{i+1,j} - \mathsf{P}_{i-1,j}\right) \quad \text{and} \quad h_x\,(p_{i,j+\frac{1}{2}} - p_{i,j-\frac{1}{2}}) \approx \frac{h_x}{2}\left(\mathsf{P}_{i,j+1} - \mathsf{P}_{i,j-1}\right)$$

which simple ignore the values of u and p at cell (i, j).

The spurious modes can be avoided by using a one-sided scheme, e.g., **forward** differences for the div terms and **backward** differences for the grad terms. For the continuity equation this is equivalent to taking

$$u_{i+\frac{1}{2},j} \approx \mathsf{U}_{i+1,j}, \quad u_{i-\frac{1}{2},j} \approx \mathsf{U}_{i,j},$$

$$v_{i,j+\frac{1}{2}} \approx \mathsf{V}_{i,j+1}, \quad v_{i,j-\frac{1}{2}} \approx \mathsf{V}_{i,j}$$

thus giving

$$h_y\left(\mathsf{U}^{n+1}_{i+1,j} - \mathsf{U}^{n+1}_{i,j}\right) + h_x\left(\mathsf{V}^{n+1}_{i,j+1} - \mathsf{V}^{n+1}_{i,j}\right) = 0$$

and for the pressure terms

$$h_y\,(p_{i+\frac{1}{2},j} - p_{i-\frac{1}{2},j}) \approx h_y\left(\mathsf{P}_{i,j} - \mathsf{P}_{i-1,j}\right) \quad \text{and} \quad h_x\,(p_{i,j+\frac{1}{2}} - p_{i,j-\frac{1}{2}}) \approx h_x\left(\mathsf{P}_{i,j} - \mathsf{P}_{i,j-1}\right)$$

The only problem with such scheme is that it reduces to first order $\mathcal{O}(h_x + h_y)$, so we may ask for the next "better" alternative.

6.5.6 Another remedy: Pressure-Weighted-Interpolation (PWI)

[36]: Rhie et al. (1983), 'Numerical study of the turbulent flow past an airfoil with trailing edge separation'
[37]: Miller et al. (1988), ' Use of a pressure-weighted interpolation method for the solution of the incompressible Navier-Stokes equations on a nonstaggered grid system'

To circumvent the suboptimal order of the previous one-sided formulas, Rhie and Chow [36, 37] have proposed a scheme which is second order in space (i.e., $\mathcal{O}(h_x^2 + h_y^2)$). The ideia of the method is to add a small regularizing term to the continuity equation, more precisely, a Laplacian of the pressure, in the following way, for finite volume $K_{i,j}$

$$\int_{K_{i,j}} \nabla\cdot\mathbf{u}^{n+1}\,dv \;\approx\; \frac{1}{2\,h_x}\left(\mathsf{U}^{n+1}_{i+1,j} - \mathsf{U}^{n+1}_{i-1,j}\right) + \frac{1}{2\,h_y}\left(\mathsf{V}^{n+1}_{i,j+1} - \mathsf{V}^{n+1}_{i,j-1}\right) + \mathscr{R}_{i,j}(\mathbf{P}) = 0$$

where the regularizing term is given by

$$\mathscr{R}_{i,j}(\mathbf{P}) = \frac{h_x\,h_y}{2\mu}\left\{\left[\mathbb{L}^x_{i+1,j}(\mathbf{P}) - 2\,\mathbb{L}^x_{i,j}(\mathbf{P}) + \mathbb{L}^x_{i-1,j}(\mathbf{P})\right] + \left[\mathbb{L}^y_{i,j+1}(\mathbf{P}) - 2\,\mathbb{L}^y_{i,j}(\mathbf{P}) + \mathbb{L}^y_{i,j-1}(\mathbf{P})\right]\right\}$$

with

$$\mathbb{L}^x_{i,j}(\mathbf{P}) = \frac{1}{\alpha_{i,j}\, h_x^2}\left(\mathsf{P}_{i+1,j} - 2\,\mathsf{P}_{i,j} + \mathsf{P}_{i-1,j}\right)$$

and the coefficient $\alpha_{i,j}$ is given by[14]

$$\alpha_{i,j} = (-1) \sum_{(m,n)\neq(i,j)} c_{m,n}$$

in which $c_{m,n}$ are the coefficients involving the u unknown in the x-momentum balance equation 6.17. The expressions for the other terms and directions are analogous. The scheme works well as to the control of the spurious modes provided the body forces are sufficiently small, otherwise further modifications are necessary. Details can be found in [35, 36] and [37].

14: Notice that i and j in $\mathbb{L}^x_{i,j}(\cdot)$ does NOT denote the row and column indices of matrix $\mathbb{L}$. Recall, always, that for each pair (i,j) it corresponds a global index $\mathcal{J}_g$, so, $\mathbb{L}^x_{i,j}(\mathbf{P})$ must be understood as the $\mathcal{J}_g$–th component of the action of the Laplacian operator $\mathbb{L}$ on the global vector of unkowns $\mathbf{P}$.

6.6 Assignment 1: A practice with `OpenFOAM` - Flow around obstacle

The aim in this assignment is to study the classical phenomenon of vortex shedding that occurs when a flow past a bluff body. To that end consider the `OpenFOAM` case `VortexShedding/` to simulate the laminar transient flow around a circular obstacle by solving the incompressible Navier-Stokes equations. The case is taken from `https://wiki.openfoam.com/`, an interesting source for `OpenFOAM` cases. The problem geometry and computational grid are shown in Figure 6.5. It consists of the rectangle $[-20, 30] \times [-20, 20]$ and the obstacle is the circle of radius 1 centered at $(0, 0)$. Recall that `OpenFOAM` solve problems by the Finite Volume Method on general colocated grids.

Theodore von Kármán (Hungary(1881)–Germany(1963)).

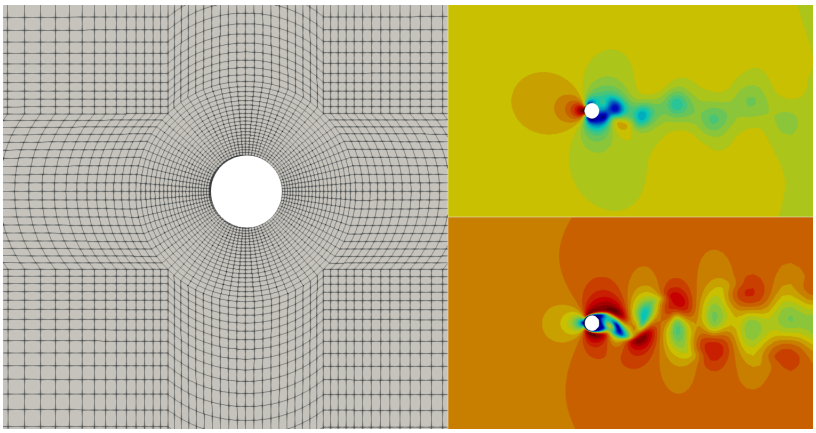

Figure 6.5: Mesh, typical velocity and pressure fields for the flow field around a circular obstacle at Re= 200 obtained with `OpenFOAM`.

1. The first task is to identify the problem setting and the different numerical ingredients involved in the solution of the problem. To that end explore the content of the different files:
   - `0/U`
   - `constant/transportProperties`
   - `constant/turbelenceProperties`

- `system/controlDict`
- `system/fvSchemes`
- `system/fvSolution`

After that you should be able to answer:

- What are the boundary conditions?
- What are the material parameters?
- What is the time marching algorithm?
- What are the discretization options to compute the gradients?
- etc., ...

2. Run the case by setting the Reynolds number to values Re= 20, 40, 80, 160, 320.

3. Visualize the results, namely, pressure, velocity and streamlines by using `paraFoam`. Activate the `surfaceLIC` plugin in `ParaFOAM` to better visualize the flow patterns. Be aware that this filter can be quite slow on fine grids.

4. For each of the Reynolds number of the previous item, identify at which time the dettaching of vortices begins to occur.

5. Plot the lift and drag forces as a function of time. These can be found in the directory `sol_postprocessing/`.

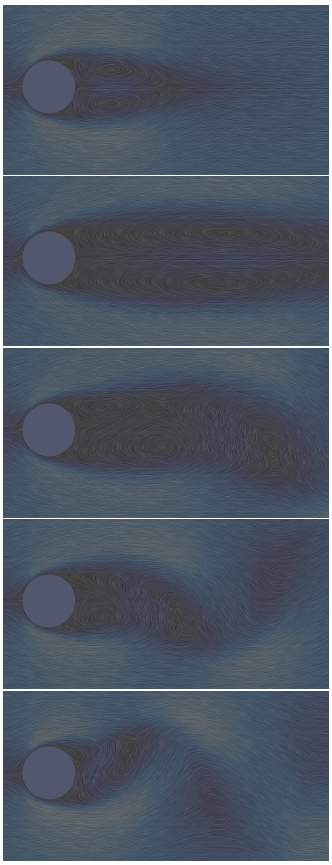

Figure 6.6: Flow field around a circular obstacle at different time instants for Re= 200 obtained with `OpenFOAM`.

6.7 The ultimate remedy to cure the spurious checkboard modes: Staggered grids

A better and more elegant way to avoid the spurious checkboard modes is to use a staggered grid (see Figure 6.1). In the *non-orthogonal* and/or *unstructured* case, its implementation is difficult. Actually, most of the software used by the industry, namely, `Fluent` and `OpenFoam`, rely on colocated grids. However, for orthogonal cartesian meshes, it is the method of choice so, it will be discussed in this section. We restrict again to the 2D case since there are no new concepts involved in the treatment of the 3D case.

In the staggered arrange, velocity unknowns are located at cell faces, more specifically, u-velocities at vertical faces and v-velocities at horizontal faces, whereas pressure unknowns are located at cell centroids. This in turn leads to different control volumes on which the x-momentum, y-momentum and continuity equations are integrated (see Figure 6.7). We denote the control volumes, respectively by $K^u_{i,j}$, $K^v_{i,j}$ and $K^p_{i,j}$. Beginning with the continuity equation, we integrate over the finite volume $K^p_{i,j}$ at which the pressure unknown $\mathsf{P}_{i,j}$ is centered, yielding[15]

$$\int_{K^p_{i,j}} \nabla \cdot \mathbf{u}^{n+1}\, dv = \int_{\partial K^p_{i,j}} \mathbf{u}^{n+1} \cdot \check{\mathbf{n}}\, d\ell \approx h_y \left(\mathsf{U}_{i+1,j} - \mathsf{U}_{i,j}\right) + h_x \left(\mathsf{V}_{i,j+1} - \mathsf{V}_{i,j}\right) = 0$$

A key point now is to realize that in the staggered arrange of unknowns,

15: At this stage we continue omiting the time dependence of variable to keep the notation simpler.

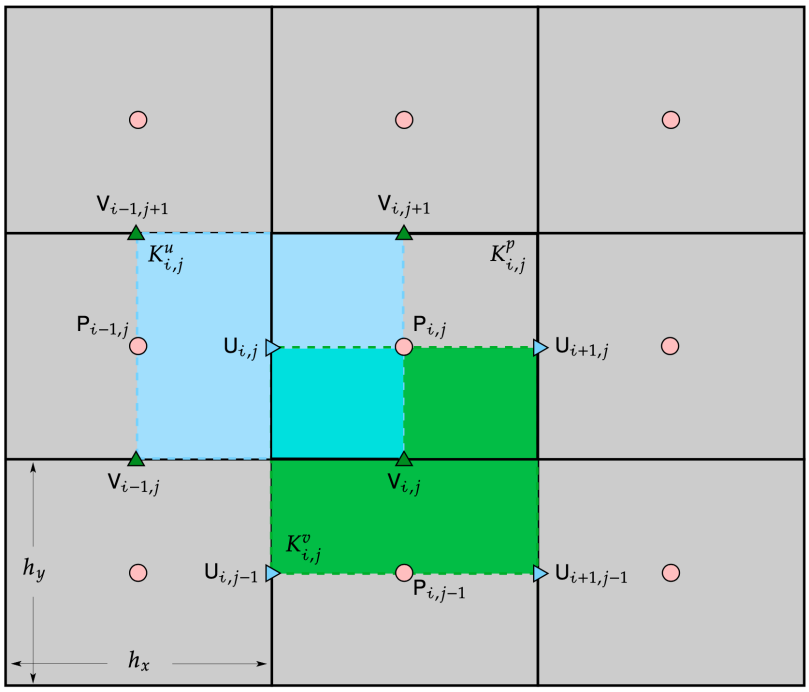

Figure 6.7: Staggered arrange of unknowns.

no further interpolation approximation is needed to obtain the face values $\mathsf{U}_{i+1,j}$, $\mathsf{U}_{i,j}$, $\mathsf{V}_{i,j+1}$ and $\mathsf{V}_{i,j}$. This can be written in terms of operators as

$$\int_{K^p_{i,j}} \nabla \cdot \mathbf{u}^{n+1}\, dv \approx h_x\, h_y\, \mathbb{D}_{i,j}(\mathbf{U}) = h_x\, h_y\, \mathbb{D}^x_{i,j}(\mathbf{U}_x) + h_x\, h_y\, \mathbb{D}^y_{i,j}(\mathbf{U}_y) = 0$$

where

$$\mathbb{D}^x_{i,j}(\mathbf{U}_x) = \frac{\mathsf{U}_{i+1,j} - \mathsf{U}_{i,j}}{h_x}, \qquad \mathbb{D}^y_{i,j}(\mathbf{U}_y) = \frac{\mathsf{V}_{i,j+1} - \mathsf{V}_{i,j}}{h_y}$$

This can also be written in matrix form by blocks as

$$\mathbb{D}\,(\mathbf{U}) = \begin{bmatrix} \mathbb{D}^x & \mathbb{0} \\ \mathbb{0} & \mathbb{D}^y \end{bmatrix} \cdot \begin{bmatrix} \mathbf{U}_x \\ \mathbf{U}_y \end{bmatrix}$$

Again, as with the Laplacian operator $\mathbb{L}^x_{i,j}$ introduced above, recall that (i,j) does not denote the row and column indices of the matrix $\mathbb{D}^x$. Instead, $\mathbb{D}^x_{i,j}(\mathbf{U}_x)$ must be understood as the global j_g–th component of the action of the divergence operator $\mathbb{D}^x$ on the global vector of unkowns $\mathbf{U}_x$.

For the x-momentum balance equation we integrate over $K^u_{i,j}$ (see Figure 6.8)

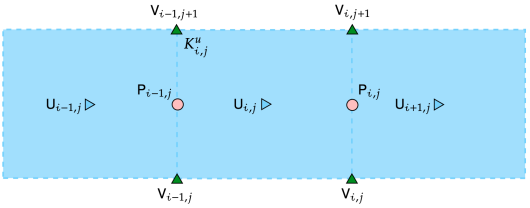

Figure 6.8: u-cells for the x-momentum balance.

$$\int_{K^u_{i,j}} \rho\, \partial_t u\, dv + \int_{\partial K^u_{i,j}} \left[\rho\, u\, (\mathbf{u} \cdot \check{\mathbf{n}}) - 2\mu\, \frac{\partial u}{\partial x}\, \check{n}_x - \mu \left(\frac{\partial u}{\partial y} + \frac{\partial v}{\partial x} \right) \check{n}_y + p \check{n}_x \right] d\ell \approx$$

$$h_x\, h_y\, \left[\rho\, \partial_t \mathbf{u}\right]_{i,j} + h_y \rho \left[u^2_{i_r,j} - u^2_{i_l,j} \right] + h_x \rho \left[(u\, v)_{i,j_t} - (u\, v)_{i,j_b} \right] -$$

$$-h_y\left(2\mu\left.\frac{\partial u}{\partial x}\right|_{i_r,j}-2\mu\left.\frac{\partial u}{\partial x}\right|_{i_l,j}\right)-h_x\left[\mu\left(\frac{\partial u}{\partial y}+\frac{\partial v}{\partial x}\right)_{i,j_t}-\mu\left(\frac{\partial u}{\partial y}+\frac{\partial v}{\partial x}\right)_{i,j_b}\right]+$$

$$+h_y\left(p_{i_r,j}-p_{i_l,j}\right) \tag{6.18}$$

Now, in the staggered grid, we will see some of the approximations become greatly simplified:

Right/Left sides: $\left[\begin{array}{lcl} u^2_{i_r,j} & = & \frac{1}{4}\left(\mathsf{U}_{i,j}+\mathsf{U}_{i+1,j}\right)^2, \\ u^2_{i_l,j} & = & \frac{1}{4}\left(\mathsf{U}_{i,j}+\mathsf{U}_{i-1,j}\right)^2, \end{array}\right.$ Top/Bottom sides: $\left[\begin{array}{lcl} (u\,v)_{i,j_t} & = & \frac{1}{4}\left(\mathsf{U}_{i,j}+\mathsf{U}_{i,j+1}\right)\left(\mathsf{V}_{i-1,j+1}+\mathsf{V}_{i,j+1}\right), \\ (u\,v)_{i,j_b} & = & \frac{1}{4}\left(\mathsf{U}_{i,j}+\mathsf{U}_{i,j-1}\right)\left(\mathsf{V}_{i-1,j}+\mathsf{V}_{i,j}\right) \end{array}\right.$

Right/Left sides: $\left[\begin{array}{lcl} \mu\left.\frac{\partial u}{\partial x}\right|_{i_r,j} & = & \mu_{i_r,j}\frac{\mathsf{U}_{i+1,j}-\mathsf{U}_{i,j}}{h_x}, \\ \mu\left.\frac{\partial u}{\partial x}\right|_{i_l,j} & = & \mu_{i_l,j}\frac{\mathsf{U}_{i,j}-\mathsf{U}_{i-1,j}}{h_x}, \end{array}\right.$ Top/Bottom sides: $\left[\begin{array}{lcl} \mu\left.\frac{\partial u}{\partial y}\right|_{i,j_t} & = & \mu_{i,j_t}\frac{\mathsf{U}_{i,j+1}-\mathsf{U}_{i,j}}{h_y}, \\ \mu\left.\frac{\partial u}{\partial y}\right|_{i,j_b} & = & \mu_{i,j_b}\frac{\mathsf{U}_{i,j}-\mathsf{U}_{i,j-1}}{h_y} \end{array}\right.$

Top/Bottom sides: $\left[\begin{array}{lcl} \mu\left.\frac{\partial v}{\partial x}\right|_{i,j_t} & = & \mu_{i,j_t}\frac{\mathsf{V}_{i,j+1}-\mathsf{V}_{i-1,j+1}}{h_x}, \\ \mu\left.\frac{\partial v}{\partial x}\right|_{i,j_b} & = & \mu_{i,j_b}\frac{\mathsf{V}_{i,j}-\mathsf{V}_{i-1,j}}{h_x} \end{array}\right.$

Right/Left sides: $\left[\begin{array}{lcl} p_{i_r,j} & = & \mathsf{P}_{i,j}, \\ p_{i_l,j} & = & \mathsf{P}_{i-1,j} \end{array}\right.$

As we did for the divergence term in the continuity equation, for the pressure gradient term we can writte

$$\int_{\partial K^u_{i,j}}[p\check{n}_x]\,d\ell \approx h_x\,h_y\,\mathbb{G}^x_{i,j}(\mathbf{P})$$

where

$$\mathbb{G}^x_{i,j}(\mathbf{P})=\frac{\mathsf{P}_{i,j}-\mathsf{P}_{i-1,j}}{h_x}$$

The approximations for the y-component of the momentum balance over control volume $K^v_{i,j}$ are left as an exercice. See Figure 6.9.

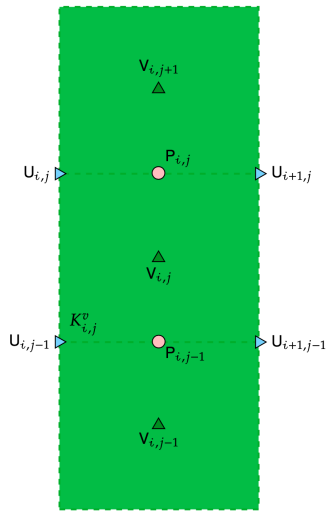

Figure 6.9: v-cells for the y-momentum balance.

6.7.1 Laplacian form of the viscous term

In the constant viscosity case we have the following identity

$$\nabla\cdot\left[\mu\left(\nabla\mathbf{u}+\nabla^\intercal\mathbf{u}\right)\right]=\mu\nabla\cdot\left(\nabla\mathbf{u}\right)+\underbrace{\mu\nabla\cdot\left(\nabla^\intercal\mathbf{u}\right)}_{=0}=\mu\nabla^2\mathbf{u}$$

The second term is zero because

$$[\nabla \cdot (\nabla^\intercal \mathbf{u})]_i = \frac{\partial}{\partial x_j}\left(\frac{\partial u_j}{\partial x_i}\right) = \frac{\partial}{\partial x_i}\left(\frac{\partial u_j}{\partial x_j}\right) = \frac{\partial}{\partial x_i}(\nabla \cdot \mathbf{u}) = [\nabla(\nabla \cdot \mathbf{u})]_i = 0$$

since, obviously $\nabla \cdot \mathbf{u} = 0$ in the incompressible case we are dealing with[16]. Hence, the discretization of the viscous term simplifies to (e.g., for the x-momentum balance):

16: Notoriously, the simplification also holds at the discrete level for the staggered scheme. The verification is left as an exercice (see Exo. 1 of Assignment 2 below).

$$-\int_{K^u_{i,j}} \{\nabla \cdot [\mu(\nabla \mathbf{u} + \nabla^\intercal \mathbf{u})]\}\, dv = -\mu \int_{\partial K^u_{i,j}} \nabla \mathbf{u} \cdot \check{\mathbf{n}}\, d\ell = -\mu \int_{\partial K^u_{i,j}} \left[\frac{\partial u}{\partial x}\check{n}_x + \frac{\partial u}{\partial y}\check{n}_y\right] d\ell =$$

$$-\mu\, h_y \left(\left.\frac{\partial u}{\partial x}\right|_{i_r,j} - \left.\frac{\partial u}{\partial x}\right|_{i_l,j}\right) - \mu\, h_x \left(\left.\frac{\partial u}{\partial y}\right|_{i,j_t} - \left.\frac{\partial u}{\partial y}\right|_{i,j_b}\right) \approx$$

$$-\mu\left(h_y \frac{\mathsf{U}_{i+1,j} - \mathsf{U}_{i,j}}{h_x} - h_y \frac{\mathsf{U}_{i,j} - \mathsf{U}_{i-1,j}}{h_x} + h_x \frac{\mathsf{U}_{i,j+1} - \mathsf{U}_{i,j}}{h_y} - h_x \frac{\mathsf{U}_{i,j} - \mathsf{U}_{i,j-1}}{h_y}\right) = -\mu\, h_x\, h_y \left(\mathbb{L}^x_{i,j}(\mathbf{U}) + \mathbb{L}^y_{i,j}(\mathbf{U})\right)$$

It can be seen that, a salient feature of the staggered discretizations is that[17]

$$\mathbb{D}^x\, \mathbb{G}^x = \mathbb{L}^x$$

17: The same does not hold for colocated grids, so we need to add stabilization terms as we have seen in 6.5.6.

or with our recurrent abuse of notation

$$\mathbb{D}^x_{i,j}(\mathbb{G}^x_{i,j}(\mathbf{U}_x)) = \mathbb{L}^x_{i,j}(\mathbf{U}_x)$$

and similar for the y-component. The same holds for the Poisson's equation for the pressure in the projection scheme, i.e., $\mathbb{D}\mathbb{G}(\mathbf{P}) = \mathbb{L}(\mathbf{P})$ (this is also left for Exo. 2 of the Assignment below).

6.7.2 Treatment of boundary conditions

As usual, boundary conditions are the hardest part to code in a PDE solver. There are several ways to deal with the boundary conditions. We can use for instance the so called ghost cells, so, we take a discretization made of $(N_x + 2) \times (N_y + 2)$ cells (see 6.10):

- $\mathbf{U} \in \mathbb{R}^{\dim_u}$
- $\mathbf{V} \in \mathbb{R}^{\dim_v}$
- $\mathbf{P} \in \mathbb{R}^{\dim_p}$

where

$$\dim_u = \dim_v = \dim_p = (N_x + 2) \times (N_y + 2)$$

and (N_x, N_y) are the interior **pressure cell-centered** cells.

Imposed velocity

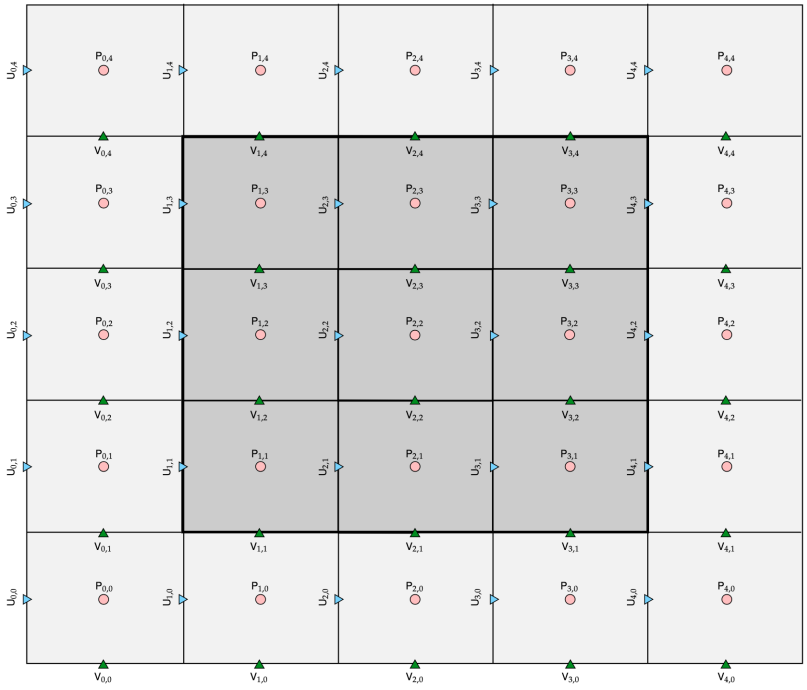

Let us suposse we aim to impose both components of velocity on a given wall. To fix the ideas consider the left vertical wall as in Figure 6.11. In such case the condition is

$$\mathbf{u}(0, y) = (u_\ell, v_\ell)$$

For the normal component to the wall is simple. The x-component of the momentum balance is simply replaced by

$$\mathsf{U}_{1,j} = u_\ell$$

For the tangent velocity v_ℓ, we introduce a **ghost** unknown $\mathsf{V}_{0,j}$ (to the left of the interior unknown $\mathsf{V}_{1,j}$) whose value must be such that

$$\mathsf{V}_{0,j} + \mathsf{V}_{1,j} - 2\,v_\ell = 0 \tag{6.19}$$

from which, by linear interpolation from $x = -h_x/2$ to $x = h_x/2$, we obtain the correct velocity at $x = 0$. For the other walls (right, bottom and top) is similar[18].

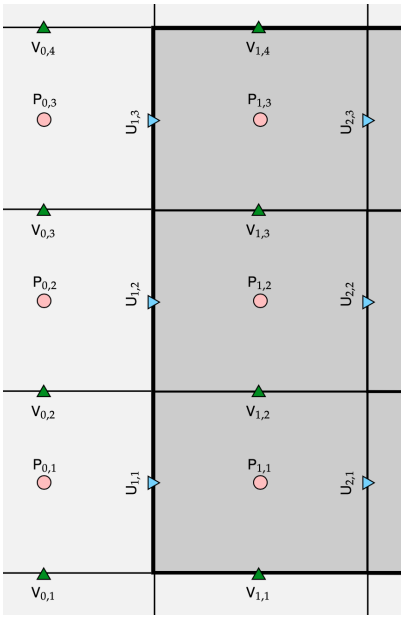

Figure 6.11: Cells adjacent to the left wall.

Imposed force

Let us consider the left vertical wall again. If we aim to impose the tangential velocity v_ℓ and the normal component of the force F^x_w, we may consider the finite volume $K^u_{1,j}$ associated to unknown $\mathsf{U}_{1,j}$ reduced by half and proceed by substituting the integral over the left side of the finite volume $i_l = 1$ by the given value, i.e.,

$$h_y \left(-2\mu \left.\frac{\partial u}{\partial x}\right|_{1,j} + p_{1,j} \right) = h_y\, F^x_w$$

18: Recall that in the current context, this discussion is limited to orthogonal cartesian grids. Also, notice that from Equation 6.19 we have

$$\frac{\mathsf{V}_{0,j} + \mathsf{V}_{1,j}}{2} = v_\ell$$

which ends up in the right-hand-side of the system. Notice that, if instead, we impose the normal velocity u_ℓ and the tangential component of the force, we work with the y-momentum balance in finite volume $K^v_{1,j}$ associated to unknown $\mathsf{V}_{1,j}$[19].

19: Recall that, for mixed boundary conditions, for the problem to be well-posed, we can not imposed both tangential components of velocity and force (or both normal components of velocity and force) simultaneously, we either impose tangential velocity and normal force or viceversa.

Boundary conditions for the pressure equation

When using the projection method of section 6.4 we have to impose some boundary condition for the pressure equation. In the staggered discretization we proceed as follows. Let us consider our vertical wall and a pressure finite volume adjacent to the wall on which the normal velocity $\mathsf{U}_{1,j} = u_\ell$ is given to us. The discrete continuity equation at time $n+1$ thus reads

$$\frac{\mathsf{U}^{n+1}_{2,j} - \mathsf{U}^{n+1}_{1,j}}{h_x} + \frac{\mathsf{V}^{n+1}_{1,j+1} - \mathsf{V}^{n+1}_{1,j}}{h_y} = \frac{\mathsf{U}^{n+1}_{2,j} - u_\ell}{h_x} + \frac{\mathsf{V}^{n+1}_{1,j+1} - \mathsf{V}^{n+1}_{1,j}}{h_y} = 0 \quad (6.20)$$

and the velocity corrector step for velocity unknowns $\mathsf{U}^{n+1}_{i,j}$ and $\mathsf{V}^{n+1}_{i,j}$

$$\mathsf{U}^{n+1}_{i,j} = \hat{\mathsf{U}}^{n+1}_{i,j} - \frac{\Delta t}{\rho}\mathbb{G}^x_{i,j}(\mathbf{P})$$

$$\mathsf{V}^{n+1}_{i,j} = \hat{\mathsf{V}}^{n+1}_{i,j} - \frac{\Delta t}{\rho}\mathbb{G}^y_{i,j}(\mathbf{P})$$

20: Notice that if the problem at hand has pure velocity BCs, the null space of the pressure matrix will be made of the constant vector $\mathbf{1} \in \mathbb{R}^{\dim p}$. In such case, the matrix must be asserted by fixing the pressure at some point or by letting the linear solver to handle the indeterminancy.

which substituting into Equation 6.20 and after some manipulations gives a modified pressure equation for those cells adjacent to the wall in which the velocity is being imposed

$$\frac{\mathsf{P}^{n+1}_{2,j} - 1\,\mathsf{P}^{n+1}_{1,j} + 0\,\mathsf{P}^{n+1}_{0,j}}{h_x^2} + \frac{\mathsf{P}^{n+1}_{1,j+1} - 2\,\mathsf{P}^{n+1}_{1,j} + \mathsf{P}^{n+1}_{1,j-1}}{h_y^2} = \frac{\rho}{\Delta t}\left(\frac{\hat{\mathsf{U}}^{n+1}_{2,j} - u_\ell}{h_x} + \frac{\hat{\mathsf{V}}^{n+1}_{1,j+1} - \hat{\mathsf{V}}^{n+1}_{1,j}}{h_y}\right)$$

which shows that actually the ghost pressure values are totally irrelevant[20]. The discussion about boundary conditions can be more extensive, specially when dealing with outflow boundaries. More details on boundary conditions for staggered and colocated arranges must be consulted in any of the references cited above.

6.8 Assignment 2: A simple Finite Volume Staggered code - Cavity flow

1. Show that for incompressible flows with the staggered scheme, the identity $\nabla \cdot \nabla^\intercal \mathbf{u} = 0$ automatically holds at the discrete level.

2. Program a small python script that builds the $\mathbb{D}$ and $\mathbb{G}$ matrix operators of the staggered scheme for a 3×3 grid. Visualize the strucuture of such matrizes as well as of their product $\mathbb{DG}$.

3. Consider an outflow boundary (e.g., the right wall) on which

we aim to impose the condition

$$\frac{\partial \mathbf{u}}{\partial x} = 0$$

How this condition tranlates into the pressure equation in the segregated approach?.

Consider the Navier-Stokes problem on the 2D square cavity $\Omega = [0,1]^2$ with constant and uniform density ρ and viscosity μ:

$$\begin{cases} \rho\left(\dfrac{\partial \mathbf{u}}{\partial t} + (\mathbf{u}\cdot\nabla)\,\mathbf{u}\right) - \mu\,\nabla^2\mathbf{u} + \nabla p &= \mathbf{0} & \text{in } \Omega \\ \nabla\cdot\mathbf{u} &= 0 & \text{in } \Omega \\ \mathbf{u}(\mathbf{x},0) &= \mathbf{0} & \text{in } \Omega \\ \mathbf{u}(\mathbf{x},t) &= (0,0) & \text{in } \Gamma_l \cup \Gamma_b \cup \Gamma_r \\ \mathbf{u}(\mathbf{x},t) &= (u_t,0) & \text{in } \Gamma_t \end{cases}$$

Consider the finite volume formulation of the projection method on a staggered grid implemented in the script `nsfvm.py`.

4. Make sure to understand the different sections of the code. Notice that the implementation is particularly simple because we are assuming uniform discretization (h_x, h_y), constant properties and an explicit formulation for time integration.

5. Complete the missing parts in the code pointed out with the string `#.....#`, namely, the implementation of some parts of the **advective** and **viscous terms** in the x and y-momentum equations, the RHS in the pressure equation and the y-component of the velocity corrector.

6. Consider discretizations with $N_x \times N_y = 32\times 32$, 64×64 and 128×128, $u_t = 1$, $\mu = 0.001$ and $\rho = 1$. Measure the computational times involved in the different steps of the code, namely, **Initial setting** and **Solver** (considering separately, Velocity predictor, Pressure solver and Velocity corrector). Measure the total times and the cost per time step.

7. Consider Reynolds numbers equal to Re= 1, 10, 100 and 1000. Show the velocity fields at different times, including: contours, profiles, streamlines and vectors. Typical results are shown in the figure.

8. Program the advection of a passive scalar governed by the

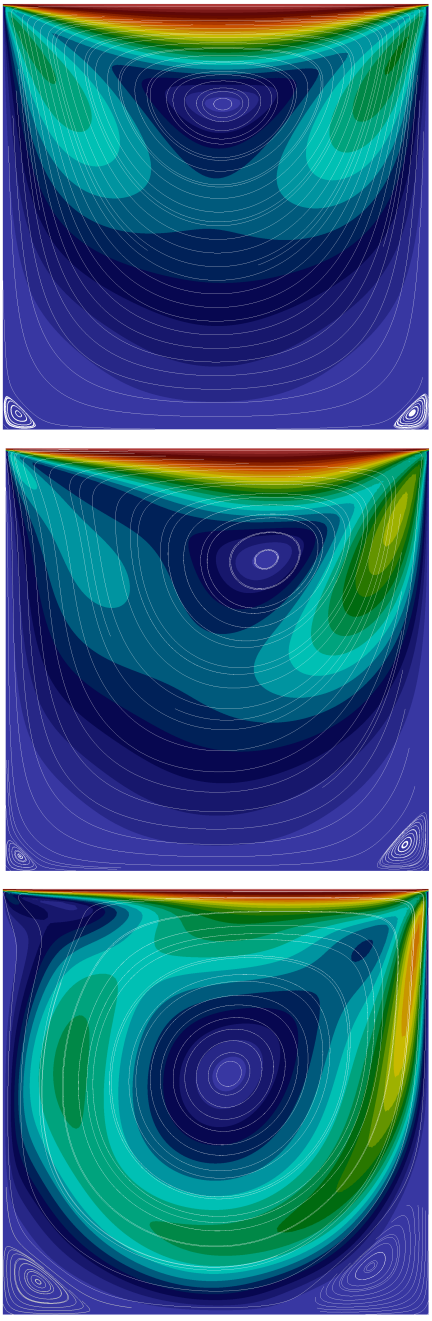

Figure 6.12: Expected steady state result in the 2D the cavity flow for Re= 10 (top), Re= 100 (middle), Re= 1000 (bottom).

following conservation law

$$\begin{cases} \dfrac{\partial \psi}{\partial t} + \nabla \cdot (\mathbf{u}\psi) = 0 & \text{in } \Omega \\ \psi(\mathbf{x}, 0) = e^{-\frac{(x-x_0)^2+(y-y_0)^2}{0.1^2}} & \text{in } \Omega \\ \psi(\mathbf{x}, t) = 0 & \text{on } \partial\Omega \end{cases} \tag{6.21}$$

above ψ represents the concentration of a species A being advected by the fluid velocity field.

- Which is the natural choice of finite volumes to locate the ψ unknowns?
- Experiment with different positions (x_0, y_0) for the initial Gaussian distribution of ψ on a grid with 128×128 and the different Reynolds numbers of the previous point.
- Compute the quantity

$$\mathcal{M}_A(t) = \int_\Omega \rho\, \psi(\mathbf{x}, t)\, dv$$

and plot as a function of time considering different time steps that honour the time step restrictions for the NS problem.

6.9 Further comments

6.9.1 Other temporal schemes: ABCN

The temporal discretizations discussed so far are first order in Δt. A temporal scheme that is very often used to enhance the accuracy of numerical results is the ABCN method, which consists in using the Adams-Bashforth (AB) method to deal with the non-linear term and the midpoint or Crank-Nicolson (CN) for the viscous terms. The scheme reads:

$$\begin{cases} \rho \dfrac{\mathbf{U}^{n+1} - \mathbf{U}^n}{\Delta t} + \rho \left[\dfrac{3}{2}\mathbb{A}(\mathbf{U}^n) - \dfrac{1}{2}\mathbb{A}(\mathbf{U}^{n-1}) \right] - \dfrac{1}{2}\left[\mathbb{V}(\mathbf{U}^{n+1}) + \mathbb{V}(\mathbf{U}^n) \right] + \mathbb{G}(\mathbf{P}^{n+1}) = \mathbf{F}^{n+\frac{1}{2}} \\ \mathbb{D}(\mathbf{U}^{n+1}) = \mathbf{0} \end{cases}$$

The proposed scheme is second order accurate in Δt. It is also simple, since it avoids any iterative process to handle the nonlinearities and finally, it avoids the stringent time step restrictions associated to the diffusive terms.

Now, in order to proceed with the pressure-velocity decoupling, we introduce an auxiliary field $\hat{\mathbf{P}}$, such that [21]

$$\mathbb{G}\,\hat{\mathbf{P}} = \mathbb{G}\,\mathbf{P}^{n+1} - \frac{1}{2}\left[\mathbb{V}(\mathbf{U}^{n+1}) - \mathbb{V}(\hat{\mathbf{U}}) \right]$$

21: This comes from taking the viscous operator at time level $n+1$ in the equation above and writting

$$\mathbb{V}(\mathbf{U}^{n+1}) = \mathbb{V}(\mathbf{U}^{n+1}) + \mathbb{V}(\hat{\mathbf{U}} - \hat{\mathbf{U}})$$

followed by the three steps:

- **Velocity predictor solver:**

$$\rho \frac{\hat{\mathbf{U}} - \mathbf{U}^n}{\Delta t} + \rho \left[\frac{3}{2} \mathbb{A}(\mathbf{U}^n) - \frac{1}{2} \mathbb{A}(\mathbf{U}^{n-1}) \right] - \frac{1}{2} \left[\mathbb{V}(\hat{\mathbf{U}}) + \mathbb{V}(\mathbf{U}^n) \right] = \mathbf{F}^n$$

- **Pressure solver:**

$$\mathbb{D}\,\mathbb{G}\,\hat{\mathbf{P}} = \frac{\rho}{\Delta t} \mathbb{D}\,\hat{\mathbf{U}}$$

- **Velocity corrector:**

$$\mathbf{U}^{n+1} = \hat{\mathbf{U}} - \frac{\Delta t}{\rho} \mathbb{G}\,\hat{\mathbf{P}}$$

6.9.2 Other decoupling strategies

Besides the projection method presented above, there exist other strategies that are used in practice to solve the pressure-velocity coupling. To conclude this chapter, we briefly comment on one called the SIMPLE method, applied to the stationary case, although the extension to the transient case is possible. SIMPLE is an acronysm for **Semi-Implicit Method for Pressure Linked Equation**. The method consists in computing pressure and velocity in an interative manner. To that end we begin with an initial guess for the pressure $\hat{\mathbf{P}}$ and solve for the velocity $\hat{\mathbf{U}}$ from

$$\mathbb{M}_{\text{diag}} \hat{\mathbf{U}} = \mathbb{M}_{\text{off}} \hat{\mathbf{U}} - \mathbb{G}\,\hat{\mathbf{P}}$$

where the operator $\mathbb{M}_{\text{diag}}$ contains the diagonal contributions of the Advection and Viscous operators and $\mathbb{M}_{\text{off}}$ the off-diagonal ones. Now, we propose a correction $(\tilde{\mathbf{U}}, \tilde{\mathbf{P}})$, such that the solution is

$$\mathbf{U} = \hat{\mathbf{U}} + \tilde{\mathbf{U}}, \qquad \mathbf{P} = \hat{\mathbf{P}} + \tilde{\mathbf{P}}$$

and the correction satisfy

$$\mathbb{M}_{\text{diag}} \tilde{\mathbf{U}} = \mathbb{M}_{\text{off}} \tilde{\mathbf{U}} - \mathbb{G}\,\tilde{\mathbf{P}}$$

However, if we ignore the off-diagonal terms, we easily derive a Poisson's equation for $\tilde{\mathbf{P}}$ by applying the divergence operator and substituing $\mathbf{U} - \hat{\mathbf{U}}$, i.e.,

$$\mathbb{L}\,\tilde{\mathbf{P}} = \mathbb{M}_{\text{diag}}^{-1} \left(\mathbb{D}\hat{\mathbf{U}} - \mathbb{D}\mathbf{U} \right) = \mathbb{M}_{\text{diag}}^{-1} \mathbb{D}\hat{\mathbf{U}}$$

This process is repeated until some convergence criterion is satisfied. The method, however, can converge slowly. More details about the SIMPLE method and its variants (SIMPLER, SIMPLEST, SIMPLEC, etc.), the PISO method, and others, can be consulted in [7, 8] or any classical reference on the subject. Most of them are available in `Fluent`, `OpenFOAM` and other CFD software.

[7]: Versteeg et al. (2007), *An Introduction to Computational Fluid Dynamics. The finite volume method.*
[8]: Jasak (1996), 'Error Analysis and Estimation for the Finite Volume Method with Applications to Fluid Flows'

COMPUTATIONAL ASPECTS OF TURBULENCE MODELING

7

"Albert Einstein's son, Hans, was a famous hydraulic engineering professor who developed important equations for sediment transport in rivers. When reporters asked Albert what he thought of his son's career, he replied, "He is working on a more difficult problem."

– The Fascinating life and Theory of Albert Einstein, Walter C. Mih.

7.1 Prelude 121
7.2 What is turbulence? Qualitative aspects 121
7.3 The Averaged Navier-Stokes equations (RANS) 122
7.4 Computational Modeling of Turbulence 127
7.5 Assignment 1: Turbulent flows 129
7.6 Assignment 2: RANS equations in openFOAM . 130

7.1 Prelude

This aim of this chapter is to present some aspects involved in the numerical simulation of turbulent incompressible flows. We begin by describing the concept of turbulent flow in a rather informal way. Second we introduce the so called Averaged Navier-Stokes equations and the simplest 2-equation model of turbulence: the k–ε model.

7.2 What is turbulence? Qualitative aspects

Majority of flows found in practice and engineering applications are turbulent. Many of us possibly have an intuitive notion of what a turbulent flow is, a a qualitative definition being:

Definition 7.2.1 *(**Deepseek**) Turbulence refers to a complex and irregular flow regime characterized by chaotic changes in pressure and flow velocity. Unlike laminar flow, where the fluid moves in smooth, parallel layers with minimal mixing, turbulent flow involves highly disordered motion, eddies, and vortices of varying sizes.*

Definition 7.2.2 *(**Chatgpt**) Turbulence is a complex, chaotic state of fluid motion characterized by irregular, three-dimensional vortices, rapid velocity fluctuations, and enhanced mixing. It occurs at high Reynolds numbers when inertial forces dominate over viscous forces, leading to the breakdown of laminar flow.*

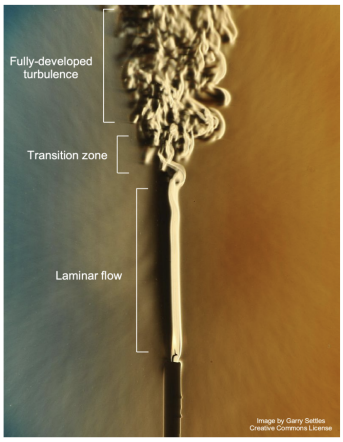

Example of a plume transitioning from laminar to turbulent. Taken from Introduction to Aerospace Flight Vehicles.

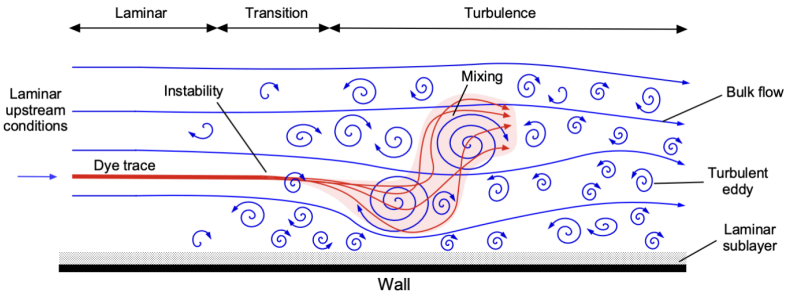

Figure 7.2: Illustration of a laminar to turbulent transition for the flow over a plate. Taken from Introduction to Aerospace Flight Vehicles.

Turbulence is a multiscale phenomena and turbulent flows occurs typically after transitioning from a laminar flow, due to the unstable nature

of such flows at high Re numbers. Some of these processes are illustrated in Figure 7.2 and Figure 7.1.

Some big names in the history of turbulence modeling are Reynolds, von Karman, Kolmogorov, Taylor and Prandtl, who surveyed and established the foundations of modern theories. A thorough study of this topic involving both theoretical and computational aspects is out of the scope of this course that would certainly consume more than one entire course. Here we will limit ourselves to describe some basic aspects.

O. Reynolds (Ireland, 1842–1912).

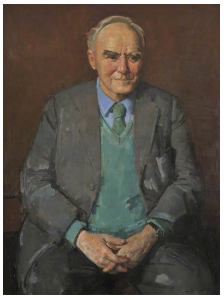

I. G. Taylor (England, 1886–1975).

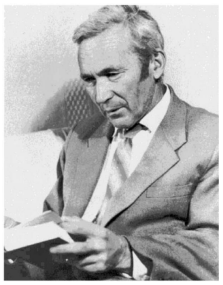

A. N. Kolmogorov (Russia, 1903–1987).

T. von Kármán (Hungary(1881)–Germany(1963)).

L. Prandtl (Germany 1875–1953).

In turbulent flows:

- Large-scale eddies are the most significant structures and help transport bulk momentum and energy;
- Intermediate-scale eddies, are essential in transferring energy from the large-scales eddies to the smallest ones;
- Small-scale eddies (1 mm or less), are responsible for energy dissipation and kinetic energy conversion into heat.
  This is illustrated in Figure 7.9.

An important observation to be made is that turbulence is essentially a 3D phenomenon:

- Vortex Stretching is a key mechanism that drives turbulence in 3D flows. This process transfers energy from larger scales to smaller scales, creating the famous energy cascade.
- Turbulence relies on nonlinear interactions between different scales of motion in 3D leading to fine-scale chaotic behavior, whereas in 2D flows, the nonlinear interactions are restricted, so the flow tends to organize into large-scale coherent structures.
- In 3D, energy is efficiently dissipated at small scales due to viscous effects. This dissipation is crucial for maintaining the energy cascade and sustaining turbulence. In 2D flows, energy dissipation is less effective.
- Mathematically, the Navier-Stokes equations, have different properties in 2D and 3D. In 3D, the equations allow for the development of chaotic behavior, which is a key feature of turbulence.

We recommend the reading of Chapter 13 of [1] to gain more insights into qualitative and quantitative aspects of turblence. For a more detailed description of the aforementioned concepts excellent references are also [38, 39][1].

7.3 The Averaged Navier-Stokes equations (RANS)

Consider the flow in shown in figure 7.8. It shows several instantaneous velocity fields at different instants of time obtained by a so called Direct Numerical Simulation (DNS) taken from `Johns Hopkins Turbulence Database`, which is nothing but the numerical resolution of the Navier-Stokes equations, possibly performed with a discretization scheme similar to those that has been studied in previous chapters, considering a full resolution mesh and time step needed to capture all of the spatial and

1: Despite the comments about the 3D nature of turbulence, the concept of "2D turbulence" and chaotic behaviors in 2D flows, have also received a great deal of attention as can be consulted in [39]. In any case, take this with some caution.

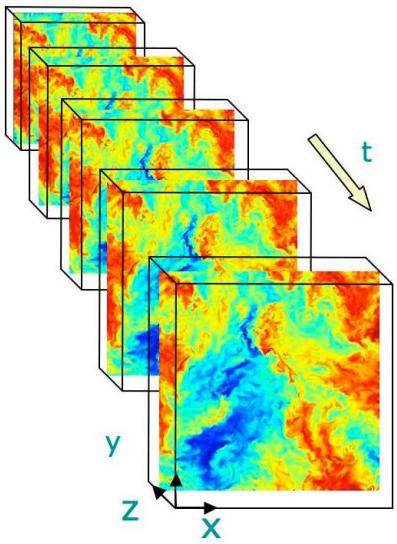

Figure 7.8: Several snapshots of a turbulent flow from a DNS computation.

temporal scales present in the flow. **Althought the flow patterns look quite complex and chaotic, the key observation to be made here is that:**

The flow exhibits **random fluctuations** around mean values, however, these mean values are quite **deterministic**.

In light of such observation, it is reasonable to introduce an additive decomposition of the flow variables into a mean or average value plus a fluctuating part:

$$\mathbf{u}(\mathbf{x},t) = \bar{\mathbf{u}}(\mathbf{x},t) + \mathbf{u}'(\mathbf{x},t), \quad p(\mathbf{x},t) = \bar{p}(\mathbf{x},t) + p'(\mathbf{x},t) \tag{7.1}$$

where the bar over a variable indicates its mean value, which is obtained after applying an averaging or mean operator, that will denoted by $\langle\cdot\rangle$ in what follows, i.e.[2],

$$\langle \mathbf{u}(\mathbf{x},t)\rangle = \bar{\mathbf{u}}(\mathbf{x},t), \quad \langle p(\mathbf{x},t)\rangle = \bar{p}(\mathbf{x},t)$$

Obviously, the decomposition above applies componentwise, i.e.,

$$u_i(x_k,t) = \bar{u}_i(x_k,t) + u_i'(x_k,t) \tag{7.2}$$

We need to precise how to compute the mean values. The first situation to consider is when these mean values do not vary with time, which is the case if the forcing terms and boundary conditions are also invariant with time. This situation is illustrated in figure Figure 7.10. In such case we define the temporal mean as:

$$\bar{\mathbf{u}}(\mathbf{x}) = \langle \mathbf{u}(\mathbf{x},t)\rangle \triangleq \lim_{t_{\text{avg}}\to\infty} \frac{1}{t_{\text{avg}}} \int_0^{t_{\text{avg}}} \mathbf{u}(\mathbf{x},t)\,dt \tag{7.3}$$

The other situation that arise is when the average values do change with time, as illustrated in Figure 7.11. In this case, a definition that makes more sense is the **ensemble** average, that would correspond to the mean

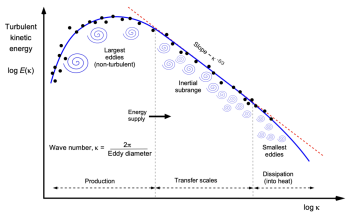

Typical spectra in log–log scale of the turbulent kinetic energy E as a function of $\kappa = \dfrac{2\pi}{D_{\text{eddy}}}$, where D_{eddy} stands for the diameter of eddies. Taken from `Introduction to Aerospace Flight Vehicles`.

2: Hereafter, we assume isothermal flow conditions, otherwise a similar decomposition should be made for the temperature field T and the energy conservation law must be solved together This would be relevant in thermally buoyant flows.

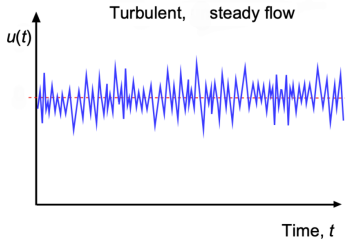

Figure 7.10: Stationary turbulent flow.

over a series of experiments or realizations of the flow:

$$\bar{\mathbf{u}}(\mathbf{x},t) = \langle \mathbf{u}(\mathbf{x},t) \rangle \triangleq \frac{1}{N_{\text{exp}}} \sum_{n=1}^{N_{\text{exp}}} \mathbf{u}^{(n)}(\mathbf{x},t) \tag{7.4}$$

In both cases, the "mean operator" is linear and the following properties are relevant:

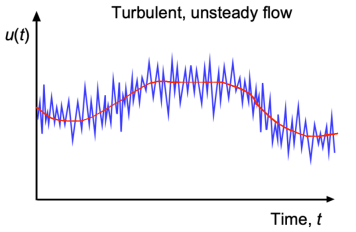

Figure 7.11: Non-stationary turbulent flow.

Definition 7.3.1 *For any scalar, vector or tensor quantity* $a(\mathbf{x},t) = \bar{a}(\mathbf{x},t) + a'(\mathbf{x},t)$*, the following properties hold:*

$$\langle \bar{a} \rangle = \bar{a} \tag{7.5}$$

$$\langle a + b \rangle = \bar{a} + \bar{b} \tag{7.6}$$

$$\langle \alpha\, a \rangle = \alpha\, \bar{a} \tag{7.7}$$

$$\langle a' \rangle = 0 \tag{7.8}$$

$$\left\langle \frac{\partial a}{\partial s} \right\rangle = \frac{\partial \langle a \rangle}{\partial s} = \frac{\partial \bar{a}}{\partial s} \tag{7.9}$$

$$\left\langle \int_{\mathcal{D}} a\, ds \right\rangle = \int_{\mathcal{D}} \langle a \rangle\, ds = \int_{\mathcal{D}} \bar{a}\, ds \tag{7.10}$$

where s *denotes any independent variable (*$\mathbf{x}$ *or* t*).*

The proof of these properties is left as an exercise.

The starting point for the RANS equations are the conservation of mass and linear momentum equations:

Mass conservation

$$\int_{\partial\Omega} \mathbf{u} \cdot \check{\mathbf{n}}\, ds = 0 \quad \Rightarrow \quad \nabla \cdot \mathbf{u} = 0 \tag{7.11}$$

Momentum conservation

$$\int_{\Omega} \rho \frac{\partial \mathbf{u}}{\partial t}\, dv + \int_{\partial\Omega} \boldsymbol{p} \cdot \check{\mathbf{n}}\, ds = \int_{\Omega} \mathbf{f}\, dv \quad \Rightarrow \quad \rho \frac{\partial \mathbf{u}}{\partial t} + \nabla \cdot \boldsymbol{p} = \mathbf{f} \tag{7.12}$$

where the *momentum flux* is defined by

$$\boldsymbol{p} = -\boldsymbol{\sigma} + \rho\, (\mathbf{u} \otimes \mathbf{u})$$

and the stress tensor, for the Newtonian case is

$$\boldsymbol{\sigma} = -p\, \mathbf{I} + \mu(\nabla \mathbf{u} + \nabla \mathbf{u}^{\intercal}) = -p\, \mathbf{I} + 2\mu \mathbf{D}(\mathbf{u})$$

Now, we substitute the decompositions (7.1). For the continuity we have:

$$\int_{\partial\Omega} (\bar{\mathbf{u}} + \mathbf{u}') \cdot \check{\mathbf{n}}\, ds = 0 \tag{7.13}$$

and apply the mean operator

$$\left\langle \int_{\partial\Omega} (\bar{\mathbf{u}} + \mathbf{u}') \cdot \check{\mathbf{n}}\, ds \right\rangle = \int_{\partial\Omega} \langle \bar{\mathbf{u}} + \mathbf{u}' \rangle \cdot \check{\mathbf{n}}\, ds = \int_{\partial\Omega} \langle \bar{\mathbf{u}} \rangle \cdot \check{\mathbf{n}}\, ds = \int_{\partial\Omega} \bar{\mathbf{u}} \cdot \check{\mathbf{n}}\, ds = 0 \tag{7.14}$$

i.e., the mean component of the velocity field satisfies the continuity equation. Similarly, for the momentum equation

$$\left\langle \int_{\Omega} \rho \frac{\partial(\bar{\mathbf{u}} + \mathbf{u}')}{\partial t}\, dv + \int_{\partial\Omega} \boldsymbol{\pi} \cdot \check{\mathbf{n}}\, ds \right\rangle = \left\langle \int_{\Omega} (\bar{\mathbf{f}} + \mathbf{f}')\, dv \right\rangle \tag{7.15}$$

$$\begin{aligned} \int_{\Omega} \rho \frac{\partial \langle \bar{\mathbf{u}} + \mathbf{u}' \rangle}{\partial t}\, dv + \int_{\partial\Omega} \langle (\bar{p} + p')\, \mathbb{I} \cdot \check{\mathbf{n}} \rangle\, ds \; - \int_{\partial\Omega} 2\mu \mathbf{D}(\langle \bar{\mathbf{u}} + \mathbf{u}' \rangle) \cdot \check{\mathbf{n}}\, ds + \\ + \int_{\Omega} \rho \langle (\bar{\mathbf{u}} + \mathbf{u}') \otimes (\bar{\mathbf{u}} + \mathbf{u}') \rangle \cdot \check{\mathbf{n}}\, ds \quad = \\ = \quad \int_{\Omega} \left\langle \bar{\mathbf{f}} + \mathbf{f}' \right\rangle dv \\ = \quad \int_{\Omega} \bar{\mathbf{f}}\, dv \end{aligned} \tag{7.16}$$

All terms are dealt easily applying the previous properties of the mean operator. The only term that deserves some attention is

$$\langle (\bar{\mathbf{u}} + \mathbf{u}') \otimes (\bar{\mathbf{u}} + \mathbf{u}') \rangle = \langle \bar{\mathbf{u}} \otimes \bar{\mathbf{u}} + \bar{\mathbf{u}} \otimes \mathbf{u}' + \mathbf{u}' \otimes \bar{\mathbf{u}} + \mathbf{u}' \otimes \mathbf{u}' \rangle = \bar{\mathbf{u}} \otimes \bar{\mathbf{u}} + \langle \mathbf{u}' \otimes \mathbf{u}' \rangle$$

since the mean of the two cross terms in the middle are zero.

$$\begin{aligned} \int_{\Omega} \rho \frac{\partial \bar{\mathbf{u}}}{\partial t}\, dv + \int_{\partial\Omega} \bar{p}\, \mathbb{I} \cdot \check{\mathbf{n}}\, ds \; - \int_{\partial\Omega} 2\mu \mathbf{D}(\bar{\mathbf{u}}) \cdot \check{\mathbf{n}}\, ds + \\ + \int_{\Omega} (\rho \bar{\mathbf{u}} \otimes \bar{\mathbf{u}} + \rho \langle \mathbf{u}' \otimes \mathbf{u}' \rangle) \cdot \check{\mathbf{n}}\, ds \quad = \quad \int_{\Omega} \bar{\mathbf{f}}\, dv \end{aligned} \tag{7.17}$$

This is essentially the original momentum equation for $\bar{\mathbf{u}}$, except that we have an additional term involving the fluctuations. By defining the so called Reynolds stresses[3]

$$\boldsymbol{\tau}^{\mathrm{Re}}(\mathbf{u}') = -\rho \, \langle \mathbf{u}' \otimes \mathbf{u}' \rangle$$

we finally end up with

$$\int_{\Omega} \rho \frac{\partial \bar{\mathbf{u}}}{\partial t}\, dv - \int_{\partial\Omega} \boldsymbol{\sigma}(\nabla \bar{\mathbf{u}}, \bar{p}) \cdot \check{\mathbf{n}}\, ds \; + \int_{\partial\Omega} \rho\, (\bar{\mathbf{u}} \otimes \bar{\mathbf{u}}) \cdot \check{\mathbf{n}}\, ds - \int_{\partial\Omega} \boldsymbol{\tau}^{\mathrm{Re}}(\mathbf{u}') \cdot \check{\mathbf{n}}\, ds = \quad = \quad \int_{\Omega} \bar{\mathbf{f}}\, dv \tag{7.18}$$

In summary, the final set of equations to be solved are:

3: The Reynolds stresses are defined by a tensor which in Cartesian coordinates reads:

$$\boldsymbol{\tau}^{\mathrm{Re}}(\mathbf{u}') = -\rho \begin{bmatrix} u_1'^2 & u_1'u_2' & u_1'u_3' \\ u_2'u_1' & u_2'^2 & u_2'u_3' \\ u_3'u_1' & u_3'u_2' & u_3'^2 \end{bmatrix}$$

for which a **closure model** is needed. This will be introduced later on when discussing the turbulence models.

Reynolds Average NS equations

Find $\bar{\mathbf{u}}$ and $\bar{p}$ such that

$$\begin{aligned} \int_{\partial\Omega} \bar{\mathbf{u}} \cdot \check{\mathbf{n}}\, ds &= 0 \\ \int_\Omega \rho \frac{\partial \bar{\mathbf{u}}}{\partial t}\, dv - \int_{\partial\Omega} \boldsymbol{\sigma}(\nabla\bar{\mathbf{u}}, \bar{p}) \cdot \check{\mathbf{n}}\, ds + & \\ + \int_{\partial\Omega} \rho\, (\bar{\mathbf{u}} \otimes \bar{\mathbf{u}}) \cdot \check{\mathbf{n}}\, ds - \int_{\partial\Omega} \boldsymbol{\tau}^{\mathrm{Re}}(\mathbf{u}') \cdot \check{\mathbf{n}}\, ds &= \int_\Omega \bar{\mathbf{f}}\, dv \end{aligned}$$

or in differential (non-conservative) form:

$$\begin{aligned} \nabla \cdot \bar{\mathbf{u}} &= 0 \\ \rho \frac{D\bar{\mathbf{u}}}{Dt} - \nabla \cdot \left(2\mu \nabla^S \bar{\mathbf{u}}\right) + \nabla \bar{p} - \nabla \cdot \boldsymbol{\tau}^{\mathrm{Re}}(\mathbf{u}') &= \bar{\mathbf{f}} \end{aligned}$$

As usual, these equations must be supplemented with appropriate initial and boundary conditions, to be discussed later on.

Why not to solve the full NS equations? Kolmogorov's scales

In 1941, Kolmogorov postulated that the smallest scales of turbulence are **universal**, which means they are similar (or invariant) for every turbulent flow. He hypothesized that these scales depend only on the kinematic viscosity $\nu = \mu/\rho$ and ε, the average rate of dissipation of turbulence kinetic energy per unit mass, which is

$$\varepsilon = 2\,\nu\, \langle \mathbf{D}(\mathbf{u}') : \mathbf{D}(\mathbf{u}') \rangle, \quad \mathbf{D}_{ij}(\mathbf{u}') = \frac{1}{2}\left(\frac{\partial u_i'}{\partial x_j} + \frac{\partial u_j'}{\partial x_i}\right)$$

and quantifies how fast turbulent kinetic energy

$$k = \frac{1}{2}\langle u_i' u_i' \rangle = \frac{1}{2}\langle \|\mathbf{u}'\|^2 \rangle$$

is dissipated into heat by viscosity. Concretely, the Kolmogorov's scales are:

- Kolmogorov's lenght scale: $\eta = \sim \left(\frac{\nu^3}{\varepsilon}\right)^{1/4} \sim L\,\mathrm{Re}^{-3/4}$
- Kolmogorov's time scale: $\tau \sim \left(\frac{\nu}{\varepsilon}\right)^{1/2} \sim \frac{L}{U}\mathrm{Re}^{-1/2}$

where L and U are typical length and velocity scales of mean flow[4].

4: It is to be noticed that we have use the symbol $\sim$ to denote that these estimates are based on dimensional arguments.

As a consequence, if we aim to execute a Direct Numerical simulation (DNS) of the Navier-Stokes equations, i.e., having full spatial and temporal resolution, we need a prohibitively refined mesh and time step. Just to give an example, for the flow of water on a pipe of radius $L = 0.1$m at Re number in the order of 10^4 ($U \approx 1$m/s), a situation easily encountered in real life, the smallest eddies to be resolved are in the order 0.1mm, leading to a time step of 0.001s and a 3D mesh

with approximately 10^{12} cells[5].

5: Clearly, the situation is much worst at higher Reynolds numbers and larger scale flows, as in rivers or atmospheric flows.

7.4 Computational Modeling of Turbulence

7.4.1 Turbulence models

Boussinesq postulated that the Reynolds stresses should be expressed as:

$$\boldsymbol{\tau}^{\text{Re}}(\mathbf{u}') \leftarrow -\frac{2}{3}\rho\, k\, \mathbb{I} + 2\,\mu_t\, \mathbf{D}(\bar{\mathbf{u}}) \tag{7.19}$$

where μ_t is called the turbulent viscosity[6]. Therefore, the momentum equation becomes[7]:

$$\rho \frac{D\bar{\mathbf{u}}}{Dt} - \nabla \cdot [2\,(\mu + \mu_t(\bar{\mathbf{u}}))\, D(\bar{\mathbf{u}})] \; + \; \nabla \bar{p} \quad = \quad \bar{\mathbf{f}}$$

Prandtl was the first to propose a concrete model for the turbulent viscosity[8]

$$\mu_t = \rho\, \ell^2 \sqrt{2\, \mathbf{D}(\bar{\mathbf{u}}) : \mathbf{D}(\bar{\mathbf{u}})}$$

where the so called mixing length ℓ is given by, if we denote by y the distance to the wall :

- **von Karman model:**
$$\ell(y) = \kappa\, y,$$
where κ is almost a universal constant, for which several theories have been proposed [**turb2**].

- **Empirical expression - Nikuradse's law:** (see Spalding, 1972)
$$\frac{\ell(y)}{L} = 0.14 - 0.08 \left(\frac{y}{L}\right)^2 - 0.06 \left(\frac{y}{L}\right)^4$$
$L = R$ for a pipe.

- **Two-equation models - One example: the k–ε model**
The applicability of the previous models is quite limited to specific situations. In general, μ_t must be obtained by solving some additional problem. One of the most popular models is the k–ε. In this model it is postulated that
$$\mu_t = \frac{c_\mu\, \rho\, k^2}{\varepsilon}$$
where $c_\mu = 0.09$. Since we do not aim to track the actual fluctuations of the velocity field in the RANS equations, the idea is to model two fundamental average fields that depend on them, namely, the turbulent kinetic energy per unit mass contained in the fluctuations k and the turbulent dissipation per unit mass ε, i.e., the rate at which the energy stored in the fluctuations is dissipated. Therefore, we must solve two additional equations to model the behavior of such quantities.These are convection-diffusion-reaction equations that are coupled together and read[9]

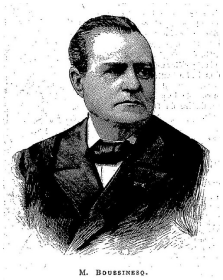

J. Boussinesq (France 1842–1929).

6: This modeling assumption agrees well with experiments, particularly if there are no large wakes and if the boundary layer is attached to the walls.

7: The bulk term in (7.19) is in general absorbed into the pressure term for convenience, which leads to a modified pressure $\bar{p}^*$. However, we will omit the $*$ in the sequel to simplify the notation.

8: The model was inspired by the concept of molecular diffusion.

9: Notice that the model is highly nonlinear, however, in many cases the equations are solved in a segregated form.

$$\frac{\partial k}{\partial t} + \bar{\mathbf{u}} \cdot \nabla k - \nabla \cdot (D_k \nabla k) + \varepsilon = \frac{2\,\mu_t}{\rho}\mathbf{D}(\bar{\mathbf{u}}) : \mathbf{D}(\bar{\mathbf{u}})$$
$$\frac{\partial \varepsilon}{\partial t} + \bar{\mathbf{u}} \cdot \nabla \varepsilon - \nabla \cdot (D_\varepsilon \nabla \varepsilon) + c_2 \frac{\varepsilon^2}{k} = \frac{2\,c_1}{k}\mathbf{D}(\bar{\mathbf{u}}) : \mathbf{D}(\bar{\mathbf{u}})$$

where

$$D_k = \frac{1}{\rho}\left(\frac{\mu_t}{\sigma_k} + \mu\right), \quad D_\varepsilon = \frac{1}{\rho}\left(\frac{\mu_t}{\sigma_\varepsilon} + \mu\right), \quad c_1 = 0.126, \quad c_2 = 1.92, \quad \sigma_k = 1, \quad , \sigma_\varepsilon = 1.3$$

are standard values adjusted by experiments.

There are also other models, such as Spalart-Allmaras, k–ω, Algebraic models, etc., that can be found in the literature.

7.4.2 Boundary conditions - Wall laws

The imposition of boundary conditions in the RANS models for wall–bounded shear flows deserves some attention. The typical situation we find is illustrated in 7.13. In this picture we clearly notice for the turbulent case, there are two important regions, namely, one in the close vicinity of the wall, exhibiting large gradients in $\bar{\mathbf{u}}$ and other, far from the wall, where the average velocity profile is essentially uniform[10].

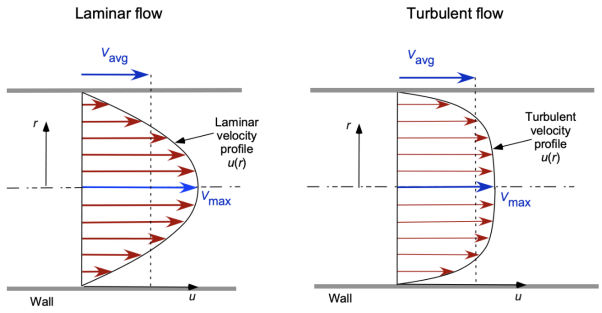

10: In the close vicinity of the wall, viscous effects are comparable or even more important than inertial ones. Eventually, there also exists the so called buffer layer above the viscous one, in which inertial and viscous effects balance eachother.

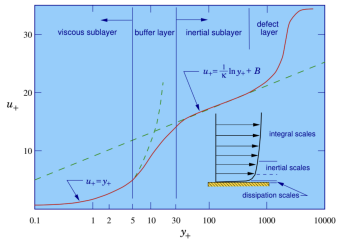

Figure 7.14: Law of the wall (Taken from Introductory Lecture Notes on Turbulence, Physics, Mathematics and Modeling by J. M. McDonough.

One problematic points is the enforcement of the appropriate boundary condition at solid walls when solving the RANS equation for the average velocity. The natural choice would be

$$\bar{\mathbf{u}} = 0 \quad \mathbf{x} \in \partial\Omega_S$$

This choice does not agree well with experiments. The core ideia to assert this problem is to impose a boundary condition at a fictitious wall (which most of the times is so close to the physical wall, that it is taken to be the same for simplicity), but considering that this wall is located in the turbulent dominated region, where the averaged equations are expected to be valid. We will see that it is more reasonable to impose a drag law as boundary condition. To that end we need some additional work. First, it is found that many turbulent flows exhibit the following velocity profile that is commonly written in terms of the non-dimensional variables u^+ and y^+,

$$u^+ = \frac{\bar{u}}{\sqrt{\tau_w/\rho}} = \frac{1}{\kappa}\ln(E\,y^+), \quad y^+ = \frac{y\sqrt{\tau_w/\rho}}{\nu} \in [20, 100]$$

where κ and E are to be determined by experiments[11]. If we evaluate this wall law at $y^+ = 30$ (within the inertial sublayer) we can obtain a boundary for the gradient of $\bar{u}$ by isolating τ_w. Generalizing this we can write

$$-2(\mu + \mu_t) D(\bar{\mathbf{u}}) \cdot \check{\mathbf{n}} = \frac{\rho}{C} \|\bar{\mathbf{u}}\|^2$$

where $\sqrt{C} = \dfrac{1}{\kappa} \ln(30\, E)$. As for the normal component of the velocity, we logically consider:

$$\bar{\mathbf{u}} \cdot \check{\mathbf{n}} = 0$$

At inflows the situation is simpler, we usually impose:

$$\bar{\mathbf{u}} = \bar{\mathbf{u}}_{\text{inlet}}$$

however the values of k and ε must also be given.

11: Typical values are $\kappa = 0.4$ and $E = 9$.

7.4.3 Final comments - LES models

Large eddy simulation (LES) is an intermediate option between DNS and RANS modeling. The main idea in the LES approach is to introduce a spatial filter (such as box, Gaussian, spectral cut-off, etc.) to separate the resolved scales (large and intermediate eddies) from the unresolved scales (the smalles eddies). For the latter, a so called subgrid scale (SGS) model must be adopted. Although, the LES approach is cheaper than DNS, it can still be quite computationally expensive when compared to RANS. In LES the filtered variable is obtained by convolution, i.e.,

$$\mathcal{F}\{\mathbf{u}(\mathbf{x}, t)\} = \widetilde{\mathbf{u}}(\mathbf{x}, t) = \int_\Omega G(\mathbf{x} - \mathbf{x}', \Delta)\, \mathbf{u}(\mathbf{x}', t)\, dv$$

and similarly for the pressure, where G is the filter function and Δ the typical size of the filter. Notice that, although the filter operation comutes with time derivatives, the same does not hold for spatial derivatives in general, so this will lead to additional errors. The filtered equations read

$$\begin{aligned} \nabla \cdot \widetilde{\mathbf{u}} &= 0 \\ \frac{\partial \widetilde{\mathbf{u}}}{\partial t} + \nabla \cdot (\widetilde{\mathbf{u} \otimes \mathbf{u}}) - \nu \nabla^2 \widetilde{\mathbf{u}} + \frac{1}{\rho} \nabla \widetilde{p} &= \widetilde{\mathbf{f}} \end{aligned}$$

The whole point is how to deal with the term $\widetilde{\mathbf{u} \otimes \mathbf{u}}$, for which we introduce the unresolved turbulent stresses and use again the Boussinesq Hypothesis

$$\boldsymbol{\tau} = \widetilde{\mathbf{u} \otimes \mathbf{u}} - \widetilde{\mathbf{u}} \otimes \widetilde{\mathbf{u}} = -2\, \nu_t \mathbf{D}(\widetilde{\mathbf{u}})$$

where ν_t is the subgrid scale viscosity, for which a model is needed to close the problem. The final momentum equation becomes

$$\frac{\partial \widetilde{\mathbf{u}}}{\partial t} + \nabla \cdot (\widetilde{\mathbf{u}} \otimes \widetilde{\mathbf{u}}) - \nu \nabla^2 \widetilde{\mathbf{u}} + \frac{1}{\rho} \nabla \widetilde{p} + \nabla \cdot \boldsymbol{\tau} = \widetilde{\mathbf{f}}$$

7.5 Assignment 1: Turbulent flows

This assignment is related to analyzing the turbulent flow on a periodic channel from the `Johns Hopkins Turbulence Database`. There are several benchmarks that can be retrieved from the database, most of them obtained via DNS computations of the Navier-Stokes equations, in general using spectral methods, since for one or two of the spatial dimensions, periodicity can be assumed.

The activity is based on `DEMO_JHTDB_incomp.ipynb` and the following points should be addressed:

1. Study the description of the problem given in the website and make sure to understand the different conditions under which the DNS simulation was conducted
2. Make a little research about spectral methods that were used to compute such DNS solutions.
3. Choose some arbitrary points in the domain and show the evolution of relevant quantities of the flow as a functions of time (velocity, pressure, kinetic energy, etc.)
4. Chose some arbitrary instants and plot the velocity profile in the streamwise direction, i.e., the u_2 as a function of $x_2 \in [-1, 1]$.
5. For the previous point, now retrieve the solution at several times and compute and plot the average velocity profile. Show the results as a function of the size of the sample.
6. Show contours of velocity on 2D planes and also 3D views of the flow.

7.6 Assignment 2: RANS equations in `openFOAM`

(This assignment is optional for undergrad students)

In this assignment the RANS equations with the k-ε model will be solved using the `openFOAM` software in `simpleFOAM`. The objective of this assignment is to run the example available in the website and conduct numerical experiments to characterize the numerical solution for the flow on a long pipe. Explore the different options available and elaborate a short report.

Bibliography

Here are the references in citation order.

[1] Pijush K. Kundu and Ira M. Cohen. *Fluid Mechanics, Fourth Edition*. Ed. by Elsevier. 2008 (cited on pages ii, 1, 43, 44, 122).

[2] Frank M. White. *Fluid Mechanics, Seventh Edition*. Ed. by McGraw-Hill. 2011 (cited on pages ii, 1, 2, 43, 45, 47).

[3] Brian J. Kirby. *Micro- and Nanoscale Fluid Mechanics: Transport in Microfluidic Devices*. Ed. by Cambridge University Press. 2010 (cited on pages ii, 11).

[4] Panayiotis Papadopoulos. *Lecture notes, ME185: Introduction to Continuum Mechanics*. 2020 (cited on pages ii, 7).

[5] Gustavo C. Buscaglia. *Lecture notes: Introduction to Computational Fluid Mechanics*. 2017 (cited on page ii).

[6] Robert Eymard, Thierry Gallouët, and Raphaèle Herbin. *Finite Volume Methods*. Ed. by P.G. Ciarlet and J.L. Lions. Vol. 7. 2003 (cited on pages 30, 35).

[7] H K Versteeg and W Malalasekera. *An Introduction to Computational Fluid Dynamics. The finite volume method.* Ed. by Pearson - Prentice Hall. 2007 (cited on pages 34, 120).

[8] Hrvoke Jasak. 'Error Analysis and Estimation for the Finite Volume Method with Applications to Fluid Flows'. PhD thesis. Department of Mechanical Engineering Imperial College of Science, Technology and Medicine, 1996 (cited on pages 34, 120).

[9] J. Pontes, N. Mangiavacchi, and G.R. Anjos. *An Introduction to Compressible Flows with Applications: Quasi-One-Dimensional Approximation and General Formulation for Subsonic, Transonic and Supersonic Flows*. SpringerBriefs in Mathematics. Springer International Publishing, 2019 (cited on page 49).

[10] J. Pontes and N. Mangiavacchi. *Fenômeos de Transferência*. Matemática Aplicada. SBM, 2021 (cited on page 49).

[11] Randall J LeVeque. *Finite volume methods for hyperbolic problems*. Vol. 31. Cambridge university press, 2002 (cited on pages 59, 61, 69, 74, 78, 88, 90).

[12] Johannes Martinus Burgers. 'A mathematical model illustrating the theory of turbulence'. In: *Advances in applied mechanics*. Vol. 1. Elsevier, 1948, pp. 171–199 (cited on page 59).

[13] Se E Buckley and MCi Leverett. 'Mechanism of fluid displacement in sands'. In: *Transactions of the AIME* 146.01 (1942), pp. 107–116 (cited on page 59).

[14] James William Thomas. *Numerical partial differential equations: finite difference methods*. Vol. 22. Springer Science & Business Media, 2013 (cited on page 61).

[15] José Alberto Cuminato and Messias Meneguette. *Discretização de equações diferenciais parciais: técnicas de diferenças finitas*. Sociedade Brasileira de Matemática, 2013 (cited on pages 61, 74).

[16] Randall J LeVeque. *Finite difference methods for ordinary and partial differential equations: steady-state and time-dependent problems*. SIAM, 2007 (cited on pages 66, 70, 74).

[17] Gerald Beresford Whitham. *Linear and nonlinear waves*. Vol. 42. John Wiley & Sons, 2011 (cited on page 77).

[18] Helge Holden and Nils Henrik Risebro. *Front tracking for hyperbolic conservation laws*. Vol. 152. Springer, 2015 (cited on page 77).

[19] Gordon D Smith. *Numerical solution of partial differential equations: finite difference methods*. Oxford university press, 1985 (cited on page 77).

[20] Siddhartha Mishra. 'Numerical methods for conservation laws and related equations'. In: *Lecture Notes, ETH Zurich* (2010), p. 74 (cited on pages 78, 84, 88, 90).

[21] Peter D Lax. 'Hyperbolic systems of conservation laws II'. In: *Communications on pure and applied mathematics* 10.4 (1957), pp. 537–566 (cited on page 82).

[22] Olga Arsen'evna Oleinik. 'Discontinuous solutions of non-linear differential equations'. In: *Uspekhi Matematicheskikh Nauk* 12.3 (1957), pp. 3–73 (cited on page 82).

[23] Sergei Konstantinovich Godunov. 'A difference scheme for numerical solution of discontinuous solution of hydrodynamic equations'. In: *Math. Sbornik* 47 (1959), pp. 271–306 (cited on pages 84, 88).

[24] Philip L Roe. 'Approximate Riemann solvers, parameter vectors, and difference schemes'. In: *Journal of computational physics* 43.2 (1981), pp. 357–372 (cited on page 85).

[25] Kurt O Friedrichs and Peter D Lax. 'Systems of conservation equations with a convex extension'. In: *Proceedings of the National Academy of Sciences* 68.8 (1971), pp. 1686–1688 (cited on page 86).

[26] Vladimir Vasil'evich Rusanov. 'Calculation of interaction of non-steady shock waves with obstacles'. In: *J. Comput. Math. Phys.* 1 (1961), pp. 267–279 (cited on page 87).

[27] Björn Engquist and Stanley Osher. 'Stable and entropy satisfying approximations for transonic flow calculations'. In: *Mathematics of Computation* 34.149 (1980), pp. 45–75 (cited on page 87).

[28] Helen C Yee. 'A class of high resolution explicit and implicit shock-capturing methods'. In: (1989) (cited on page 89).

[29] Philip L Roe. 'Some contributions to the modelling of discontinuous flows'. In: *Large-scale computations in fluid mechanics* (1985), pp. 163–193 (cited on page 90).

[30] Bram Van Leer. 'Towards the ultimate conservative difference scheme. IV. A new approach to numerical convection'. In: *Journal of computational physics* 23.3 (1977), pp. 276–299 (cited on page 90).

[31] Gerhard Wanner and Ernst Hairer. *Solving ordinary differential equations II*. Vol. 375. Springer Berlin Heidelberg, 1996 (cited on page 92).

[32] Sigal Gottlieb and Chi-Wang Shu. 'Total variation diminishing Runge-Kutta schemes'. In: *Mathematics of computation* 67.221 (1998), pp. 73–85 (cited on page 92).

[33] Sigal Gottlieb, Chi-Wang Shu, and Eitan Tadmor. 'Strong stability-preserving high-order time discretization methods'. In: *SIAM review* 43.1 (2001), pp. 89–112 (cited on page 92).

[34] A. J. Chorin. 'Numerical Solution of the Navier-Stokes Equations'. In: *Math. Comp.* 22 (1968), pp. 745–762 (cited on page 103).

[35] Pieter Wesseling. *Principles of Computational Fluid Dynamics*. Ed. by Springer. 2001 (cited on pages 108, 109, 111).

[36] C.M. Rhie and W.L. Chow. 'Numerical study of the turbulent flow past an airfoil with trailing edge separation'. In: *AIAA J.* 21 (1983), pp. 1525–1532 (cited on pages 110, 111).

[37] T.F. Miller and F.W. Schmidt. ' Use of a pressure-weighted interpolation method for the solution of the incompressible Navier-Stokes equations on a nonstaggered grid system'. In: *Num. Heat Transfer* 14 (1988), pp. 213–233 (cited on pages 110, 111).

[38] Stephen B. Pope. *Turbulent Flows*. Cambridge University Press, 2000 (cited on page 122).

[39] P.A. Davidson. *Turbulence, An Introduction for Scientists and Engineers*. Oxford University Press, 2004 (cited on page 122).

Alphabetical Index

Adams-Bashforth/Crank-Nicolson (ABCN), 119
Advection equation, 71
Averaged Navier-Stokes equations, 122

Boussinesq, 127

Cauchy problem, 74
Cauchy's stress tensor, 9
Cauchy-Riemann equations, 46
Cavity flow, 117
Cell-centered discretization, 24
Central scheme, 75
CFL condition, 68–70
Characteristic curves, 68
Checkboard pattern, 105
Colocated grid, 105
Computational aspects of turbulence modeling, 127
Conservation of energy principle, 11
Conservation of linear momentum principle, 9
Conservation of mass principle, 8
Consistency, 70
Continuum hypothesis, 1
Convergence, 70
Courant number, 69

Dirichlet boundary condition, 10
Domain of dependence, 69

Einstein's convention, 3
Exact solution, 70, 71

Finite difference method (FDM), 20
Finite Element method (FEM), 37
Finite volume mesh, 24
Finite volume method (FVM), 24
Flux consistency, 73
Fourier series, 74
Fourier's law, 12
Fully developed flow, 16

Global error, 70, 73

Helholtz-Hodge decomposition, 103

Internal energy, 11

Kronecker symbol, 3

Lax equivalence theorem, 70, 74
Lax-Friedrichs scheme, 72, 76
Lax-Richtmyer stability, 74
Lax-Wendroff scheme, 72, 76
LES, 129
Lipschitz continuity, 73
Local truncation error, 71

Material description, 4
Material points, 4
Material time derivative, 5

Navier-Stokes equations, 100
Neumann boundary condition, 10
Newtonian constitutive law, 12
Newtonian fluid, 18
No-slip boundary condition, 10

One-sided discretization, 110

Partition, 24
Poisson's problem, 15
Potential flows, 43
Potential function, 43
Potential lines, 47
preface, ii
Pressure-Weighted-Interpolation, 110

Referential description, 4
Reynolds transport theorem, 6

Spatial description, 4
Stability, 70, 73, 74
Stabilization term, 110
Staggered grid, 112
Steady motion, 6
Stream function, 45
Streamlines, 47

Tensors fields, 2
Transient heat equation, 16
Turbulence models, 127

Upwind , 71
Upwind scheme, 76

Vector fields, 2
Vertex-centered discretization, 24
Von Karman vortices, 111
von Neumann stability, 74

Wall laws, 128